Sara Raquel Vilela Pais

Mestre em Genética Molecular e Biomedicina

Identification and characterization of CteG, a novel *Chlamydia trachomatis* type III secretion effector protein

Dissertação para obtenção do Grau de Doutor em
Biociências Moleculares

Orientador: Luís Jaime Mota, Professor Auxiliar, Faculdade de Ciências e Tecnologia, Universidade NOVA de Lisboa

Júri:

Presidente:	Doutora Maria João de Reis Madeira Crispim Romão
Arguentes:	Doutora Sandra Manuela Rodrigues Sousa Cabanes
	Doutora Isaura Isabel Gonçalves Simões
Vogais:	Doutor Luís Manuel Valla Teixeira
	Doutora Isabel Maria Godinho de Sá Nogueira
	Doutor Luís Jaime Gomes Ferreira da Silva Mota

FACULDADE DE CIÊNCIAS E TECNOLOGIA
UNIVERSIDADE NOVA DE LISBOA

Sara Raquel Vilela Pais

Mestre em Genética Molecular e Biomedicina

Identification and characterization of CteG, a novel *Chlamydia trachomatis* type III secretion effector protein

Dissertação para obtenção do Grau de Doutor em
Biociências Moleculares

ACKNOWLEDGMENTS

First, I would like to thank my supervisor Luís Jaime Mota for mentoring me since I first arrived in the laboratory to do my Master's thesis with almost no laboratory experience. His constant guidance, support and availability and all the fruitful discussions and critics helped me become the researcher that I am today. I will always be grateful.

Also, I would like to acknowledge Isabel Sá Nogueira and Adriano Henriques for taking part on my thesis committee, and our collaborators Vítor Borges and João Paulo Gomes from Instituto Nacional de Saúde Pública Dr. Ricardo Jorge and Charlotte Key and Derek Fisher from Southern Illinois University. I thank the MolBioS PhD Program for accepting me and to Fundação para a Ciência e Tecnologia for financial support.

To all my colleagues of the Infection Biology Lab, Joana Bugalhão, Irina Franco, Filipe Almeida, Nuno Charro, Maria Cunha, Lia Domingues, Catarina Milho, Inês Pereira, Beatriz Costa and Maria Luís, a big thank you. Your companionship and all the helpful advices and discussions made this PhD thesis a more enriching experience. Besides, all the laughs shared inside and out of the laboratory made these PhD years more pleasant and enjoyable. Special thanks to Joana Bugalhão, who was a constant presence. Thanks for all the enthusiastic discussions and for the friendship. Also, thanks to Catarina Milho, Beatriz Costa, Ana Luzia and Inês Pereira for contributing to the work presented here in this thesis. Further, I thank my colleagues with whom I share the "Aquário", Raquel Portela, Inês Grilo, Bárbara Gonçalves and Cynthia Barroco for the all the relaxing breaks and chats.

I also would like to thank Carolina Cassona and Diana Espadinha, my resilient companions from the MolBioS PhD Program, for all the shared experiences and support.

Finally, I thank my parents and my brother for their constant love and patience and to Ana, Inês and Patrícia for all the support and for all the adventures.

FUNDING

This work was supported by Fundação para a Ciência e a Tecnologia (FCT) through grants PTDC/IMI-MIC/1300/2014 and PTDC/BIA-MIC/28503/2017, and by Unidade de Ciências Biomoleculares Aplicadas (UCIBIO), which is financed by national funds from FCT (UID/Multi/04378/2013) and co-financed by the European Regional Development Fund (ERDF) under the PT2020 Partnership Agreement (POCI-01-0145-FEDER-007728). SVP was supported by PhD fellowship PD/BD/52210/2013 within the scope of the PhD program Molecular Biosciences (PD/00133/2012) funded by FCT.

RESUMO

Chlamydia trachomatis é uma bactéria patogénica, intracelular obrigatória, que em células eucarióticas reside num vacúolo membranar. Durante o seu ciclo de desenvolvimento, esta bactéria usa um sistema de secreção do tipo III, que permite o transporte de proteínas efetoras para o citoplasma da célula hospedeira. Estas proteínas efetoras modificam vários processos e organelos das células hospedeiras, permitindo que as bactérias sobrevivam no ambiente intracelular.

Para identificar novas proteínas efetoras de *Chlamydia*, foram infetadas células de mamífero com estirpes de *C. trachomatis* que expressavam proteínas candidatas com um duplo péptido de hemaglutinina na extremidade C-terminal. Análises por microscopia de imunofluorescência revelaram que a proteína CT105/CteG era transportada para a célula hospedeira infetada. Observou-se que CT105/CteG associava-se inicialmente ao complexo de Golgi e que com a progressão da infeção, acumulava-se na membrana plasmática. Mostrou-se que esta mudança da localização de CT105/CteG é independente da integridade de filamentos de actina e microtúbulos. Além disso, quando diferentes regiões de CT105/CteG (656 resíduos de aminoácidos) foram expressas ectopicamente em células de mamífero, os primeiros 100 resíduos de CT105/CteG foram identificados como contendo uma região que direcionava a proteína para o Golgi. Apesar de uma estirpe de *C. trachomatis* com *ct105*/*cteG* inativado não ter apresentado um defeito no crescimento intracelular da bactéria, a expressão de CT105/CteG em *Saccharomyces cerevisiae* causou um defeito no transporte de proteínas para o vacúolo. Isto sugere que a função de CT105/CteG seja alterar o transporte vesicular em células eucarióticas. Por fim, a análise de várias estirpes de *C. trachomatis* sugeriu que o *ct105*/*cteG* é apenas transcrito em estirpes causadoras de linfogranuloma venéreo, indicando uma função de CT105/CteG neste contexto.

Em conclusão, neste trabalho foi identificada e caracterizada a primeira proteína efetora de *C. trachomatis* que se associa com o complexo de Golgi, ajudando a uma melhor compreensão das interações bactéria-hospedeiro.

Termos chave: Interações bactéria-hospedeiro; *Chlamydia trachomatis*; Sistema de secreção do tipo III; Golgi; tráfego vesicular

ABSTRACT

Chlamydia trachomatis is an obligate intracellular bacterial pathogen that resides in eukaryotic host cells within a membrane-bounded vacuole, termed inclusion. Throughout its characteristic biphasic developmental cycle, the bacterium uses a type III secretion system, which allows the direct delivery of effector proteins into the host cell cytoplasm. These effector proteins are thought to modify a variety of host cell processes enabling the bacteria to survive and multiply within the intracellular environment.

To identify novel type III secretion effectors of *Chlamydia*, mammalian host cells were infected by *C. trachomatis* strains independently expressing previously identified candidate effectors with a double hemagglutinin tag at their C-termini. Immunofluorescence microscopy analysis revealed that CT105/CteG (*Chlamydia trachomatis* effector associated with the Golgi) was delivered into infected host cells, where initially (~ 16 to 20 h post-infection) associated with the Golgi complex and as the developmental cycle progressed (~30 to 40 h post-infection) accumulated at the plasma membrane. The change of subcellular localization of CT105/CteG in the host cell during infection was shown to be independent of intact actin filaments and microtubules. Furthermore, when ectopically expressing different regions of CT105/CteG (656 amino acid residues) in mammalian cells, the first 100 residues of the protein were identified as containing a Golgi-targeting region. Although a *C. trachomatis ct105*/*cteG* mutant did not display a defect in intracellular growth, CT105/CteG induced a vacuolar protein sorting defect when expressed in *Saccharomyces cerevisiae*. This suggested that CteG could function in modifying eukaryotic vesicular transport. Lastly, *ct105*/*cteG* was mostly transcribed in *C. trachomatis* strains causing lymphogranuloma venereum, indicating that CT105/CteG might contribute to the characteristic tropism of these strains.

In conclusion, we have identified and characterized CT105/CteG, the first chlamydial effector found to associate with the Golgi complex, thus expanding the portfolio of known chlamydial effectors and increasing the understanding of host-pathogen interactions.

Keywords: Host-pathogen interactions, *Chlamydia trachomatis*, Type III secretion, Golgi, membrane trafficking

TABLE OF CONTENTS

Page

Acknowledgements I

Funding III

Resumo V

Abstract VII

Table of contents IX

Figure index XIII

Table index XV

List of abbreviations XVII

1 INTRODUCTION 1

1.1 Discovery of the *Chlamydia* pathogen 3

1.2 Taxonomy of *Chlamydia* 3

1.2.1 The *Chlamydiae* 3

1.2.2 The *Chlamydiaceae* 4

1.3 The human pathogen *Chlamydia trachomatis* 6

1.3.1 *C. trachomatis* strains 6

1.3.2 Medical importance and public health 6

1.3.3 Diagnostic, treatment and vaccine 7

1.4 *C. trachomatis* genetics 8

1.4.1 *C. trachomatis* genome 8

1.4.2 The virulence plasmid 8

1.4.3 Genetic manipulation of *Chlamydia* 9

1.4.3.1 Transformation of *Chlamydia* and development of stable shuttle vectors 10

1.4.3.2 Mutagenesis 11

1.4.3.2.1 Random mutagenesis 11

1.4.3.2.2 Site-directed mutagenesis 11

1.5 *Chlamydia trachomatis* pathogenesis 12

1.5.1 The type III secretion system of *Chlamydia trachomatis* 14

1.5.1.1 Chlamydial T3S effectors 16

1.5.1.1.1 Inc (inclusion membrane) proteins 17

1.5.1.1.2 Non-Inc T3S effector proteins 17

1.5.1.2 Chlamydial T3S chaperones 19

1.5.1.3 Chlamydial T3S-independent effectors 20

1.5.2 Modulation of host cells by *C. trachomatis* 21

1.5.2.1 Attachment and entry 21

Page

1.5.2.2 Repositioning and stability of the inclusion in the host cell 21
1.5.2.3 Subversion of host cell trafficking pathways and nutrient acquisition 21
1.5.2.4 Golgi fragmentation 23
1.5.2.5 Host cell exit 24
1.6 General aims 25

2 MATERIALS AND METHODS 27
2.1 Plasmids, oligonucleotides, and DNA manipulation 29
2.2 Cells lines and transient transfection 29
2.3 *E. coli* and *Y. enterocolitica* growth conditions 30
2.4 Maintenance and manipulation of *C. trachomatis* strains 30
2.4.1 Infection of HeLa 229 cells with *C. trachomatis* 30
2.4.2 Transformation of *C. trachomatis* 31
2.4.3 Clonal isolation of *C. trachomatis* by plaque assay purification 32
2.4.4 Construction of a *C. trachomatis ct105::aadA* mutant strain 32
2.4.5 Quantification of infectious progeny 33
2.5 *Y. enterocolitica* T3S assays 33
2.6 Yeast strains, invertase assays and toxicity analysis 34
2.7 Antibodies and fluorescent dyes 34
2.8 Drug treatments 35
2.9 Immunoblotting 35
2.10 Fluorescence microscopy 36
2.11 Real-time quantitative PCR (RT-qPCR) 36

3 RESULTS 37
3.1 Identification of candidate type iii secretion effectors of *Chlamydia trachomatis* 39
3.1.1 Ectopic expression of candidate T3S effectors of *C. trachomatis* in mammalian cells 39
3.1.2 Expression of epitope-tagged candidate chlamydial T3S effectors in *C. trachomatis* 41
3.1.2.1 Construction of *C. trachomatis* transformation vectors 41
3.1.2.2 Construction of strains with plasmid-encoded candidate *C. trachomatis* T3S effectors 44
3.1.3 Assessment of the delivery of candidate chlamydial T3S effectors by *C. trachomatis* into the host cell cytoplasm 45
3.1.4 The first 20 amino acids of CT105 contain a T3S signal 47
3.1.5 Full-length orthologues of CT105 are only present in *C. muridarum* and *C. suis* . 49

Page

3.1.6 The *C. trachomatis ct105* gene is likely only expressed in lymphogranuloma venereum (LGV) strains 51

3.2 The *C. trachomatis* effector CT105 associates with the Golgi complex and plasma membrane of infected host cells 53

3.2.1 Characterization of the *C. trachomatis* strain producing plasmid-encoded CT105-2HA 53

3.2.2 Analysis of the delivery of CT105-2HA into host cells during *C. trachomatis* developmental cycle 56

3.2.3 CT105-2HA localizes at the Golgi complex in *C. trachomatis*-infected cells 59

3.2.4 CT105-2HA localizes at the host cell plasma membrane in *C. trachomatis*-infected cells 61

3.2.5 Bacterially-delivered CT105-2HA changes its main localization in the host cell cytoplasm as the *C. trachomatis* developmental cycle progresses 62

3.2.6 The change in the main localization of CT105-2HA during infection from the Golgi to the plasma membrane is independent of intact host microfilaments and microtubules 64

3.2.7 The localization of bacterially-delivered CT105-2HA at the host cell plasma membrane is independent of the timing of the protein expression during the *C. trachomatis* developmental cycle 66

3.2.8 The first 100 amino acid residues of CT105 are sufficient to target the protein to the Golgi in uninfected mammalian cells 66

3.2.9 CT105 appears in filamentous structures within host cells 73

3.3 The *Chlamydia trachomatis* effector CT105 can interfere with vesicular trafficking in eukaryotic cells 75

3.3.1 CT105 is not essential for intracellular replication of *C. trachomatis* in infected tissue culture cells 75

3.3.2 CT105 induces a vacuolar protein sorting defect when ectopically expressed in *S. cerevisiae* 78

4 DISCUSSION AND CONCLUSIONS 81

4.1 Mechanism of delivery of CT105 83

4.2 CT105 is modified within *C. trachomatis* 84

4.3 CT105 has a dual localization within host cells during *C. trachomatis* infection 85

4.4 CT105 disrupts vesicular trafficking in eukaryotic cells 86

4.5 CT105 is likely relevant for the tropism of LGV strains 87

4.6 Outlook on other candidate T3S effectors of *C. trachomatis* 88

4.7 Hypothetic mode of action for CT105 during *C. trachomatis* infection 88

4.8 Future work 89

4.9 Conclusions and final remarks 91

Page

REFERENCES 93
ANNEXES 111

FIGURES INDEX

		Page
Figure 1.1	Phylogenetic 16S rRNA tree showing relationships among members of the phylum *Chlamydiae* …….……..	4
Figure 1.2	Phylogenetic reconstruction of the *Chlamydia* genus ……..……	5
Figure 1.3	Transmission electron micrograph of different *C. trachomatis* morphologic forms ……..…….	13
Figure 1.4	Schematic representation of the *C. trachomatis* developmental cycle	14
Figure 1.5	The T3SS of *C. trachomatis* ……....…….....	15
Figure 1.6	*Chlamydia-host interactions*.…….. ……..	24
Figure 3.1	Localization of candidate T3S effectors of *C. trachomatis* when ectopically expressed in mammalian cells ..…….….	40
Figure 3.2	*C. trachomatis* transformation vectors …….....	42
Figure 3.3	Construction of *C. trachomatis* L2/434-derived strains expressing candidate chlamydial T3S effectors ...…….. ….	45
Figure 3.4	Analysis of the delivery of the candidate T3S effectors by *C. trachomatis* L2/434 into the host cell ...…….. …….…….……	46
Figure 3.5	The first 20 amino acids of CT105 are sufficient and necessary to drive T3S by *Y. enterocolitica* ……..……..….	48
Figure 3.6	The first 20 amino acids of CT105 are necessary for the delivery of the protein into the host cell by *C. trachomatis* L2/434 ……..…….	49
Figure 3.7	mRNA levels of *ct105* in different *C. trachomatis* strains ….....	51
Figure 3.8	Putative promoter region of *ctl0360/ct105* in different *C. trachomatis* strains	52
Figure 3.9	Characterization of *C. trachomatis* L2/434 strain harboring pCT105-2HA ….	54
Figure 3.10	Kinetics of expression of CT105-2HA during infection by *C. trachomatis* L2/434	55
Figure 3.11	CT105-2HA is modified in *C. tracho*matis L2/434 ……..	56
Figure 3.12	*C. trachomatis* L2/434 produces CT105-2HA early during infection ……...	57
Figure 3.13	The subcellular localization of bacterially-delivered CT105-2HA changes in infected cells as the *C. trachomatis* developmental cycle progresses ……	58
Figure 3.14	CT105-2HA expressed under the control of the tetracycline promoter is delivered into the host cell by *C. trachomatis* L2/434 ……..……..	59
Figure 3.15	CT105-2HA associates with the Golgi complex in *C. trachomatis*-infected cells ……..…	61
Figure 3.16	CT105-2HA localizes at the host cell plasma membrane in *C. trachomatis*-infected cells ……	62

Page

Figure 3.17 CT105-2HA changes its subcellular localization during *C. trachomatis* infection …… 63

Figure 3.18 Subcellular localization of CT105-2HA expressed under the control of the tetracycline promoter in *C. trachomatis*-infected cells ……... 63

Figure 3.19 CT105-2HA changes in its subcellular localization during *C. trachomatis* infection is independent of intact host microfilaments and microtubules …… 65

Figure 3.20 Bacterially-translocated localizes at the host cell plasma membrane regarding the timing of its expression by *C. trachomatis* ……..…… 66

Figure 3.21 Ectopic expression of CT105 in HeLa cells ……..…….. 67

Figure 3.22 The first 100 amino acids of CT105 are target to the Golgi complex …… 69

Figure 3.23 CT105 fusions to the N-terminus of mEGFP …..…… 70

Figure 3.24 The first 100 amino acids of CT105 associate with the *trans*-Golgi …..…….. 71

Figure 3.25 *C. trachomatis* L2/434 strains harboring plasmids encoding truncated versions of CT105 were not detected in the host cell cytoplasm ……..……... 72

Figure 3.26 CT105 localizes in filamentous structures in non-infected and *Chlamydia*-infected cells …… 74

Figure 3.27 Verification of intron insertion in the *C. trachomatis ct105*::*aadA* mutant strain …….. 76

Figure 3.28 A *C. trachomatis ct105::aadA* insertional mutant is not defective for intracellular growth in tissue culture cells ……..…….. 77

Figure 3.29 The CT105 Chlamydia trachomatis effector protein does not affect host cell Golgi morphology during infection ……..…… 78

Figure 3.30 CT105 induces a vacuolar protein sorting defect in *S. cerevisiae* …… 79

Figure 3.31 Phenotypic characterization of *S. cerevisiae* strains expressing CT105 ...…. 80

Figure 4.1 Schematic model for CT105 mode of action during *C. trachomatis* infection of epithelial cells ……..…… 89

TABLE INDEX

		Page
Table 3.1	Predicted promoter regions of candidate T3S effectors of *C. trachomatis* ….	43
Table 3.2	Potential orthologues of *C. trachomatis* CT105 (CTL0360) in other *Chlamydiae* ……..……..……..	50
Table A.1	Plasmids used in this work ……..…….	113
Table A.2	Oligonucleotides used in this work ……..……	119
Table A.3	*Saccharomyces cerevisiae* strains used in this work ……..….	122

LIST OF ABBREVIATIONS

2HA	Double hemagglutinin
AB	Aberrant body
ATCC	American Type Culture Collection
BFA	Brefeldin A
BHI	Brain heart infusion
bla	Amplicilin resistance gene
cAMP	Cyclic adenosine monophosphate
Cas9	CRISPR associated protein 9
CEL I	Mismatch specific endonuclease
COPII	Coatomer protein II complex
CPAF	*Chlamydia* protease-like activity factor
CPY-Inv	Carboxypeptidase Y – invertase
CRISPRi	Clustered regularly interspaced short palindromic repeats interference
CyaA	*Bordetella pertussis* adenylate cyclase
DAPI	4',6-diamidino-2-phenylindole
DFA	Direct immunofluorescence assays
DMEM	Dulbecco's modified eagle medium
DMSO	Dimethyl sulfoxide
DNA	Deoxyribonucleic acid
EB	Elementary body
ECACC	European Collection of Authenticated Cell Cultures
EGFP	Enhanced fluorescent protein
EHEC	Enterohaemorrhagic *Escherichia coli*
ELISA	Enzyme-linked immunosorbent assays
EMS	Ethyl methanesulfonate
ENU	*N*-ethy-*N*-nitrosurea
EPEC	Enteropathogenic *Escherichia coli*
ER	Endoplasmic reticulum
ESCRT	Endosomal sorting complexes required for transport
FBS	Foetal bovine serum
FITC	Fluorescein isothiocyanate
FRAEM	Fluorescence-reported allelic exchange mutagenesis
FRU	Fructose
GAL	Galactose
GCIP	Grap2 cyclin D-interacting protein
GFP	Green fluorescent protein
GSK	Glycogen synthase kinase
HBSS	Hank's balanced salt solution
HRP	Horseradish peroxidase
Hsp60	Heat shock protein 60
IFN-γ	Interferon gamma
IFU	Inclusion forming units
Inc	Inclusion membrane
INSA	Portuguese National Institute of Health Dr. Ricardo Jorge
Inv	Invertase
LGV	Lymphogranuloma venereum
MCS	Multiple cloning site
mEGFP	Monomeric enhanced green fluorescent protein
MHC	Major histocompatibility complex
MOMP	Major outer membrane protein
mRNA	Messenger RNA
rRNA	Ribosomal RNA
MTOC	Microtubule-organizing centre

MVB	Multivesicular body
NAAT	Nucleic acid amplification tests
NCBI	National Center of Biotechnology Information
NEM	*N*-ethylmaleimide
OD_{600}	Optical density at 600 nm
ORF	Open reading frame
ori	Origin of replication
p.i.	Post-infection
PBS	Phosphate-buffered saline
PCR	Polymerase chain reaction
PDZ	Postsynaptic Density95/Disc Large/Zonula Occludens-1
PFA	Paraformaldehyde
PGK1	Phosphoglycerate kinase 1
Pmps	Polymorphic outer membrane proteins
P_{tet}	Tetracycline promoter
RB	Reticulate body
RNA	Ribonucleic acid
rRNA	Ribosomal RNA
RT-qPCR	Real-time quantitative PCR
SET	Su(var)3-9, Enhancer-of-zeste and Trithorax
SDS	Sodium dodecyl sulphate
SDS-PAGE	SDS-polyacrylamide gel electrophoresis
SNX	Sorting nexins
SPG	Sucrose-phosphate-glutamate buffer
SPI-1	*Salmonella* pathogenesis island-1
sRNA	Small RNA
STI	Sexually transmitted infections
T2SS	Type II secretion system
T3S	Type III secretion
T3SS	Type III secretion system
TCA	Trichloroacetic acid
TILLING	Targeting-induced local lesions in genomes
T_{incD}	*incD* terminator
TSS	Transcription start site
WHO	World Health Organization
YNB-Ura	Yeast nitrogen base uracil dropout

1 INTRODUCTION

1.1 DISCOVERY OF THE *CHLAMYDIA* PATHOGEN

In 1907, Ludwig Halberstadter and Stanislaus von Prowazek were examining Giemsa-stained smears of conjunctival scrapings from subjects with trachoma when they identified intracytoplasmatic inclusions arranged around the nucleus like a cloak. This was the first description of the etiological agent of trachoma which was named Chlamydozoa, derived from the Greek word “khlamús”, meaning cloak (Halberstaedter and von Prowazek, 1907). Later, similar inclusions were identified in scrapings from adults with urethritis and cervicitis, from newborns with nongonococcal conjunctivitis (Lindner, 1910), and in samples obtained from patients with lymphogranuloma venereum (LGV) (Durand *et al.*, 1913). In 1935, the agent was classified as a virus because it was able to pass through bacterial filters and unable to grow on agar or liquid media (Miyagawa *et al.*, 1935). This was accepted until 1966, when alongside with the emergence of electron microscopy, *Chlamydia* was reclassified as bacterium, due to the presence of DNA, RNA, a cell wall similar to Gram-negative bacteria, and the ability to undergo binary fission (Moulder, 1966).

1.2 TAXONOMY OF *CHLAMYDIA*

1.2.1 The *Chlamydiae*

Until the 1990’s, the phylum *Chlamydiae* was thought to have only one genus, the *Chlamydia*. However, the improvement and the increase accessibility to DNA sequencing set the grounds to the discovery of additional *Chlamydiae.* Over the last 25 years, the diversity of the *Chlamydiae* increased from one to nine families: *Chlamydiaceae*, *Parachlamydia*, *Waddliaceae*, *Simkaminiaceae*, *Rhabdochlamydiaceae*, *Criblamydiaceae*, *Piscichlamydiaceae*, *Clavichlamydiaceae* and *Parilichlamydiaceae* (Figure 1.1) (Horn, 2008). Despite covering a great host range and an ubiquitous distribution in the environment, all *Chlamydiae* share the obligate intracellular lifestyle within eukaryotic cells, a unique biphasic developmental cycle and more than 80% 16S ribosomal RNA (rRNA) and/or 23S rRNA sequence identity (Everett, 2000). The non-*Chlamydiaceae* are also referred as *Chlamydia*-like bacteria or environmental *Chlamydia* and exist as symbionts of free-living amoeba and of other eukaryotic hosts (Horn, 2008).

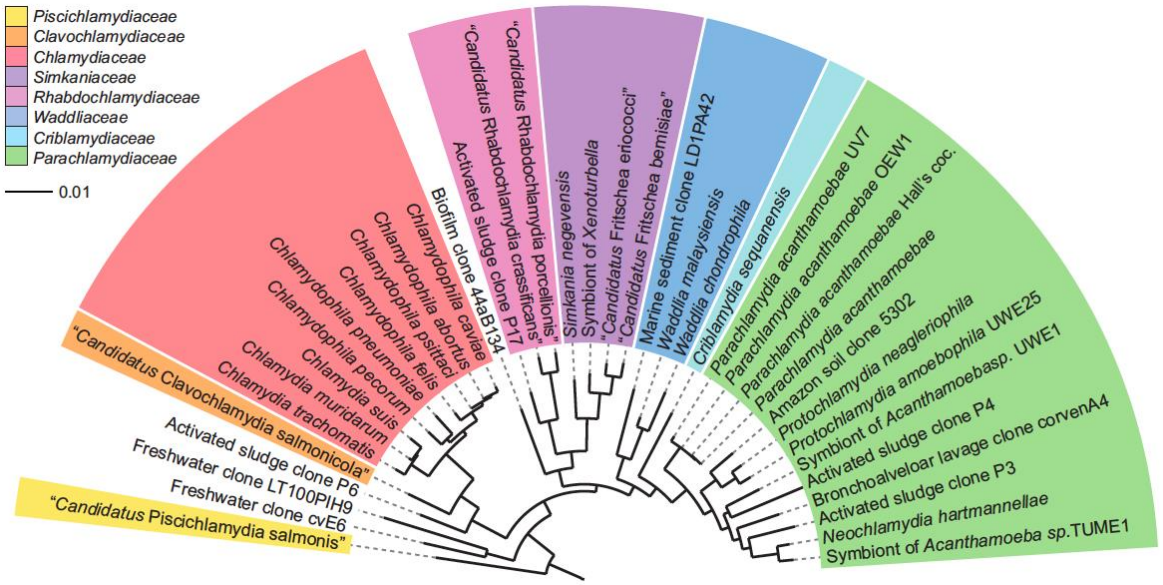

Figure 1.1 Phylogenetic 16S rRNA tree showing relationships among members of the phylum *Chlamydiae*. Representatives of all recognized families. Bar, 10% estimated evolutionary distance. Reprinted from Horn 2008.

1.2.2 The *Chlamydiaceae*

Based on the analysis of rRNA gene sequences, it was proposed the division of *Chlamydiacea* into two genera, *Chlamydia* and *Chlamydiophyla* (Everett *et al.*, 1999). However, this division raised controversy, as the thresholds used were not consistent with those from other bacteria taxa, all genomes were highly similar and there were no distinct phenotypic features between the recently created genera. Therefore, most of the researchers in the field continued to use the one genera nomenclature and a reunification for the genera was proposed (Sachse *et al.*, 2015). Although there are still doubts on the nomenclature, a single *Chlamydia* genus comprising all the known *Chlamydiaceae* species is the more accepted classification. The *Chlamydiaceae* family comprises 11 different species that infect a variety of hosts (Figure 1.2):

- *Chlamydia trachomatis* is an exclusive human pathogen causing ocular and genital infections. It is the most studied and characterized *Chlamydia* species (see Section 1.3);
- *Chlamydia pneumoniae* is another human pathogen and the major cause of community acquired pneumonia (Brown, 2012). It has been linked to several chronic diseases in humans such as atherosclerosis, osteoporosis, multiple sclerosis, and Alzheimer disease, although scarce data supports these associations. Besides infecting humans, *C. pneumoniae* infects amphibians, reptiles and other mammals (Roulis *et al.*, 2013);
- *Chlamydia psittacci* is the cause of avian respiratory disease and has a high impact on poultry farming and bird breeding. Transmission from birds to humans has been reported, when humans are in contact with infected birds. *C. psitacci* has been also isolated from other mammalian hosts, such as dogs, cats, pigs, cattle, sheep and horses (Longbottom and Coulter, 2003);
- *Chlamydia avium* and *Chlamydia gallinaceae* infect pigeons and poultry, respectively. These were previously included in the *C. psitacci* species. (Sachse *et al.*, 2014).

- *Chlamydia pecorum* is a pathogen of livestock (cattle, sheep, goats and pigs) (Walker *et al.*, 2015) and wild animals such as the koalas. In fact, *C. pecorum* is a major cause of the decline of the koalas in Australia (Polkinghorne *et al.*, 2013);
- *Chlamydia abortus* causes abortion in sheep and goat due to infection of the placenta and therefore has a significant economic impact, particularly in Europe. Although rare, transmission to humans has been reported and pregnant women exposed to infected animals are at risk of abortion (Longbottom and Coulter, 2003);
- *Chlamydia felis* is a frequent cause of infection in cats causing conjunctivitis and pneumonitis (Cai *et al.*, 2002). Infection of humans is rare and does not cause severe illness however transmission can occur to humans in close contact with cats (Hartley *et al.*, 2001);
- *Chlamydia caviae* is a pathogen of guinea pigs causing conjunctivitis and genital infections. These have been used as a model of sexual transmission of *Chlamydia* (Rank *et al.*, 2003) and to the study of genital tract infection and disease pathology (Rank and Sanders, 1992);
- *Chlamydia muridarum* infects mice causing pneumonitis and is widely used as a model to study genital chlamydial infections (Barron *et al.*, 1981).
- *Chlamydia suis* is a common pathogen of pigs. It is the only chlamydial species known to have naturally acquired genes that confer antibiotic resistance, as it contains tetracycline resistant genes (*tetC* islands) (Dugan *et al.*, 2004).

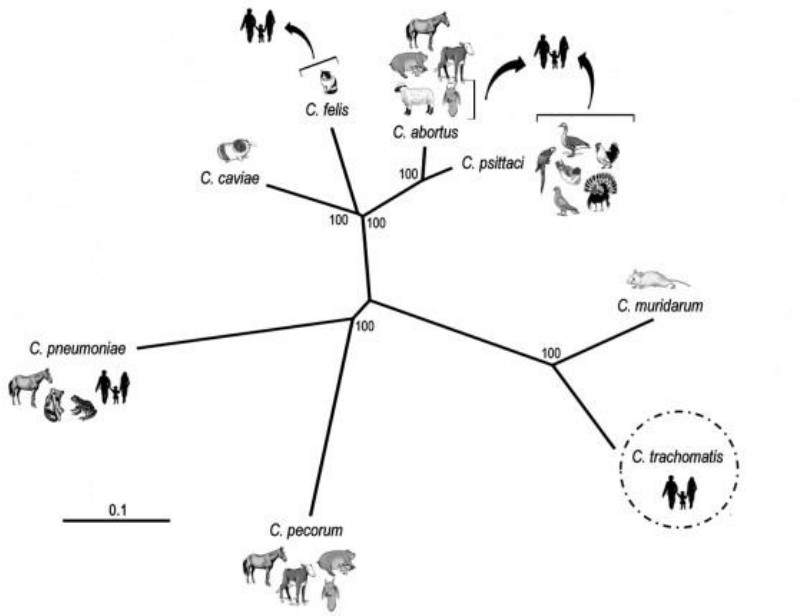

Figure 1.2 Phylogenetic reconstruction of the *Chlamydia* genus. *Chlamydiaceae* species and the respective natural hosts are shown in the figure and arrows depicted the cases of zoonotic transmission. *C. suis, C. avium and C. gallinacea* are not represented due to lack of sequence data. Tree topology is based on the accumulation of single-nucleotide polymorphisms (SNPs) on 600 orthologous genes shared among the species. Reprinted from Nunes *et a.l*, 2014.

1.3 THE HUMAN PATHOGEN *CHLAMYDIA TRACHOMATIS*

1.3.1 *C. trachomatis* strains

C. trachomatis is an exclusive obligate intracellular human pathogen and the most studied *Chlamydia* species. *C. trachomatis* are conventionally divided into 15 major serovars (A to L), depending on the immunoreactivity of the *C. trachomatis* major outer membrane protein (MOMP), or the genotyping and sequencing of *ompA* (the gene encoding MOMP). Serovars A to C mainly infect ocular epithelial cells, serovars D to K mainly infect urogenital epithelial cells, and lymphogranuloma venereum (LGV) strains (serovars L1 to L3) are also sexually transmitted but are more invasive and can infect macrophages and monocytes and spread into lymph nodes (Schachter, 1999).

All sequenced genomes of *C. trachomatis* are similar in size (1.04-1.05 Mb), exhibit more than 99% nucleotide sequence identity and have a high degree of synteny (Stephens *et al.*, 2009; Harris *et al.*, 2012; Seth-Smith *et al.*, 2013). Nevertheless, a small region in the genome (10 to 50 kb corresponding to 45-49 genes) named plasticity zone (PZ) has a high degree of genetic divergence between the different serovars and is likely involved in the different tissue tropisms (Read *et al.*, 2000). For example, the tryptophan operon (*trpRBA*) and the gene encoding cytotoxin CT166 are localized in this region. The tryptophan operon is present in all *C. trachomatis* strains, but only in the genital strains the tryptophan synthase (encoded by *trpBA*) is active and able to synthesize tryptophan from indole, a compound found in the genital tract and thought to be produced by the resident microbiota. During infection, the host immune system produces interferon gamma (IFN-γ), which limits the availability of tryptophan. However, genital strains are able to produce their own tryptophan and can survive in the genital tract environment (A Shaw *et al.*, 2000; Fehlner-Gardiner *et al.*, 2002; Caldwell *et al.*, 2003). Cytotoxin CT166 is a protein involved in the disassembly of actin filaments during bacterial internalization, which has been called the “cytopathic effect” (Thalmann *et al.*, 2010). Although present (complete or truncated) in ocular and genital strains, the gene encoding CT166 is deleted in LGV strains (Carlson *et al.*, 2004). Besides the PZ region, other genes across the genome might contribute to the variability among different *C. trachomatis* serovars, such as the highly variable polymorphic outer membrane proteins (Pmps) (Gomes *et al.*, 2006) and different secreted virulence proteins (Lutter *et al.*, 2010; Almeida *et al.*, 2012).

1.3.2 Medical importance and public health

C. trachomatis infections are a public health concern worldwide. Ocular strains are the major causative agent of preventable infectious blindness (trachoma), whereas urogenital strains are the most common cause of bacterial sexually transmitted infections.

Ocular infections caused by *C. trachomatis* serovars A to C produce a conjunctival inflammation that can lead to the scarring of the eyelid. Repeated infections can result in severe eye scarring and ultimately cause irreversible blindness. Transmission occurs through the contact with eye or nose discharges of infected people (Taylor *et al.*, 2014). *C. trachomatis* ocular infections are endemic in the poorest and rural areas of Africa, Central and South America, Asia, Australia and Middle East, mainly

due the lack of hygiene standards. *C. trachomatis* is responsible for visual impairment or blindness of about 1.9 million people, causing approximately 1.4% of all blindness (Taylor *et al.*, 2014; Trachoma Fact Sheet, World Health Organization (WHO), 2018)

C. trachomatis serovars D to K infect urogenital epithelial cells leading to cervicitis in women and urethritis in men. Infections are asymptomatic in approximately 70% of women and 50% of men. (Harryman *et al.*, 2014). If the infections are left untreated, bacteria ascend to the upper genital tract in 15 – 40% of the cases and leads to serious sequelae among woman including pelvic inflammatory disease (PID), tubal infertility, ectopic pregnancy, and chronic pelvic pain (O'Connell and Ferone, 2016). The World Health Organization (WHO) estimated that, in 2012, 131 million new cases of *C. trachomatis* infections occurred among adolescents and adults (15 - 49 years old), which corresponds to a 4.2% prevalence of *C. trachomatis* infections worldwide (Sexually transmitted infections (STIs) Fact Sheet, World Health Organization (WHO), 2016). In Portugal, the data on *C. trachomatis* infections is still limit as the report of *C. trachomatis* infections became mandatory only in 2014. The Portuguese National Institute of Health (INSA) inquiry revealed a prevalence of 2.7% of *C. trachomatis* infections among the 4,866 people inquired (INSA Inquiry 2015-2016, 2016).

C. trachomatis serovars L1 to L3 cause lymphogranuloma venereum (LGV), an inguinal syndrome normally characterized by genital ulceration and painful inguinal lymphadenopathy (Mabey and Peeling, 2002). LGV strains are endemic in Africa, Southeast Asia, South America and the Caribbean; however, in recent years, LGV has emerged in Europe and North America, mainly in men who have sex with men, as a leading cause of ulcerative proctitis (Mabey and Peeling, 2002; Martin-Iguacel *et al.*, 2010).

1.3.3 Diagnostic, treatment and vaccine

Antibiotic therapy has been shown to be effective in the treatment of primary ocular and urogenital *C. trachomatis* infections. The current guidelines of the WHO recommend the use of azithromycin and doxycycline (Reyburn, 2010) . Nevertheless, the major concern in *C. trachomatis* infections is the fact that these are commonly asymptomatic and can go undiagnosed and untreated (van de Laar and Morré, 2007). Repeated infections are also common and associated with a high risk of developing serious sequelae, such as blindness due to the ocular infections and infertility due to the urogenital infections (Darville and Hiltke, 2010). Therefore, tools to diagnose *C. trachomatis* are of major importance. Infections can be diagnosed either by culturing, direct immunofluorescence assays (DFAs), or enzyme-linked immunosorbent assays (ELISAs). However, the method of choice have been the nucleic acid amplification tests (NAATs), as they are highly sensitive and specific in detection of *C. trachomatis* in medical samples (Meyer, 2016) .

Currently, there are no licensed vaccines for *C. trachomatis* and the development of a vaccine still has low priority on the public health agenda, as these bacterial infections cause significant morbidity but no mortality. Several evidences from animal models and human studies suggested that the vaccine is feasible and a MOMP-based vaccine is already in phase I clinical trials (Gottlieb *et al.*, 2016; Poston *et al.*, 2017).

1.4 *C. TRACHOMATIS* GENETICS

1.4.1 *C. trachomatis* genome

The first complete chlamydial genome (*C. trachomatis* serovar D) was published in 1998 (Stephens, 1998). However, with the rapid development of the DNA sequencing technologies, the number of sequenced *C. trachomatis* genomes have increased rapidly. To date, there are 85 complete *C. trachomatis* genomes deposited in National Center of Biotechnology Information (NCBI) database. The typical *C. trachomatis* chromosome has approximately 1 Mbp and is predicted to encode about 900 protein-coding genes. The small genome suggests that, during adaptation to the host, *C. trachomatis* lost a large number of genes, as *Chlamydia*-like and free living bacteria have larger genomes (~2Mp) (Mendonça *et al.*, 2011). Nevertheless, *C. trachomatis* maintained the minimal machinery required for DNA replication, transcription and translation, for protein secretion, for basic lipid metabolism and for essential functions in aerobic respiration (Stephens, 1998; Yao, Cherian, *et al.*, 2015). Still, *C. trachomatis* relies on the host to obtain basic nutrients as some of its metabolic pathways are incomplete (e.g., tricarboxilic acid cycle or the biosynthesis of some amino acids) (Stephens, 1998)

1.4.2 The virulence plasmid

C. trachomatis harbors a 7.5 kb cryptic plasmid, first described in 1980 (Lovett *et al.*, 1980). The plasmid is low copy with up to 8 copies per cell, non-conjugative, non-integrative and, in the majority of the *Chlamydia* species, it does not possess antibiotic resistance genes (Pickett *et al.*, 2005; Ferreira *et al.*, 2013). The exception is plasmid of *C. suis*, which integrates and contains tetracycline resistance genes (Dugan *et al.*, 2004; Dugan *et al.*, 2007).

The plasmid is highly conserved among different *Chlamydia* species, ranging from 68 to 99% of nucleotide identity (Thomas *et al.*, 1997; Pickett *et al.*, 2005), and among different *C. trachomatis* strains it only differs in 1% of the nucleotide sequence (Thomas *et al.*, 1997; Ferreira *et al.*, 2013). The chlamydial plasmid carries 8 open reading frames (ORFs), which are all transcribed and translated during the developmental cycle (Palmer and Falkow, 1986; Ricci *et al.*, 1993; Ricci *et al.*, 1995), and 2 small antisense RNAs (sRNAs) (Ricci *et al.*, 1993; Albrecht *et al.*, 2009). The nomenclature is quite diverse among different species. pORF1 designates the open reading frame (ORF) immediately downstream from the origin of replication of the plasmid. However, in *C. trachomatis* this corresponds to Pgp7. This will be the nomenclature used below.

The Pgp1, -2, -6 proteins and the DNA sequence within *pgp8*, but not the Pgp8 protein, are required for plasmid maintenance (Gong *et al.*, 2013; Song *et al.*, 2013; Y Liu *et al.*, 2014). Pgp1 is a predicted DnaB-like helicase and Pgp8 is a putative integrase/recombinase. Pgp2 and Pgp6 are proteins of unknown function (Ricci *et al.*, 1995; Thomas *et al.*, 1997). The *pgp8* DNA coding sequence comprises a small antisense RNA (sRNA-2), which may play a role in plasmid maintenance although other features of the *pgp8* DNA coding sequence might contribute to this function (Gong *et al.*, 2013).

Pgp4 is a transcriptional regulator of virulence-associated chlamydial genes. Deletion of *pgp4* results in reduction of gene expression of *pgp3* (~ 4-fold) and of chromosomal genes that include *glgA,* a gene associated with accumulation of glycogen within the inclusion lumen (~ 8-fold), and a few genes encoding secreted proteins (~2- to 23-fold) (Song *et al.*, 2013). In addition, *pgp4* was shown to be required to particular egress mechanism (lytic exit) of *Chlamydia* from host cells (Chunfu Yang *et al.*, 2015).

Pgp5 is a negative regulator of the genes regulated by Pgp4, thus leading to the hypothesis that the chlamydial plasmid might aid in the modulation of chlamydial gene expression in response to environmental cues from the host, microbiome and co-infection (Y Liu *et al.*, 2014).

Pgp3 protein is associated with the chlamydial outer membrane (Comanducci *et al.*, 1993) and is secreted into the inclusion lumen and host cell cytosol (Z Li *et al.*, 2008). It has been demonstrated to be one of the most immunodominant antigens in humans infected by *C. trachomatis* (Wang *et al.*, 2010). Different activities have been reported for this plasmid-encoded protein. Pgp3 binds and neutralizes the anti-microbial peptide LL-37 (Hou *et al.*, 2015) and activates macrophages to produce inflammatory cytokines (Z Li *et al.*, 2008). In addition, the Pgp3/LL-37 complex is able to induce neutrophils to secrete inflammatory cytokines (Hou *et al.*, 2018) In mice, Pgp3 promotes *C. muridarum* survival in the lower genital tract and bacterial ascension to the upper genital tract (Yuanjun Liu *et al.*, 2014). Overall, this indicates that Pgp3 is a major virulence factor with an important role in *Chlamydia* pathogenesis.

sRNA-2 (antisense to *pgp8*) is the most abundant of all the plasmid transcripts (Ferreira *et al.*, 2013) and may play a role in plasmid maintenance through the regulation of *pgp8*, as described above (Gong *et al.*, 2013). sRNA-7 (antisense to *pgp5*) is not important to plasmid maintenance (Gong *et al.*, 2013) nor to negative transcriptional regulation associated with *pgp5* (Y Liu *et al.*, 2014), and its function is unknown.

Plasmid-deficient *C. trachomatis* strains are rare but have already been detected in patient isolates. These plasmidless strains are associated with impaired glycogen accumulation within the inclusion (Matsumoto *et al.*, 1998; O'Connell and Nicks, 2006) and have attenuated virulence in mice (O'Connell and Nicks, 2006; Sigar *et al.*, 2014). This suggests that the plasmid contributes to *Chlamydia* pathogenicity *in vivo*.

1.4.3 Genetic manipulation of *Chlamydia*

The study of the biology, pathogenesis and transmission of *C. trachomatis* has been hindered by the lack of tools for its genetic manipulation. The major constraints have been related with its obligate intracellular lifestyle, its characteristic biphasic developmental cycle, and the lack of evidence of recent acquisition of foreign DNA. However, in the last 10 years, methods for genetic manipulation broadly used in other bacteria have been successfully adapted to *C. trachomatis*. Although these procedures still need optimization, *C. trachomatis* is no longer genetically intractable.

1.4.3.1 Transformation of *Chlamydia* and development of stable shuttle vectors

In 1994, Tam and colleagues described for the first time the transformation of *C. trachomatis* (Tam *et al.*, 1994). The DNA used consisted in a *C. trachomatis–Escherichia coli* shuttle plasmid carrying a chloramphenicol acetyltransferase (*cat*) cassette under the control of a *Chlamydia* native promoter. However, the transformation revealed to be transient and the plasmid was lost after 4 passages/rounds of infection. Recent data showed that the transformed plasmid lacked a region within *pgp1* that is essential for plasmid maintenance.

In 2009, Binet and Maurelli designed a suicide plasmid containing a synthetic rRNA with single mutations that conferred resistance to kasugamycin and spectinomycin. By transforming *C. psittaci* with this plasmid using electroporation, a mutant was successfully obtained by means of allelic exchange (Binet and Maurelli, 2009). However, the methodology was not followed-up, probably due to the extremely low efficiencies of transformation and to the fact that *C. psittaci* requires high levels of containment.

In 2011, a landmark study by the laboratory of Ian Clarke was published describing a method for stable transformation of *C. trachomatis* (Wang *et al.*, 2011). A shuttle vector comprising the native chlamydial plasmid fused to an *E. coli* cloning vector was constructed to allow replication in both bacteria, and a β-lactamase gene was also added for selection of the transformants. The reasoning for the choice of this selection marker was that in the presence of β-lactams *C. trachomatis* enters a persistent state characterized by the arrest of the development cycle, in which bacteria are maintained in an aberrant non-infectious form. Therefore, the introduction of this plasmid in *C. trachomatis* would allow the transformed bacteria to avoid this persistent state in the presence of penicillin and continue the infection cycle. Another advantage of this marker is the fact that aberrant (non-transformed) and non-aberrant (transformed) bacteria have a distinct morphology that can be easily distinguished using conventional light microscopy. To introduce the recombinant plasmid in *C. trachomatis*, the classic method of *E. coli* chemical transformation was adapted. The plasmid DNA and elementary bodies (infectious form of the bacteria) were incubated in a $CaCl_2$ buffer followed by infection of epithelial cells and selection using penicillin during several rounds of infection. During this process, the native plasmid is replaced by the recombinant plasmid due to plasmid incompatibility and transformants can be stably maintained over numerous passages, even in the absence of the selection marker.

The development of the procedure described by the laboratory of Ian Clarke laid the basis for genetic manipulation of *C. trachomatis*. The shuttle vector used has been the backbone to second generation recombinant plasmids, which allow expression of a variety of fluorescent proteins (Agaisse and Derré, 2013; Campbell *et al.*, 2014), native or conditional control of gene expression (Agaisse and Derré, 2013; Wickstrum *et al.*, 2013; Bauler and Hackstadt, 2014), and to monitor protein delivery into the cytoplasm of infected host cells using different reporter epitope tags or enzymes (FLAG, Cya, GSK, TEM-1, split-GFP) (Bauler and Hackstadt, 2014; Mueller and Fields, 2015; Wang *et al.*, 2018).

1.4.3.2 Mutagenesis

1.4.3.2.1 Random mutagenesis

The development of the techniques to random mutagenize *C. trachomatis* were also a big step in the study of the biology of this bacterium. Kari and colleagues described the construction of an isogenic *C. trachomatis* mutant strain (Kari *et al.*, 2011) by a method derived from targeting-induced local lesions in genomes (TILLING), a plant genetics tool which combines chemical mutagenesis with a sensitive DNA screen to identify single nucleotide changes in a target gene. Low-levels of the mutagenizing agent ethyl methanesulfonate (EMS) were used to generate *C. trachomatis* strains with one mutation per genome. These mutants were expanded in subpopulations and screened for specific mutations by denaturing and reannealing PCR amplicons of the target gene followed digestion of the amplicons with a mismatch specific endonuclease (CEL I). Furthermore, subpopulations carrying the mutations in the target gene were sequenced. If a desired mutation was present, bacteria were isolated and further analyzed.

Subsequently, Nguyen coupled chemical mutagenesis with genome sequencing and DNA exchange to identify mutations responsible for characteristic phenotypes, in a forward genetics approach (Nguyen and Valdivia, 2012). *C. trachomatis* were again treated with the mutagenizing agent EMS but in higher concentrations than those used by Kari and colleagues, thus generating 3 to 20 mutations per genome. By plaque assay, clonal populations were isolated, and the morphology of the plaques were analyzed. Clones sharing the same plaque morphology were sequenced and searched for common mutations. Afterwards, mutants of interest were segregated by lateral gene transfer and homologous recombination. This method was further updated by Kokes (Kokes *et al.*, 2015) using as mutagenizing agent either EMS or *N*-ethy-*N*-nitrosurea (ENU) to create a collection of 934 mutant strains. The screen was performed by both plaque morphology and whole genome sequencing analysis.

1.4.3.2.2 Site-directed mutagenesis

Although the random mutagenesis was a great addition to the molecular genetics toolbox of *Chlamydia*, methods to specifically target the chlamydial chromosome were not yet available. In 2013, Johnson and Fisher adapted the TargeTron system (at the time marketed by Sigma Aldrich) to perform site-specific mutagenesis of *C. trachomatis*. This system is based on a mobile group II intron that can be retargeted by the alteration of DNA sequences within the intron and thus allowing site-specific gene insertions. The system was modified with the insertion of a chlamydial native promoter to allow the expression of the intron insertion machinery in *C. trachomatis.* A β-lactamase gene (*bla)* was added as a marker to select for the mutated strains. Using this system, it was possible to insertionally inactivate the gene encoding IncA, a *Chlamydia* protein that inserts in the membrane of the inclusion (Johnson and Fisher, 2013). Later, a re-modification of the system also allowed the use of spectinomycin as a selection marker (Lowden *et al.*, 2015). The success of this method has been proved, as it was used to mutate an antagonist of the chlamydial anti-sigma factor (Thompson *et al.*, 2015), other inclusion

membrane proteins (Weber, Nicholas F. Noriea, *et al.*, 2016; Sixt *et al.*, 2017; Weber *et al.*, 2017; Almeida *et al.*, 2018), and chlamydial GroEL chaperonins (Illingworth *et al.*, 2017).

In 2016, Mueller *et al*. described a system for fluorescence-reported allelic exchange mutagenesis (FRAEM) (Mueller *et al.*, 2016). The vector used consisted in a plasmid with *pgp6* (a gene required for plasmid maintenance) under the control of the tetracycline promoter, thus allowing a controlled removal of the plasmid upon mutagenesis. In addition, the plasmid contained a cassette encoding both β-lactamase and the green fluorescent protein (GFP) flanked by chlamydial DNA corresponding to approximately 3 kb of the genomic sequence upstream and downstream from the gene targeted for mutagenesis. This allowed allelic exchange of the gene of interest by the *bla/gfp* cassette. Stable mutations of *trpA*, *tmeA*/*ct694*/*ctl0063*, *tmeB*/*ct695*/*ctl0064*, and *ct696*/*ctl0065* were successfully achieved, confirming the functionality of the FRAEM system.

More recently, a system using clustered regularly interspaced short palindromic repeats interference (CRISPRi) based on an inducible catalytically inactive CRISPR associated protein 9 (Cas9) allowed the conditional knockdown of the *incA* gene. Nevertheless, the system still requires improvements in the stability of the plasmid, minimization of off-target effects and leaky expression to be considered attainable for mutagenesis of *C. trachomatis* (Ouellette, 2018).

1.5 *CHLAMYDIA TRACHOMATIS* PATHOGENESIS

C. trachomatis, like all *Chlamydiae*, are obligate intracellular bacteria that have a distinctive biphasic developmental cycle comprising the interconversion between two distinctive morphological forms, the elementary body (EB) and the reticulate body (RB) (Abdelrahman and Belland, 2005) (Figure 1.3). EBs are the infectious, non-replicative and extracellular form of the bacteria. They can temporally survive in the extracellular environment between infections, due to a highly crosslinked cell wall that confers resistance to osmotic and physical stress. These are the smaller form of the bacteria (~ 0.3 µm in diameter) and have a highly compact nucleoid. Although previously thought as being metabolically inactive, recent studies suggest that their metabolic and biosynthetic activity is high and depends on D-glucose as a source of energy (Omsland *et al.*, 2014). The RBs (~ 1 µm in diameter) are the non-infectious but replicative form of the bacteria. They are more fragile than EBs due the lack of a cross-linked outer membrane. They have a more relaxed chromatin and are metabolically active as they are involved in nutrient acquisition and replication (Hackstadt *et al.*, 1985; Barry *et al.*, 1992; Abdelrahman and Belland, 2005; Omsland *et al.*, 2014). *C. trachomatis* RBs can have an enlarged and aberrant morphology, designate as aberrant bodies (ABs). These are viable but non-infectious bacteria that result from *Chlamydia* entering in a state of persistence, where metabolism is slowed down and RB to EB conversion is hampered. This state is reversible and has been shown to be induced by several factors such as cytokines (IFN-γ), nutrient starvation and antibiotics (e.g., β-lactams) (Beatty *et al.*, 1994; Hogan *et al.*, 2004).

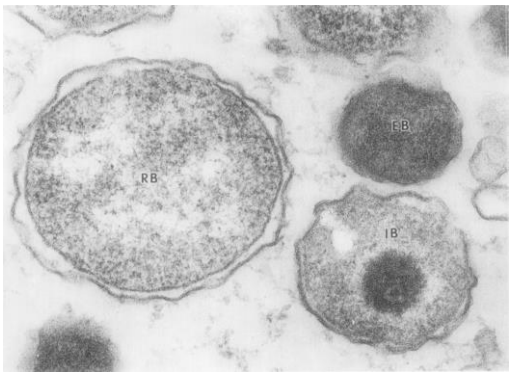

Figure 1.3 Transmission electron micrograph of different *C. trachomatis* morphologic forms. EB, elementary body. RB, reticulate body. IB, intermediate body, a conversion intermediate between EBs and RBs. Magnification x160,000. Reprinted form Philips *et al.* 1984

The developmental cycle of *C. trachomatis* is completed in 36 to 96 h (depending on the strains, e.g., for *C. trachomatis* LGV strains the cycle is about 48 h) (Miyairi *et al.*, 2006). It comprises an entry phase, where bacteria attach to the extracellular side of the host cell plasma membrane and are subsequently internalized in a membrane-bound vacuole, normally designated as inclusion. Then, the inclusion migrates to the perinuclear region of the host cell (Clausen *et al.*, 1997) and avoids fusion with lysosomes, as it mostly devoid of known markers of the endocytic pathway (Heinzen *et al.*, 1996). EBs differentiate into RBs thus starting bacterial replication, which is supported by the acquisition of nutrients (lipids, amino acids and iron) from the host cell. Chlamydial replication has been presumed to occur by binary fission, however recent studies have reported different observations where one supports the hypothesis of replication by polarized cell division (Abdelrahman *et al.*, 2016) and the other by binary fission (Lee *et al.*, 2018). Those studies have been performed using different microscopy tecniques, and thus the mechanism of *Chlamydia* replication will require further clarification. Chlamydial replication is accompanied by the expansion of the inclusion and, later, RBs asynchronously convert into EBs. This process has been suggested to be regulated by the size of the RBs (Lee *et al.*, 2018). Finally, EBs are released either by host cell lysis or extrusion of the inclusion and can undergo another round of infection on neighboring cells (Abdelrahman and Belland, 2005).

Throughout the developmental cycle, *Chlamydia* modulates host cellular functions (section 1.5.2) and one of the mechanisms used is the type III secretion system (T3SS; see Section 1.5.1), a mechanism of bacterial protein transport, that is likely crucial to the growth and survival of the bacteria within the host cell.

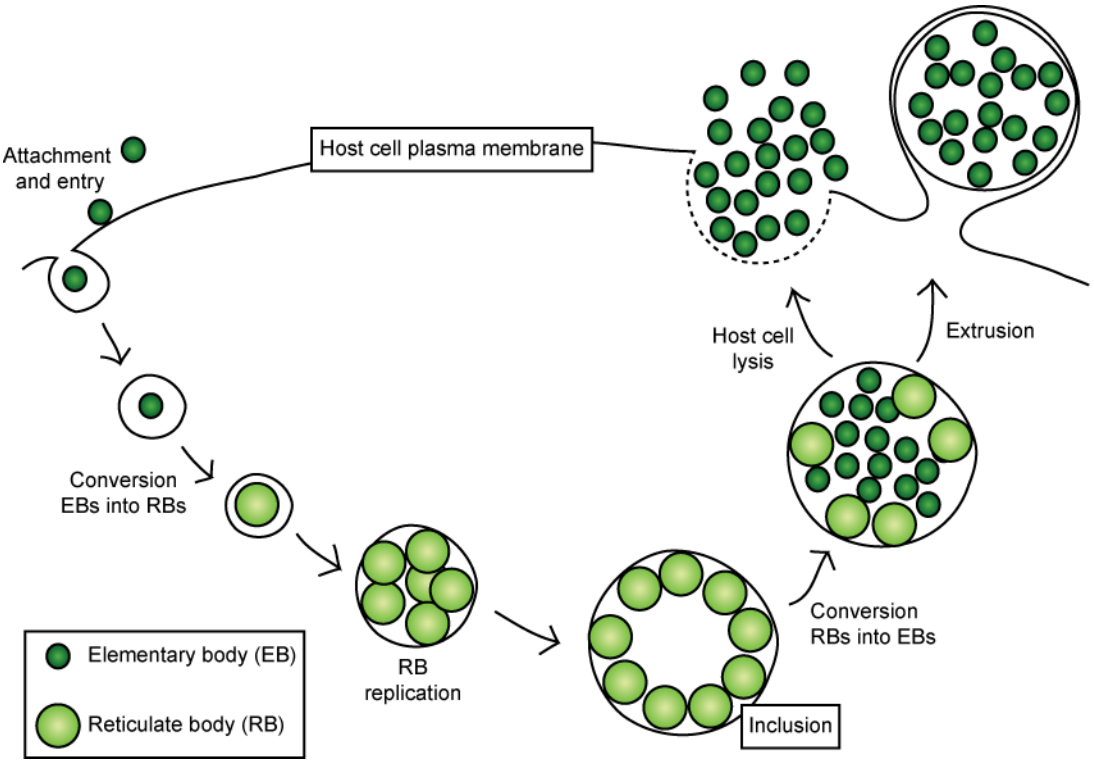

Figure 1.4 Schematic representation of the *C. trachomatis* developmental cycle. *C. trachomatis* infection starts with the attachment of the infectious elementary bodies (EBs) to the surface of epithelial cells. After entry, bacteria become enclosed within a membrane-bound vacuole, named inclusion, where EBs differentiate in non-infectious reticulate bodies (RBs). Later in the cycle, RBs differentiate back into EBs and are then released, either by host cell lysis or extrusion, to undergo another round of infection.

1.5.1 The type III secretion system of *Chlamydia trachomatis*

Protein secretion is an essential process for prokaryotic cells (and for all cells), allowing the transport of proteins to membrane compartments or to the extracellular space, whether this is the environment, another bacterium or a eukaryotic cell. To cross to the extracellular space, proteins from Gram-negative bacteria encounter a barrier composed by at least two phospholipid membranes and a peptidoglycan layer (Costa *et al.*, 2015). Therefore, it is not surprising that these bacteria have evolved a variety of mechanisms of protein secretion, specific to their needs. The type III, type IV and type VI secretion systems (T3SS, T4SS, T6SS, respectively) allow the direct delivery of proteins and DNA, in a one-step process, through large multiprotein complexes, functioning as nanomachines, spanning both inner and outer bacterial membrane. Although these nanomachines appear similar and serve the same purpose, they have different evolutionary origins and functions. For instance, proteins of the T3SSs are evolutionary related to those of the bacterial flagellum and secrete proteins capable of manipulating eukaryotic host cells. The proteins of the T4SSs are evolutionary related to those of bacterial conjugation systems possessing a pilus-like structure. T4SS allow the transport of proteins, but its main physiological role is the transport of plasmid DNA by conjugation. Lastly, the proteins of T6SSs are homologous to those of phage tails. In fact, while T6SSs also transport proteins into eukaryotic cells, their most common function is the injection of proteins into other bacteria. They are important to bacterial communication/competition and interaction with the environment (Costa *et al.*, 2015).

Non-flagellar T3SSs are exclusive of Gram-negative bacteria and are widely spread among bacterial pathogens of animals and plants, but are also involved in the establishment of symbiotic relationships between bacteria and eukaryotic hosts (Galán *et al.*, 2014). These systems allow the direct delivery into the cytoplasm of eukaryotic cells of bacterial proteins, named type III secretion (T3S) effectors, which promote bacterial growth and survival by interfering with host cell processes. T3SSs comprise an injectisome, a multi-protein complex embedded in the two bacterial membranes consisting in a basal apparatus, a needle complex topped by a tip complex and a translocation pore inserted in a host membrane (the host plasma membrane and the inclusion membrane, in the case of *Chlamydia*). The injectisome forms a continuous channel that enables the one-step delivery of the T3S effectors, which can have specific T3S chaperones to aid their secretion (Figure 1.5) (Cornelis, 2006; Galán and Wolf-Watz, 2006).

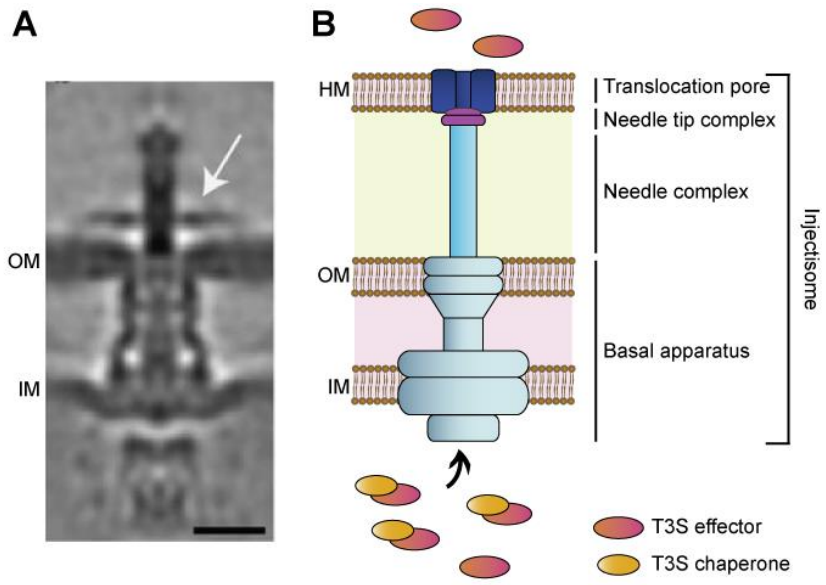

Figure 1.5 The T3SS of *C. trachomatis*. (A) Cryo-electron tomogram of host-free T3SS of *C. trachomatis;* scale 15 nm; Reprinted from Nans *et al.* 2015 **(B)** Schematic representation of a prototypical T3SS. The injectisome basal apparatus is embedded in the bacterial outer (OM) and inner (IM) membranes and is topped by a needle-like structure. Upon activation of the T3SS, translocator proteins are secreted and inserted at the host membrane (HM), forming the translocation pore. T3S effectors in bacterial cytosol can interact with T3S chaperones that aid secretion through the injectisome.

Typically, T3SSs are encoded in a few operons, either in pathogenicity islands in the bacterial chromosome (e.g., S*almonella*) or in virulence plasmids (e.g., *Yersinia* and *Shigella*) (Hueck, 1998). These systems have lost the motility genes of the flagellar apparatus and acquired components necessary for secretion and delivery of proteins across an eukaryotic cell membrane (Abby and Rocha, 2012). They are typically horizontally acquired and highly conserved even among bacteria with distinct evolutionary origins (Gophna *et al.*, 2003).

Likely, the first observation of the chlamydial T3SS was made by Matsumoto and colleagues in 1973, which described the presence of rosette-like structures and projections on the surface of both EBs and RBs in different chlamydial species (Matsumoto, 1973). With the advent of DNA sequencing, genomic analysis confirmed the presence of T3S encoding genes in all sequenced *Chlamydiaceae* and

environmental *Chlamydiae* (Stephens, 1998; Kalman *et al.*, 1999; Read *et al.*, 2000; Read *et al.*, 2003; Thomson *et al.*, 2005; Azuma *et al.*, 2006; Bertelli *et al.*, 2010). Normally, T3SS structural components are clustered together; however, the genes encoding the T3SS in *Chlamydia* are in at least four clusters (Kalman *et al.*, 1999) organized in multiple operons (Hefty and Stephens, 2007). Genes that code for T3SS have usually different G+C content (40-45%) when compared with the genome; however, this does not occur in *Chlamydia* indicating that recent gene integration did not occur and suggesting that chlamydial T3SS might represent a primordial system (Stephens, 1998; Abby and Rocha, 2012).

The chlamydial T3SS is thought to be activated in extracellular EBs upon contact with the host cell plasma membrane, resulting in the secretion of translocon proteins and followed by secretion of early effectors. Subsequently, within host cells, secretion is maintained in RBs by their association with the inclusion membrane which is accompanied by *de novo* expression of T3SS genes. When the transition of RBs to EBs occurs, RBs detach from the inclusion membrane and are thought to lose their protein secretion ability (Hansen-Wester and Hensel, 2001).

1.5.1.1 Chlamydial T3S effectors

Although the T3S injectisome is conserved among bacteria, normally T3S effectors do not have significant amino acid identity, but often have common structural features and perform similar functions. All effectors are thought to share a T3S signal localized at the N-terminus of the protein (approximately in the first 20 amino acid residues) (Sory *et al.*, 1995; Lloyd *et al.*, 2001). This signal is responsible to direct the protein for secretion and has been showed to be recognized by the T3SSs of different bacteria. The T3S signal is not cleavable, is unstructured and disordered, and enriched in serine, threonine, isoleucine and proline, but a clear consensus sequence is still unknown, despite of extensive studies (Wang *et al.*, 2013). Upon secretion and delivery into the host cell, T3S effectors can perform a variety of functions that have been found to be crucial to the survival of many pathogenic bacteria.

In *C. trachomatis*, T3S effector genes have been predicted to represent approximately 5-10% of the coding capacity of the genome. Their initial identification and study mostly relied on the use of (i) complex bioinformatic tools to predict T3S signals (Arnold *et al.*, 2009; Samudrala *et al.*, 2009; Löwer and Schneider, 2009), (ii) use of heterologous T3SS such as *Salmonella* (Ho and Starnbach, 2005), *Shigella* (Subtil *et al.*, 2005; Jewett *et al.*, 2006; Pennini *et al.*, 2010; Muschiol *et al.*, 2011; Furtado *et al.*, 2013), or *Yersinia* (Fields and Hackstadt, 2000; Clifton *et al.*, 2004; Chellas-Géry *et al.*, 2007; Hower *et al.*, 2009; Pais *et al.*, 2013; Hovis *et al.*, 2013; da Cunha *et al.*, 2014), and (iii) *Saccharomyces cerevisiae* to phenotypically characterize the effects of overexpression of candidate effectors (Sisko *et al.*, 2006; Kumar *et al.*, 2006). In addition, the identification of T3S effectors during *C. trachomatis* infection relied on the ability to produce specific antibodies against the proteins of interest and on their immunolocalization within host cells. More recently, the tools to genetically manipulate *C. trachomatis* strains have been used to study chlamydial T3S effectors.

1.5.1.1.1 Inc (inclusion membrane) proteins

The inclusion membrane (Inc) proteins are the most studied *C. trachomatis* T3S effectors. These proteins are characterized by a bilobed hydrophobic motif that likely mediates their insertion in the inclusion membrane (Rockey *et al.*, 2002). Therefore, they can be identified using bioinformatics prediction tools and by immunofluorescence microscopy analysis of their presumed localization in the *C. trachomatis* inclusion. Inc proteins, which are at the host-bacteria interface, have been shown to modulate host cytoskeleton dynamics (Kokes *et al.*, 2015; Mital *et al.*, 2015; Dumoux *et al.*, 2015; Wesolowski *et al.*, 2017), vesicular and non-vesicular transport (Rzomp *et al.*, 2006; Delevoye *et al.*, 2008; Derré *et al.*, 2011; Mirrashidi *et al.*, 2015), release of the bacteria from host cells (Lutter *et al.*, 2013; Nguyen *et al.*, 2018) and inhibition of host cell death (Sixt *et al.*, 2017; Weber *et al.*, 2017). Moreover, Inc proteins have been hypothesized to contribute to the different tissue tropism and invasion characteristics of different *C. trachomatis* serovars (Lutter *et al.*, 2012; Almeida *et al.*, 2012).

1.5.1.1.2 Non-Inc T3S effector proteins

In addition to the Inc proteins, there are chlamydial T3S effectors that are delivered into the host cell and which do not possess the characteristic bilobed hydrophobic motif and mostly do not localize at the inclusion membrane. Their study is more challenging, as their primary structure normally lacks obvious distinguishable features.

CT456/TarP (translocated actin-recruitment phosphoprotein) is likely the most studied T3S effector of *C. trachomatis*. TarP is synthesized at the late stages of the developmental cycle, pre-packed into EBs but only delivered into the host cell within minutes after EBs attachment. Once the EBs enter host cell, TarP is readily phosphorylated and recruits actin to the entry sites. TarP comprises an actin-binding domain at its C-terminus that associates with both G- and F-actin and induces actin nucleation and polymerization independently of host cell factors. At the N-terminus, TarP contains tyrosine-repeated regions which have been shown to be phosphorylated by the host cell kinases Src, AbII and Syk family (Mehlitz *et al.*, 2008; Jewett *et al.*, 2008). Phosphorylated TarP interacts with guanidine exchange factors, Sos1/Eps8/Abi1, and Vav2, which activate the small GTPase Rac allowing WAVE2 and Arp2/3-mediated nucleation of actin at the host cell entry sites (Lane *et al.*, 2008). Both actin nucleators, TarP and Arp2/3, act synergistically to enhance the rate of formation of actin filaments (Jiwani *et al.*, 2012). TarP has been shown to interact with vinculin to mediate actin recruitment and assembly at the host cell plasma membrane, and with adaptor protein SHC1 to induce host cell survival early during chlamydial infection (Mehlitz *et al.*, 2010). TarP has also been associated to the tropism of different C*. trachomatis* strains, as LGV strains contain higher number of tyrosine-rich repeat regions and less predicted actin binding domains, in contrast with TarP of the ocular strains (Lutter *et al.*, 2010).

CT694/TmeA (translocated membrane-associated effector A) is a T3S effector important for infectivity and invasion of *C. trachomatis.* TmeA is delivered into the host cell in the early-steps of infection (Hower *et al.*, 2009; McKuen *et al.*, 2017). The C-terminus of TmeA interacts with human AHNAK affecting the formation of host cell actin stress fibers. However, this does not seem to be

essential to invasion, probably due to redundancy among effectors acting at this stage (e.g., TarP) (Hower *et al.*, 2009; McKuen *et al.*, 2017). Furthermore, ANNAK recruitment to the nascent inclusions was found to be independent of TmeA (McKuen *et al.*, 2017). Moreover, TmeA contains a membrane binding domain (MDL) at the N-terminus that targets the protein, at least when ectopically expressed, to the mammalian plasma membrane. It is believed that this might be important to target the protein to the entry sites (Bullock *et al.*, 2012). Moreover, *ct695/tmeB,* which is co-transcribed with *ct694/tmeA*, encodes a T3S substrate that is transported into the host cell by *C. trachomatis* during invasion and at later times during the development cycle. TmeB localized at the inclusion membrane although no predicted transmembrane domain was found in this protein (Mueller and Fields, 2015). No defects for invasion and intracellular growth were observed for a *C. trachomatis tmeB* mutant (McKuen *et al.*, 2017) and the function of this protein remains to be elucidated.

CT875/TepP (translocated early phosphoprotein) is delivered into the host cell where is tyrosine-phosphorylated by Src family kinases, similarly to TarP (Carpenter *et al.*, 2017). TepP interacts with and recruits to the nascent inclusion the host proteins Crk and Crk-L, which are host scaffolding proteins that organize cytoskeletal rearrangement and signal transduction events (Birge *et al.*, 2009; Chen *et al.*, 2014; Carpenter *et al.*, 2017). TepP also interacts and recruits phosphoinositide-3-kinase (PI3K) to nascent inclusions modulating a type I IFN response (Carpenter *et al.*, 2017). Replication of *C. trachomatis* was found to be enhanced by expression of TepP (Carpenter *et al.*, 2017).

CT847 is a T3S substrate found to interact with the mammalian Grap2 cyclin D interacting protein (GCIP). As GCIP levels decreased during infection and by the addition of a T3SS inhibitor, CT847 is thought to be implicated in this effect during chlamydial infection (Chellas-Géry *et al.*, 2007).

CT737/NUE (nuclear effector) is transported into the host cell nucleus during infection where associates with chromatin. NUE contains SET [Su(var)3-9, Enhancer-of-zeste and Trithorax] domains, characteristic of proteins related to chromatin remodeling, and has histone methyltransferase activity with the ability to target host histones. This effector performs auto-methylation that leads to the increase of its enzymatic activity (Pennini *et al.*, 2010).

CT619, CT620, CT621, CT711 and CT712 are T3S substrates all comprising a unique domain of unknown function (DUF582). CT620 and CT621 have been shown to be delivered into the host cell cytoplasm and CT620 and CT711 were shown to localize in the host cell nucleus of infected cells. Although the DUF582 domain was shown to interact with the Hrs host protein (and Tsg101 for CT619), depletion of these and of other host proteins involved in the late steps of the endosomal sorting complexes required for transport (ESCRT) machinery assembly did not affect *C. trachomatis* internalization and development (Hobolt-Pedersen *et al.*, 2009; Muschiol *et al.*, 2011; Vromman *et al.*, 2016).

CT622 is a recently identified T3S effector that is delivered into the host cell cytosol. Although no specific function was found for this protein, a *C. trachomatis* mutant strain with the corresponding gene inactivated showed reduced infectivity and a growth defect (Gong *et al.*, 2011; Cossé *et al.*, 2018).

Chlamydial proteins CT089/CopN and CT529/Cap1, were found to localize at the inclusion membrane, although they did not contain the characteristic bilobal hydrophobic domain present in Inc proteins (Rockey *et al.*, 2002). Their function as T3S effectors remains unknown.

In addition to the T3S effectors described above, other candidate T3S effectors of *C. trachomatis* were found to be delivered into the host cells and to contribute to *C. trachomatis* pathogenesis: CT868/ChlaDub1/Cdu1, CT166/cytotoxin and Lda (Lipid droplet associated) proteins (Belland *et al.*, 2001; Kumar *et al.*, 2006; Wang *et al.*, 2018).

ChlaDub1 is a predicted cysteine protease likely to have deubiquitinating and deneddylating activities in the host cell, (Misaghi *et al.*, 2006). ChlaDub1 suppressed the NF-κB pathway when ectopically expressed in epithelial cells (Le Negrate *et al.*, 2008). Moreover, ChlaDub1 was shown to localize to the inclusion membrane (Wang *et al.*, 2018) where it stabilized by deubiquination of the anti-apoptotic host protein Mlc-1 (Fischer *et al.*, 2017), and likewise also stabilized GLUT1 (glucose transporter 1), which was shown to be upregulated in *Chlamydia*-infected cells (Wang *et al.*, 2017)

As already mentioned (section 1.3.1), CT166/cytotoxin is a protein cytotoxic for host cells (Belland *et al.*, 2001) and has been suggested to induce actin reorganization, that might involve the glycosylation of Rac1 (Thalmann *et al.*, 2010).

The Lda proteins (Lda1/CT156, Lda2/CT163, and Lda3/CT473) were found to be translocated into the eukaryotic host cell and to have affinity for host cell lipid droplets. They were proposed to contribute to the recruitment of lipid droplets into the inclusion lumen. Lipid droplets are neutral lipid-rich eukaryotic organelles and their recruitment may serve to the transport of essential lipids or vesicular transport proteins to the chlamydial inclusion (Kumar *et al.*, 2006).

1.5.1.2 Chlamydial T3S chaperones

T3S chaperones are bacterial strictly cytosolic proteins that bind T3S substrates and aid their secretion by different mechanisms, such as: preventing substrate degradation, maintaining substrates in a partially unfolded secretion-competent state, preventing aggregation and premature/incorrect interactions, targeting substrates to the T3SS, and/or regulating hierarchy of secretion. These T3S specific chaperones have been characterized as low molecular mass acidic proteins with ability to form dimers and to bind downstream from the T3S signal (Feldman and Cornelis, 2003; Parsot *et al.*, 2003). Depending on their substrate, T3S chaperones can be divided in three different classes: class I (Slc1, Mcsc, Scc1, Scc4, Scc3, in *C. trachomatis*) bind T3S effectors, class II (Scc2/Scc3, in *C. trachomatis*) bind proteins forming the translocon, and class III (CdsE and CdsG, in *C. trachomatis*) bind the T3S needle subunit

In *C. trachomatis*, although a high number of T3S substrates have already been identified, the number of known T3S chaperones it is still reduced. CT043/Slc1 (SycE-like chaperone 1) binds and enhances secretion of chlamydial T3S effectors TarP, TmeA, TepP and T3S substrate CT695/TmeB (Brinkworth *et al.*, 2011; Pais *et al.*, 2013; Chen *et al.*, 2014). Slc1 has been proposed to control the hierarchy of secretion of their interacting T3S effectors (Chen *et al.*, 2014). CT260/Mcsc (multiple cargo secretion chaperone) binds and stabilizes Cap1 and Inc proteins CT225 and CT618 (Spaeth *et al.*, 2009). The T3S chaperone CT584 binds and stabilizes the T3S substrate CT082 promoting its secretion (Pais *et al.*, 2013). Furthermore, CT584 has been proposed to be the main component of the chlamydial T3S needle tip complex based on an initial biophysical characterization (Markham *et al.*, 2009), however,

the subsequent elucidation of its three dimensional structure, revealed it does not resembles T3S tip proteins (Stone *et al.*, 2012). CT635 has been recently proposed as a candidate T3S chaperone of CT622 as both proteins interact. Nevertheless, CT635 could not stabilize or aid secretion of CT622 (Cossé *et al.*, 2018).

1.5.1.3 Chlamydial T3S-independent effectors

Additionally, other chlamydial proteins are delivered into the host cell independently of the T3SS and have been found to play important roles in *C. trachomatis* infection. CT441/Tsp is a protease found to cleave host NF-κB in *C. trachomatis* infected cells (Lad, Li, *et al.*, 2007; Lad, Yang, *et al.*, 2007). As already mentioned in section 1.4.2, Pgp3 is a plasmid-encoded protein found to be secreted into the cytosol of infected cells (Z Li *et al.*, 2008) and which plays an important role in *C. trachomatis* infection.

Another protein transported into the host cell is CT858/CPAF (*Chlamydia* protease-like activity factor), a widely studied chlamydial protein with serine protease activity and several proposed functions. Initial reports, indicated that CPAF targeted and cleaved several host cell and *Chlamydia* proteins during infection (Pirbhai *et al.*, 2006; Chen *et al.*, 2009; Christian *et al.*, 2010; Jorgensen *et al.*, 2011). However, subsequent studies found that the cleavage of many of the described CPAF targets occurred post-lysis and not under biological conditions (Chen *et al.*, 2012). The generation of a *C. trachomatis cpaf* mutant strain allowed re-evaluation of the previously characterized functions of CPAF (Snavely *et al.*, 2014). CPAF is produced in RBs as an inactive zymogen that upon its secretion into the inclusion lumen, possibly by a type II secretion system (T2SS), autocatalyzes into the active protease. This activation has been suggested to be regulated by the host cell protease inhibitor protein PI15 (Huang *et al.*, 2008; Chen, Lei, Flores, *et al.*, 2010; Chen, Lei, Lu, *et al.*, 2010; Snavely *et al.*, 2014; Prusty *et al.*, 2018). In the host cell, after loss of the inclusion membrane integrity, CPAF was found to target vimentin filaments and nuclear envelope protein lamin-associated protein-1 (LAP1). This occurs before loss of plasma membrane permeability and cell lysis, suggesting a function for CPAF in the release of EBs from the host cell during the late stages of infection (Snavely *et al.*, 2014). Moreover, CPAF has been implicated in the evasion of the host immune system by suppressing the oxidative burst, interfering with chemical-mediated activation of neutrophils and targeting host anti-chlamydial peptides to degradation (Tang *et al.*, 2015; Rajeeve *et al.*, 2018). CPAF, together with T3S effectors, was found to suppress the innate immune signaling (decreased β-interferon and proinflammatory cytokine synthesis) by inhibiting NF-κB p65 nuclear translocation (Patton *et al.*, 2016). CPAF expression has been found to be negatively regulated by the chlamydial plasmid, but only in LGV strains, implicating a function in macrophage infection tropism and invasiveness (Patton *et al.*, 2018). In addition, CPAF was found to promote *C. trachomatis* survival in the mouse lower genital tract (Yang *et al.*, 2016), and *C. trachomatis* CPAF-deficient mutants displayed impaired intracellular growth (Snavely *et al.*, 2014). Overall, CPAF showcases the complexity and diversity of functions for a single chlamydial protein during *C. trachomatis* infection.

1.5.2 Modulation of host cells by *C. trachomatis*

1.5.2.1 Attachment and entry

The attachment of *C. trachomatis* EBs to the host cell surface begins with a reversible electrostatic interaction with host heparan sulphate proteoglycans (Su *et al.*, 1996). This is followed by irreversible high affinity binding of host cell receptors, such as manose-6-phophate receptor, PDGFRβ, β1-integrin, and Ephrin A2, to bacterial counterparts MOMP, OmcB and PmpD. *Chlamydia* uses more than one receptor for invasion as single depletion of these host receptors is not sufficient to block entry (Elwell *et al.*, 2008; Subbarayal *et al.*, 2015). Additionally, host protein disulfide isomerase (PDI) was shown to be implicated in the entry of *Chlamydia*. It was speculated this could be due to reducing disulfide bonds in proteins involved in bacterial adhesion, such as host receptors and bacterial proteins (e.g., MOMP, Pmps, T3SS needle) (Conant and Stephens, 2007; Abromaitis and Stephens, 2009). After attachment, most of the EBs are internalized in an actin-dependent process orchestrated by *C. trachomatis* with the contribution of known chlamydial effectors TarP, TmeA, TepP and CT166 (see section 1.5.1.1.2).

1.5.2.2 Repositioning and stability of the inclusion in the host cell

Upon entry, *C. trachomatis* EBs become enclosed in a membrane-bound vacuole (the inclusion) whose membrane is readily modified by the insertion of Inc proteins. Insertion of these proteins allows interactions between bacteria and the host cell (E I Shaw *et al.*, 2000; Rockey *et al.*, 2002). Subsequently, the inclusion is directed from the entry sites towards the centrosome/microtubule-organizing centre (MTOC) (Grieshaber *et al.*, 2003) via the microtubule motor dynein, in a process involving *C. trachomatis* proteins. Inc protein CT850 interacts with the dynein light chain DYNLT1 (Mital *et al.*, 2015) and once at MTOC, Src kinases control the association between the inclusion and centrosomes (Mital and Hackstadt, 2011). Inc proteins IncB, CT101 and CT222, have been found at these contact points suggesting a potential contribution of these proteins to the transport of the inclusions (Mital *et al.*, 2015).

As the inclusion expands, actin and intermediate filaments progressively associate with inclusion. The actin cytoskeleton is key to maintain inclusion stability as disruption of actin filaments results in the rupture of the inclusion membrane and leakage of bacteria into the host cell cytoplasm. Host small GTPase RhoA is involved in this this process as it is recruited to the inclusion and its depletion leads to a decrease of the actin scaffolds around the inclusion (Kumar and Valdivia, 2008). In addition, host septins co-localize with the actin surrounding the inclusion and were found to be important to the assembly of actin fibers around the inclusion (Ouellette and Carabeo, 2010b).

1.5.2.3 Subversion of host cell trafficking pathways and nutrient acquisition

To survive within the intracellular environment *C. trachomatis* modulates the host cell trafficking pathways either promoting or inhibiting fusion with host cell compartments.

Eukaryotic small GTPases of the Rab family are major regulators of vesicle fusion. During *C. trachomatis* infection, Rab4, Rab11 and Rab14, which normally mostly associated with recycling endosomes, and Rab1 and Rab6, which are associated with endoplasmic reticulum (ER)-Golgi trafficking, are recruited to the inclusion membrane (Rzomp *et al.*, 2003). Moreover, *C. trachomatis* Inc CT229/CpoS binds multiple Rab proteins involved in a multiplicity of pathways (e.g. ER to Golgi transport, retrograde transport, exocytosis, and lipid droplet formation), suggesting that this protein could be involved in the recruitment of Rabs to the inclusion membrane (Rzomp *et al.*, 2006; Mirrashidi *et al.*, 2015; Sixt *et al.*, 2017). The recruitment of Rab proteins together with their respective host interacting proteins were shown to be involved in nutrient acquisition to the inclusion by fusion or interaction with host vesicles. Rab6, Rab11 and Rab14 were shown to be involved in acquisition of sphingomyelin from the Golgi (Rejman Lipinski *et al.*, 2009; Moore *et al.*, 2011b) and Rab4 and Rab11 in the acquisition of iron from the slow transferrin recycling pathway (Rzomp *et al.*, 2003; Ouellette and Carabeo, 2010a).

Besides recruiting Rab proteins, *C. trachomatis* also recruits to the inclusion host Soluble NSF (N-ethylmaleimide-sensitive factor (SNARE) proteins, which drive vesicle fusion in eukaryotic cells. For instance, the normally Golgi-localized SNAREs Syntaxin 6 and GS15 (Moore *et al.*, 2011a; Pokrovskaya *et al.*, 2012) and the endocytic SNAREs Vamp3, Vamp7 and Vamp8 (Delevoye *et al.*, 2008; Paumet *et al.*, 2009) localize around the inclusion in *C. trachomatis* infected cells. Interestingly, *C. trachomatis* Inc proteins IncA, InaC and IPAM contain SNARE-like motifs (Delevoye *et al.*, 2008), which bind to host SNAREs Vamp3, Vamp7 and Vamp8 and inhibit host membrane fusion (Paumet *et al.*, 2009). Moreover, IncA contains two SNARE-like motifs which are required for homotypic fusion of inclusions (Ronzone and Paumet, 2013; Ronzone *et al.*, 2014; Weber, Nicholas F Noriea, *et al.*, 2016) and also interacts with host Vamp8 likely to inhibit fusion with lysosomes (Delevoye *et al.*, 2008; Weber, Nicholas F Noriea, *et al.*, 2016). Although the *C. trachomatis* inclusion avoids fusion with the lysosomes, this organelle is thought to be a source of amino acids to the bacteria (Ouellette *et al.*, 2011).

Host sorting nexin (SNXs) proteins (Aeberhard *et al.*, 2015), which are involved in protein sorting from the endosomes to the Golgi apparatus (Seaman, 2012), are also recruited to inclusion membrane by *C. trachomatis*. The IncE protein interacts and recruits SNX5/6 allowing the bacteria to disrupt trafficking to the *trans*-Golgi network (Mirrashidi *et al.*, 2015; Elwell *et al.*, 2017).

Moreover, *C. trachomatis* intercepts multivesicular bodies (MVBs), intermediate endocytic compartments that are a source of sphingolipids and cholesterol crucial to chlamydial intracellular growth (Beatty, 2006; Beatty, 2008). As already mentioned above (section 1.5.1.1.2), *Chlamydia* also targets lipid droplets. The uptake of lipid droplets by the chlamydial inclusion may involve chlamydial proteins Lda1, Lda3, the inclusion membrane-associated effector protein Cap1, and the Inc proteins CT618, IncG and IncA (Kumar *et al.*, 2006; Saka *et al.*, 2015).

C. trachomatis also highjacks non-vesicular trafficking pathways involved in the transport of lipids, which have been found to be incorporated into the bacterial cell (e.g., sphingomyelin, cholesterol, phosphatidylcholine, and phosphatidylinositol). During infection, the Inc protein CT005/IncV interacts with host vesicle-associated membrane proteins (VAPs) present in the ER mediating the formation of ER-inclusion multiple contact sites (Stanhope *et al.*, 2017). Moreover, VAPs interact with ceramide transport protein (CERT), which is recruited to the inclusion by IncD providing additional stability to these

multiple contact sites and also allowing the direct transfer of ceramide (the precursor of sphingomyelin) from the ER to the inclusion (Derré *et al.*, 2011; Agaisse and Derré, 2014). In the absence of CERT and sphingomyelin, bacterial replication and inclusion size decreases (Derré *et al.*, 2011). Overall these suggests that ER-inclusion multiple contact sites are important to the transport of ceramide and consequently to the synthesis of sphingomyelin at the inclusion membrane.

*C. trachoma*tis also acquires saturated fatty acids for *de novo* membrane synthesis (Yao, Dodson, *et al.*, 2015), which have been found to be essential for bacterial replication (Yao *et al.*, 2014; Yao, Dodson, *et al.*, 2015)

1.5.2.4 Golgi fragmentation

A hallmark of *C. trachomatis* infection is the fragmentation of the Golgi complex into mini stacks that surround the inclusion (Heuer *et al.*, 2009). This requires the depolymerization of acetylated and detyrosinated tubulin (Al-Zeer *et al.*, 2014), which may act as anchors for the Golgi mini stacks around the inclusion. Until now, InaC/CT813 (an Inc protein) is the only chlamydial effector found to be required for the repositioning of the Golgi complex. InaC was found to bind and recruit the small GTPases Arf1 and Arf4 to the inclusion membrane and indirectly activate Arf1. Moreover, absence of InaC, or depletion of Arf1 or Arf4 during infection, could prevent Golgi dispersal and decreased the presence of detyrosinated or acylated tubulin, suggesting that InaC/CT813 hijacks Arf GTPases to control Golgi positioning (Kokes *et al.*, 2015; Wesolowski *et al.*, 2017).

Golgi fragmentation has been thought to enhance lipid delivery, as depletion of Rab6 and Rab11 abolished Golgi fragmentation in infected cells and led to a reduction in the infectivity, in the formation of EBs and in the delivery of sphingolipids to the inclusion (Rejman Lipinski *et al.*, 2009). However, Golgi fragmentation was shown to be dispensable for dynamin-mediated sphingolipid acquisition into *C. trachomatis* inclusions (Gurumurthy *et al.*, 2014) and infection with a *C. trachomatis inaC* mutant strain revealed normal trafficking of sphingolipids into the inclusion (Kokes *et al.*, 2015). Therefore, additional studies will be required to clarify the importance of Golgi fragmentation during *C. trachomatis* infection.

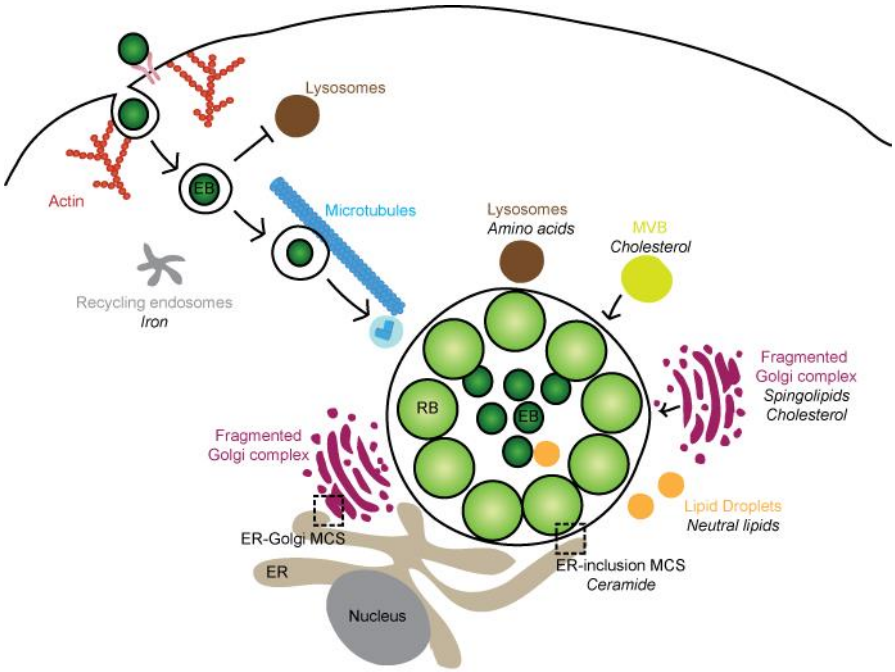

Figure 1.6 *Chlamydia*-host interactions. Following attachment to the host cell plasma membrane, *Chlamydia* enters in the host cell in a process dependent on actin rearrangements involving both host and bacterial proteins. The bacteria become enclosed within a bacterially-modified vacuole, named the inclusion. This nascent inclusion is transported along microtubules to the MTOC and expands as bacterial replication occurs. During this stage, the inclusion interacts, via bacterial effectors, with multiple host cell organelles, including the Golgi complex, the endoplasmic reticulum (ER), lipid droplets, multivesicular bodies (MVBs) and lysosomes. Delivery of essential host lipids to the inclusion involves vesicular trafficking from Golgi complex, MVBs and lipid droplets and non-vesicular trafficking from membrane contact sites (MCS) formed between the ER and the inclusion. Amino acids are acquired from protein degradation within the lysosomes. EB, elementary body; RB, reticulate body. Adaptation of Bastidas *et al.* 2013.

1.5.2.5 Host cell exit

At the end of the developmental cycle, the EBs enclosed in the inclusion can be released either by host cell lysis or extrusion of the inclusion. The aggressiveness of *C. trachomatis* strains seems to be related with the exit mechanism, as LGV-strains tend to be release by host cell lysis whereas non-LGV genital or ocular strains by extrusion (Hybiske and Stephens, 2007).

The lytic exit consists in sequential permeabilizations of the inclusion, host organelles and then plasma membrane leading to host cell death. Inclusion disruption is dependent on cysteine proteases whereas plasma membrane disruption and *Chlamydia* release is a calcium-dependent process (Hybiske and Stephens, 2007). CPAF has been suggested to play a role in lytic exit, since a *C. trachomatis cpaf* mutant strain failed to lyse infected epithelial cells. However, it was suggested that CPAF has an indirect role in this process (Snavely *et al.*, 2014; Chunfu Yang *et al.*, 2015). Moreover, it was shown that plasmid-encoded Pgp4, a regulator of chromosomal genes (see section 1.4.2), was required for lysis, probably by regulating T3S effector genes related to the modulation of the host cell cytoskeleton (Chunfu Yang *et al.*, 2015).

Exit by extrusion of the inclusion is a process similar to exocytosis, where the contraction of the inclusion and plasma membranes results in the detachment of a separate double membrane compartment enclosing the bacteria. In opposition to the lytic exit, extrusion exit leaves the host cell

intact (Hybiske and Stephens, 2007). For extrusion, actin polymerization and elements of the myosin phosphatase pathway are required (Lutter *et al.*, 2013). The Inc protein CT228 was found to interact with and recruit myosin phosphatase-targeting subunit 1 (MYPT1), a component of the myosin phosphatase complex, to inclusion membrane microdomains rich in Src kinase. Yet the mechanisms regulating the activity of myosin phosphatase have not been defined (Lutter *et al.*, 2013). Moreover, another Inc protein (MrcA/CT101) interacts with host calcium channel and a receptor for inositol-trisphosphate, ITPR3. Both ITPR3 and the calcium sensor STIM-1 were found to be recruited to Src rich microdomains at the inclusion (Nguyen *et al.*, 2018). Reduction of chlamydial release by extrusion was inhibited by disruption of the *mrcA* gene, depletion of ITPR3 or STIM1, or by using calcium chelator (Nguyen *et al.*, 2018). The calcium chelator also led to the loss of myosin motor activity (Nguyen *et al.*, 2018). Overall, this suggested that the calcium signaling pathways also play an important role in the regulation of the extrusion mechanism by *C. trachomatis*.

1.6 GENERAL AIMS

The general goal of this project was to improve our understanding of the mechanisms used by *C. trachomatis* to infect and survive within host cells and, therefore, to provide insights on how host cells can be manipulated by bacterial pathogens.

Previous results from our laboratory identified chlamydial proteins that were secreted in a T3S-dependent manner, when using *Y. enterocolitica* as a heterologous T3SS (Pais *et al.*, 2013; da Cunha *et al.*, 2014). In this work, we aimed to characterize and analyze the function of the previously identified putative *C. trachomatis* T3S effectors CT053, CT082, CT105, CT429, CT696 and CT849. To achieve this, our specific aims were:

- To construct *C. trachomatis* strains expressing the putative T3S effectors fused to an epitope tag, by using state of the art techniques for genetic manipulation of *C. trachomatis*;

- To analyze whether these putative T3S effectors were delivered into the host cell during infection and where they localized;

- To search for the function of a putative T3S effector shown to be delivered into the host cells and analyze its importance during *C. trachomatis* infection.

2 MATERIALS AND METHODS

2.1 PLASMIDS, OLIGONUCLEOTIDES, AND DNA MANIPULATION

The plasmids used in this work, their main characteristics and construction details, are described in Annexes Table A1. The DNA primers used in their construction are listed in Annexes Table A2. Plasmids were constructed and purified using standard molecular biology procedures with Phusion high-fidelity DNA polymerase (Thermo Fisher Scientific), restriction enzymes (Thermo Fisher Scientific), T4 DNA Ligase (Thermo Fisher Scientific), DreamTaq DNA polymerase (Thermo Fisher Scientific), NZYTaqII (NZYTech), DNA clean & concentrator™-5 kit and Zymoclean™ gel DNA recovery kit (Zymo Research), and GeneElute Plasmid Miniprep kit (Sigma Aldrich) or NZYMidiprep kit (NZYTech), according to the instructions of the manufacturers.

The backbone plasmids used in this work were: p2TK2-SW2 (Agaisse and Derré, 2013), used to construct *Chlamydia trachomatis* expression plasmids encoding 2HA, GSK or CyaA; pSVP247 (da Cunha *et al.*, 2017), a derivative of p2TK2-SW2 (Agaisse and Derré, 2013), used to generate *C. trachomatis* expression plasmids encoding proteins with a 2HA at their C-termini; pmEGFP-N1 and pmEGFP-C1 [both constructed from pEGFP-N1 (Clontech) and pEGFP-C1 (Clontech), respectively, where the gene encoding enhanced green fluorescent protein (EGFP) was replaced by a gene encoding monomeric EGFP (mEGFP) from pLAMP1-mGFP (Falcón-Pérez *et al.*, 2005) and pEF6/*Myc*-His A (Thermo Fisher Scientific), used to generate mammalian transfection plasmids; pLJM3 used to generate *Yersinia enterocolitica* plasmids for type 3 secretion (T3S) assays, which enabled expression of cloned genes driven by the promoter of the *Y. enterocolitica yopE* gene (Marenne *et al.*, 2003); pYES2-GFP (Rodríguez-Escudero *et al.*, 2005) and pKS84 (De Felipe *et al.*, 2008), used to generate yeast expression plasmids encoding fusions to the C- or N-terminus of GFP, respectively. Furthermore, pBOMB4-Tet-mcherry (Bauler and Hackstadt, 2014) and Lyn11-FRB-mcherry (Hammond *et al.*, 2012) were used to amplify the tetracycline promoter (P_{tet}) and the nucleotide sequence encoding the Lyn11 peptide, respectively. The accuracy of the nucleotide sequence of all the inserts in the constructed plasmids was confirmed by DNA sequencing.

2.2 CELL LINES AND TRANSIENT TRANSFECTION

HeLa 229 and Vero cells (from the European Collection of Authenticated Cell Culture; ECACC) were maintained in high-glucose Dulbecco's modified Eagle Medium (DMEM; Thermo Fisher Scientific) supplemented with heat-inactivated 10% (v/v) foetal bovine serum (FBS; Thermo Fisher Scientific) at 37°C in a humidified atmosphere of 5% (v/v) CO_2. Cells were checked for *Mycoplasma* by conventional PCR either using the Venor® GeM Advance kit (Minerva Biolabs) or as described (Uphoff and Drexler, 2011).

HeLa 229 cells were transfected by using the jetPEI reagent (Polyplus-transfection) accordingly to the instructions of the manufacture. Briefly, to HeLa 229 cells previously seeded in 24-well plates, 250 ng of plasmid DNA and 1.5 µl of JetPei reagent were added per well. This was scaled-up when necessary. The plate was centrifuged at 180 x *g* for 5 min at room temperature and subsequently incubated for 24 h at 37°C in a 5% (v/v) CO_2 atmosphere. The transfected cells were then collected for

immunoblotting or fixed for immunolabeling. In experiments involving simultaneous infection by *C. trachomatis* and transfection, transfection was performed at time zero of infection (see section 2.4.1).

2.3 *E. COLI* AND *Y. ENTEROCOLITICA* GROWTH CONDITIONS

Escherichia coli TOP10 (Thermo Fisher Scientific) or NEB® 10β (New England Biolabs) were used for construction and purification of plasmids, and *E. coli* ER2925 (New England Biolabs) was used to amplify and purify plasmids for transformation of *C. trachomatis*.

Yersinia enterocolitica ΔHOPEMT (MRS40 pIML421 [$yopH_{\Delta 1\text{-}352}$, $yopO_{\Delta 65\text{-}558}$, $yopP_{23}$, $yopE_{21}$, $yopM_{23}$, $yopT_{135}$]), deficient for the *Yersinia* T3S effectors YopH, O, P, E, M, and T, but T3S-proficient (Iriarte and Cornelis, 1998) and T3S-deficient *Y. enterocolitica* ΔHOPEMT ΔYscU (MRS40 pFA1001 [$yopH_{\Delta 1\text{-}352}$, $yopO_{\Delta 65\text{-}558}$, $yopP_{23}$, $yopE_{21}$, $yopM_{23}$, $yopT_{135}$, $yscU_{\Delta 1\text{-}354}$) (Almeida *et al.*, 2012) were used for T3S assays. The *yscU* gene encodes an essential component of the *Y. enterocolitica* T3S system, and the $yscU_{\Delta 1\text{-}354}$ mutation is non-polar (Sorg *et al.*, 2007).

E. coli or *Y. enterocolitica* were routinely grown in liquid or solid Luria-Bertani (LB) medium (NZYtech) with the appropriate antibiotics and supplements at 37°C and 30°C, respectively. Plasmids were introduced into *E. coli* or *Y. enterocolitica* by electroporation.

2.4 MAINTENANCE AND MANIPULATION OF *C. TRACHOMATIS* STRAINS

C. trachomatis prototype strains B/Har36, C/TW3, E/Bour, L2/434, and L3/404 (from the American Type Culture Collection; ATCC) and clinical strains F/CS465-95 and L2b/CS19-08 (from the collection of the Portuguese National Institute of Health) were propagated in HeLa 229 cells using standard techniques [see section 2.4.1; (Scidmore, 2005);]. Throughout this work, the gene nomenclature of the annotated *C. trachomatis* D/UW3 strain was used (Stephens, 1998).

2.4.1 Infection of HeLa 229 cells with *C. trachomatis*

For immunofluorescence analysis, 5 x 10^4 HeLa 229 cells were seeded in 24-well plates, previously filled with 13 mm glass coverslips (VWR). For immunoblotting, 1 x 10^5 HeLa 229 cells were seeded in 24-well plates (2 cm^2/well). Scaling-up was done accordingly [6-well plate (10 cm^2/well), or tissue culture flasks with a surface area of 25 cm^2 (T25) or 75 cm^2 (T75)]. The next day, cells were incubated with Hank's balanced salt solution (HBSS) for 15 min at 37ºC in a humidified atmosphere of 5% (v/v) CO_2, while the *C. trachomatis* inocula (previously titrated infectious particles, as described in (Scidmore, 2005)) were prepared in sucrose-phosphate-glutamate buffer (SPG; 0.2 mM sucrose, 17 mM Na_2HPO_4, 3mM NaH_2PO_4, 5 mM L-glutamic acid) in the appropriate volume: 0.2 ml for 24-well plates, 0.5 ml for 6-well plates, 1 ml for T25 or 3 ml for T75. HBSS was then removed and the *C. trachomatis* inocula were added and incubated for 30 min at 37ºC in a humidified atmosphere of 5% (v/v) CO_2 (for 24- and 6-well plates) or 1 h at room temperature with gentle rocking (for T25 and T75 flasks). At this point, the inocula

were removed and DMEM supplemented with 10% (w/v) FBS and 10 µg/ml of gentamicin was added. This step was considered time zero of the infection. In experiments where HeLa 229 cells were infected with *C. trachomatis* L2/434 harboring a plasmid encoding CT105-2HA under the control of a tetracycline promoter (pSVP302/pTet-CT105-2HA; Annexes Table A1), anhydrotetracycline was added to 20 ng/ml at time zero of infection. Infected cells were harvested at the indicated times post-infection (p.i.) and analyzed by immunoblotting or immunofluorescence microscopy.

2.4.2 Transformation of *C. trachomatis*

Transformation of *C. trachomatis*, first reported by the laboratory of Ian N. Clarke (Wang *et al.*, 2011), was done essentially as described by Agaisse and Derré (Agaisse and Derré, 2013). Approximately, 20 µl of a cellular extract containing *C. trachomatis* EBs stored in SPG were added to 6 µg of plasmid DNA diluted in 200 µl of $CaCl_2$ buffer (10 mM Tris pH 7.4, 50 mM $CaCl_2$). The mixture was then homogenized and incubated for 30 min at room temperature. Meanwhile, 4 x 10^6 HeLa 229 cells were trypsinized [using TrypLE™ Express (Thermo Fisher Scientific)] and centrifuged for 5 min at 237 x *g* and at room temperature. Cells were washed with phosphate-buffered saline (PBS) and resuspended in 200 µl of $CaCl_2$ buffer. The cells were added to the mixture and incubated 20 min at room temperature. The whole mixture (cells, plasmid DNA, and *Chlamydia*) was split in two wells from a 6-well plate (each containing 3 ml of pre-warmed DMEM supplemented with 10% (v/v) FBS) and incubated for 44 h at 37ºC in a 5% (v/v) CO_2 atmosphere. At 16 h after transformation, the medium was replaced with DMEM supplemented with 10% (v/v) FBS, 0.3 U/ml penicillin G or 250 µg/ml of spectinomycin. At 44 h after transformation, the medium was removed, and the cells were osmotically lysed with 1 ml of sterile H_2O (MilliQ®) per well. The lysates were pooled together and centrifuged for 5 min at 237 x *g* at room temperature, after which 2 ml of the supernatant were added to 2 ml of 2xSPG (0.4 mM sucrose, 34 mM Na_2HPO_4, 6 mM NaH_2PO_4, 10 mM L-glutamic acid). This was then used as inoculum to add to newly seeded HeLa 229 cells (1.3 x 10^6 cells in a 25 cm^2 surface area flask), previously equilibrated in HBSS. After an incubation of 1 h at room temperature with gentle rocking, the inoculum was removed, and DMEM supplemented with 10% (v/v) FBS, 0.3 U/ml penicillin G or 250 µg/ml of spectinomycin, and 1 µg/ml cycloheximide was added. The cells were then incubated for 44 h at 37ºC in a 5% (v/v) CO_2 atmosphere. Then, the infected cells were osmotically lysed with 1 ml of sterile H2O (MilliQ®) and lysate was centrifuged for 5 min at 237 x *g* and at room temperature. After, the 1 ml of the supernatant was added to 1 ml of 2xSPG and used to re-infect newly seeded HeLa 229 cells (1.3 x 10^6 cells in 25 cm^2 surface area flasks), previously equilibrated in HBSS. After an incubation of 1 h at room temperature and gentle rocking, the inoculum was removed, and DMEM supplemented with 10% (v/v) FBS, 1 U/ml penicillin G or 250 µg/ml of spectinomycin, and 1 µg/ml cycloheximide was added. The cells were then incubated for 3 days at 37ºC in a 5% (v/v) CO_2 atmosphere. At this point, the presence of wild type inclusions, as detected by phase-contrast microscopy, indicated a successful transformation. The infected cells containing transformed *C. trachomatis* were collected, lysed and used to re-infect newly seeded HeLa 229 cells (1.3 x 10^6 cells in a 25 cm^2 surface area flask), as previously described, except the medium added was DMEM supplemented with 10% (v/v) FBS, 10 U/mL penicillin G or 500 µg/ml of

spectinomycin, and 1 µg/mL cycloheximide. The cells were incubated 44 h at 37ºC in a 5% (v/v) CO_2 atmosphere. The transformed *C. trachomatis* was continually passaged for approximately 5 rounds of re-infection, then stored at -80ºC.

2.4.3 Clonal isolation of *C. trachomatis* by plaque assay purification

Further, the constructed strains were plaque purified similarly as previously described (Nguyen and Valdivia, 2013). First, 4 x 10^5 Vero cells were seeded per well in a 6-well plate. Cells were incubated at 37ºC in the presence of 5% (v/v) CO_2 for about 24 h and allowed to form a confluent and homogeneous monolayer. Aliquots of infectious particles of the transformed *C. trachomatis* strains were thawed on ice and six 10-fold serial dilutions in a volume of 1 ml were performed. Prior to infection, Vero cells were washed once with HBSS. Each well was infected with 500 µl of the respective dilution, swirled to ensure an even mixture and incubated for 30 min at 37ºC in a humidified atmosphere of 5% (v/v) CO_2. The inocula was removed and DMEM supplemented with 10% (v/v) FBS, 1 U/ml of penicillin G and 1 µg/ml of cycloheximide was added. The cells were incubated at 37ºC in the presence of 5% (v/v) CO_2 for 24 h. An overlay solution of 0.54 % (w/v) Seakam® agarose (Lonza) in DMEM (without phenol red) containing 10% (v/v) FBS, 1 U/ml of penicillin G and 1 µg/ml of cycloheximide was prepared and kept in a warm water bath at 55ºC before adding to the infected cells. The media was carefully aspirated from each well of the 6-well plates with the infected Vero cells and 2 ml of the overlay solution was quickly added to each well. Agarose was allowed to completely solidify at room temperature for 15 min. Additionally, after the overlay solution had solidified, 2 ml of complete DMEM (without phenol red) were added on top. Cells were then incubated at 37ºC in the presence of 5% (v/v) CO_2 for approximately 6 days. At this point, plaques were usually visible with naked eye. Isolated plaques were picked using a 200 µl sterile barrier pipette tip. Tips were then placed in a 1.5 ml tube previously loaded with 100 µl of DMEM containing 10% (v/v) FBS, 1 U/ml of penicillin G and 1 µg/ml of cycloheximide. Media was carefully removed from a 96-well plate, seeded the day before with 1 x 10^4 Vero cells per well, and the 100 µl of DMEM containing each plaque were added. After inoculating the wells, the 96-well plate was centrifuged at 2,200 x *g* for 30 min at 15ºC. Cells were incubated at 37ºC in the presence of 5% (v/v) CO_2 for 2 days. Each well of the 96-well plate containing Vero cells infected with plaque purified *C. trachomatis* were lysed by osmotic shock through incubation in 100 µl of H_2O for 10 min. After this, 100 µl of 2xSPG were added to each well. This 200 µl solution containing the infectious particles was then added to each well of a 24-well plate seeded in the previous day with 2 x 10^5 HeLa 229 cells per well. Infection proceeded as described above. This way each plaque-purified clone was propagated into HeLa 229 cells providing a higher number of viable bacteria to be stored. Stock aliquots were stored at - 80ºC and after titrated for further experiments.

2.4.4 Construction of a *C. trachomatis ct105::aadA* mutant strain

A *C. trachomatis ct105::aadA* mutant was generated in collaboration with us by the group of Derek J. Fisher (Southern Illinois University, USA) using group II intron-based insertional mutagenesis, as

previously described (Johnson and Fisher, 2013; Key and Fisher, 2017). Briefly, intron-insertion sites in the *C. trachomatis* L2/434 *ctl0360* gene (orthologue of *ct105* in *C. trachomatis* strain D/UW3) were identified using the TargeTron® algorithm (Sigma). Then, the intron in pDFTT3*aadA* (Annexes Table A1) (Key and Fisher, 2017) was retargeted for *ctl0360* using standard molecular biology procedures and the DNA primers listed in Annexes Table A2. The *ctl0360* mutator plasmid [pDFTT296; (Annexes Table A1)] was then used to transform *C. trachomatis* L2/434.

2.4.5 Quantification of infectious progeny

HeLa 229 cells infected by *C. trachomatis* strains for different times were lysed by osmotic shock (10 min incubation in sterile H_2O). Dilutions of these lysates in SPG were used to infect freshly seeded HeLa 229 cells. The newly infected cells were fixed after 24 h post-infection, *C. trachomatis* were immunolabeled using anti *C. trachomatis* major outer membrane protein (MOMP) antibodies (see section 2.7), and the number of inclusion forming units (IFUs/ml) was calculated after determination of the number of infected cells/field of view by immunofluorescence microscopy (Scidmore, 2005) (see section 2.10).

2.5 *Y. ENTEROCOLITICA* T3S ASSAYS

T3S assays were done as previously described (Sorg *et al.*, 2007). Briefly, *Y. enterocolitica* strains harboring the plasmids encoding the hybrid proteins were diluted from overnight cultures to an optical density at 600 nm (OD_{600}) of 0.1 in brain heart infusion (BHI) medium supplemented with 20 mM sodium oxalate, 20 mM $MgCl_2$ and 0.4% (w/v) glucose and grown for 2 h at 28ºC with 150 rpm shaking. The bacterial cultures were then quickly shifted to 37ºC and incubated for an additional 4 h with 150 rpm shaking. After incubation, OD_{600} of the cultures was measured and culture supernatants and bacterial pellets were separated by a centrifugation of 1 min, at room temperature (RT) and 17,000 x *g*. Proteins in the supernatant were precipitated with 10% (w/v) trichloroacetic acid (TCA). The TCA protein precipitate corresponding to 1 ml of the culture was resuspended in OD_{600} x 10 µl of SDS-polyacrylamide gel electrophoresis (SDS-PAGE) loading buffer [50 mM Tris-HCl, pH 6.8, 2.0% (w/v) SDS, 10% (v/v) glycerol, 0.1 M β-mercaptoethanol, 0.1% (w/v) bromophenol blue], while the bacterial pellet, corresponding to 1.5 ml of the culture, was resuspended in OD_{600} x 100 µl of SDS-PAGE loading buffer. Both fractions were denatured at 100ºC for 10 min.

In these experiments, we used *Y. enterocolitica* ΔHOPEMT or ΔHOPEMT ΔYscU strains carrying the plasmids described in Annexes Table A1. The proteins in bacterial pellets (non-secreted) and culture supernatants (secreted) were analyzed by immunoblotting.

2.6 YEAST STRAINS, INVERTASE ASSAYS AND TOXICITY ANALYSIS

Saccharomyces cerevisiae strains used in this work (listed in Annexes Table A3) were grown in plates with yeast nitrogen base uracil dropout (YNB-Ura) supplemented with 2% (w/v) fructose (non-inducing media) or 2% (w/v) galactose (inducing media) for 3 days, at 25°C.

For the qualitative invertase (Inv) assays, *S. cerevisiae* NSY01-derived strains harboring GFP fusion proteins previously grown for 3 days in plates containing inducing and non-inducing media were overlaid with agar containing glucostat reagent [125 mM sucrose, 100 mM sodium acetate, pH 5.5, 0.5 mM *N*-ethylmaleimide (NEM), 10 µg/ml horseradish peroxidase, 8 U/ml glucose oxidase, and 2 mM *O*-dianisidine]. Defects on trafficking were assessed by the intensity of the brow precipitate formed, where brown colonies indicate a defect in trafficking in contrast with white colonies (normal trafficking) (Shohdy *et al.*, 2005; Franco *et al.*, 2012).

For the quantitative Inv assays, *S. cerevisiae* NSY01-derived strains harboring GFP fusion proteins were grown for 3 days in plates containing inducing media. Briefly, yeasts scraped from the plates were resuspended in 0.1M of sodium acetate buffer, pH 4.9. Then, for total Inv activity, yeasts were lysed by addition of Triton-X and four freeze/thaw cycles. For secreted Inv activity yeasts were not lysed. Further, the samples were then tested for Inv activity by the addition of glucostat reagent. Reactions were stopped by using 6 M HCl, and the absorbance at 540 nm was measured. One unit of Inv activity is defined as the amount of enzyme that hydrolyzes sucrose to produce 1 µmol of glucose per minute at 30°C. Values for secreted and total Inv activity were obtained and used to calculate the percent secreted. Relative secreted Inv was normalized by setting GFP as the minimum value and Vps4^{E233Q} as the maximum value (Darsow *et al.*, 2000; Shohdy *et al.*, 2005).

For the phenotypic characterization of yeast growth defects of *S. cerevisiae* expressing GFP fusion proteins were grown to late-log phase and 10-fold serial dilutions (cells corresponding to an OD_{600} of 1 correspond to the first dilution) were spotted on yeast nitrogen base uracil dropout (YNB-Ura) supplemented with 2% (w/v) fructose (non-inducing media) or 2% (w/v) galactose (inducing media) agar plates and grown 3 days at 30°C.

2.7 ANTIBODIES AND FLUORESCENT DYES

For immunoblotting the following primary antibodies were used: mouse monoclonal anti-chlamydial Hsp60 (A57-B9; Thermo Fisher Scientific; 1:1,000); goat polyclonal anti-MOMP of *C. trachomatis* (Abcam; 1:1,000); rat monoclonal anti-HA (3F10; Roche; 1:1,000); mouse monoclonal anti-α-tubulin (clone B-5-1-2; Sigma Aldrich; 1:1,000); mouse monoclonal anti-TEM-1 (QED Bioscience; 1:500); rabbit polyclonal anti-SycO (1:1,000) (Letzelter *et al.*, 2006); goat polyclonal anti-GFP (Sicgen; 1:1,000); mouse anti-phosphoglycerate kinase 1(PGK1) (Life Technologies; 1:1,000).

For immunofluorescence the following primary antibodies were used: goat anti-*C. trachomatis* fluorescein isothiocyanate (FITC)-conjugated polyclonal antibody (Millipore; 1:100); goat polyclonal anti-MOMP of *C. trachomatis* (Abcam; 1:500), rat monoclonal anti-HA (3F10; Roche; 1:200); mouse anti-CT442 (a gift from Guangming Zhong; (Zhongyu Li *et al.*, 2008); 1:200); rabbit polyclonal anti-Cap1 (a

gift from Agathe Subtil; (Gehre *et al.*, 2016); 1:2,000; rabbit polyclonal anti-GM130 (Sigma Aldrich; 1:200); mouse monoclonal anti-TGN46 (clone TGN46-8; Sigma Aldrich; 1:200), mouse monoclonal anti-α-tubulin (clone B-5-1-2; Sigma Aldrich; 1:200); mouse monoclonal anti-vimentin (Sigma Aldrich; 1:200).

For immunoblotting, the secondary antibodies were all horseradish peroxidase (HRP)-conjugated (GE Healthcare and Jackson ImmunoResearch; 1:10,000). For immunofluorescence, the secondary antibodies were all from Jackson ImmunoResearch and used at 1:200: Rhodamine Red-X-conjugated anti-rat; DyLight 488-conjugated anti-goat; AF488-conjugated anti-mouse; DyLight 405-conjugated anti-goat; AF488-conjugated anti-rabbit; Cy5-conjugated anti-mouse. Acti-stain™ 670 phalloidin (Cytoskeleton), and DAPI (Thermo Fisher Scientific) were used to stain filamentous actin and DNA, respectively.

2.8 DRUG TREATMENTS

To induce Golgi fragmentation, HeLa 229 cells were incubated with 1 µg/ml of brefeldin A (BFA) [Sigma; stock solution at 5 mg/ml in dimethyl sulfoxide (DMSO)] for 1 h and then either fixed immediately or washed with medium without BFA and incubated for 1 h before fixation. To disrupt microtubules, HeLa 229 cells were incubated in the presence of 1 µg/ml nocodazole (stock solution at 5 mg/ml in DMSO; Sigma). To disrupt the actin cytoskeleton, *C. trachomatis*-infected cells were incubated in the presence of 2 µM cytochalasin D (stock solution at 5 mg/ml in DMSO; Sigma) or 500 nM latrunculin B (stock solution at 1 mg/ml in DMSO; Sigma) in serum-free DMEM.

2.9 IMMUNOBLOTTING

To harvest infected or transfected HeLa 229 cells, they were washed once with PBS and then trypsinized using TrypLE™ Express (Thermo Fisher Scientific) by incubation during 5 min at 37°C in a 5% (v/v) CO_2 atmosphere. The cells were then collected, pelleted by a brief centrifugation, washed 2 times with ice-cold PBS, and stored as a pellet at -20°C until use. Prior to SDS-PAGE, the cells were thawed, resuspended in an appropriate volume of SDS-PAGE loading buffer. The proteins were further denatured by an incubation of 5 min at 100°C, followed by addition of benzonase (Novagen) to destroy DNA and reduce the viscosity of the samples.

To prepare *Chlamydia*-enriched extracts, the infected HeLa 229 cells were lysed by osmotic shock (15 min in sterile H_2O). Lysates were centrifuged at 170 x *g* for 10 min at 4°C. The supernatants were then centrifuged at 24,000 x *g* for 10 min at 4°C and resulting pellets washed 2 times with ice-cold PBS. The bacteria-enriched pellets were resuspended in an appropriate volume of SDS-PAGE loading buffer and the proteins were further denatured by an incubation of 5 min at 100°C.

To prepare yeast extracts, cells were grown for 3 days at 30ºC in YNB-Ura plates supplemented with 2% (w/v) fructose and then streaked into YNB-Ura supplemented with 2% (w/v) galactose. Cells corresponding to an OD_{600} of 2.5 were used for immunoblotting.

Samples were separated by 12% (v/v) SDS-PAGE and transferred onto 0.2 µm nitrocellulose membranes (Bio-Rad) using Trans-Blot Turbo Transfer System (BioRad). Immunoblot detection was

done with SuperSignal® West Pico Chemiluminescent Substrate (Thermo Fisher Scientific) or SuperSignal® West Femto Maximum Sensitivity Substrate (Thermo Fisher Scientific) (as indicated in figure legends) and exposure to Amersham Hyperfilm ECL (GE Healthcare).

2.10 FLUORESCENCE MICROSCOPY

Infected and uninfected HeLa 229 cells were fixed either in PBS containing 4% (w/v) paraformaldehyde (PFA) for 10 min at room temperature or in methanol (-20°C) for 10 min, as indicated in figure legends. For immunostaining, the antibodies were diluted in PBS containing 10% (v/v) horse serum (when fixation was done with PFA, 0.1% (v/v) Triton X-100 was added to allow permeabilization of cells). After immunolabeling, the cells were consecutively washed with PBS and H_2O. The coverslips were assembled using Aqua-poly/Mount (Polysciences) on microscopy glass slides, and the cells were examined by conventional fluorescence microscopy or by confocal microscopy.

S. cerevisiae expressing GFP fusion proteins were grown in YNB-Ura supplemented with 2% (w/v) galactose (inducing media) agar plates and grown 3 days at 30°C. Live cells were scrapped from the plates, resuspended in water and imaged live using brightfield and conventional fluorescence microscopy. Images were processed and assembled using Fiji software (Schindelin *et al.*, 2012).

2.11 REAL-TIME QUANTITATIVE PCR (RT-qPCR)

To quantify the mRNA levels of *ct105* during the developmental cycle of *C. trachomatis* strains B/Har36, C/TW3, E/Bour, F/CS465-95, L2/434, L2b/CS19-08 and L3/404, RT-qPCR measurements were performed in collaboration with us by the group of João Paulo Gomes (Instituto Nacional de Saúde Dr. Ricardo Jorge, Portugal) as previously described (Almeida *et al.*, 2012), using primers listed in Annexes Table A2. To compare by RT-qPCR the mRNA levels of *ct105* during the developmental cycle of *C. trachomatis* strains L2/434 or L2/434 harboring pCT105-2HA (pSVP264/pCT105-2HA; Annexes Table A1), a 6-well plate seeded with HeLa 229 cells was inoculated by each strain at a multiplicity of infection of 50 and cells were harvested at the indicated times post-infection by trypsinization. Total RNA was isolated using NZY Total RNA Isolation Kit (NZYtech). For each RNA sample, cDNA was generated using iScript cDNA Synthesis Kit (Bio-Rad) accordingly with the manufacturer's instructions. RT-qPCR was performed using *ct105* and *16S* primers (Annexes Table A2) and SsoFast EvaGreen Supermix (Bio-Rad). For each time point, quantitative PCR was performed on each cDNA sample (including an RT-negative sample) using Rotor Gene 6000 (Corbett Life Science). For normalization, ratios to the *16s* rRNA transcript were obtained. Data analysis was carried out with Rotor-Gene 6000 software. Unless otherwise indicated, RT-qPCR results were based in three independent experiments.

3 RESULTS

3.1 IDENTIFICATION OF CANDIDATE TYPE III SECRETION EFFECTORS OF *CHLAMYDIA TRACHOMATIS*

In previous studies, the *Chlamydia trachomatis* proteins CT053, CT082, CT105, CT429, CT696 and CT849 were identified as candidate type III secretion (T3S) substrates, using *Yersinia enterocolitica* as a heterologous host (Pais *et al.*, 2013; da Cunha *et al.*, 2014). Here, we analyzed whether these previously identified proteins localized at specific sites within mammalian cells or if they were delivered by *C. trachomatis* into host cells, which could indicate a potential function in the host cytoplasm during chlamydial infection.

3.1.1 Ectopic expression of candidate T3S effectors of *C. trachomatis* in mammalian cells

To investigate the localization of the candidate T3S effectors of *C. trachomatis* when ectopically expressed in mammalian cells, we constructed transfection plasmids encoding enhanced green fluorescent protein (EGFP, 27 kDa) and *C. trachomatis* candidate T3S effectors fused to the C-terminus of EGFP (EGFP-CT053, 44 kDa; EGFP-CT082, 86 kDa; EGFP-CT105, 95 kDa; EGFP-CT429, 66 kDa; EGFP-CT696, 72 kDa; EGFP-CT849, 44 kDa). HeLa cells were transfected for 24 h with the constructed plasmids and subsequent immunoblotting of whole cell extracts confirmed the expression of EGFP-CT429, EGFP-CT696 and EGFP-CT849 proteins of the predicted molecular mass (Figure 3.1A). EGFP-CT053, EGFP-CT082 and EGFP-CT105 migrated on SDS-PAGE at higher molecular mass than predicted. However, the differences between the predicted and observed molecular mass were similar to when 2HA-tagged versions of the proteins were expressed in *Y. enterocolitica* (Pais et al., 2013, da Cunha et al., 2014).

Next, to determine the localization in HeLa cells of the ectopically expressed proteins, the transfected cells were fixed 24 h after transfection, stained with 4',6-diamidino-2-phenylindole (DAPI) and analyzed by fluorescence microscopy (Figure 3.1B). EGFP-CT053 and EGFP-CT429 showed a cytosolic localization similarly to EGFP alone (Figure 3.1B). For EGFP-CT082 and EGFP-CT849 the proteins were mostly cytosolic (Figure 3.1B), but not comparable to EGFP alone, and in some transfected cells they appeared to localize at the cell periphery (Figure 3.1B; indicated with arrows). EGFP-CT105 accumulated at the cell periphery (Figure 3.1B) but filamentous structures and aggregates could also be observed, as will be described in further detail (Figure 3.26). As for EGFP-CT696, the protein aggregated in rod-like structures spread in the cell (Figure 3.1B). Overall, among the proteins studied, this indicated CT105 and CT696 as the stronger candidates to be chlamydial T3S effectors.

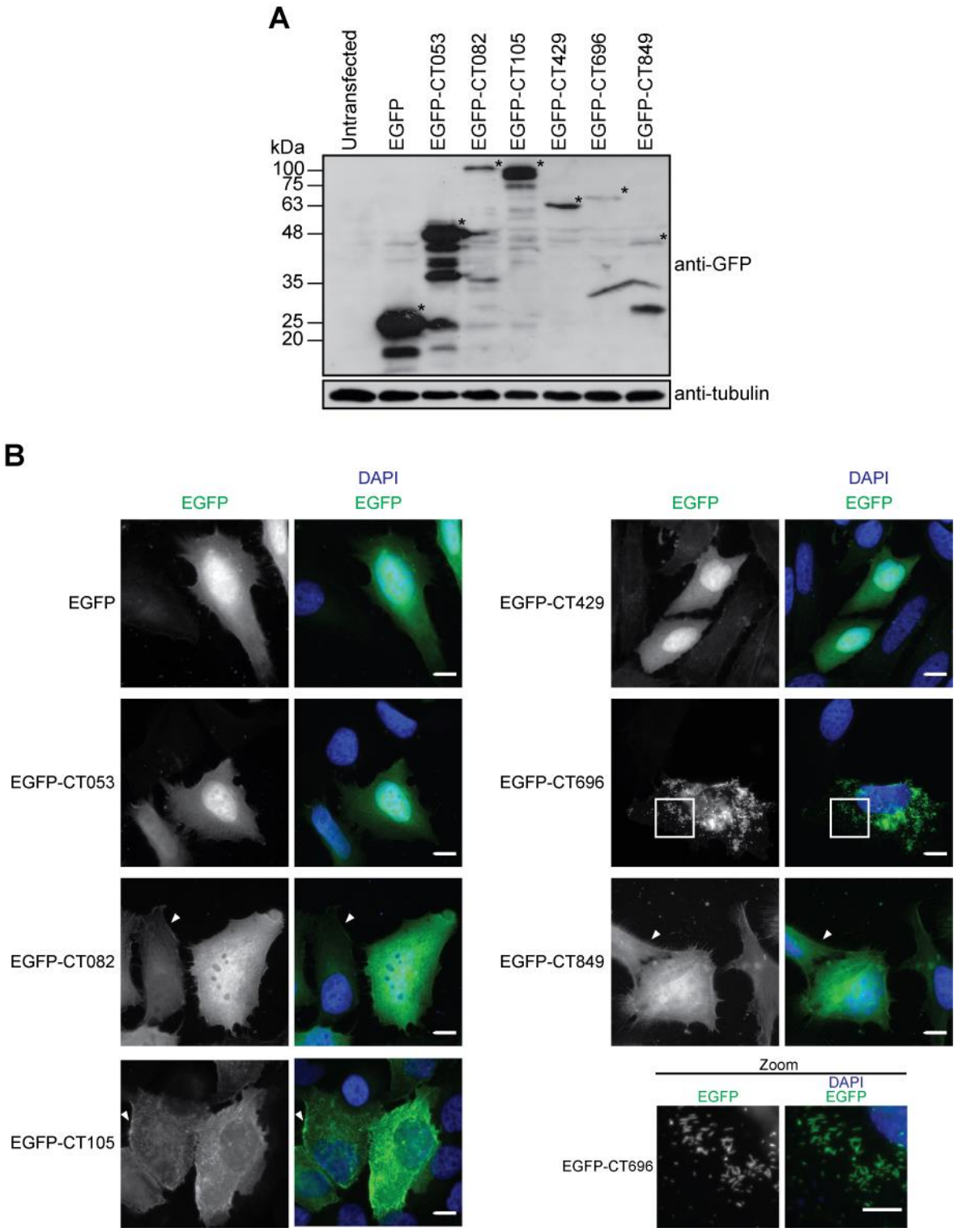

Figure 3.1 Localization of candidate T3S effectors of *C. trachomatis* when ectopically expressed in mammalian cells. HeLa 229 cells were transfected for 24 h with plasmids encoding EGFP or candidate T3S effector fused to the C-terminus of EGFP. **(A)** Whole cell extracts of transfected cells were analyzed by immunoblotting using antibodies against GFP and α-tubulin (HeLa loading control) using SuperSignal® West Pico detection kit (Thermo Fisher Scientific). **(B)** Transfected cells were fixed with 4% (w/v) PFA, stained with DAPI, and imaged by fluorescence microscopy. Arrows indicate accumulation of the proteins at the periphery of the cell. Scale bars, 10 µm. A region of EGFP-CT696 (delimitated by the white square) was zoomed to show the rod-like structures (right lower panel). Scale bar, 5 µm.

3.1.2 Expression of epitope-tagged candidate chlamydial T3S effectors in *C. trachomatis*

The description of a methodology allowing the transformation of *C. trachomatis* was a breakthrough in the *Chlamydia* field (Wang *et al.*, 2011). Since then, several improvements have been made to the protocol, including the development of second generation plasmid vectors with different selection markers, promoters and epitope tags (Agaisse and Derré, 2013; Wickstrum *et al.*, 2013; Campbell *et al.*, 2014; Bauler and Hackstadt, 2014; Mueller and Fields, 2015; Wang *et al.*, 2018). To directly analyze the delivery of the chlamydial candidate T3S effectors into the host cell cytoplasm during infection, we took advantage of the methods for transformation of *C. trachomatis*. We constructed suitable *Chlamydia* expression plasmids and, subsequently, *C. trachomatis* strains individually expressing from a plasmid tagged candidate T3S effectors.

3.1.2.1 Construction of *C. trachomatis* transformation vectors

We started by constructing vectors that would allow expression of candidate T3S effector proteins in *C. trachomatis* using as backbone the vector p2TK2-SW2 (Agaisse and Derré, 2013). All the constructed transformation vectors were derivatives of the native virulence plasmid of *C. trachomatis* (pSW2) and therefore contained all elements necessary for the replication and maintenance of the plasmid in *C. trachomatis*. Also, they comprised an *E. coli* origin of replication to allow the shuttle between the two bacteria, therefore facilitating molecular cloning. In addition, all these vectors encoded for β-lactamase, enabling selection during transformation of *C. trachomatis*, and contained the terminator of the *incDEFG* operon (*incD* terminator) to halt transcription (Figure 3.2). Three different vectors were constructed to express proteins fused either to a double hemagglutinin (2HA) peptide (pSVP247; Figure 3.2A), glycogen synthase kinase (GSK) peptide (pSVP277; Figure 3.2B), or calmodulin-dependent adenylate cyclase (CyaA) from *Bordetella pertussis* (pSVP268; Figure 3.2C). The pSVP247 vector was designed to allow the visualization of the protein by immunofluorescence microscopy using the 2HA epitope-tag and its localization upon delivery. In the case of pSVP277, if the fusion proteins were delivered into the host, the GSK tag would be phosphorylated by host cell kinases and this could be detected by immunoblotting using an antibody against phosphorylated GSK (Bartra and Plano, 2017). As for pSVP268, upon delivery, the calmodulin-dependent CyaA would lead to an increase of the production of cyclic adenosine monophosphate (cAMP) in the host cell that could be detected using a specific enzymatic assay (Sory and Cornelis, 1994).

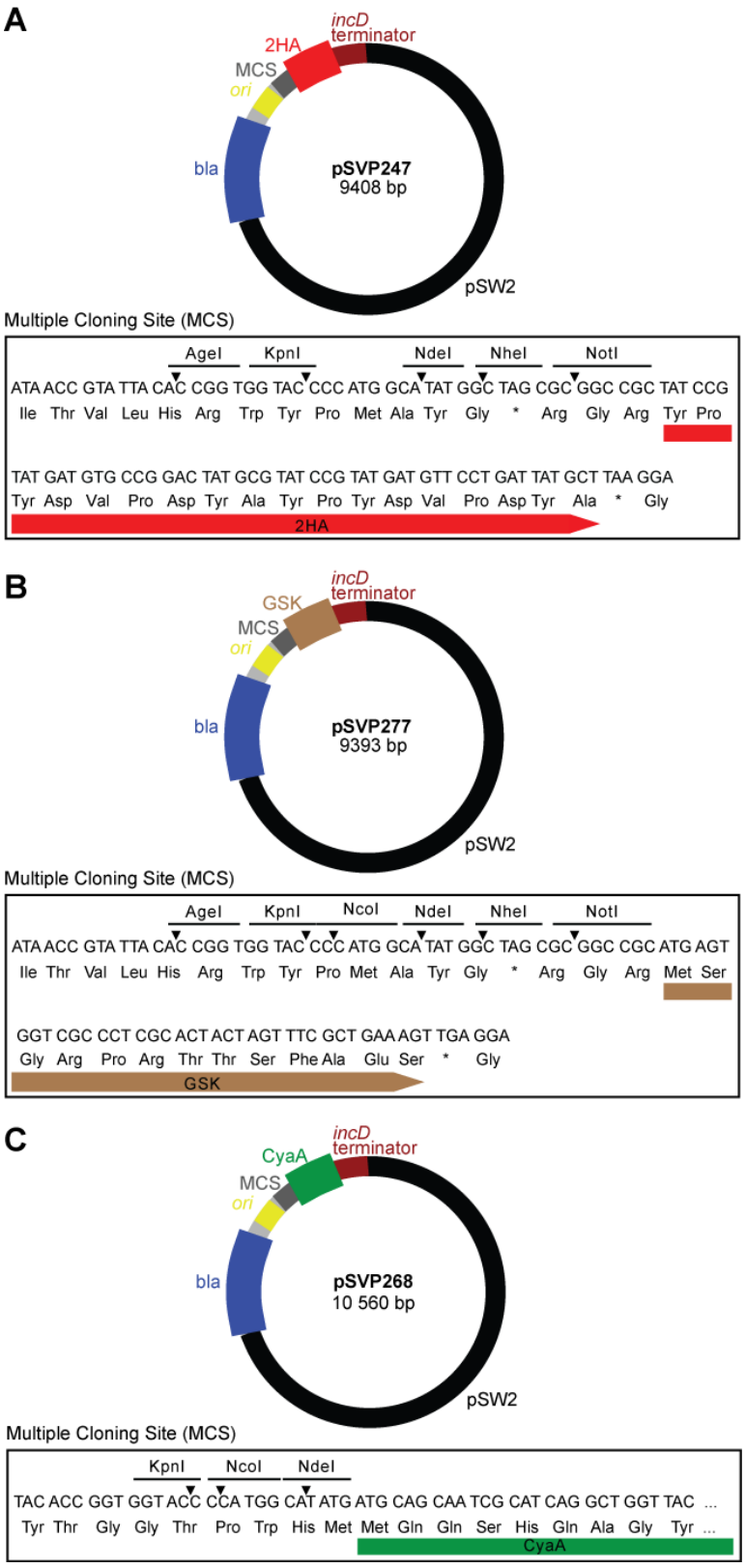

Figure 3.2 *C. trachomatis* transformation vectors. Different vectors were constructed to allow fusion of selected proteins **(A)** to a double hemagglutinin (2HA) or **(B)** GSK (brown) epitope tags or **(C)** to calmodulin-dependent CyaA (green). The pSW2 plasmid backbone (Wang *et al.*, 2011) is shown in black, the *Escherichia coli* origin of replication (*ori*) in yellow, the ampicillin resistance gene (*bla*) in blue, the multiple cloning site (MCS) in grey and *incD* terminator in dark red. The DNA sequence of the MCS with unique restriction sites are depicted in the box below the plasmid map (Details of plasmid construction are in Annexes Table A1)

Table 3.1 Predicted promoter regions of candidate T3S effectors of *C. trachomatis*.

***C. trachomatis* strain D (NC_000117.1)**	***C. trachomatis* strain L2b/UCH-1/proctitis (NC_010280.2)**	***C. trachomatis* strain L2/434/Bu (NC_010287.1)**	**Gene position**	**Transcription start site (TSS) position** (Albrecht *et al.*, 2009)	**Sequences of the predicted promoter region**
CT053	CTLon0304	CTL0309	382456..382902, complement	383902	…AATACT**TTGGAA**TGAGTATTTTACTAGCCAAAATCTCTCCTGATCTATTTGTT**TATGCC**TGCTCAC **-35** **-10** TTGCTCTATCTG**A**GCAAAAGATGCAGTTACCCTTGGTAGGAAGCAAGTAAATTGGCTCTCAGG **+1** GGGTTTCCGGTTTCAATCATAGAACAGGACTATTTACGA**ATG**… **Start**
CT082	CTLon0333	CTL0338	416611..418293	416578	…TCATAA**TTCACT**GTTTCAGTTTAAAAT**TATTAT**TACCC**A**TTCATTGGTTTTTTGTTTTTTAGGAAAA **-35** **-10** **+1** AATC**ATG** **Start**
CT105	CTLon0356	CTL0360	442875..444845	442794	…AATAAT**TTGTTT**TAACAACTGTTTAATAGT**TTTAAT**TTTTAAA**G**TGTGAAAAACAGGTTTTATATGT **-35** **-10** **+1** AGAATTTCCTGTTAAAAATAAAAAATCCTTACAAGAATCCGGGAGTTAAAGGT**ATG**… **Start**
CT429	CTLon0684	CTL0688	817103..818092, complement	818099	…ATAAAA**TTGAGG**ATAACACAAGAGAGAGTTGCTATC**TAACAG**AGCATCCCCTATACT**G**GAGCCT **-35** **-10** **+1** **ATG**… **Start**
CT696	CTLon0065	CTL0065	78483..79661	78440	…GGAAT**ATCTAA**GAACATTTTCTAATAGGGAAGAGGA**TAAATA**GCGTGAAATAA**T**ACTGATTATGT **-35** **-10** **+1** GAAGAATAGGCAAAAAGACCTAAATCCTTAT**ATG**… **Start**
CT849	CTLon0221	CTL0221	277967..278446, complement	278480	…CTTATT**TTTAAA**ACAAATTATTATTTTTAT**TAAAGA**GAGAAATTGCTGGTAAA**A**TAAAAAATAAAAA **-35** **-10** **+1** CCAAAAAAATTTTTTAGAAT**ATG**… **Start**

Our strategy consisted in first constructing pSVP247 derived plasmids encoding 2HA epitope-tagged proteins because they would allow a more direct assessment of the delivery of the proteins and could provide additional information on protein subcellular localization. Moreover, the candidate T3S effectors were expressed under the control of their predicted promoters, based on previously identified transcription start sites (TSS) (Albrecht *et al.*, 2009) from where the σ^{66}-like promoter regions -10 and -35 were deduced (Table 3.1). The reasoning to express the genes under the control of their endogenous promoter instead of an inducible promoter, such as the tetracycline promoter (Wickstrum *et al.*, 2013), was to allow regulation, and therefore a timing of expression, similar to the respective endogenous genes during the *C. trachomatis* developmental cycle. As will be described, because we could identify a potential T3S effector using the pSVP247 plasmid backbone, and considering the time required to generate transformed *C. trachomatis* strains, plasmids pSVP277 and pSVP268 were not further used in this work.

3.1.2.2 Construction of strains with plasmid-encoded candidate *C. trachomatis* T3S effectors

The next step was the construction of *C. trachomatis* strains expressing the candidate T3S effectors. The transformation was performed as described in the Materials and Methods (see section 2.4.2). We constructed *C. trachomatis* L2/434 derived strains harboring plasmids encoding the candidate T3S substrates with a 2HA tag at their C-termini (pCT053-2HA, pCT082-2HA, pCT105-2HA, pCT429-2HA, CT696-2HA and pCT849-2HA). Next, to confirm transformation with the correct plasmids, PCR was performed using as template whole cell extracts of the *C. trachomatis* L2/434 derived strains and specific primers (Annexed Table A2). Amplicons of the expected size were obtained for all strains (pCT053-2HA, 1.4 kb; pCT082-2HA, 2.4 kb; pCT105-2HA, 2.7 kb; pCT429-2HA, 1.8 kb; pCT696-2HA, 1.9 kb; and pCT849-2HA, 1.4 kb) (Figure 3.3A).

The expression of the candidate T3S substrates was assessed by immunoblotting of extracts of HeLa cells infected for 40 h with the *C. trachomatis* strains harboring plasmids encoding CT053-2HA (predicted molecular mass of 17 kDa), CT082-2HA (60 kDa), CT105-2HA (68 kDa), CT429-2HA (39 kDa), CT696-2HA (46 kDa) or CT849-2HA (18kDa). The production of 2HA-tagged proteins was confirmed (Figure 3.3B). However, the strains producing CT053-2HA, CT082-2HA and CT105-2HA also showed species migrating on SDS-PAGE at a molecular mass different from the one predicted for the full-length proteins (Figure 3.3B), as previously observed when identical 2HA-tagged versions of the proteins were produced in *Y. enterocolitica* (Pais *et al.*, 2013; da Cunha *et al.*, 2014) and when EGFP versions were ectopically expressed in mammalian cells (Figure 3.1A). Moreover, CT696-2HA and CT849-2HA were produced in much lower amounts than the other proteins (Figure 3.3B). Overall, these experiments confirmed that the constructed *C. trachomatis* strains expressed the expected 2HA-epitope tagged proteins.

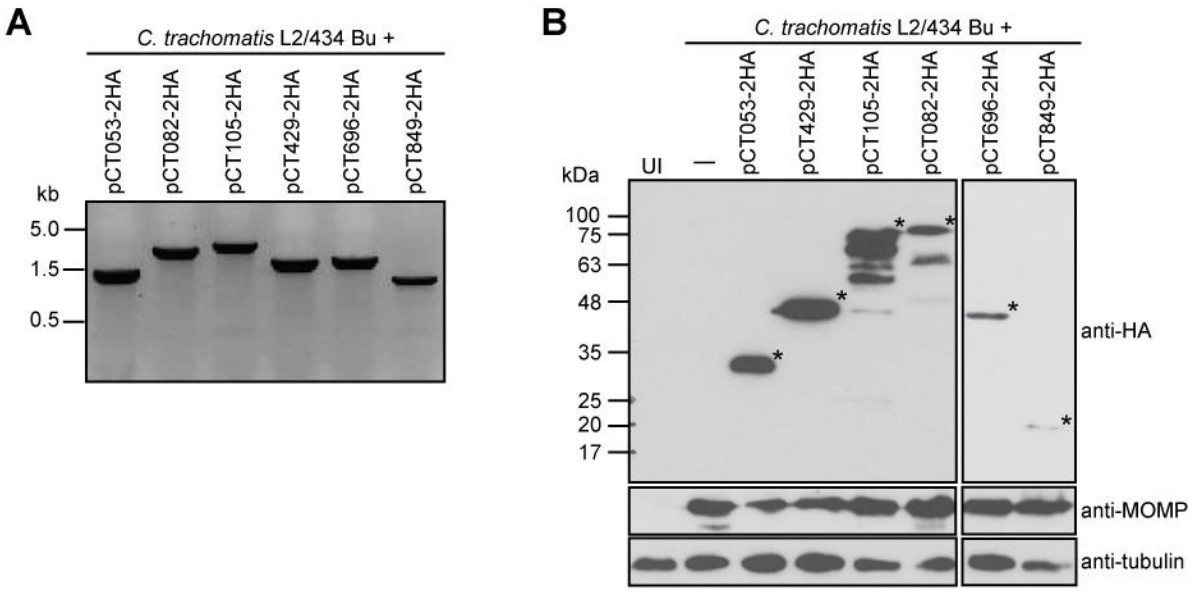

Figure 3.3 Construction of *C. trachomatis* L2/434-derived strains expressing candidate chlamydial T3S effectors. HeLa cells were infected by *C. trachomatis* L2/434-derived strains harboring the indicated plasmids, encoding the indicated candidate T3S effectors with a 2HA epitope tag at their C-termini. **(A)** Transformation of the indicated plasmids was confirmed by PCR using specific primers of the plasmid (primers 1978 and 1979; Annexes Table A2) **(B)** At 40 h post-infection (p.i.), whole cell extracts were analyzed by immunoblotting with antibodies against HA, *C. trachomatis* major outer membrane protein (MOMP) (bacterial loading control) and α-tubulin (HeLa loading control) using SuperSignal® West Pico detection kit (Thermo Fisher Scientific), or SuperSignal® West Femto detection kit (Thermo Fisher Scientific) for CT696-2HA and CT849-2HA. Asterisks indicate the bands likely corresponding to the full-length proteins.

3.1.3 Assessment of the delivery of candidate chlamydial T3S effectors by *C. trachomatis* into the host cell cytoplasm

To analyze the subcellular localization of CT053-2HA, CT082-2HA, CT105-2HA, CT429-2HA, CT696-2HA, and CT849-2HA in *Chlamydia*-infected cells, HeLa cells were infected with *C. trachomatis* L2/434-derived strains harboring the corresponding plasmids. The infected cells were fixed at 20 or 40 h post-infection (p.i.), immunolabeled for HA and for *C. trachomatis* major outer membrane protein (MOMP), stained with DAPI, and then analyzed by fluorescence microscopy. At 20 h or 40 h p.i. (Figure 3.4), CT053-2HA, CT082-2HA, CT429-2HA, CT696-2HA, and CT849-2HA were only detected within the inclusion and/or co-localizing with the *C. trachomatis* MOMP signal (Figure 3.4). In agreement with the immunoblotting data (Figure 3.3B), the levels of CT849-2HA were very low and nearly undetectable by fluorescence microscopy (Figure 3.4). In contrast, at both times p.i. analyzed, CT105-2HA was detected outside of the inclusion, indicating it is bacterially-delivered into the cytoplasm of infected host cells (Figure 3.4).

Altogether, as plasmid-encoded CT105-2HA was the only protein showed to be delivered into the host cell by *C. trachomatis* and as ectopically expressed EGFP-CT105 localized at specific sites of the mammalian cells, this suggests that CT105 might be a potential T3S effector of *C. trachomatis*.

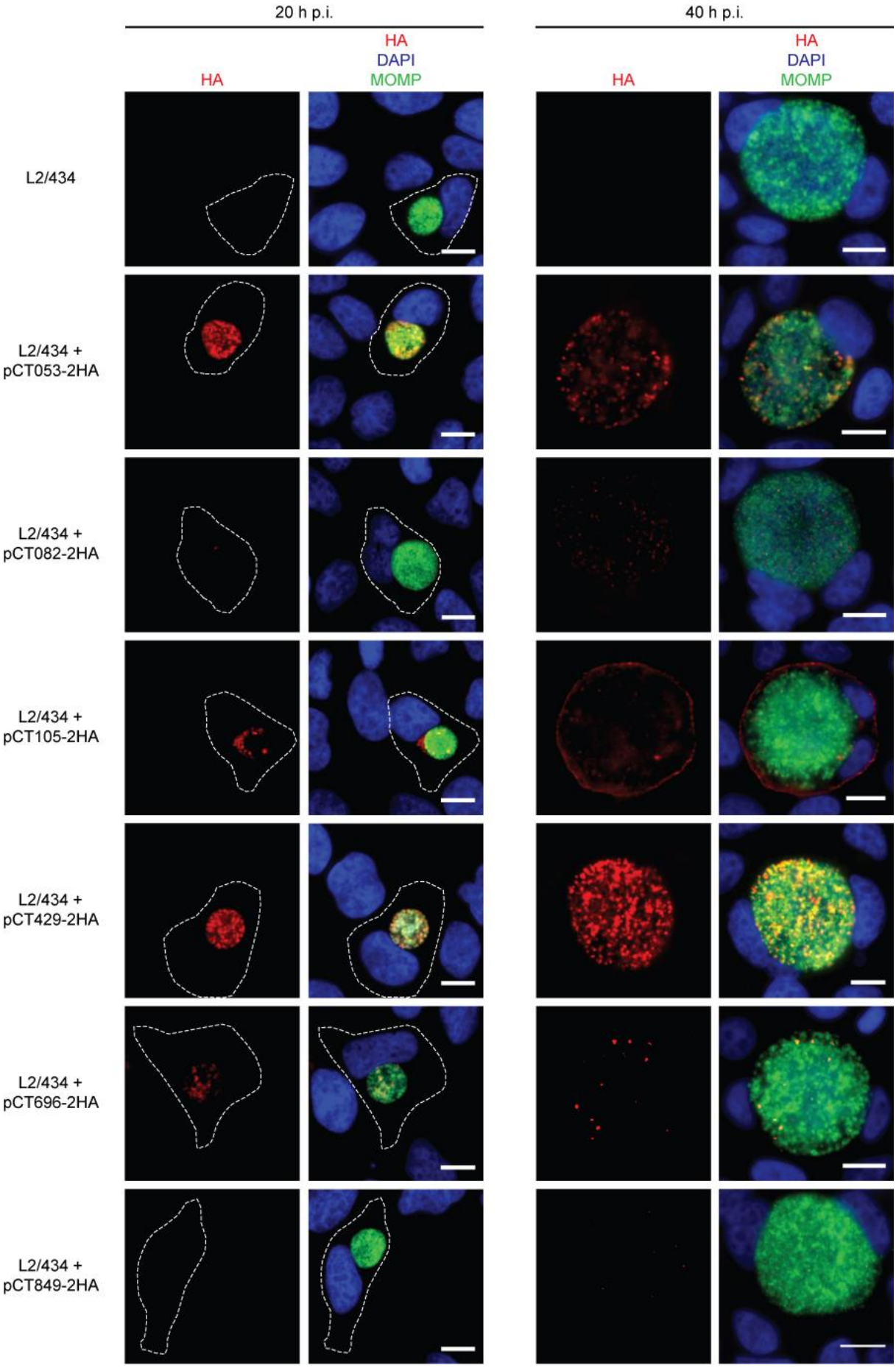
20 h p.i.
40 h p.i.
HA
HA
DAPI
MOMP
HA
HA
DAPI
MOMP
L2/434
L2/434 + pCT053-2HA
L2/434 + pCT082-2HA
L2/434 + pCT105-2HA
L2/434 + pCT429-2HA
L2/434 + pCT696-2HA
L2/434 + pCT849-2HA

Figure 3.4 Analysis of the delivery of the candidate T3S effectors by *C. trachomatis* L2/434 into the host cell. HeLa cells were infected by *C. trachomatis* L2/434-derived strains harboring the indicated plasmids, encoding chlamydial candidate T3S effectors (CT053, CT082, CT429, CT105, CT696, CT849) with a 2HA epitope tag at their C-termini. At 20 h and 40 h p.i., cells were fixed with 4% (w/v) PFA, stained with DAPI (blue), immunolabeled with antibodies against HA (red), *C. trachomatis* MOMP (green) and appropriate fluorophore-conjugated secondary antibodies, and imaged by fluorescence microscopy. Scale bars, 10 µm.

3.1.4 The first 20 amino acids of CT105 contain a T3S signal

A common feature of T3S effectors proteins is the presence of a secretion signal at their N-terminal region (Sory *et al.*, 1995; Lloyd *et al.*, 2001). Although the T3S signal has been extensively characterized, a clear consensus sequence was not yet identified. In addition, the T3S signal is universal and thus a T3S substrate of one bacterial system can be recognize and secreted by other bacterial T3S systems (T3SSs).

To analyze the T3S signal of CT105, *Y. enterocolitica* was used as a heterologous T3SS. *In vitro* T3S assays were performed using *Y. enterocolitica* T3S-proficient (ΔHOPEMT) and T3S-deficient (ΔHOPEMT ΔYscU) strains expressing the mature form of TEM-1 β-lactamase (TEM-1) or the first 20 or 40 amino acids of CT105 fused to TEM-1 ($CT105_{20}$-TEM-1 and $CT105_{40}$-TEM-1). Subsequently, bacterial pellets and culture supernatants were immunoblotted and secretion by the T3S-proficient strains was verified for $CT105_{20}$-TEM-1, as previously described (da Cunha *et al.*, 2014), and for $CT105_{40}$-TEM-1 (Figure 3.5A). In the T3S-deficient strain neither of the proteins was secreted (Figure 3.5A). Next, *in vitro* T3S assays were performed using *Y. enterocolitica* T3S-proficient strains expressing full-length CT105 and CT105 lacking the first 20 or 40 amino acids with a 2HA epitope tag at their C-terminus ($CT105_{FL}$-2HA, $CT105_{\Delta 20}$-2HA and $CT105_{\Delta 40}$-2HA). The analysis of the bacterial pellets and culture supernatants revealed that $CT105_{FL}$-2HA was secreted, as previously described (da Cunha *et al.*, 2014), but not $CT105_{\Delta 20}$-2HA or $CT105_{\Delta 40}$-2HA (Figure 3.5B).

Overall, these results indicate that secretion of CT105 was dependent on a functional T3SS and that the first 20 amino acids of CT105 were sufficient and necessary to drive T3S in *Y. enterocolitica*.

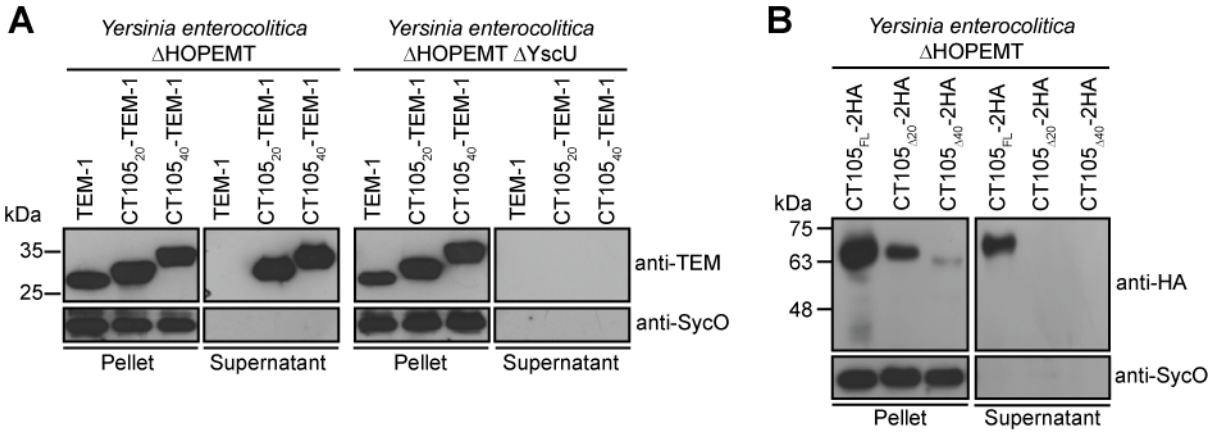

Figure 3.5 The first 20 amino acids of CT105 are sufficient and necessary to drive T3S by *Y. enterocolitica*. **(A)** *Y. enterocolitica* T3S-proficient (ΔHOPEMT) and T3S-deficient (ΔHOPEMT ΔYscU) strains were used to analyze secretion of TEM-1 (mature form of TEM-1 β-lactamase) and TEM-1 fusions to the first 20 or 40 amino acids of CT105 (CT105$_{20}$-TEM-1 and CT105$_{40}$-TEM-1, respectively). **(B)** *Y. enterocolitica* T3S-proficient (ΔHOPEMT) strains were used to analyze secretion of full-length CT105 (CT105$_{FL}$), CT105 lacking the first 20 amino acids (CT105$_{\Delta20}$), and CT105 lacking the first 40 amino acids (CT105$_{\Delta40}$) with a C-terminal 2HA epitope tag. After performing *in vitro* T3S assays, proteins in culture supernatants (secreted proteins) and in bacterial pellets (non-secreted proteins) were analyzed by immunoblotting with antibodies against TEM, HA and SycO using SuperSignal® West Pico detection kit (Thermo Fisher Scientific). SycO is a strictly cytosolic *Yersinia* T3S chaperone and it was used as a control to show that proteins in the culture supernatant did not result from bacterial lysis or contamination during fractionation. This experiment was performed in collaboration with Maria Beatriz Costa (master student in the host laboratory).

To confirm that the first 20 amino acids of CT105 were necessary to drive secretion in *C. trachomatis*, HeLa cells were infected with *C. trachomatis* strains carrying plasmids encoding full-length CT105 or CT105 lacking the first 20 amino acids with a 2HA epitope tag at the C-terminus (respectively, pCT105-2HA and pCT105$_{\Delta20}$-2HA). At 40 h p.i., extracts of infected cells were analyzed by immunoblotting and expression of CT105-2HA (68 kDa) and CT105$_{\Delta20}$-2HA (66 kDa) was confirmed (Figure 3.6A; indicated with asterisks). However, for CT105-2HA, an additional form of the protein migrated in the SDS-PAGE at a higher molecular mass (Figure 3.6A; indicated with an arrow).

Moreover, HeLa cells infected with *C. trachomatis* strains harboring pCT105-2HA or pCT105$_{\Delta20}$-2HA were fixed at 20 h and 40 h p.i. and analyzed by fluorescence microscopy using antibodies against HA and Cap1/CT529 (a chlamydial protein localized at the inclusion membrane). CT105-2HA was delivered into the host cell as previously described (Figure 3.4), but CT105$_{\Delta20}$-2HA was only detected inside the bacteria and not in the host cell (Figure 3.6B). Overall, we found that CT105 has a T3S signal within its first 20 amino acids, which allowed the delivery of CT105 by *C. trachomatis* into the host cell cytoplasm.

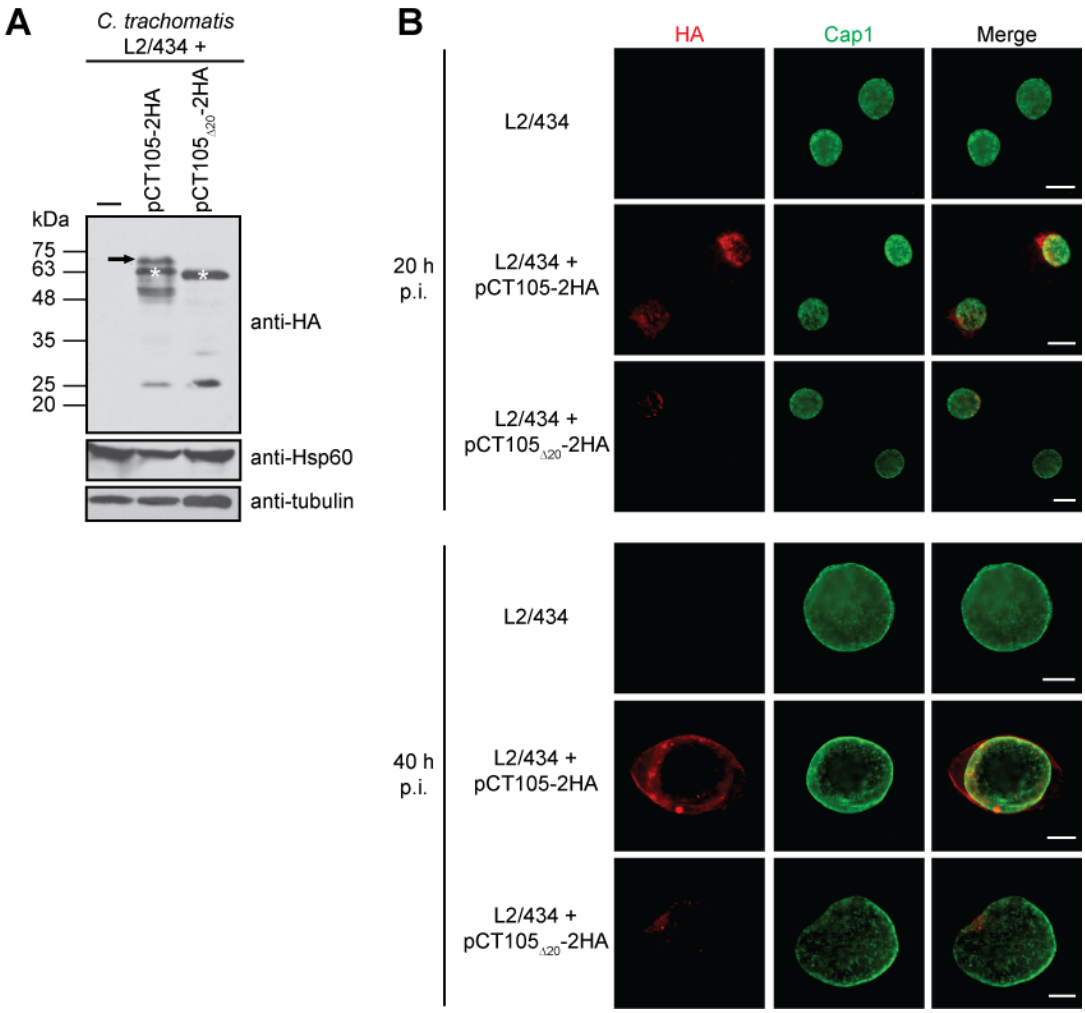

Figure 3.6 The first 20 amino acids of CT105 are necessary for the delivery of the protein into the host cell by *C. trachomatis* L2/434. HeLa cells were infected by *C. trachomatis* L2/434 and derived strains harboring full-length CT105 and CT105 lacking the first 20 amino acids with a C-terminal 2HA epitope tag (pCT105-2HA and pCT105$_{\Delta 20}$-2HA, respectively). **(A)** At 40 h p.i., whole cell extracts were analyzed by immunoblotting with antibodies against HA, *C. trachomatis* Hsp60 (bacterial loading control) and α-tubulin (HeLa loading control) using SuperSignal® West Pico detection kit (Thermo Fisher Scientific) for Hsp60 and α-tubulin, or SuperSignal® West Femto detection kit (Thermo Fisher Scientific) for HA. Asterisks indicate the bands likely corresponding to the full-length proteins. Arrow indicates protein species migrating at higher molecular mass. **(B)** At 20 h and 40 h p.i., infected cells were fixed with 4% (w/v) PFA and immunolabeled with antibodies against HA (red), *C. trachomatis* Cap1 (chlamydial protein located at the inclusion membrane; green) and appropriate fluorophore-conjugated secondary antibodies, and imaged by fluorescence microscopy. Scale bars, 10 µm. This experiment was performed in collaboration with Maria Beatriz Costa (master student in the host laboratory).

3.1.5 Full-length orthologues of CT105 are only present in *C. muridarum* and *C. suis*

Chlamydiaceae infect a wide range of hosts and T3S effectors are among the proteins thought to be implicated in the adaptation to the different niches. T3S effectors are involved in interactions with the host and therefore can elucidate on *Chlamydiaceae* evolution (Jewett *et al.*, 2010; Lutter *et al.*, 2010; Almeida *et al.*, 2012).

CT105 is a protein of 656 amino acid residues whose sequence does not show significant similarity to other proteins except for potential orthologues in another *Chlamydia* spp. However, full-length orthologues of CT105 were only found in *C. muridarum* and *C. suis* (Table 3.2). In *C. suis* and in other

Chlamydia spp. different open reading frames might encode proteins with some identity (between 30-22%) to only some parts of the amino acid sequence of CT105 (Table 3.2).

Table 3.2 Potential orthologues of *C. trachomatis* CT105 (CTL0360) in other *Chlamydiae*[a]

	Cover	Id	Protein	aa range (CTL0360)	aa range (target protein)	Protein length (aa)	E-value
C. abortus	38%	28%	CAB376	361-612	400-683	732	2e-14
C. avium	14%	30%	M832_01180	334-428	121-212	304	7e-4
	23%[b]	22%[b]	M832_01160	277-429	51-183	479	0.14[b]
C. caviae	41%	27%	CCA_00389	297-570	339-570	726	4e-20
	56%	26%	CCA_00390	282-651	416-782	898	3e-17
	12%	27%	CCA_00297	290-370	55-125	445	0.003
	15%	25%	CCA_00298	294-397	77-168	533	0.003
C. felis	69%	26%	CF0619	143-601	223-644	737	2e-19
	54%	24%	CF0618	301-656	406-758	816	2e-12
	15%	25%	CF0705	294-397	79-170	536	2e-05
	20%	23%	CF0706	290-422	55-176	447	9e-04
C. gallinacea	24%	22%	M787_003335	269-429	51-194	439	0.005
	26%[b]	24%[b]	M787_003340	300-427	69-179	451	0.057[b]
C. muridarum	99%	53%	TC_0381	1-651	1-644	650	0.0
C. pecorum	56%	28%	CpecS_0642	284-654	143-509	597	6e-29
	55%	26%	CpecS_0639	290-652	181-533	566	2e-24
	39%	23%	CpecS_0640	331-587	190-444	463	3e-16
C. pneumoniae	17%	30%	CPn0405	233-350	132-245	258	8e-10
	23%	22%	CPn0404	401-555	12-165	339	7e-07
C. psittaci	71%	25%	CPSIT_0422	189-654	72-523	610	9e-26
	35%	27%	CPSIT_0421	366-597	403-643	733	2e-13
C. suis	99%	47%	Q499_0113	4-654	7-648	650	7e-170
	72%	28%	Q499_0114	177-651	141-603	607	3e-44

[a] Orthologues of the *C. trachomatis* protein CT105 in other *Chlamydiae* were searched by PSI-BLAST. An individual PSI-BLAST search was performed between CT105 (using the amino acid sequence of CTL0360, from *C. trachomatis* serovar L2 strain 434/Bu) and a representative strain from each *Chlamydia* spp. (*C. abortus* strain S26/3, *C. avium* strain 10DC88, *C. caviae* strain GPIC, *C. felis* Fe/C-56, *C. gallinacean* 08-1274/3, *C. muridarum* strain Nigg, *C. pecorum* VR-629, *C. pneumoniae* strain CWL029, *C. psittaci* strain 6BC, *C. suis* strain MD56). Another individual PSI-BLAST search was performed between each protein and members of the other *Chlamydiae* families, but no significant hits were found. Cover, indicates % of coverage, and Id indicates % of identity; aa, amino acid.
[b] E-value worse than threshold.

3.1.6 The *C. trachomatis ct105* gene is likely only expressed in lymphogranuloma venereum (LGV) strains

Depending on the invasiveness and tissue tropism, *C. trachomatis* can be grouped into ocular (serovars A to C), urogenital (serovars D to K) and LGV (serovars L1 to L3) strains. Moreover, tissue tropism differences have been previously linked to T3S effectors (Lutter *et al.*, 2012; Almeida *et al.*, 2012).

As previously noted (Borges and Gomes, 2015), analysis of the mRNA levels of *ct105* by reverse transcription quantitative PCR (RT-qPCR) in different *C. trachomatis* strains revealed that the gene is significantly expressed in LGV strains (serovars L1 to L3) (Figure 3.7).

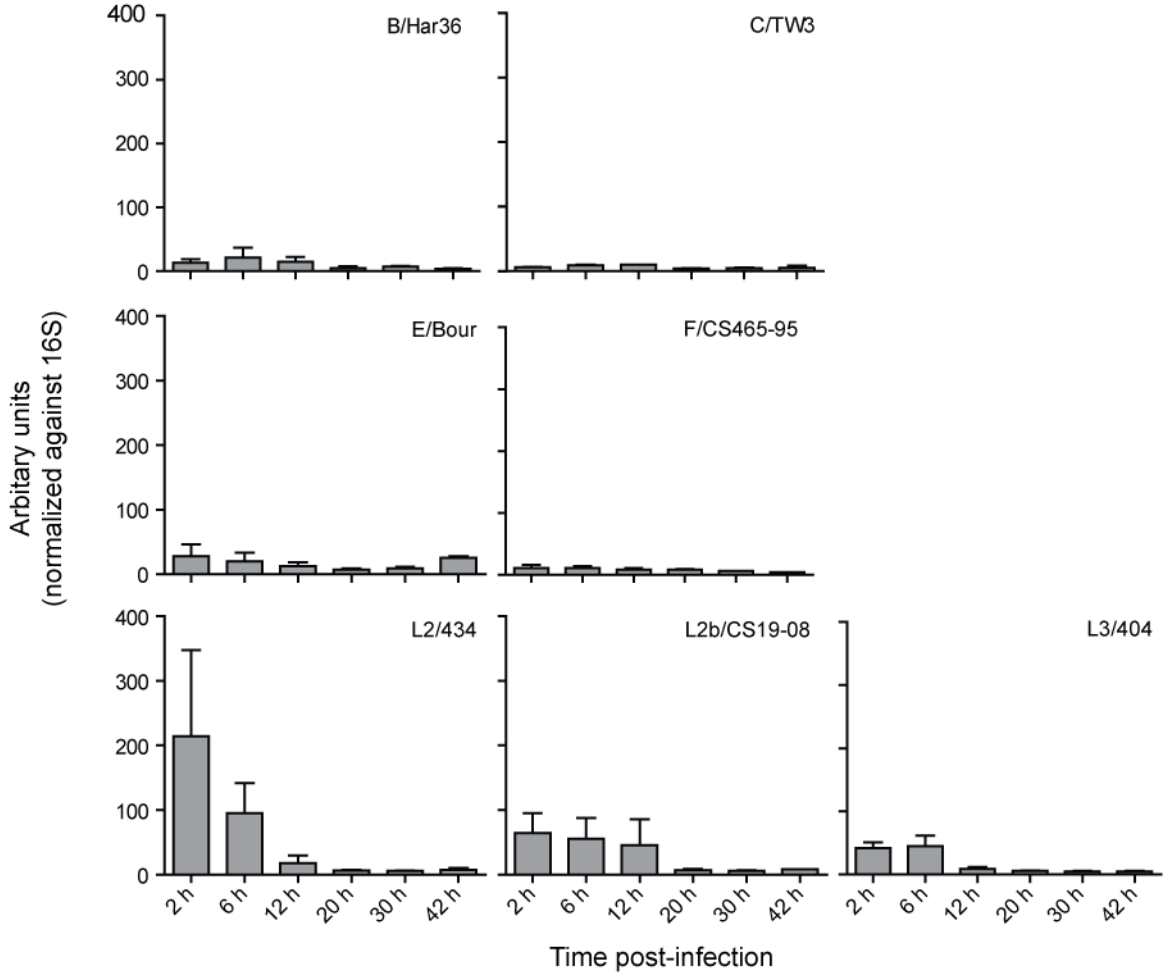

Figure 3.7 mRNA levels of *ct105* in different *C. trachomatis* strains. The mRNA levels of *ct105* were analyzed by real-time quantitative PCR (RT-qPCR) during the developmental cycle of *C. trachomatis* ocular (B/Har36, C/TW3), urogenital (E/Bour, F/CS465-95) or lymphogranuloma venereum (LGV) (L2/434, L2b/CS19-08, L3/404) strains, at the indicated time-points. The expression values (mean ± standard error of the mean) resulted from raw RT-qPCR data ($x10^5$) of *ct105* gene normalized to that of the *16S* rRNA gene and are from two independent experiments (except for strain C/TW3 where only one experiment was performed). This experiment was performed in collaboration with Vítor Borges and João Paulo Gomes (National Institute of Health Dr. Ricardo Jorge, Portugal).

Furthermore, also as previously noted (Borges and Gomes, 2015), considering the promoter region of *ct105* based on the transcription start site identified in *C. trachomatis* LGV strain L2b/UCH-1/proctitis

(Albrecht *et al.*, 2009), *C. trachomatis* non-LGV strains (serovars A to K) lack 74 nucleotides upstream from the putative -10 region recognized by *C. trachomatis* σ^{66} (Figure 3.8). It has also been previously shown that *ct105* is a pseudogene in *C. trachomatis* ocular strains (serovars A to C), where a stop codon in position 379 inactivates the gene or leads to the production of a protein with 126 amino acid residues (Borges *et al.*, 2012). Therefore, among *C. trachomatis* serovars, active CT105 is mostly produced by LGV strains.

Summarizing, our results showed that the first 20 amino acid of CT105 contained a T3S signal and were necessary to the delivery of the protein into the host cell. Moreover, as mRNA levels of *ct105* were mostly expressed in LGV strains and as *ct105* promoter region in LGV strains contained specific nucleotides, altogether this suggests that CT105 might contribute to characteristic tropism of LGV strains.

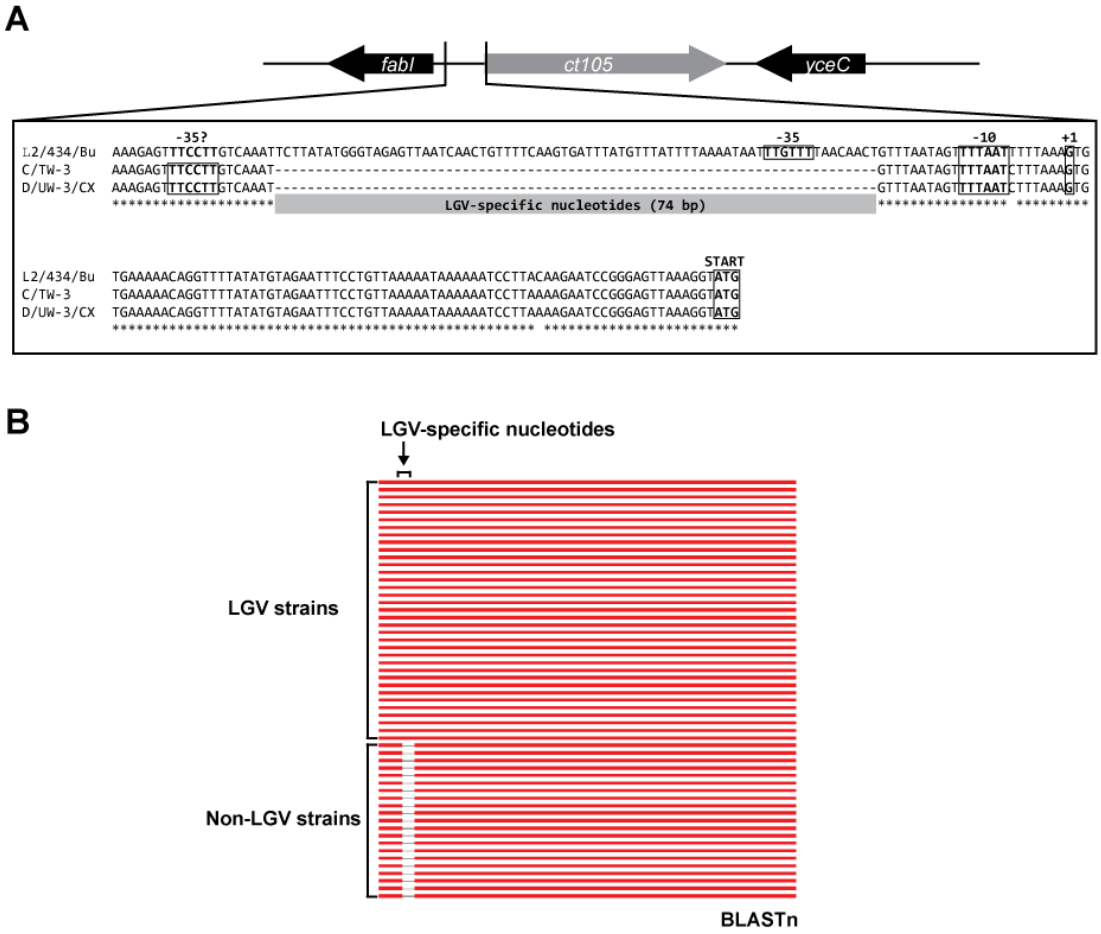

Figure 3.8 Putative promoter region of *ctl0360/ct105* in different *C. trachomatis* strains. (A) Representation of the genetic organization of *ctl0360/ct105* and the nucleotide sequence of the putative promoter region of *ctl0360/ct105* in *C. trachomatis* L2/434 (LGV strain), C/TW-3 (ocular strain) and D/UW-3/CX (urogenital strain).The sequences have the annotation of the putative transcription start site (+1), the predicted -10 and -35 hexamers, the start codon (Start) and the 74-bp LGV-specific nucleotides, based on the transcription start site identified in *C. trachomatis* LGV strain L2b/UCH-1/proctitis (Albrecht et al., 2010). **(B)** BLAST nucleotide (BLASTn) analysis of the genomic region of *ctl0360/ct105* highlights the LGV-specific nucleotides (arrow). This analysis was performed in collaboration with Vítor Borges and João Paulo Gomes (National Institute of Health Dr. Ricardo Jorge, Portugal).

3.2 THE *C. TRACHOMATIS* EFFECTOR CT105 ASSOCIATES WITH THE GOLGI COMPLEX AND PLASMA MEMBRANE OF INFECTED HOST CELLS

The chlamydial protein CT105 was identified as a T3S substrate that is delivered by *C. trachomatis* into the host infected cells, thus indicating a possible function for CT105 in the modulation of host cell functions to aid growth and survival of *C. trachomatis* within the intracellular environment.

Here, we carried out a more detailed analysis of the expression and localization of CT105-2HA. First, we analyzed the effects of overexpression of the plasmid-encoded CT105-2HA in *C. trachomatis* and further analyzed the subcellular localization of CT105 and the protein regions responsible for specific targeting which could contribute to uncovering the function of CT105 during *C. trachomatis* infection.

3.2.1 Characterization of the *C. trachomatis* strain producing plasmid-encoded CT105-2HA

To further analyze the expression and subcellular localization of CT105 in infected cells, we characterized the *C. trachomatis* L2/434 strain harboring pCT105-2HA (L2/434+pCT105-2HA), which expresses endogenous CT105 from the chromosome and CT105-2HA from a plasmid.

The profile of expression of *ct105* (based on its mRNA levels detected by RT-qPCR) during the developmental cycle of *C. trachomatis* was similar between the parental (L2/434) and derived (L2/434+pCT105-2HA) strains (Figure 3.9A). In agreement with previous observations (Figure 3.7) (da Cunha *et al.*, 2014), the highest levels of *ct105* mRNA were detected at 2 h p.i. (Figure 3.9A). Furthermore, at 2 h p.i., the strain harboring pCT105-2HA showed a 10-fold increase in the mRNA levels of *ct105* relative to the parental strain (Figure 3.9A). This is consistent with the approximetely 8 copies per cell of the *Chlamydia*-virulence plasmid (Pickett *et al.*, 2005; Ferreira *et al.*, 2013), which is the backbone of plasmid pCT105-2HA. As judged by quantifying the number of infectious progeny at different times of the developmental cycle, expression of plasmid-encoded CT105-2HA in *C. trachomatis* had no significant impact on chlamydial growth in cell culture (Figure 3.9B) and did not affect the size of the inclusion (Figure 3.9C).

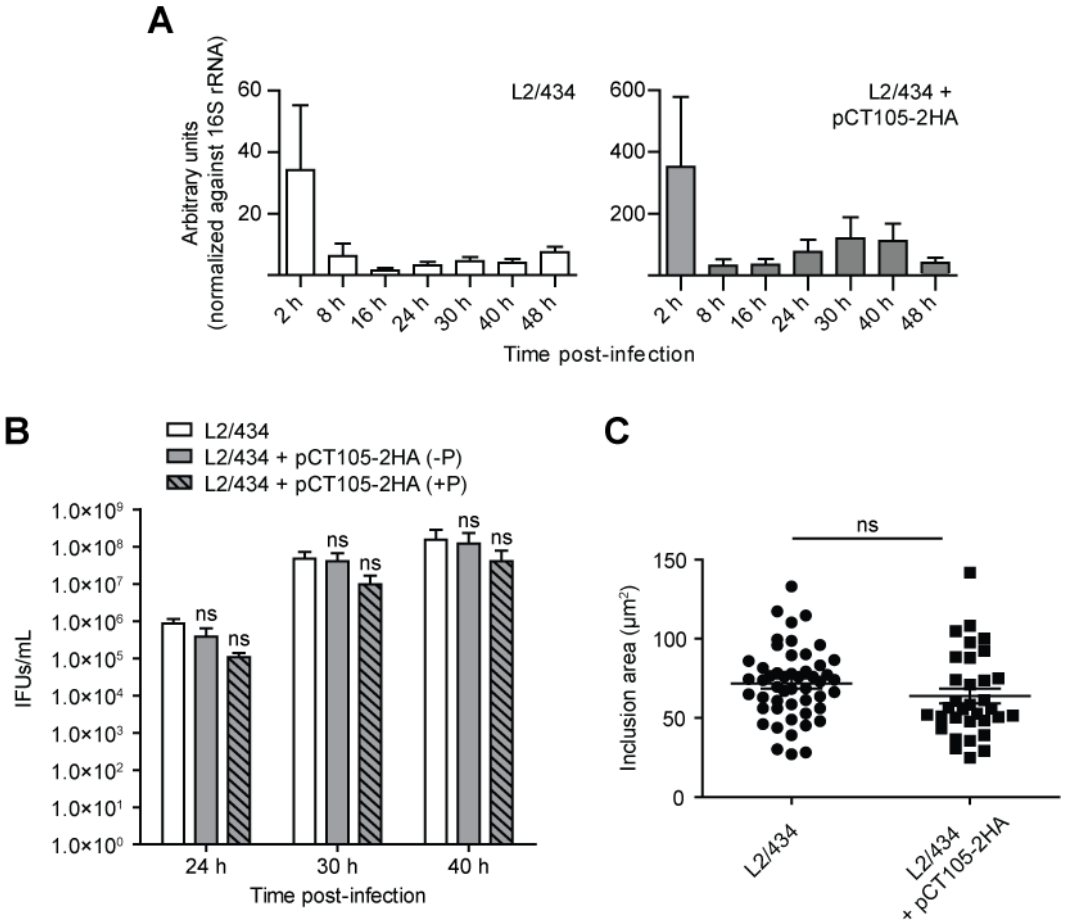

Figure 3.9 Characterization of *C. trachomatis* L2/434 strain harboring pCT105-2HA. (A) *ct105* mRNA levels of *C. trachomatis* L2/434 and *C. trachomatis* L2/434 harboring pCT105-2HA were analyzed by real-time quantitative PCR (RT-qPCR) at the indicated times post-infection. The expression values (mean ± standard error of the mean) resulted from raw RT-qPCR data of the *ct105* gene normalized to that of the *16S* rRNA gene and are from three independent experiments. **(B)** HeLa cells were infected with the indicated *C. trachomatis* strains at a multiplicity of infection of 1, in the absence (-P) or presence (+P) of 1 U/mL of penicillin G. Recoverable inclusion forming units (IFUs) were determined at 24, 30, and 40 h post-infection. Data are mean ± standard error of the mean of three independent experiments. P-values were obtained by one-way ANOVA and Dunnett post-test analyses relative to the parental L2/434 strain; ns, not significant ($P > 0.05$). **(C)** Hela cells were infected by the indicated *C. trachomatis* strains for 20 h. Cells were fixed with 4% (w/v) PFA, immunolabeled with antibodies against *C. trachomatis* MOMP and appropriate fluorophore-conjugated secondary antibody and imaged by fluorescence microscopy. The inclusion area was measured for 30 particles randomly chosen from independent images using Fiji software. P-values were obtained by t-test analyses; ns, not significant ($P \geq 0.05$).

In extracts of HeLa cells infected with *C. trachomatis* L2/434 harboring pCT105-2HA, we could detect CT105-2HA by immunoblotting from 16 h to 40 h p.i. (Figure 3.10B). Moreover, several other protein species were consistently observed between 20 h to 40 h p.i., which were particularly evident at 30 h or 40 h p.i. (Figure 3.10B), suggesting modification and/or degradation of CT105-2HA. We performed an identical analysis using a *C. trachomatis* strain harboring a plasmid encoding CT105-2HA under the control of a tetracycline-inducible promoter (pTet-CT105-2HA). Nevertheless, a similar expression kinetics and the same protein species were observed (Figure 3.10A and 3.10C).

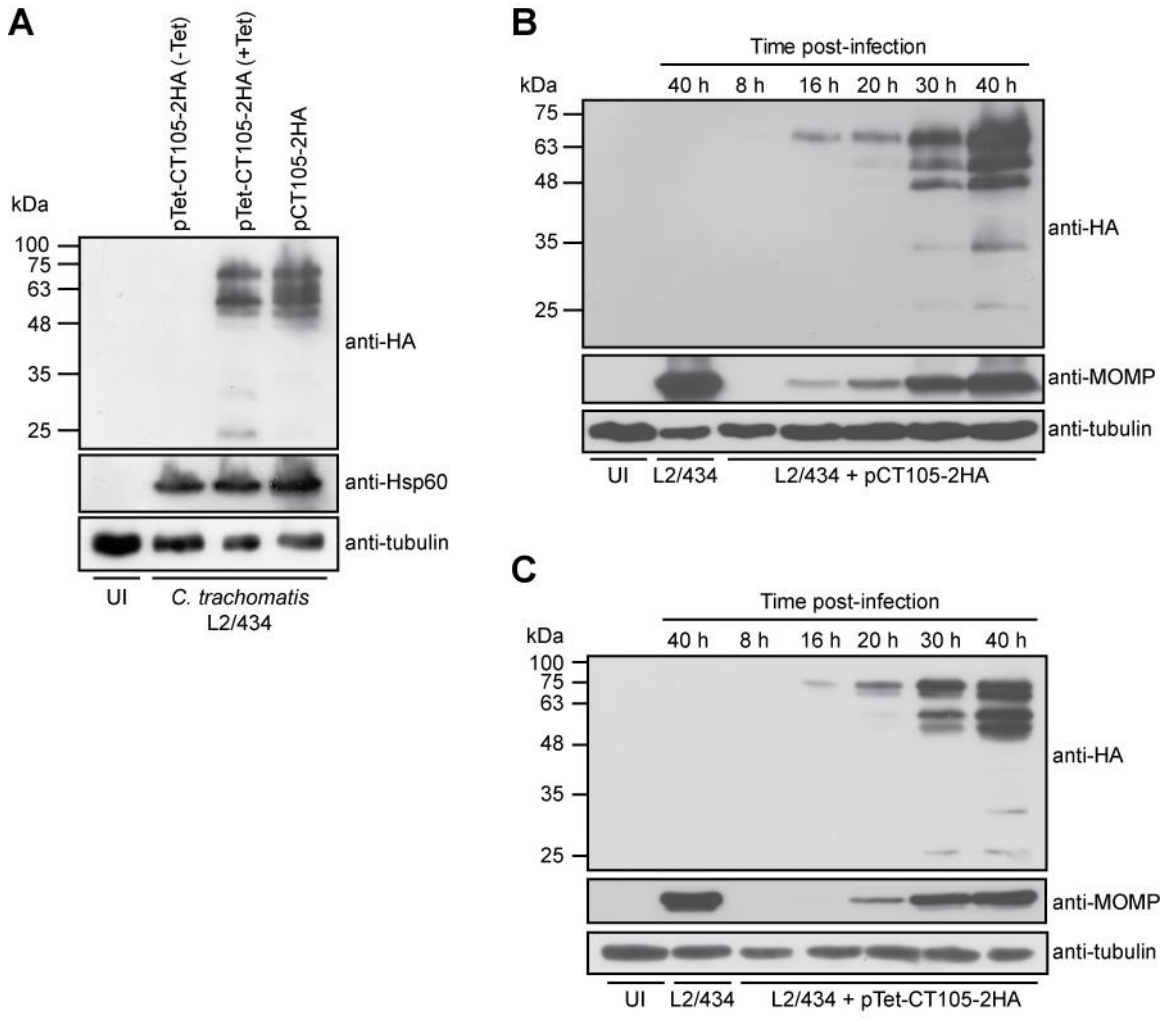

Figure 3.10 Kinetics of expression of CT105-2HA during infection by *C. trachomatis* L2/434. (A) HeLa cells were left uninfected (UI) or infected for 40 h by *C. trachomatis* L2/434, L2/434 harboring pCT105-2HA or L2/434 harboring pTet-CT105-2HA. In cells infected by L2/434 harboring pTet-CT105-2HA, anhydrotetracycline was either not added (-Tet) or added (+Tet). Total extracts were analyzed by immunoblotting with antibodies against HA, *C. trachomatis* Hsp60 (bacterial loading control) and α-tubulin (HeLa loading control). **(B)** and **(C)** Total extracts of UI cells or of cells infected for 8, 16, 20, 30, or 40 h by **(B)** *C. trachomatis* L2/434 harboring pCT105-2HA or by **(C)** *C. trachomatis* L2/434 harboring pTet-CT105-2HA were analyzed by immunoblotting with antibodies against HA, *C. trachomatis* MOMP (bacterial loading control) and α-tubulin (HeLa loading control). Immunoblotting detection was done using SuperSignal® West Pico detection kit (Thermo Fisher Scientific) for *C. trachomatis* Hsp60 or MOMP, and α-tubulin, or SuperSignal® West Femto detection kit (Thermo Fisher Scientific) for HA. In cells infected by *C. trachomatis* L2/434 harboring pTet-CT105-2HA, anhydrotetracycline was added to 20 ng/mL at time zero of infection.

To understand if these protein species that appear in anti-HA immunoblots of HeLa cells infected by *C. trachomatis* producing CT105-2HA were dependent of bacterial or host cell factors, extracts of *E. coli*, *Y. enterocolitica* and *C. trachomatis* strains harboring pTet-CT105-HA were analyzed by immunoblotting. Although the lower molecular mass protein species were similar among the analyzed bacterial strains (Figure 3.11A), the protein species with the highest molecular mass was only detected in *C. trachomatis* whole cell extracts (Figure 3.11A), suggesting a modification of CT105 during chlamydial infection. Next, we questioned whether this modification occurred inside or outside the bacteria. Therefore, immunoblotting of extracts of HeLa cells infected by *C. trachomatis* L2/434 harboring either pCT105-2HA or pTet-CT105-2HA, or of corresponding *Chlamydia*-enriched extracts, showed the presence of the protein species with the highest molecular mass both in whole cell and

Chlamydia-enriched extracts (Figure 3.11B). In addition, for CT105$_{\Delta 20}$-2HA, which was not secreted by *Y. enterocolitica* (Figure 3.5B) and apparently not delivered into the host cells by *C. trachomatis* (Figure 3.6B), an additional protein species of high molecular mass was not detected by immunoblotting (Figure 3.6A). Altogether, these results suggest a modification of CT105 inside *C. trachomatis* that requires the first 20 amino acid residues of the protein.

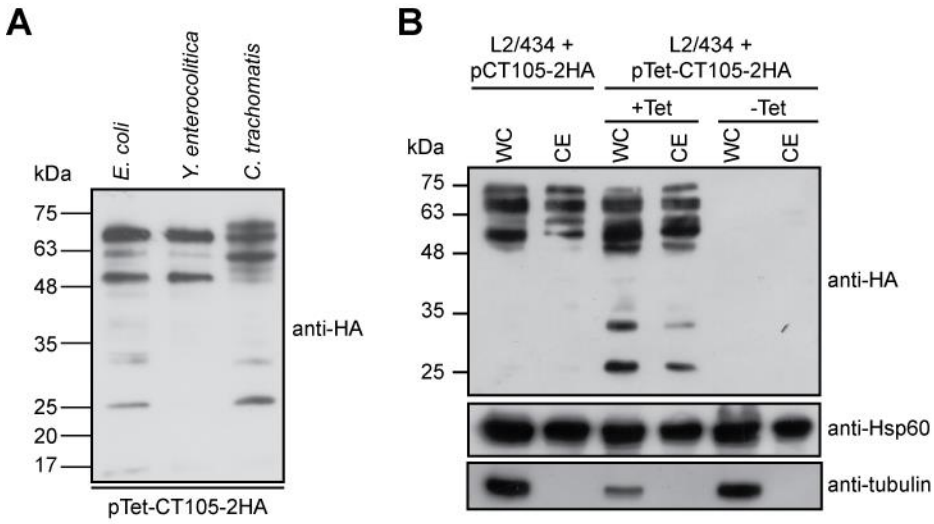

Figure 3.11 CT105-2HA is modified in *C. trachomatis* L2/434. (A) Total extracts of the indicated bacterial strains harboring pTet-CT105-2HA were analyzed by immunoblotting with antibodies against HA. The induction conditions to express CT105-2HA in each bacterial strain are described in Materials and Methods. **(B)** HeLa cells were infected for 40 h by the indicated *C. trachomatis* strains. In cells infected by L2/434 harboring pTet-CT105-2HA, anhydrotetracycline was either not added (-Tet) or added (+Tet) to 20 ng/mL at time zero of infection. Whole cell (WC) and *Chlamydia*-enriched (CE) extracts (see Materials and Methods) were analyzed by immunoblotting with antibodies against HA, *C. trachomatis* Hsp60 (bacterial loading control) and α-tubulin (HeLa loading control). Immunoblotting detection was done using SuperSignal® West Pico detection kit (Thermo Fisher Scientific) for Hsp60 and α-tubulin, or SuperSignal® West Femto detection kit (Thermo Fisher Scientific) for HA. This experiment was performed in collaboration with Inês Serrano Pereira (PhD student in the host laboratory).

3.2.2 Analysis of the delivery of CT105-2HA into host cells during *C. trachomatis* developmental cycle

To further detail the kinetics of delivery of CT105-2HA during infection, HeLa cells were infected by *C. trachomatis* L2/434 harboring pCT105-2HA. Infected cells were fixed at 2, 4, 8, 16, 20, 30, and 40 h p.i., immunolabeled with antibodies against HA, *C. trachomatis* MOMP, and Inc protein CT442, and analyzed by fluorescence microscopy. At 2, 4, and 8 h. p.i., CT105-2HA could be detected co-localizing with the signal for *C. trachomatis* Hsp60 (Figure 3.12), indicating its presence within the bacterial cells.

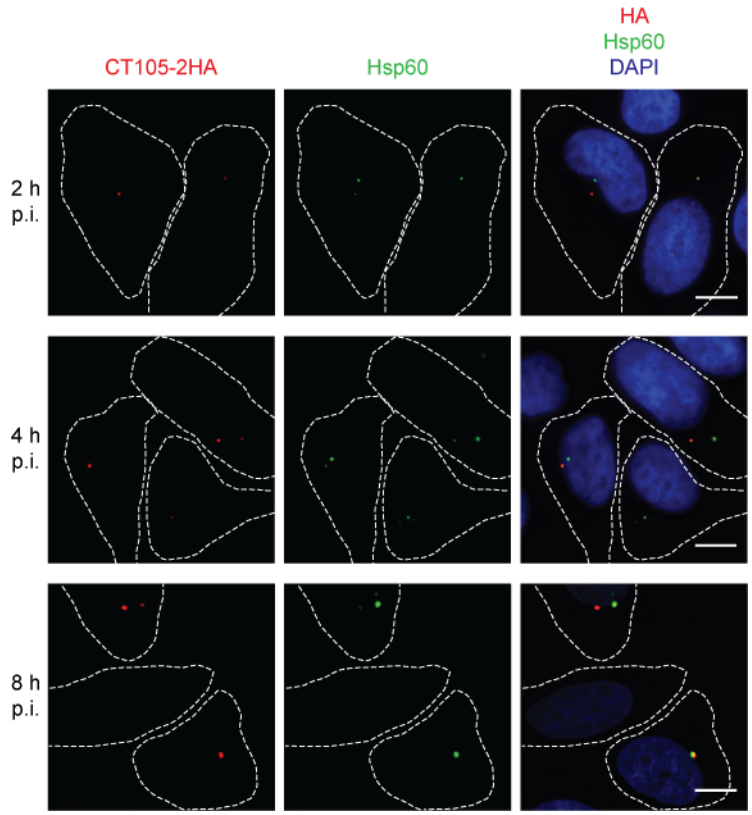

Figure 3.12 *C. trachomatis* L2/434 produces CT105-2HA early during infection. HeLa cells were infected by *C. trachomatis* L2/434 harboring pCT105-2HA for 2, 4, and 8 h p.i. Cells were fixed with 4% (w/v) PFA, stained with DAPI (blue), immunolabeled with antibodies against HA (red) and *C. trachomatis* Hsp60 (green), and appropriate fluorophore-conjugated secondary antibodies, and imaged by fluorescence (2 h and 4 h p.i.) or confocal fluorescence (8 h p.i.) microscopy. Confocal image corresponds to single *z* section. Scale bars, 10 µm.

At 16 and 20 h p.i., CT105-2HA was detected outside of the inclusion in approximately 37% and 90% of the infected cells, respectively (Figure 3.13); at 30 and 40 h p.i., the protein was found outside of the inclusion in all infected cells (Figure 3.13). While at 16, 20, and 30 h p.i. CT105-2HA was detected in the host cell cytoplasm concentrated at one of the sides of the inclusion, at 30 h p.i. the protein was also detected at the periphery of the infected cells (Figure 3.13). Furthermore, at 40 h p.i., CT105-2HA was mostly seen at the periphery of the infected cells (Figure 3.13). A similar localization was observed for *C. trachomatis* L2/434 harboring pTet-CT105-2HA (Figure 3.14).

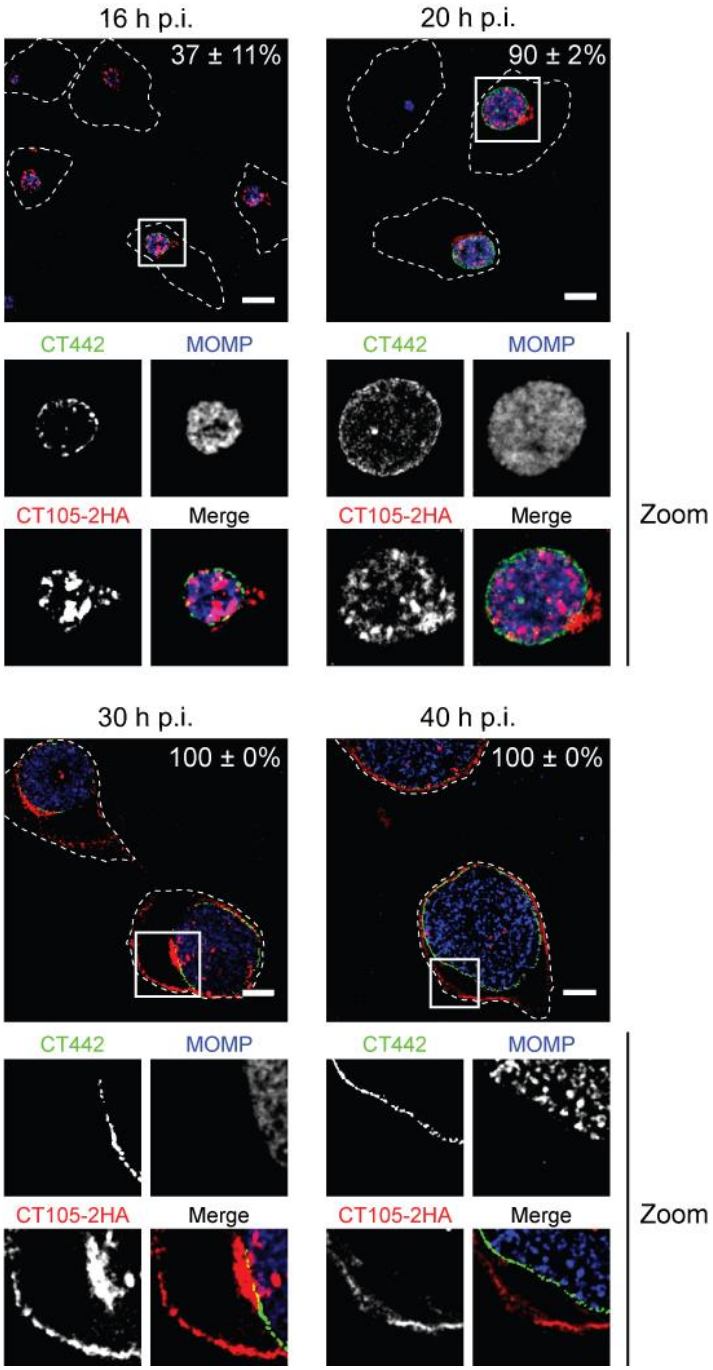

Figure 3.13 The subcellular localization of bacterially-delivered CT105-2HA changes in infected cells as the *C. trachomatis* developmental cycle progresses. HeLa cells were infected by *C. trachomatis* L2/424 harboring pCT105-2HA for 16, 20, 30, or 40 h. Infected cells were fixed with 4% (w/v) PFA and immunolabeled with antibodies against HA (red), *C. trachomatis* MOMP (blue), and the inclusion membrane protein CT442 (green), and appropriate fluorophore-conjugated secondary antibodies, and imaged by confocal fluorescence microscopy. Images correspond to single *z* sections. The values indicate the number of infected cells showing CT105-2HA outside of the inclusion, in the cytoplasm of the infected host cell. Data are the mean ± standard error of the mean of three independent experiments (n ≥ 25). In the area delimited by a white square (upper panels) images were zoomed (lower panels). Scale bars, 10 µm.

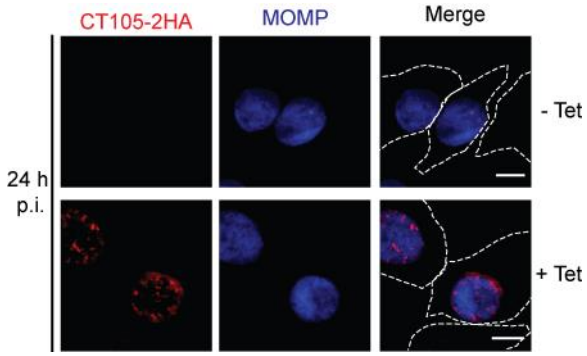

Figure 3.14 CT105-2HA expressed under the control of the tetracycline promoter is delivered into the host cell by *C. trachomatis* L2/434. HeLa cells were infected by *C. trachomatis* L2/434 harboring pTet-CT105-2HA and fixed with 4% (w/v) PFA at 24 h p.i. During infection, anhydrotetracycline was either not added (-Tet) or added (+Tet) to 20 ng/mL at time zero of infection. Fixed cells were immunolabeled with antibodies against HA (red) and *C. trachomatis* MOMP (blue), and appropriate fluorophore-conjugated secondary antibodies. Cells were imaged by fluorescence microscopy. Scale bars, 10 µm.

3.2.3 CT105-2HA localizes at the Golgi complex in *C. trachomatis*-infected cells

The accumulation of CT105-2HA near the inclusion in the cytoplasm of infected cells suggested it could localize at the Golgi complex. This immunofluorescence signal of CT105-2HA also appeared less compact at longer times of infection, which was evocative of the Golgi fragmentation seen in *C. trachomatis* infected-cells (Heuer *et al.*, 2009). To analyze this, HeLa cells infected by *C. trachomatis* L2/434 harboring pCT105-2HA were fixed at 16, 20, 30, and 40 h p.i. and then immunolabeled using antibodies against HA, *C. trachomatis* MOMP, GM130 (*cis*-Golgi marker), and TGN46 (*trans*-Golgi network [TGN] marker). Subsequent analysis by fluorescence microscopy revealed that CT105-2HA localized in the Golgi region at 16, 20, and 30 h, and that this was much less evident at 40 h p.i. (Figure 3.15A). There was not a perfect co-localization of CT105-2HA with the *cis*- and *trans*-Golgi markers, but the immunofluorescence signal of CT105-2HA near the inclusion accompanied the dispersion of the Golgi complex during infection (Figure 3.15A). To further confirm the association of CT105-2HA with the Golgi, HeLa cells infected by the L2/434 strain harboring pCT105-2HA were treated with brefeldin A (BFA), which induces reversible Golgi fragmentation (Lippincott-Schwartz *et al.*, 1989). Specifically, at 19 h p.i., the infected cells were either incubated for 1 h with BFA or with dimethyl sulfoxide (DMSO)-solvent alone (as control) and then fixed. In addition, the infected cells were incubated for 1 h with BFA, washed out from the BFA, incubated for 1 h, and then fixed. The cells were immunolabeled with antibodies against HA, *C. trachomatis* MOMP, and GM130, and analyzed by fluorescence microscopy. In the DMSO-treated infected cells, CT105-2HA accumulated in the Golgi region (Figure 3.15B), similarly to untreated cells infected for 16 or 20 h p.i. (Figure 3.15A). In cells treated with BFA, the GM130-labeled Golgi fragmented into small vesicles and the immunofluorescence signal of CT105-2HA became dispersed and mostly below the limit of detection (Figure 3.15B). In cells treated with BFA and subsequently washed-out of the drug, both the GM130-labeled Golgi and CT105-2HA appeared mostly compact and near the inclusion (Figure 3.15B). Overall, this showed that CT105-2HA associates with the Golgi upon the detection of its delivery by *C. trachomatis* into the cytoplasm of infected host cells, at 16-20 h p.i.

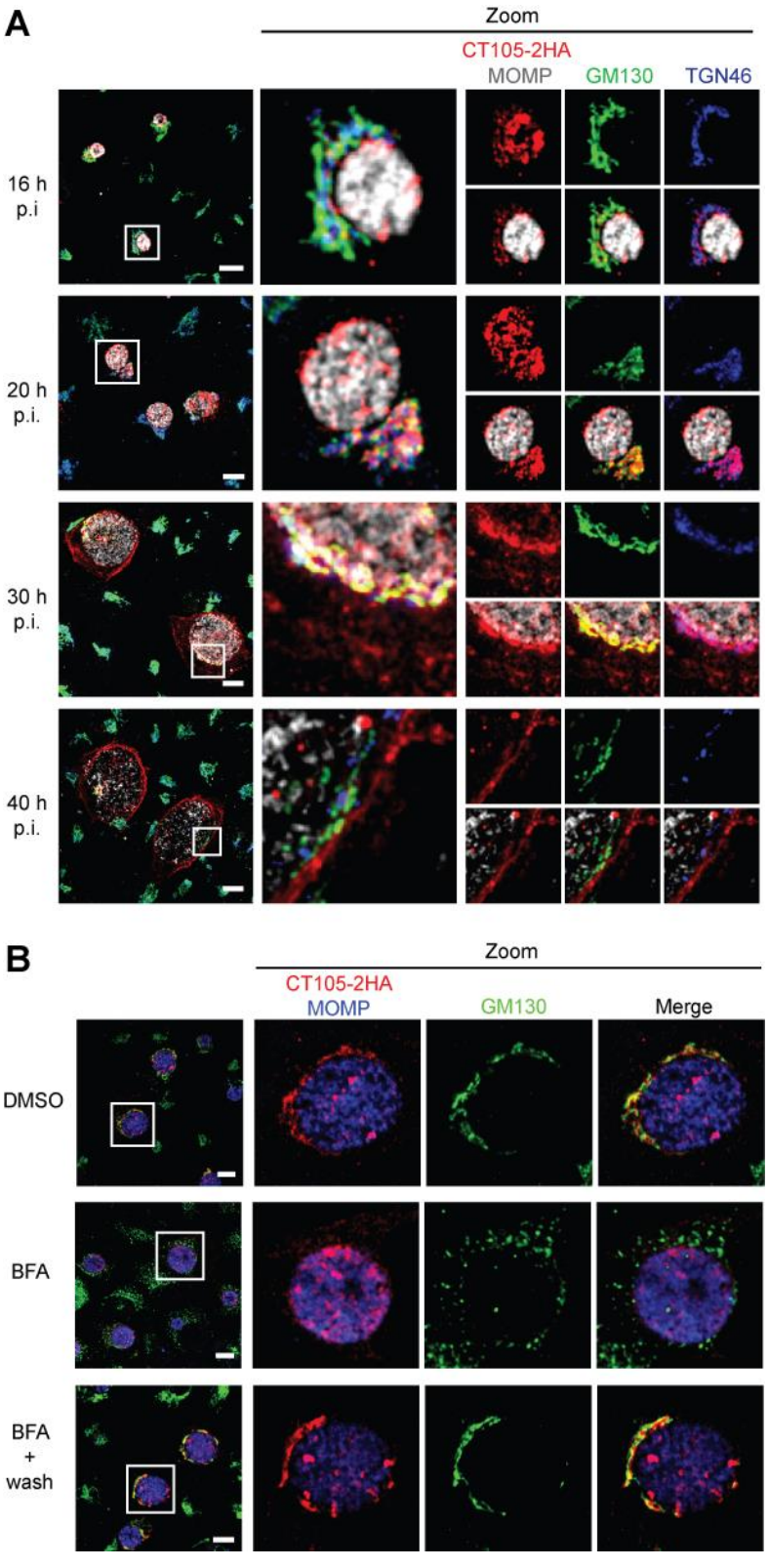
A
Zoom
CT105-2HA
MOMP
GM130
TGN46
16 h p.i
20 h p.i.
30 h p.i.
40 h p.i.
B
Zoom
CT105-2HA
MOMP
GM130
Merge
DMSO
BFA
BFA + wash

Figure 3.15 CT105-2HA associates with the Golgi complex in *C. trachomatis*-infected cells. HeLa cells were infected by *C. trachomatis* L2/434 encoding CT105-2HA. **(A)** At the indicated times p.i., cells were fixed with 4% (w/v) PFA, immunolabeled with antibodies against HA (red), *C. trachomatis* MOMP (gray), GM130 (green), and TGN46 (blue), and appropriate fluorophore-conjugated secondary antibodies. In the area delimited by a white square (left-side panels) images were zoomed (middle and right-side panels). **(B)** At 19 h p.i., cells were treated for 1 h with DMSO or 1 µg/ml BFA. Then, the cells were either fixed with 4% (w/v) PFA (upper and middle panels) or washed with complete medium lacking BFA and incubated for an additional 1 h and then fixed with 4% (w/v) PFA (lower panels). Fixed cells were immunolabeled with antibodies against HA (red), *C. trachomatis* MOMP (gray), and GM130 (green), and appropriate fluorophore-conjugated secondary antibodies. In the area delimited by a white square (left-side panels) images were zoomed (right-side panels). All immunolabeled cells were examined by confocal fluorescence microscopy, and images correspond to single *z* sections. Scale bars, 10 µm.

3.2.4 CT105-2HA localizes at the host cell plasma membrane in *C. trachomatis*-infected cells

CT105-2HA was also detected in the periphery of host cells at 30 or 40 h p.i. by *C. trachomatis* (Figure 3.16A), which suggested it could localize at or near the plasma membrane. To analyze this, HeLa cells were infected for 30 and 40 h p.i. by *C. trachomatis* L2/434 harboring CT105-2HA and transfected with a plasmid encoding a palmitoylated/myristoylated peptide from Lyn kinase (Lyn11) [targeting proteins to the plasma membrane (Inoue *et al.*, 2005) fused to monomeric EGFP (Falcón-Pérez *et al.*, 2005) (Lyn11-mEGFP)]. The cells were then fixed, immunolabeled using antibodies against HA and *C. trachomatis* MOMP, stained for the actin cytoskeleton with fluorescent-conjugated phalloidin, and analyzed by fluorescence microscopy. Although CT105-2HA did not show a perfect co-localization with either Lyn11-mEGFP or with phalloidin-stained cortical actin (Figure 3.16B and 3.16C), this showed that at 30 and 40 h p.i., CT105-2HA localizes at the plasma membrane.

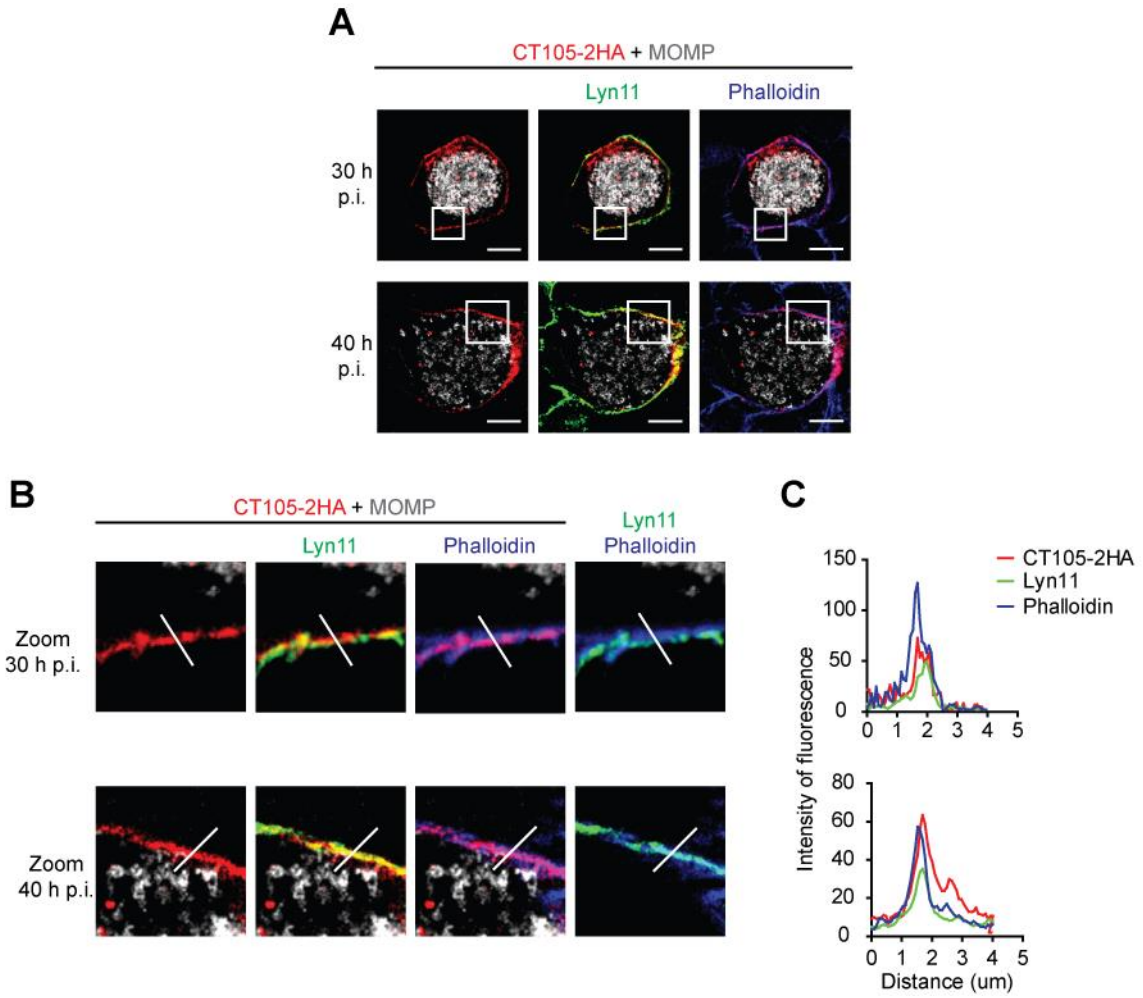

Figure 3.16 CT105-2HA localizes at the host cell plasma membrane in *C. trachomatis*-infected cells. HeLa cells were infected by *C. trachomatis* L2/434 encoding pCT105-2HA and transfected with a plasmid encoding the plasma membrane marker Lyn11-mEGFP (green). **(A)** At 30 or 40 h p.i., cells were fixed with 4% (w/v) PFA, stained with phalloidin (blue), and immunolabeled with antibodies against HA (red) and *C. trachomatis* MOMP (gray), and appropriate fluorophore-conjugated secondary antibodies. Cells were imaged by confocal fluorescence microscopy and images correspond to single *z* sections. Scale bars, 10 µm. **(B)** Images were zoomed in the area delimited by a white square in **(A)**. **(C)** Co-localization profile graphs of the fluorescence signal of CT105-2HA, Lyn11 and phalloidin at the region indicated with a line in **(B)**.

3.2.5 Bacterially-delivered CT105-2HA changes its main localization in the host cell cytoplasm as the *C. trachomatis* developmental cycle progresses

The number of infected cells showing bacterially-translocated CT105-2HA outside of the inclusion and at the Golgi or at the plasma membrane were enumerated. HeLa cells were infected by strain L2/434 harboring pCT105-2HA and fixed at 16, 20, 30, and 40 h p.i. Then cells were immunolabeled for HA, for GM130 and for *C. trachomatis* MOMP and analyzed by fluorescence microscopy for CT105-2HA in the Golgi region or in the cell periphery. At 16 h p.i., CT105-2HA accumulated at the Golgi region in all infected cells showing the protein outside of the inclusion (Figure 3.17). At 20, 30, and 40 h p.i., the number of cells showing CT105-2HA outside of the inclusion and only at the Golgi region was progressively less frequent (88 ± 6%, 17 ± 7%, and 7 ± 2%, respectively) (Figure 3.17). In contrast, at 20, 30, and 40 h p.i., the number of cells showing CT105-2HA outside of the inclusion and only in the

periphery of the cell was progressively more frequent (2 ± 1%, 15 ± 1%, and 61 ± 9%, respectively) (Figure 3.17). Infected cells showing CT105-2HA outside of the inclusion and both at the Golgi region and in the periphery of the host cell could also be identified and were much more frequent at 30 h p.i. (69 ± 8%) than at 20 and 40 h p.i. (10 ± 6%, and 33 ± 9%, respectively) (Figure 3.17).

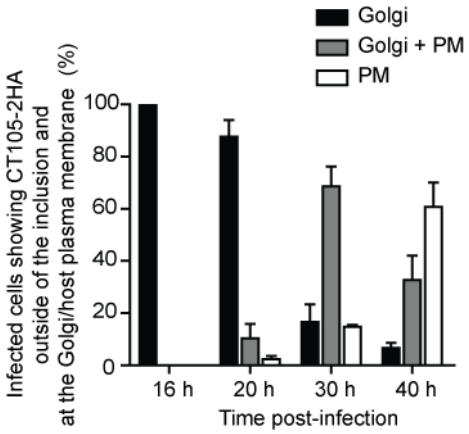

Figure 3.17 CT105-2HA changes its subcellular localization during *C. trachomatis* infection. HeLa cells were infected by *C. trachomatis* L2/434 harboring pCT105-2HA. Infected cells were fixed with 4% (w/v) PFA at 16, 20, 30 or 40 h p.i. and immunolabeled with antibodies against HA, *C. trachomatis* MOMP, and GM130, and appropriate fluorophore-conjugated secondary antibodies. Fluorescence microscopy was used to enumerate cells showing CT105-2HA only at the Golgi, only at the plasma membrane (PM), or both at the Golgi and at the plasma membrane (Golgi + PM). Data are mean ± standard error of the mean (SEM) of three independent experiments (n ≥ 25).

Altogether, in *C. trachomatis*-infected cells, initial delivery of CT105-2HA into the host cell cytoplasm (first detected at 16 h p.i.) results in its accumulation at the Golgi region, but as infection progresses this localization of the protein becomes less frequent and CT105-2HA accumulates more often at the periphery of the cell. These observations were recapitulated by the analysis of HeLa cells infected by *C. trachomatis* L2/434 harboring pTet-CT105-2HA (Figure 3.18).

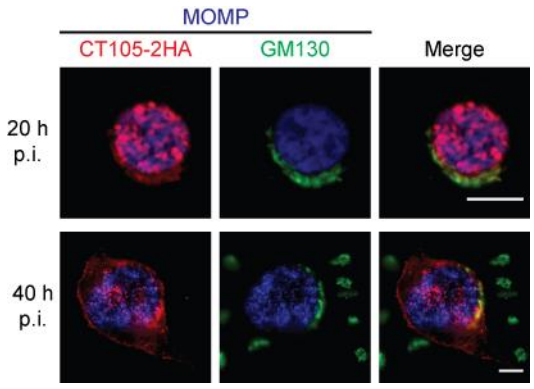

Figure 3.18 Subcellular localization of CT105-2HA expressed under the control of the tetracycline promoter in *C. trachomatis*-infected cells. HeLa cells were infected by *C. trachomatis* L2/434 harboring pTet-CT105-2HA and fixed with 4% (w/v) PFA at the indicated times post-infection (p.i.). During infection, anhydrotetracycline was added to 20 ng/mL at time zero of infection. Fixed cells were immunolabeled with antibodies against HA (red), *C. trachomatis* MOMP (blue), and GM130 (green), and by appropriate fluorophore-conjugated secondary antibodies. Cells were imaged by fluorescence microscopy. Scale bars, 10 µm.

3.2.6 The change in the main localization of CT105-2HA during infection from the Golgi to the plasma membrane is independent of intact host microfilaments and microtubules

The previous results suggested that CT105-2HA could be transported from the Golgi to the plasma membrane in vesicles associated with the microtubule and actin cytoskeleton. To test this possibility, we infected HeLa cells with *C. trachomatis* harboring pCT105-2HA and at 20 h p.i., when CT105-2HA mostly localizes at the Golgi region (Figure 3.17), we incubated the cells in the presence of dimethyl sulfoxide (DMSO) solvent as control, of cytochalasin D or lantrunculin B (to inhibit actin polymerization, but each drug promotes depolymerization of microfilaments by different mechanisms), or of nocodazole (to prevent tubulin polymerization, and thereby depolymerize microtubules) (Figure 3.19A). The cells were then fixed at 30 h p.i., when CT105-2HA mostly localizes near the plasma membrane (Figure 3.17), and immunolabeled for HA and *C. trachomatis* MOMP. Fluorescence microscopy was then used to enumerate infected cells showing CT105-2HA near the plasma membrane (Figure 3.19B). We observed a statistically significant difference in the localization of CT105-2HA near the plasma membrane when microfilaments were disrupted with cytochalasin D (Figure 3.19B). However, the small difference relative to DMSO-treated cells, and the absence of a significantly different effect upon disruption of the microfilaments with lantrunculin B (Figure 3.19B), suggests this should have no biological significance. Furthermore, disruption of the microtubule network also did not significantly affect the localization of CT105-2HA near the plasma membrane (Figure 3.19B). Therefore, CT105-2HA changes its predominant localization during infection of host cells by *C. trachomatis* from the Golgi to the plasma membrane, but this is likely independent of intact host microfilaments and microtubules.

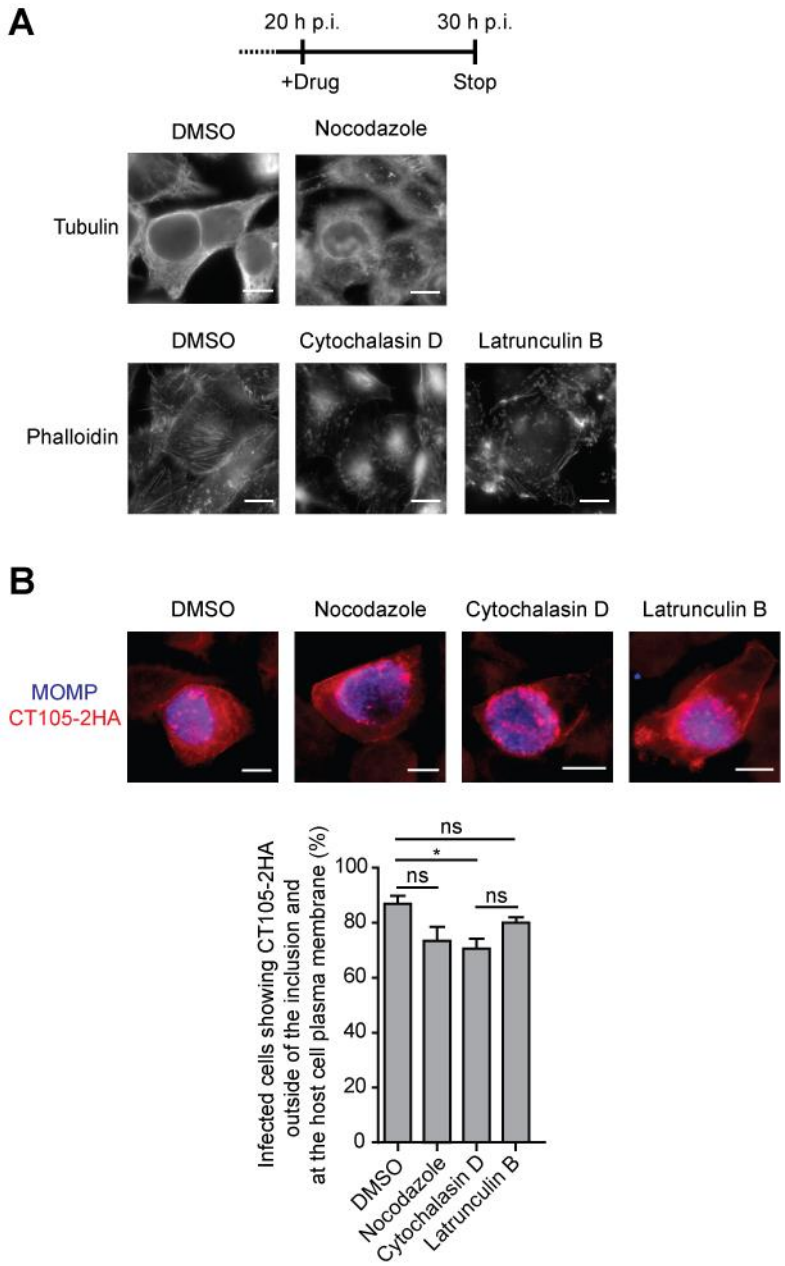

Figure 3.19 CT105-2HA changes in its subcellular localization during *C. trachomatis* infection is independent of intact host microfilaments and microtubules. HeLa cells were infected by *C. trachomatis* L2/434 encoding pCT105-2HA. At 20 h p.i., infected cells were treated with DMSO, 1 µg/ml nocodazole, 2 µM cytochalasin D or 500 nM latrunculin. At 30 h p.i., the cells were fixed with 4% (w/v) PFA or methanol. **(A)** Cells were immunolabeled with an antibody against α-tubulin and an appropriate fluorophore-conjugated secondary antibody or stained with fluorescent-conjugated phalloidin. **(B)** To enumerate cells showing CT105-2HA at the periphery of the cell/plasma membrane by fluorescence microscopy, cells were immunolabeled with antibodies against HA (red), *C. trachomatis* MOMP (blue), and appropriate fluorophore-conjugated secondary antibodies. Data are mean ± SEM of three independent experiments (n = 50). P-values were obtained by one-way ANOVA and Bonferroni post-test analyses; *statistical significant ($P < 0.05$); ns, not significant. Cells were imaged by fluorescence microscopy. Scale bars, 10 µm.

3.2.7 The localization of bacterially-delivered CT105-2HA at the host cell plasma membrane is independent of the timing of the protein expression during the *C. trachomatis* developmental cycle

Moreover, we analyzed whether the delivery and subcellular localization of CT105-2HA at the plasma membrane required expression of CT105-2HA at a specific stage on the developmental cycle of *C. trachomatis*. HeLa cells were infected with *C. trachomatis* L2/434 harboring pTet-CT105-2HA and anhydrotetracycline was not added (-Tet) or added to 20 ng/mL (+Tet) at time 0 h, 20 h, and 30 h p.i. (Figure 3.20) to induce CT105-2HA expression. At 40 h p.i. cells were fixed, immunolabeled with antibodies against HA, GM130 and *C. trachomatis* MOMP and analyzed by fluorescence microscopy. At the different times of induction, pTet-CT105-2HA localized at the host cell plasma membrane similarly to pCT105-2HA expressed under the control of *ct105* endogenous promoter (Figure 3.20). This indicates that the subcellular localization of CT105-2HA at the plasma membrane is not dependent on timing of the protein expression during the developmental stage of *C. trachomatis*.

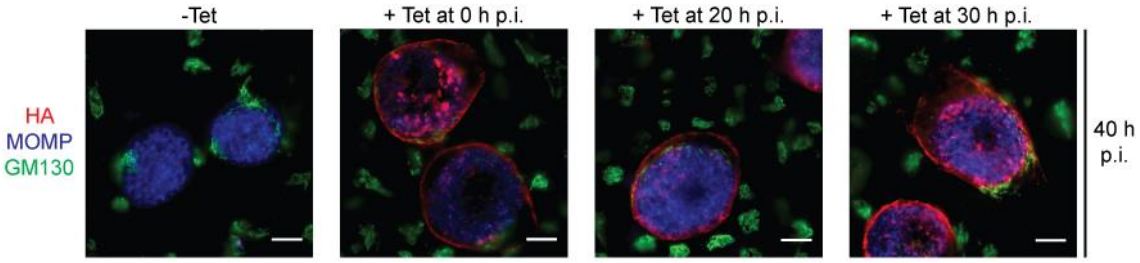

Figure 3.20 Bacterially-translocated CT105-2HA localizes at the host cell plasma membrane regarding the timing of its expression by *C. trachomatis*. HeLa cells were infected by *C. trachomatis* L2/434 harboring pTet-CT105-2HA. Anhydrotetracycline was not added (-Tet) or added to 20 ng/mL (+Tet) at 0, 20 or 30 h p.i.. At 40 h p.i. cells were fixed with 4% (w/v) PFA and immunolabeled with antibodies against HA (red), *C. trachomatis* MOMP (blue), GM130 (green) and appropriate fluorophore-conjugated secondary antibodies. Cells were imaged by fluorescence microscopy. Scale bars, 10 µm.

3.2.8 The first 100 amino acid residues of CT105 are sufficient to target the protein to the Golgi of uninfected mammalian cells

To map the regions of CT105 that could determine its different localizations within the cytoplasm of mammalian cells, we started by constructing transfection plasmids encoding full-length CT105 fused to the C- or N-termini of mEGFP (mEGFP-CT105$_{FL}$ and CT105$_{FL}$-mEGFP, respectively) or CT105-2HA. HeLa cells were transfected for 24 h with the constructed plasmids and immunoblotting of whole cell extracts confirmed the production of proteins of the predicted molecular mass (Figure 3.21A). Analysis of the transfected cells by fluorescence microscopy, showed that mEGFP-CT105$_{FL}$, CT105$_{FL}$-mEGFP, or CT105-2HA localized predominantly at the periphery of the cell (Figure 3.21B), recapitulating a main localization of CT105-2HA in cells infected by *C. trachomatis* for 30 h or 40 h (Figure 3.16 and 3.17).

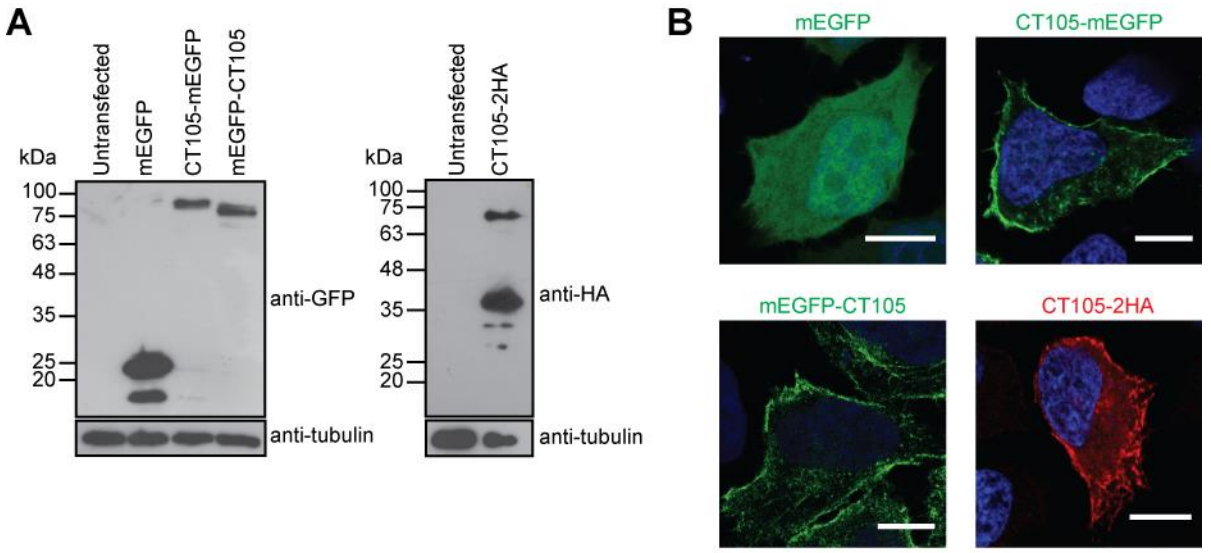

Figure 3.21 Ectopic expression of CT105 in HeLa cells. HeLa cells were either left untransfected or transfected for 24 h with plasmids encoding monomeric EGFP (mEGFP), CT105 fused to the C-terminus of mEGFP (mEGFP-CT105), CT105 fused to the N-terminus of mEGFP (CT105-mEGFP), and CT105 with a double hemagglutinin tag at its C-terminus (CT105-2HA) **(A)** Total extracts of the indicated untransfected or transfected cells were analyzed by immunoblotting with antibodies against GFP, HA and α-tubulin (HeLa loading control) using SuperSignal® West Pico detection kit (Thermo Fisher Scientific). **(B)** Cells were fixed with 4% (w/v) PFA, stained with DAPI (blue), and immunolabeled with an antibody against HA (red) and the appropriate fluorophore-conjugated secondary antibody. Scale bars, 10 µm.

We then constructed plasmids encoding different truncated/mutated versions of CT105 fused to the C-terminus of mEGFP (mEGFP-CT105$_{1\text{-}100}$, mEGFP-CT105$_{\Delta 100}$, mEGFP-CT105$_{1\text{-}320}$, mEGFP-CT105$_{\Delta 320}$, mEGFP-CT105$_{\Delta 100\text{-}320}$, or mEGFP-CT105$_{PDZ}$) (Figure 3.22A). Examination of the primary structure of CT105 revealed no predicted transmembrane domains or other obvious targeting motifs, except for a possible Postsynaptic Density95/Disc Large/Zonula Occludens-1 (PDZ) domain at the C-terminus of CT105 consisting in 3 amino acid residues (Ser-Ser-Ile) (Mu *et al.*, 2014), which is thought to be involved in protein-protein interactions. Therefore, the truncations were designed only considering the predicted secondary structure of CT105 [deduced using JPred4; (Drozdetskiy *et al.*, 2015)] and the mutation of the possible PDZ domain comprised the substitution of the three relevant amino acids residues by alanines. HeLa cells were then transfected with plasmids encoding mEGFP-CT105$_{FL}$ (predicted molecular mass of 96 kDa) mEGFP-CT105$_{1\text{-}100}$ (38 kDa), mEGFP-CT105$_{\Delta 100}$ (86 kDa) mEGFP-CT105$_{1\text{-}320}$ (60 kDa), mEGFP-CT105$_{\Delta 320}$ (65 kDa), mEGFP-CT105$_{\Delta 100\text{-}320}$ (74 kDa), or mEGFP-CT105$_{PDZ}$ (96 kDa). Immunoblotting of whole cell extracts confirmed the production of mEGFP-CT105$_{FL}$, mEGFP-CT105$_{1\text{-}100}$, mEGFP-CT105$_{\Delta 100}$, mEGFP-CT105$_{\Delta 100\text{-}320}$, mEGFP-CT105$_{\Delta 320}$ and mEGFP-CT105$_{PDZ}$ proteins of the predicted molecular mass (Figure 3.22B). The production of mEGFP-CT105$_{1\text{-}320}$ and mEGFP- CT105$_{\Delta 320}$ proteins of the predicted molecular mass was not detected (Figure 3.22B), and they were not further analyzed. HeLa cells ectopically expressing mEGFP-CT105$_{FL}$, mEGFP-CT105$_{1\text{-}100}$, mEGFP-CT105$_{\Delta 100}$, mEGFP-CT105$_{\Delta 100\text{-}320}$ or mEGFP-CT105$_{PDZ}$ were fixed, immunolabeled with antibodies against GM130, and enumerated by fluorescence microscopy for localization of the fusion protein at the cell periphery and at the Golgi. mEGFP-CT105$_{FL}$ localized near the plasma membrane in 68 ± 8% of the transfected cells, and at the Golgi in 7 ± 2% of the transfected cells (Figure 3.22C and 3.22D). However, the fluorescent signal was generally weak in the Golgi region (Figure

3.22C). Strikingly, mEGFP-CT105$_{1-100}$ localized at the Golgi region in almost all transfected cells (98 ± 1%) and was not detected at the plasma membrane (Figure 3.22C and 3.22D). In contrast, mEGFP-CT105$_{\Delta100}$ was mostly cytosolic and was never seen at the Golgi complex and only seldom (2 ± 0%) near the plasma membrane (Figure 3.22C and 3.22D). mEGFP-CT105$_{\Delta100-320}$ showed a punctate/vesicular appearance with reduced localization at the Golgi (4 ± 1%) or plasma membrane (18 ± 1%), particularly when compared with mEGFP-CT105$_{\Delta100}$ or mEGFP-CT105$_{FL}$ (Figure 3.22C and 3.22D). mEGFP-CT105$_{PDZ}$ had similar localization as mEGFP-CT105$_{FL}$ and localized near the plasma membrane in 64 ± 3% of the transfected cells, and at the Golgi in 6 ± 3% of the transfected cells (Figure 3.22C and 3.22D). Similar observations were made in HeLa cells ectopically expressing truncated versions of CT105 fused to the N-terminus of mEGFP (Figure 3.23).

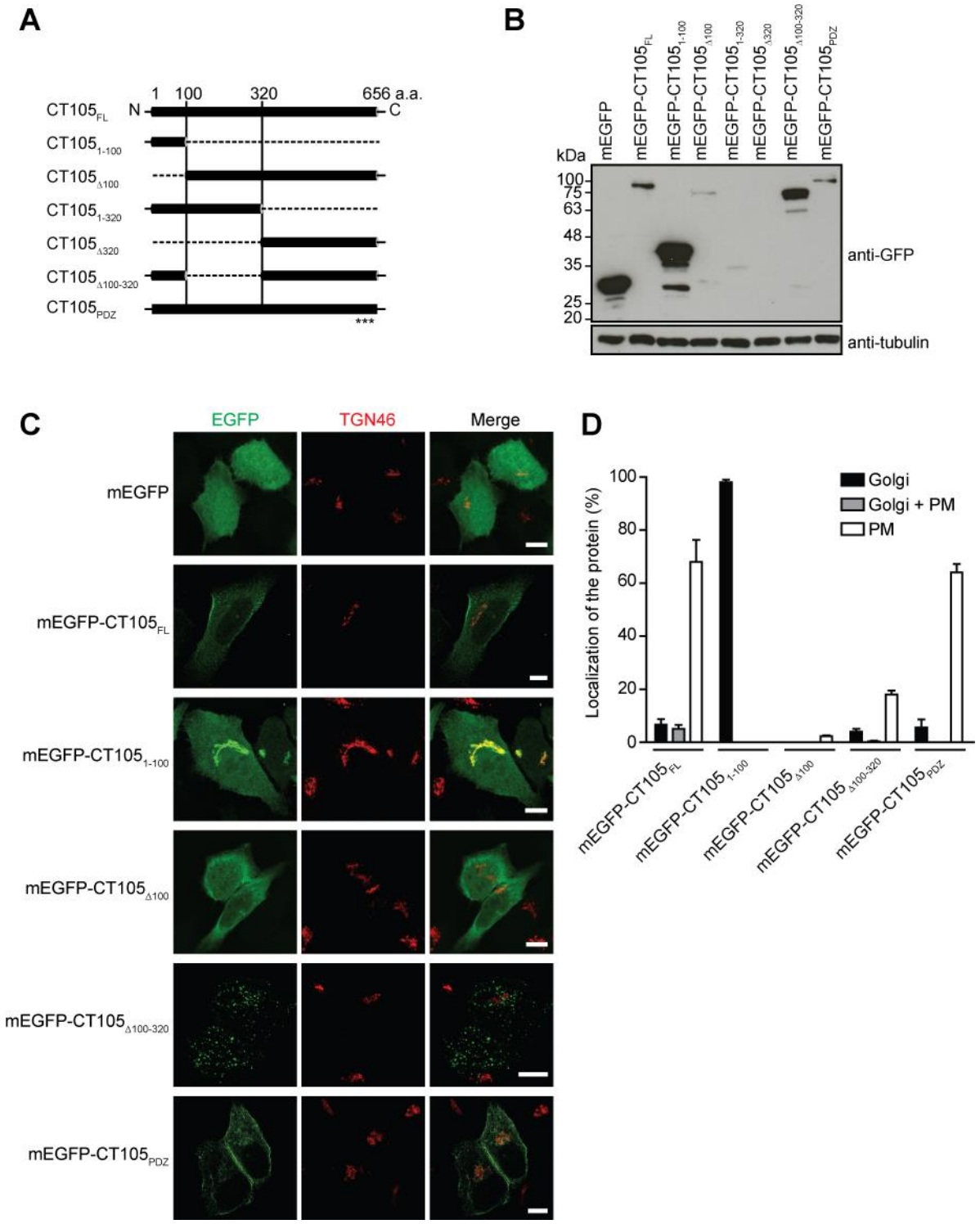

Figure 3.22 The first 100 amino acids of CT105 are targeted to the Golgi complex. HeLa cells were transfected for 24 h with plasmids encoding monomeric EGFP (mEGFP) or different versions of CT105 fused to the C-terminus of mEGFP. **(A)** Schematic representation of the mEGFP-CT105 proteins analyzed. **(B)** Total extracts of transfected cells were analyzed by immunoblotting with antibodies against GFP and α-tubulin (HeLa loading control) using SuperSignal® West Pico detection kit (Thermo Fisher Scientific). **(C)** Transfected cells were fixed with 4% (w/v) PFA, labeled with antibodies against TGN46 (red) and the appropriate fluorophore-conjugated secondary antibody, and imaged by confocal fluorescence microscopy. Images correspond to single *z* sections. Scale bars, 10 µm. **(D)** Cells immunolabeled as described in **(C)** were enumerated by fluorescence microscopy for localization of mEGFP-CT105 only at the Golgi, only at the plasma membrane (PM), or both at the Golgi and plasma membrane (Golgi + PM). Data are mean ± standard error of the mean of three independent experiments (n=100).

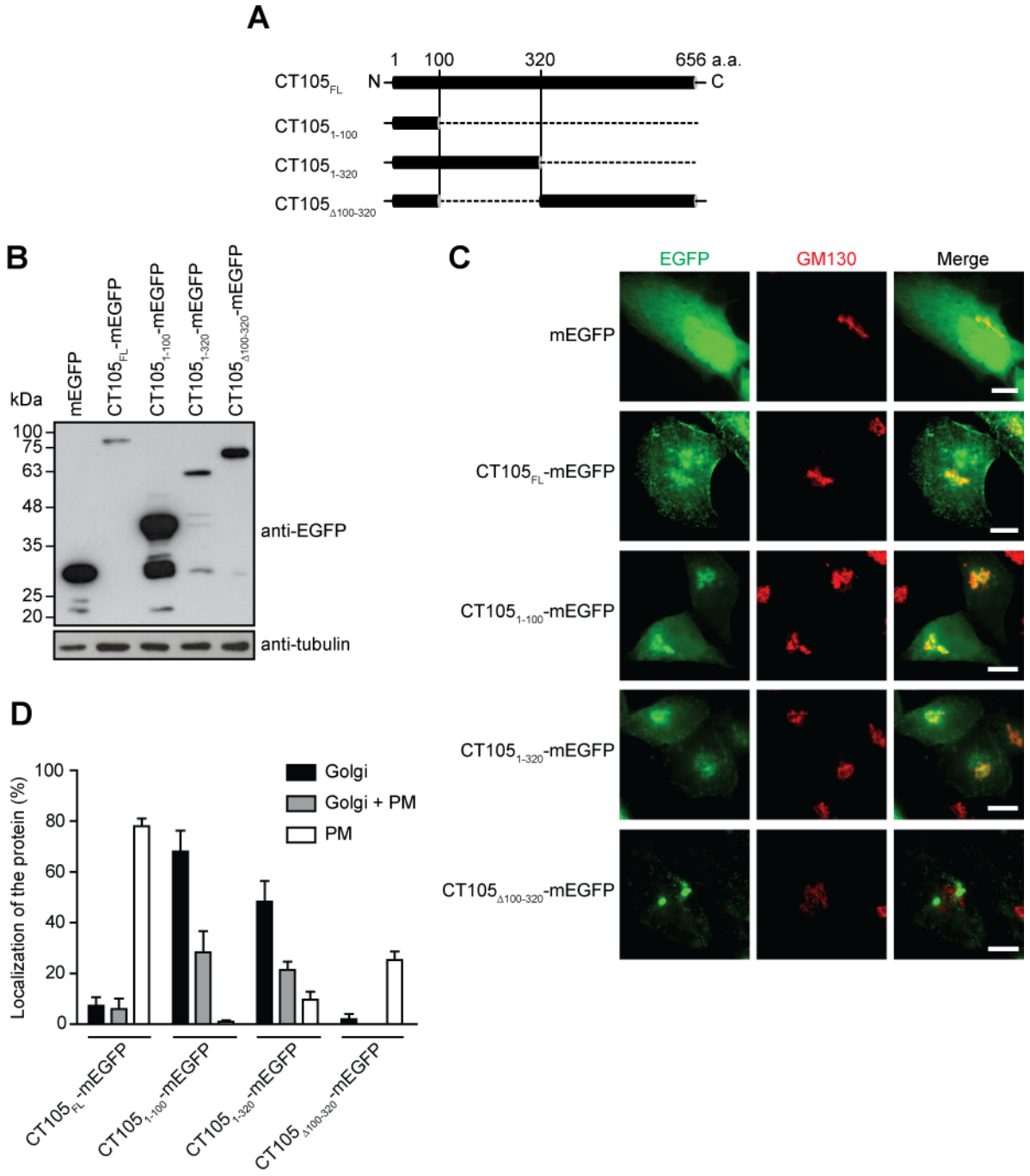

Figure 3.23 CT105 fusions to the N-terminus of mEGFP. HeLa cells were transfected for 24 h with plasmids encoding monomeric EGFP (mEGFP) or different versions of CT105 fused to the N-terminus of mEGFP. **(A)** Schematic representation of the CT105-mEGFP proteins analyzed. **(B)** Total extracts of transfected cells were analyzed by immunoblotting with antibodies against GFP and α-tubulin (HeLa loading control) using SuperSignal® West Pico detection kit (Thermo Fisher Scientific). **(C)** Transfected cells were fixed with 4% (w/v) PFA, labeled with antibodies against GM130 (red) and the appropriate fluorophore-conjugated secondary antibody, and imaged by confocal fluorescence microscopy. Images correspond to single *z* sections. Scale bars, 10 µm. **(D)** Cells immunolabeled as described in **(C)** were enumerated by fluorescence microscopy for localization of mEGFP-CT105 only at the Golgi, only at the plasma membrane (PM), or both at the Golgi and plasma membrane (Golgi + PM). Data are mean ± standard error of the mean of three independent experiments (n=100).

To confirm the association of mEGFP-CT105$_{1-100}$ with the Golgi, and to analyze its localization within the Golgi complex, HeLa cells that had been transfected for 24 h were either incubated for 1 h with BFA or DMSO (as control), and then fixed. In addition, the transfected cells were incubated for 1 h with BFA,

washed out from the BFA, incubated for 1 h, and fixed. The cells were then immunolabeled with antibodies against GM130 or TGN46 and analyzed by fluorescence microscopy. In the control DMSO-treated cells, mEGFP-CT105$_{1-100}$ localized at the Golgi region, and showed significant co-localization with TGN46 (Figure 3.24B) but not with GM130 (Figure 3.24A). BFA-induced Golgi fragmentation resulted in near complete dispersion of the fluorescence signal of mEGFP-CT105$_{1-100}$ (Figure 3.24A and 3.24B). However, BFA-induced Golgi fragmentation followed by BFA wash out revealed again a compact Golgi complex and mEGFP-CT105$_{1-100}$ in that region mostly co-localizing with TGN46 (Figure 3.24B) but not with GM130 (Figure 3.24A), as observed in the DMSO-treated cells.

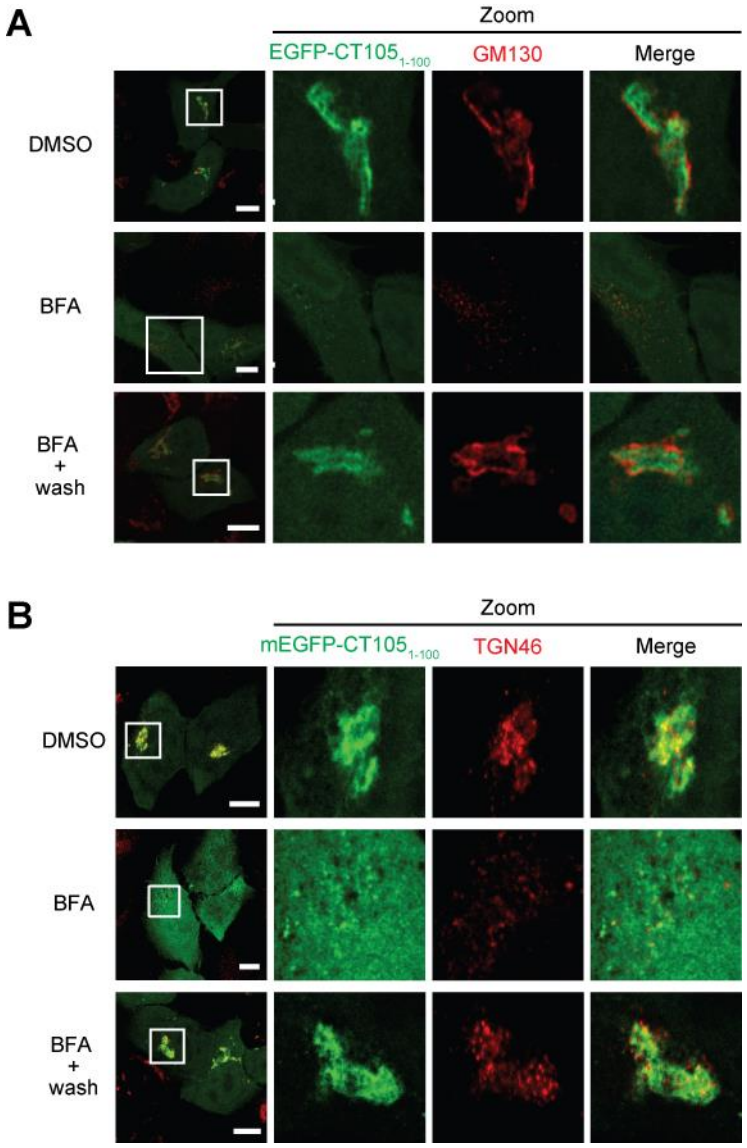

Figure 3.24 The first 100 amino acids of CT105 associate with the *trans*-Golgi. HeLa cells were transfected for 24 h with plasmids encoding mEGFP-CT105$_{1-100}$. Cells were treated for 1 h with DMSO or 1 µg/ml BFA. Then, the cells were either fixed with 4% (w/v) PFA (upper and middle panels) or washed with complete medium lacking BFA and incubated for an additional 1 h and then fixed with 4% (w/v) PFA (lower panels). The fixed cells were immunolabeled with antibodies against **(A)** GM130 (red) or **(B)** TGN46 (red), and the appropriate fluorophore-conjugated secondary antibody, and examined by confocal fluorescence microscopy. Images correspond to single *z* sections. In the area delimited by a white square (left-side panels) images were zoomed (right-side panels). Scale bars, 10 µm.

To test the importance of the different regions of CT105 for its localization in infected cells, HeLa cells were infected by *C. trachomatis* strains harboring full-length CT105 (pTet-CT105-2HA), and truncations of CT105 containing the first 100 amino acids (pTet-CT105$_{1\text{-}100}$-2HA, pTet-CT105$_{1\text{-}320}$-2HA, pTet-CT105$_{\Delta 100\text{-}320}$-2HA), as they include the T3S signal (Figure 3.5 and 3.6) and possible T3S chaperone binding sites (Woestyn *et al.*, 1996; Boyd *et al.*, 2000). At 20 h and 40 h p.i., cells were fixed and immunolabeled for HA and Cap/CT5291 (chlamydial protein localized at the inclusion membrane) and analyzed by fluorescence microscopy (Figure 3.25). Although all the proteins were expressed, neither of them was detected in the cytoplasm of host cell, and therefore we could not proceed with the analysis of the role of the different regions of CT105 in subcellular targeting during *C. trachomatis* infection.

Altogether, these results showed that ectopically expressed full-length CT105 (mEGFP-CT105$_{FL}$, CT105$_{FL}$-mEGFP, and CT105-2HA) and mutated CT105 at the PDZ domain (mEGFP-CT105$_{PDZ}$) mostly localized near the plasma membrane and mEGFP-CT105$_{1\text{-}100}$ at the Golgi, generally recapitulating the localization of CT105-2HA in infected cells. As mEGFP-CT105$_{1\text{-}100}$ showed a striking association with the TGN in uninfected cells, the first 100 amino acids of CT105 should contain a Golgi-targeting region.

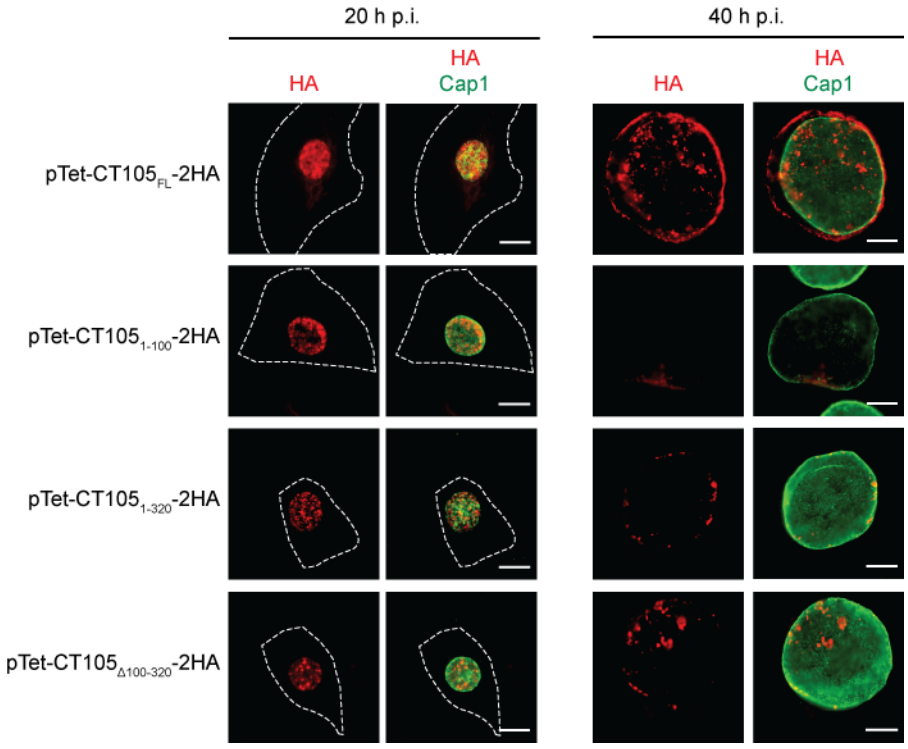

Figure 3.25 *C. trachomatis* L2/434 strains harboring plasmids encoding truncated versions of CT105 were not detected in the host cell cytoplasm. HeLa cells were infected with *C. trachomatis* L2/434 harboring pTet-C105-2HA, pTet-CT105$_{1\text{-}100}$-2HA, pTet-CT105$_{1\text{-}320}$-2HA and pTet-CT105$_{\Delta 100\text{-}320}$-2HA, and at time zero of infection anhydrotetracycline was added to 20 ng/mL. At 20 h and 40 h p.i., cells were fixed with 4% (w/v) PFA and immunolabeled with antibodies against HA (red), *C. trachomatis* Cap1 (chlamydial protein located at the inclusion membrane; green) and appropriate fluorophore-conjugated secondary antibodies. Cells were imaged by fluorescence microscopy. Scale bars, 10 µm.

3.2.9 CT105 appears in filamentous structures within host cells

In addition to the localization of CT105 at the Golgi and at the plasma membrane during *C. trachomatis* infection, CT105 appeared in filamentous structures in the host cell, which could be observed at 20 h p.i. but that become more visible in later times of infection (30 h and 40 h p.i.). These filamentous structures appeared spread in the host cell, were not associated with the inclusion membrane, and were reminiscent of host cytoskeletal filaments. Therefore, HeLa cells were infected by *C. trachomatis* harboring pTet-CT105-2HA for 30 h, fixed and labeled with antibodies against α-tubulin or vimentin to detect microtubules and intermediate filaments, respectively, or with fluorescent-conjugated phalloidin to stain the F-actin. However, significant co-localization of the filamentous CT105-2HA with the labeled host cytoskeleton components was not observed (Figure 3.26A). In addition, several other host cell proteins were labeled [endoplasmic reticulum (KDEL and PDI), Golgi (GM130, TGN46, Mannosidase II), early endosomes (EEA1), lysosomes (LAMP1 and LAMP3/CD63), cation-dependent mannose 6-phosphate receptor (CD-M6PR) and transferrin (Trf); data not shown)] but significant co-localization with filamentous CT105-2HA was not observed.

When HeLa cells were transfected by 24 h with plasmids encoding mEGFP-CT105, similar filamentous structures could be observed (Figure 3.26B). Moreover, when HeLa cells were infected with *C. trachomatis* L2/434 encoding pTet-CT105-2HA and transfected with a plasmid encoding mEGFP-CT105, fixed 24 h p.i. and immunolabeled with antibodies against HA and C*. trachomatis* MOMP, the filamentous CT105-2HA and filamentous mEGFP-CT105 co-localize (Figure 3.26C). Overall this suggests that CT105 forms filamentous structures that are not dependent on additional *C. trachomatis* factors but which seemingly do not significantly co-localized with the tested host cell markers.

Summarizing, a CT105-2HA immunofluorescence signal was detected in the host cell at 16 - 20 h p.i, where it mostly associated at the Golgi complex; as the infection progressed, at 30 and 40 h p.i., CT105-2HA predominately localized at the host cell plasma membrane. This change in the localization of CT105-2HA during infection was found to be independent of intact microfilaments or microtubules. In addition, we identified a Golgi targeting region within CT105 comprising the first 100 amino acid residues of the protein.

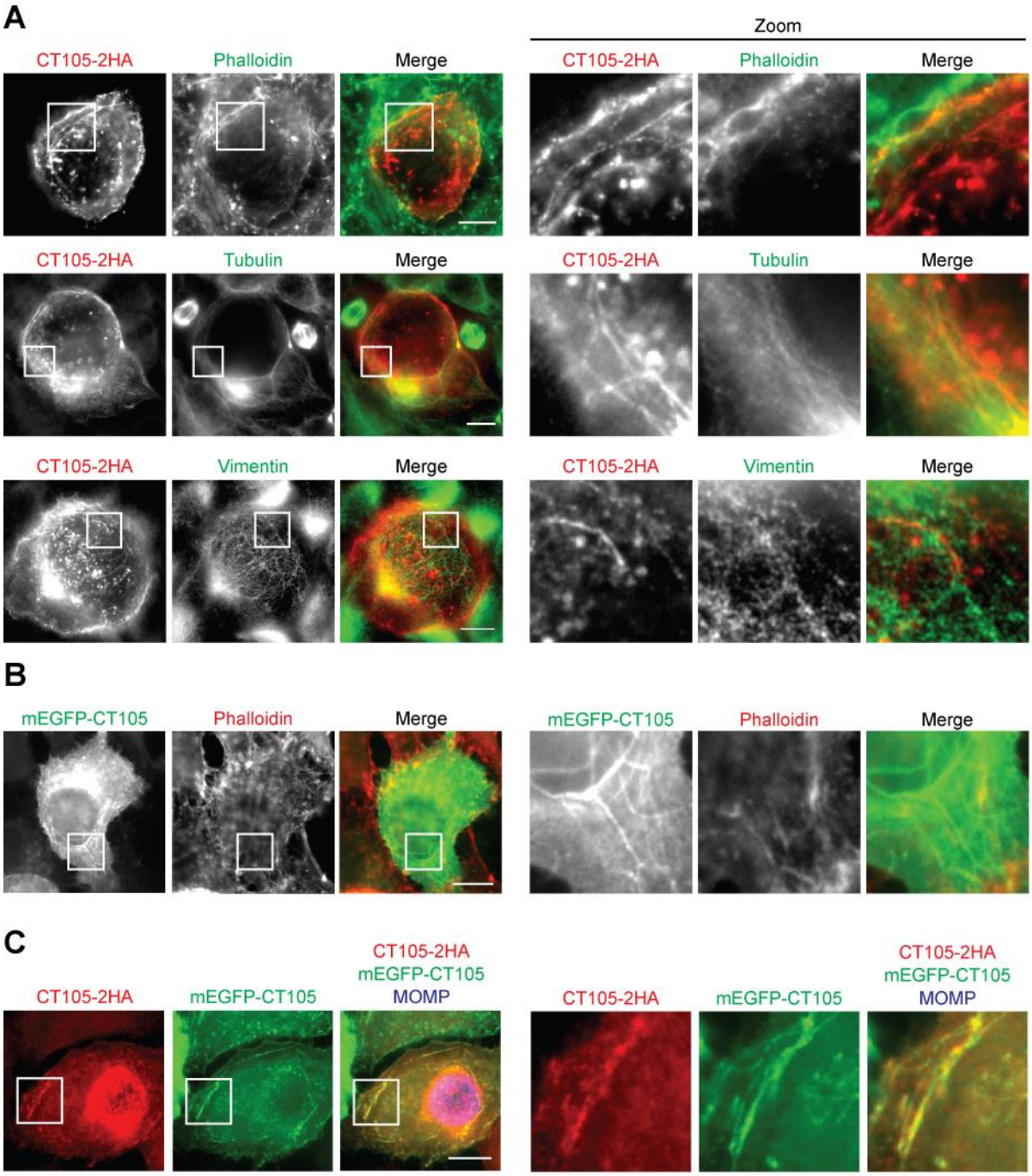

Figure 3.26 CT105 localizes in filamentous structures in non-infected and *Chlamydia*-infected cells. HeLa cells were infected *C. trachomatis* L2/434 harboring pTet-C105-2HA and at time zero of infection anhydrotetracycline was added to 20 ng/mL. At 40 h p.i., cells were fixed with 4% (w/v) PFA or methanol and immunolabeled with antibodies against HA (red) and stained/immunolabeled for the host cell cytoskeleton components (fluorescent-conjugated phalloidin or antibodies against α-tubulin and vimentin and appropriate fluorophore-conjugated secondary antibodies; green). **(B)** HeLa cells were transfected for 24 h with a plasmid encoding mEGFP-CT105, fixed with 4% (w/v) PFA and stained with fluorescent-conjugated phalloidin. **(C)** HeLa cells were infected with *C. trachomatis* L2/434 encoding pTet-CT105-2HA and transfected with a plasmid encoding mEGFP-CT105. At time zero of infection anhydrotetracycline was added to 20 ng/mL. At 24 p.i., cells were fixed with 4% (w/v) PFA, and immunolabeled with antibodies against HA (red) and *C. trachomatis* MOMP (blue), and appropriate fluorophore-conjugated secondary antibodies. Cells were imaged by fluorescence microscopy. In the area delimited by a white square (left-side panels) images were zoomed (right-side panels). Scale bars, 10 µm.

3.3 THE *CHLAMYDIA TRACHOMATIS* EFFECTOR CT105 CAN INTERFERE WITH VESICULAR TRAFFICKING IN EUKARYOTIC CELLS

We have identified CT105 as a novel *C. trachomatis* T3S substrate that is delivered into the host cell and localizes at host cell Golgi and plasma membrane during *C. trachomatis* infection. However, to designate CT105 as a T3S effector of *C. trachomatis* its function must be investigated. Although its subcellular localization has been determined, little can be inferred on the CT105 function during infection, as other bacterial T3S effectors with a Golgi localization display a variety of functions and activities such as induction of Golgi fragmentation, activity of an ubiquitin E3 ligase, interference with vesicular trafficking, causing microtubule destabilization, inactivating the host inflammasome or suppressing the host immune system (Salcedo and Holden, 2003; Gruenheid *et al.*, 2004; Tomson *et al.*, 2005; Shaw *et al.*, 2005; Jinoh Kim *et al.*, 2007; Thanabalasuriar *et al.*, 2010; Clements *et al.*, 2011; Yen *et al.*, 2015; Lin *et al.*, 2015; Yu *et al.*, 2016; Bayer-Santos *et al.*, 2016). Here, we used the recently developed methodologies to genetically manipulate *C. trachomatis* to construct and characterize a *C. trachomatis ct105* mutant strain (Johnson and Fisher, 2013). In addition we used *Saccharomyces cerevisiae,* an eukaryotic model organism previously used in the study of bacterial effector proteins (Curak *et al.*, 2009), to phenotypically characterize the effects of overexpression of CT105.

3.3.1 CT105 is not essential for intracellular replication of *C. trachomatis* in infected tissue culture cells.

To examine the importance of CT105 during the infection of tissue culture cells by *C. trachomatis*, a L2/434-derived strain where the *ct105* gene was inactivated by an insertion between nucleotides 261 and 262 of a modified group II intron containing a spectinomycin-resistance gene (*aadA*) was constructed (Figure 3.27A). The correct insertion of the intron in the *ct105::aadA* mutant strain was verified by PCR (Figure 3.27B) and locus-specific DNA sequencing. To confirm that insertion of the intron prevented production of CT105, in the absence of a specific anti-CT105 antibody, a *C. trachomatis* strain harbouring a plasmid (pCT105::aadA-2HA; Annexes Table A1) was constructed with the *ct105::aadA* mutant allele and the sequence encoding 2HA fused to the 3´end of *ct105*, and carrying the *ct105* promoter and *incD* terminator (as in pCT105-2HA; Annexes Table A1). HeLa cells were then infected for 40 h with *C. trachomatis* L2/434 harbouring either pCT105-2HA or pCT105::aadA-2HA and analysed by immunoblotting. This confirmed that the intron insertion within *ct105-2HA* prevented production of a protein detectable with anti-HA antibodies (Figure 3.27C), suggesting that the *ct105::aadA* mutant strain should not produce CT105.

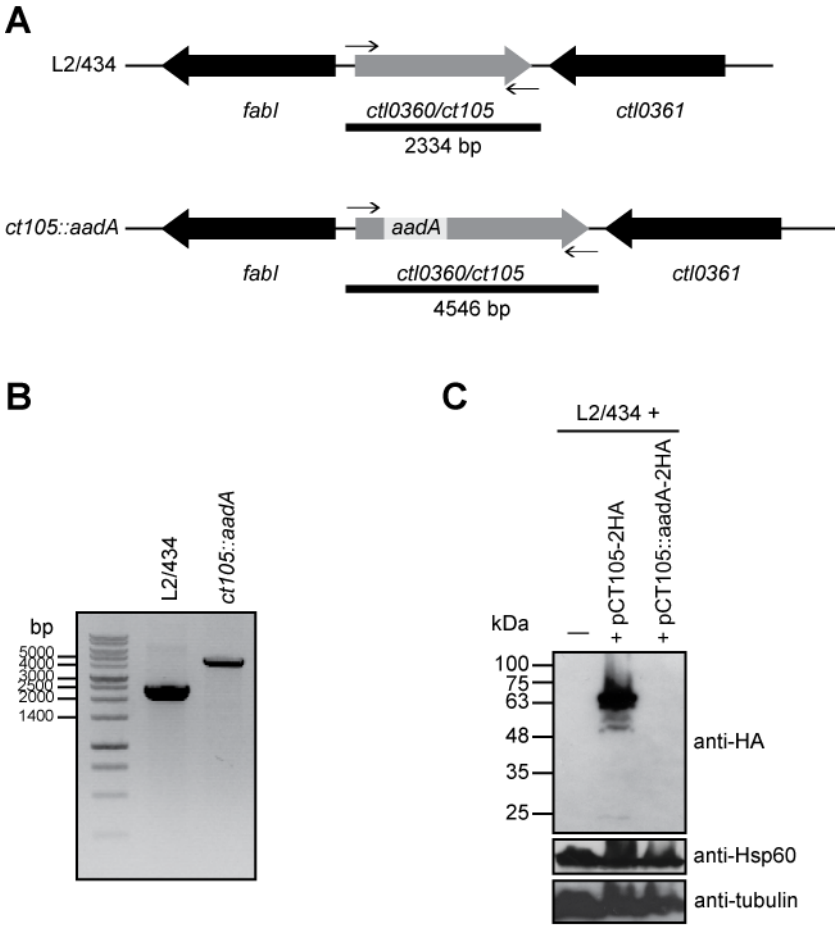

Figure 3.27 Verification of intron insertion in the *C. trachomatis ct105*::*aadA* mutant strain. A *C. trachomatis ct105*::*aadA* insertional mutant was generated in the strain L2/434 by the targeted insertion of a modified group II intron carrying a spectinomycin-resistance gene. **(A)** Representation of the *ctl0360* (orthologue of c*t105* in strain D/UW3) locus in *C. trachomatis* L2/434 and of the *ctl0360* locus in the corresponding *ct105:aadA* mutant derivative. The arrows indicate the approximate hybridization position of the DNA primers used (Annexes Table A2) in PCR reactions, yielding DNA products of the indicated length in base pairs (bp). **(B)** Agarose gel displaying the result from the PCR with the indicated primers (Annexes Table A2) and DNA templates. **(C)** Hela cells were infected by *C. trachomatis* L2/434 harboring a plasmid encoding CT105-2HA or by an identical plasmid carrying a *ct105*::*aadA*-2HA mutant allele. Whole cell extracts were analyzed by immunoblotting with antibodies against HA, *C. trachomatis* Hsp60 (bacterial loading control) and α-tubulin (HeLa loading control) using SuperSignal® West Pico detection kit (Thermo Fisher Scientific) for Hsp60 and α-tubulin, or SuperSignal® West Femto detection kit (Thermo Fisher Scientific) for HA. This experiment was performed in collaboration with Charlotte E. Key and Derek J. Fisher (Southern Illinois University, USA).

The intracellular growth of *C. trachomatis* L2/434 (parental strain), *ct105::aadA* mutant, and *ct105::aadA* mutant harboring pCT105-2HA (complemented strain) was then monitored by quantifying the production of infectious progeny during the chlamydial developmental cycle. Based on this, no significant differences between the three strains were detected (Figure 3.28A). Then, HeLa cells infected by the same strains for 24 h were fixed and immunolabeled using antibodies against *C. trachomatis* MOMP. Analysis by fluorescence microscopy revealed that the inclusion size appeared smaller in the mutant and complemented strains by comparison to the parental strain (Figure 3.28B). This was confirmed by measuring the inclusion area in cells infected by these three *C. trachomatis* strains (Figure 3.28C). Similar observations were made in cells infected by these strains for 40 h (data not shown). Because this difference in inclusion size between the mutant and the parental strain was also observed

in the complemented strain, the defect is likely not due to the absence of CT105. It is possible that intron insertion within *ct105* might have caused a polar effect in the neighboring genes. In summary, this showed that CT105 is not required for *C. trachomatis* growth in tissue culture cells.

Moreover, HeLa cells were infected by *C. trachomatis* parental, mutant or complemented strains for 20 h and cells were fixed and immunolabeled using antibodies against *C. trachomatis* MOMP and GM130 (*cis*-Golgi). In addition, considering the localization of CteG at the Golgi, we analyzed if its morphology was altered in HeLa cells infected by the *ct105::aadA* mutant, by comparison to cells infected by the parental L2/434 strain. However, significant differences in Golgi morphology were not detected between cells infected by these two *C. trachomatis* strains (Fig. 3.29A, 3.29B).

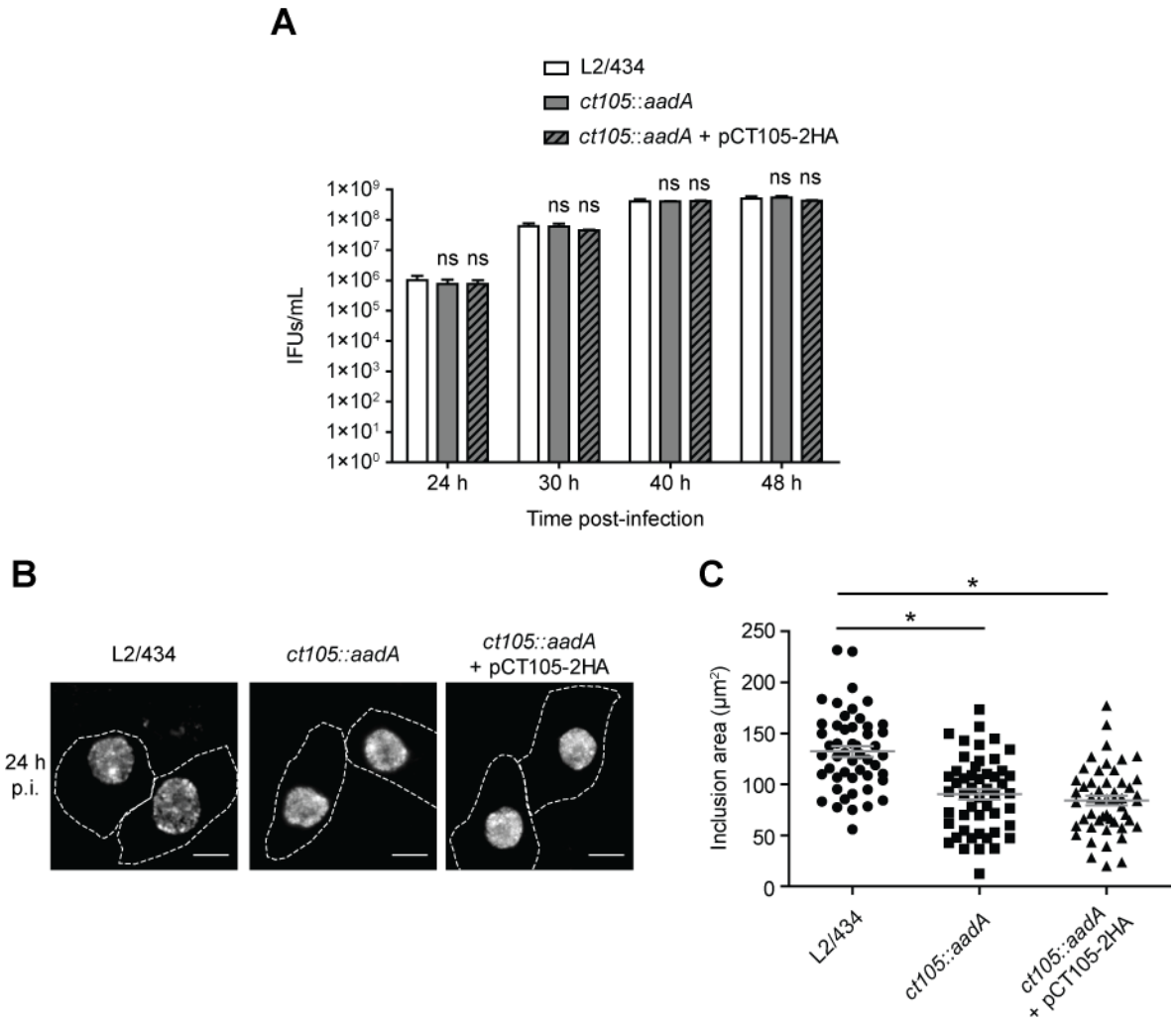

Figure 3.28 A *C. trachomatis ct105::aadA* insertional mutant is not defective for intracellular growth in tissue culture cells. HeLa cells were infected for 24, 30, or 40 h by *C. trachomatis* L2/434, *ct105::aadA* mutant or *ct105::aadA* mutant harboring pCT105-2HA at the multiplicity of infection of 1, and recoverable inclusion forming units (IFUs) were enumerated. Data ± standard error of the mean of 3 independent experiments. For each time-point, P-values were obtained by one-way ANOVA and Dunnett post-test analyses relative to the L2/434 parental strain; ns, not significant ($P \geq 0.05$). (B) Hela cells were infected for 24 h by *C. trachomatis* L2/434, *ct105::aadA* mutant, or *ct105:aadA* harbouring pCT105-2HA. Cells were fixed with methanol and labeled with goat anti-*C. trachomatis* FITC-conjugated antibody. **(C)** The inclusion area was measured (from images as those depicted in **(B)** for 50 particles randomly chosen from independent images using Fiji software. P-values were obtained by one-way ANOVA and Dunnett post-test analyses; *statistical significant ($P < 0.05$).

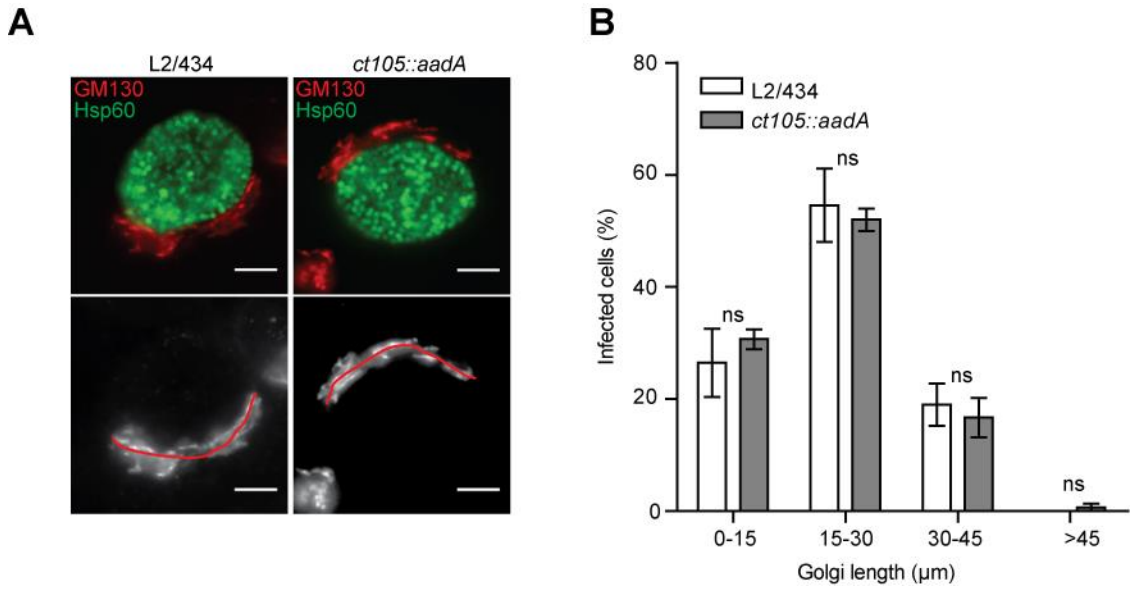

Figure 3.29 CT105 does not affect host cell Golgi morphology during infection. HeLa cells were infected by *C. trachomatis* L2/434 or *ct105::aadA* mutant for 24 h, fixed with methanol, and then immunolabeled with antibodies against GM130 (a cis-Golgi marker; red) and chlamydial Hsp60 (green), and appropriate fluorophore-conjugated secondary antibodies. **(A)** Cells were imaged by fluorescence microscopy. The length of the Golgi complex around the inclusion was measured as described (Wesolowski et al., 2017), which is illustrated by the red line. Scale bars, 5 µm. **(B)** Percentage of cells infected by *C. trachomatis* with Golgi around the inclusion of the indicated length. Data is average ± standard error of the mean from 3 independent experiments where at least 50 infected cells were analyzed for each strain. P-values were calculated by a two-tailed unpaired Student's *t*-test; ns, not significant (P > 0.05). This experiment was performed in collaboration with Inês Serrano Pereira (PhD student in the host laboratory).

3.3.2 CT105 induces a vacuolar protein sorting defect when ectopically expressed in *S. cerevisiae*

Given the localization of CT105 at the Golgi and plasma membrane in both infected and transfected mammalian cells, we hypothesized that the protein could interfere with eukaryotic vesicular trafficking. To test this, we asked if CT105 could cause a vacuolar protein sorting (VPS) defect in *S. cerevisiae* (Shohdy *et al.*, 2005), an eukaryotic model organism that has been often used to study bacterial effector proteins (Curak *et al.*, 2009). The VPS assay consists in a yeast reporter strain NSY01 (Annexes Table A3) that produces a hybrid protein composed of carboxypeptidase Y and Invertase (CPY-Inv), which normally travels to the yeast vacuole but goes to the cell surface if trafficking is disrupted. As strain NSY01 does not produce endogenous Invertase, an enzyme that hydrolyzes sucrose into glucose and fructose, normal (Vps^+) or aberrant (Vps^-) trafficking of CPY-Inv can be scored by using an agar overlay solution indicating glucose production at the cell surface by formation of a brown precipitate (Vps^+, white colonies; Vps^-, brown colonies) (Shohdy *et al.*, 2005).

Strain NSY01 was transformed with yeast expression plasmids encoding either CT105 fused to the N-terminus or C-terminus of GFP (CT105-GFP or GFP-CT105, respectively) under the control of a galactose inducible promoter (Figure 3.30A). The controls used were a NSY01 derivative strain that expressed only GFP (Figure 3.30A), which leads to a Vps^+ phenotype (Franco *et al.*, 2012), and NSY01 derivative strains expressing a dominant-negative form of the yeast ATPase Vps4 ($Vps4^{E233Q}$) (Babst *et al.*, 1998) or the *Legionella pneumophila* effector protein VipA (Figure 3.30A), both known to cause a Vps^- phenotype (Shohdy *et al.*, 2005; Franco *et al.*, 2012). In the qualitative colorimetric enzymatic assay

in solid media, it was consistently observed that GFP-CT105 or CT105-GFP induced a Vps$^-$ phenotype (Figure 3.30B). In addition, quantitative analyses in liquid media were performed and the amounts of secreted and total invertase were assessed for each strain. In this assay, both GFP-CT105 and CT105-GFP caused an increase in the levels of secreted invertase (relative to those of the control strains expressing GFP or Vps4^{E233Q}), but the difference was only statistically significant for GFP-CT105 (Figure 3.30C).

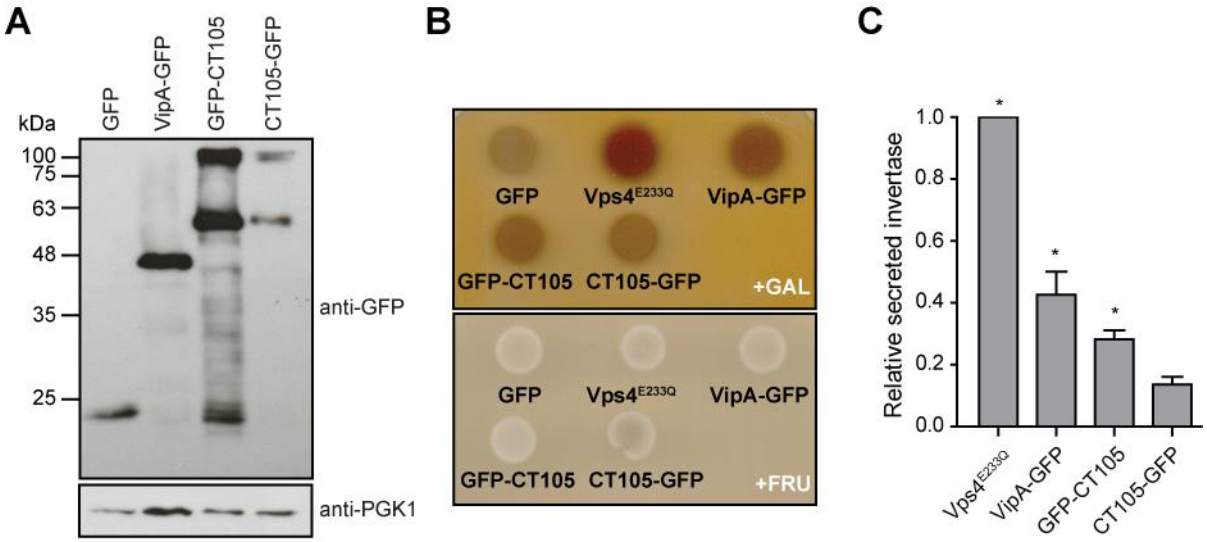

Figure 3.30 CT105 induces a vacuolar protein sorting defect in *S. cerevisiae*. *S. cerevisiae* reporter strain NSY01 producing CPY-invertase (Annexes Table A3) was transformed with plasmids encoding GFP, VipA-GFP, GFP-CT105, or CT105-GFP, where their expression is induced by 2% (w/v) galactose. A NSY01 derivative strain encoding a dominant-negative form of the yeast ATPase Vps4 (Vps4^{E233Q}) was also used. **(A)** Whole cell extracts of *S. cerevisiae* NSY01 producing the indicated proteins were analyzed by immunoblotting with antibodies against GFP and PGK1 (yeast loading control), using SuperSignal® West Pico detection kit (Thermo Fisher Scientific). **(B)** *S. cerevisiae* NSY01 strains encoding the indicated proteins were grown in solid medium in the presence of 2% (w/v) galactose (inducing conditions, +GAL) or in the presence of 2% (w/v) fructose (non-inducing conditions; +FRU). The vacuolar protein sorting (VPS) phenotype was analyzed using a sucrose overlay to assess activity of secreted invertase. A vacuolar protein sorting defect (VPS$^-$) leads to the formation of a brown precipitate. **(C)** *S. cerevisiae* NSY01 strains encoding the indicated proteins were grown in liquid medium in the presence of 2% (w/v) galactose (inducing conditions) and the relative activity of secreted invertase was quantified (see Materials and Methods). Data are mean ± standard error of the mean of five independent experiments. P-values were obtained by one-way ANOVA and Dunnett post-test analyses relative to GFP (0% of relative secreted invertase; not shown); *statistical significant ($P < 0.05$); ns, not significant.

After growing the previously described *S. cerevisiae* NSY01 strains in inducing galactose-supplemented agar plates (inducing conditions) we observed by fluorescence microscopy that GFP-CT105 and CT105-GFP localized in puncta in the yeast cytoplasm, although for GFP-CT105 the protein was mainly cytosolic (Figure 3.31A). Nevertheless, neither of the CT105 fusions was detected at the yeast plasma membrane. Furthermore, after growth of the strains in liquid media containing glucose, they were serially-diluted and plated on fructose-supplemented (non-inducing conditions; +FRU) and galactose-supplemented (inducing conditions; +GAL) agar plates. After incubation at 30°C for 3 days, yeast growth was similar between non-inducing and inducing conditions (Figure 3.31B) in each of the analyzed strains suggesting that overexpression of GFP, GFP-CT105 or CT105-GFP is not toxic and does not affect yeast growth, in contrast with previous observations (Sisko *et al.*, 2006). Also, this

indicated that the induction of the VPS defect by CT105 was not a consequence of an overall impact on yeast physiology.

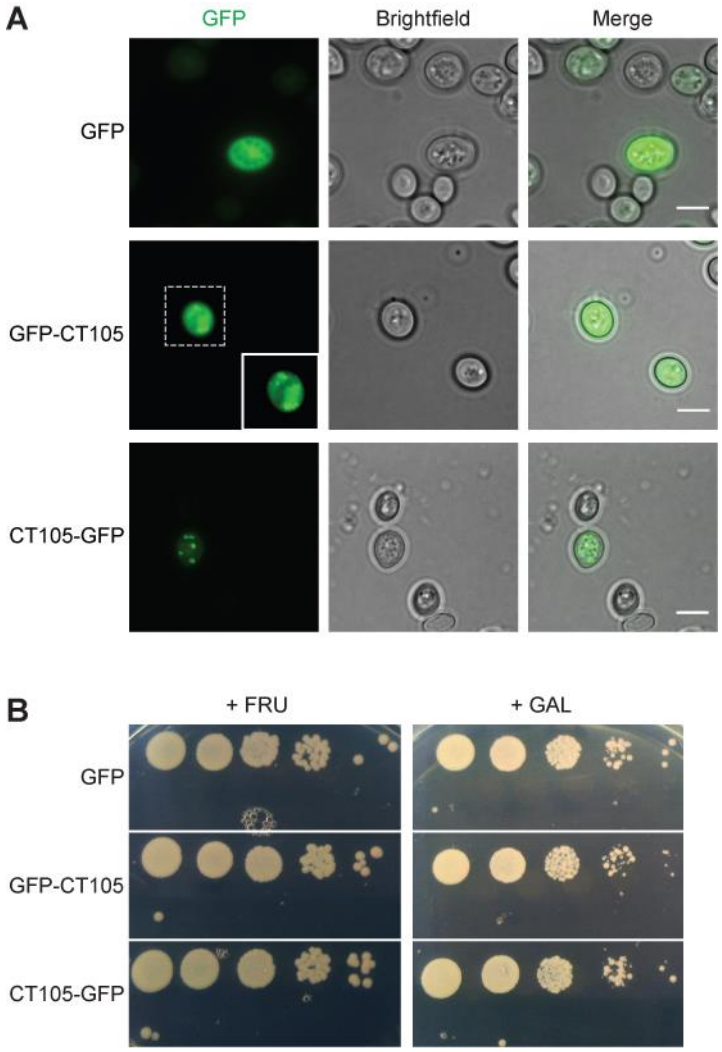

Figure 3.31 Phenotypic characterization of *S. cerevisiae* strains expressing CT105. (A) *S. cerevisiae* NSY01 strains harboring plasmids encoding GFP, GFP-CT105, or CT105-GFP were grown in 2% (w/v) galactose supplemented agar plates and cells were imaged by brightfield and fluorescence microscopy. White square shows zoomed region. Scale bars 5 μm. **(B)** *S. cerevisiae* NSY01 strains harboring plasmids encoding GFP, GFP-CT105, or CT105-GFP were grown to late log phase in 2% (w/v) glucose. Dilutions of 10-fold were spotted onto 2% (w/v) fructose (non-inducing conditions; +FRU) and 2% (w/v) galactose (inducing conditions; +GAL) supplemented agar plates and incubated at 30°C for 3 days.

In summary, CT105 was found as a non-essential gene of *C. trachomatis* infection in tissue cell culture model. However, ectopic expression of CT105 in *S. cerevisiae* induced a VPS defect, suggesting that this *C. trachomatis* protein could interfere with vesicular trafficking in infected cells. Furthermore, this is not a consequence of an overall toxic effect of CT105 in yeast cells.

4 DISCUSSION AND CONCLUSIONS

The main goal of this project was the identification and characterization of novel type III secretion (T3S) effectors of *Chlamydia trachomatis* using the techniques available to genetically modify these bacteria. Here, we have identified and characterized CT105 as a novel type III secretion (T3S) effector protein of *C. trachomatis* and as the first chlamydial effector known to be targeted to the Golgi complex of infected host cells. Upon detection of its delivery into the host cell (~ 16 - 20 h post-infection), CT105 associates with the Golgi complex possibly through its first 100 amino acid residues; as the developmental cycle progresses (~30 - 40 h post-infection), CT105 accumulates at the host plasma membrane, in a process independent from intact host cell microfilaments and microtubules.

CT105 disrupted vesicular trafficking in a yeast model but it was not essential to the developmental cycle of *C. trachomatis*, as a *ct105* mutant strain did not display an intracellular growth defect, at least in an tissue cell culture model. Furthermore, the analysis of different *C. trachomatis* strains revealed that *ct105* was mostly transcribed in lymphogranuloma venereum (LGV) strains, indicating that CT105 might be important to the tissue tropism characteristic of the LGV group.

Overall, we have demonstrated that the tools for genetic modification of *C. trachomatis* are valuable to the identification of novel T3S effectors. The identification of CT105 illustrates the diversity among chlamydial effector proteins (e.g. subcellular localization, function) despite the small genome of the bacteria. Moreover, the study of T3S effectors contributes to unveil how *C. trachomatis* interacts with the host cell and how it modulates the host cellular mechanisms to survive in the intracellular environment, thus improving our knowledge on *C. trachomatis* pathogenesis.

4.1 MECHANISM OF DELIVERY OF CT105

It had been previously shown that CT105 contains a (T3S) signal recognizable by the type III secretion system (T3SS) of *Yersinia enterocolitica* (da Cunha *et al.*, 2014). Here, we found that the T3S signal of CT105, which is comprised within the first 20 amino acid residues of the protein, was necessary and sufficient to drive T3S in *Y. enterocolitica.* This is not unexpected as T3S signals commonly locate within the first 15 - 40 amino acid residues of T3S substrates (Michiels and Cornelis, 1991). In addition, we also showed that the first 20 amino acid residues of CT105 were necessary for its delivery into the host cells infected by *C. trachomatis*. Surprisingly, when truncated versions of CT105 ($CT105_{1\text{-}100}$, $CT105_{1\text{-}320}$ and $CT105_{\Delta 100\text{-}320}$) were expressed in *C. trachomatis*, these could not be detected in the cytoplasm of host cells, although they all contained the T3S signal. While T3S signals are normally sufficient to target the protein to the secretion apparatus, in some substrates the region of the protein required for their delivery into host cells was found to be longer than the one sufficient to export by the T3SS (Sory *et al.*, 1995; Schesser *et al.*, 1996). Delivery of CT105 into the cytoplasm of infected host cells might require a region of the protein downstream from the T3S signal containing a hypothetical T3S chaperone-binding domain (Woestyn *et al.*, 1996; Boyd *et al.*, 2000; Pais *et al.*, 2013). However, a specific T3S chaperone for CT105 has not been yet identified.

Although the T3S signal frequently locates at the N-terminus of the protein substrate, this is not strictly conserved. For instance, in different bacteria, signals required for secretion/delivery were found to locate at the C-terminus of T3S substrates (e.g. T3S effector Tir from enteropathogenic *Escherichia*

coli (EPEC) (Allen-Vercoe *et al.*, 2005), T3S translocators EspB from enterohaemorrhagic *Escherichia coli* (EHEC) (Chiu *et al.*, 2003), SipB from *Salmonella* spp. (Bae Hoon Kim *et al.*, 2007), and PopD from *Pseudomonas* (Tomalka *et al.*, 2012), and T3S regulatory proteins YscU and YscP from *Yersinia* (Agrain *et al.*, 2005; Login and Wolf-Watz, 2015).

In the case of CT105, either other unidentified regions of the protein are required for its delivery into the host cell or truncated versions of CT105 have alterations in their native conformation which made such fusion proteins non-competent for T3S. Alternatively, competition between the endogenous and truncated versions of CT105 could lead to a decrease of the efficiency of delivery of the truncated proteins explaining why these could not be detected in the host cell. Experiments where the plasmids encoding the truncated versions of CT105 are introduced in the *C. trachomatis ct105::aadA* mutant strain might clarify this point.

In brief, although CT105 has a signal within its first 20 amino acid residues allowing its T3S, other determinants on the protein are required for its delivery by *C. trachomatis* into the cytoplasm of infected host cells.

4.2 CT105 IS MODIFIED WITHIN *C. TRACHOMATIS*

We found that CT105 is likely subjected to a modification within *C. trachomatis* that requires the first 20 amino acid residues of the protein. Although we could not define the nature of this modification, an obvious hypothesis is that CT105 is post-translationally modified by a *C. trachomatis* factor. Post-translational modifications (PTMs) were thought to be exclusive of eukaryotic cells for many years, but more recently they have been also found in bacteria and linked to various cellular functions including bacterial cell division and morphology (Grangeasse *et al.*, 2015). Most of the described bacterial PTMs related to virulence involve modification of host proteins, but a few modifications of bacterial proteins have been described. An example is the *Salmonella* transcription factor (HilD) that regulates *Salmonella* pathogenesis island-1 (SPI-1) genes and was found to be acylated by a bacterial acetyltransferase (Pat) thus allowing the stability of the protein and the decrease of its DNA-binding activity, which was linked to the regulation of the *Salmonella* SPI-1 T3SS (Sang *et al.*, 2016; Sang *et al.*, 2017). Moreover, the *Chlamydia* protease-like activity factor (CPAF) requires activation upon its secretion, as CPAF requires autoprocessing for proteolytic activity, where the CPAF zymogen is cleaved into the active form of the protein (Huang *et al.*, 2008; Chen, Lei, Flores, *et al.*, 2010; Chen, Lei, Lu, *et al.*, 2010; Snavely *et al.*, 2014; Prusty *et al.*, 2018). Altogether, we could speculate that the modification of CT105 could be a mechanism to regulate or to activate the protein before its delivery by *C. trachomatis* into the host cell cytoplasm. However, we could not rule out that instead of being post-translationally modified, CT105 is an unstable protein requiring a *C. trachomatis* factor such as a T3S chaperone. For example, chlamydial T3S chaperone CT584 has been shown to bind and stabilize candidate T3S effector CT082, thus enhancing its T3S (Pais *et al.*, 2013).

4.3 CT105 HAS A DUAL LOCALIZATION WITHIN HOST CELLS DURING *C. TRACHOMATIS* INFECTION

After its delivery into infected host cells, CT105 accumulates at the Golgi complex (16 - 30 h p.i.) and/or at the host cell plasma membrane (30 - 40 h p.i.), thus illustrating that *C. trachomatis* effectors can have distinct subcellular localizations (and possibly different functions) during the chlamydial developmental cycle. In addition to CT105, the *C. trachomatis* effector CT867, a deubiquitinase enzyme known as ChlaDub2/Cdu2 (Misaghi *et al.*, 2006; Fischer *et al.*, 2017) has been detected at the inclusion membrane and at the host cell plasma membrane at distinct times of infection (Wang *et al.*, 2018). Such dual localization during infection as a likely strategy to diversify effector function is reminiscent of the *Salmonella* SopB effector, which initially localizes at the host cell membrane to mediate bacterial invasion but is then redirected to the *Salmonella*-containing vacuole by host-mediated ubiquitination to modulate bacterial intracellular growth (Patel *et al.*, 2009). This precise spatial and temporal subcellular targeting of bacterial effector proteins during infection is an essential feature of their function (Hicks *et al.*, 2011).

CT105 is the first chlamydial effector shown to localize at the Golgi complex, yet at least three other bacterial effector proteins have been shown to localize at this organelle in infected host cells. These are EspI/NleA from *Escherichia coli* (Gruenheid *et al.*, 2004), GobX from *Legionella pneumophila* (Lin *et al.*, 2015), and SteD from *Salmonella enterica* (Bayer-Santos *et al.*, 2016). EspI/NleA interferes with coatomer protein II complex (COPII) function and inhibits host cell protein secretion (Jinoh Kim *et al.*, 2007), and also disrupts intestinal tight junctions (Thanabalasuriar *et al.*, 2010). In addition, EspI/NleA inhibits NLRP3 inflammasome activation (Yen *et al.*, 2015). GobX displays E3 ubiquitin ligase activity, but how this promotes *L. pneumophila* infection is unknown (Lin *et al.*, 2015). Finally, SteD interferes with the activity of a host E3 ubiquitin ligase, leading to a reduction of surface-localized major histocompatibility complex (MHC) class II molecules and suppression of T cell activation (Bayer-Santos *et al.*, 2016). Even more diverse functions have been reported among other bacterial effectors shown to interact with Golgi proteins or to localize at this organelle after ectopic expression in mammalian cells (Salcedo and Holden, 2003; Clements *et al.*, 2011; Selyunin *et al.*, 2011; Ge *et al.*, 2012; Zhe Yang *et al.*, 2015; Kim and Satchell, 2016; Yu *et al.*, 2016; Beyer *et al.*, 2017; Miller *et al.*, 2017). Overall, this shows that no specific function can be predicted for CT105 based on its localization at the Golgi.

However, CT105, and as already mentioned above, the *C. trachomatis* deubiquitinase CT867/ChlaDub2/Cdu2, was also detected at the host cell plasma membrane at late times of infection of tissue culture cells (Wang *et al.*, 2018). It is likely that effector proteins involved in chlamydial entry might also associate with the host cell plasma membrane during or immediately after bacterial uptake (Hower *et al.*, 2009; Bullock *et al.*, 2012; McKuen *et al.*, 2017), but such localization of CT105 and CT867/ChlaDub2/Cdu2 later in infection could indicate a function in host cell exit.

It is unknown how CT105 and CT867/ChlaDub2/Cdu2 are differentially directed to different host cell localizations. In the case of CT105, it is unlikely that vesicular trafficking is involved as disruption of microfilaments and microtubules did not affect its localization at the plasma membrane in infected cells. One hypothesis could be that CT105 is specifically directed to different subcellular localizations by

covalent modifications it might be subjected to and/or by changes in the lipid and/or protein composition of host cellular membranes. It is also interesting that the changes of localization of CT105 are timed with the Golgi fragmentation observed in *Chlamydia*-infected cells, suggesting that the fragmentation of the Golgi could allow the plasma membrane localization of CT105 during *Chlamydia* infection.

Analyses of the localization of hybrid proteins comprising full-length or truncated CT105 and mEGFP upon their ectopic expression in HeLa cells led to the identification of the first 100 amino acid residues of CT105 as sufficient for Golgi localization. However, this region does not display obvious motifs found in other relevant eukaryotic or bacterial proteins, and the exact molecular determinants of the Golgi localization of CT105 remain to be identified.

Other effector proteins that localize at the Golgi in infected cells use distinct mechanisms directing them to this organelle (Lee *et al.*, 2008; Thanabalasuriar *et al.*, 2010; Lin *et al.*, 2015; Bayer-Santos *et al.*, 2016). In the case of EspI/NleA, Golgi targeting is partially mediated by a Postsynaptic Density95/Disc Large/Zonula Occludens-1 (PDZ) domain on its C-terminus (Lee *et al.*, 2008). CT105 also possesses a putative PDZ domain (Mu *et al.*, 2014), but the relevant residues were not involved in its subcellular localization after ectopic expression in mammalian cells. Moreover, in contrast with our observations in infected and transfected mammalian cells, CT105 did not localize at the plasma membrane in *Saccharomyces cerevisiae* suggesting that this localization requires factor(s) not present in yeast. Other relevant questions which remain to be analyzed are whether the same determinants are responsible for Golgi localization in infected cells and which characteristics of the full-length CT105 protein enable its targeting to the plasma membrane in infected and transfected cells.

CT105 also appeared in filamentous structures spread in infected and transfected cells, suggesting that the protein can oligomerize or interact with host cell filamentous proteins independently of additional *C. trachomatis* factors. We could not identify host proteins/organelles that co-localize with these structures (e.g., host cytoskeleton and vesicular trafficking markers). Filamentous structures have been observed in *C. trachomatis*-infected cells for several Inc proteins (Bannantine *et al.*, 1998). However, they seem to emanate from the inclusion which is not the case for CT105. In the case of IncA and IncE, these tubules have been show to interact with host cell sorting nexins (SNX1, SNX2, SNX5 and SNX6), which are proteins involved in retromer endosomal membrane trafficking (Aeberhard *et al.*, 2015; Mirrashidi *et al.*, 2015). The overexpression of IncE has been associated with enhanced inclusion tubulation. Because the sorting nexin-marked tubules originate from the inclusion, it seems that they should not be involved in the tubules marked by CT105. Other components of host cell trafficking might be involved in the formation of these filamentous structures or CT105 might enhance/stabilize their formation.

4.4 CT105 DISRUPTS VESICULAR TRAFFICKING IN EUKARYOTIC CELLS

Considering the localization of CT105 within the host cell (Golgi and plasma membrane), an appealing possibility for its function would be that it contributes to nutrient acquisition by the inclusion and/or avoidance of fusion with hydrolytic compartments. However, the *C. trachomatis ct105::aadA* mutant did not reveal an obvious intracellular growth defect, which does not support these hypotheses.

The *ct105* mutant revealed smaller inclusions relative to the parental strain (suggesting a possible defect in vacuolar membrane expansion), but this could not be restored by reintroduction of *ct105* in *trans*. The inability to complement intracellular growth-like phenotypes in intron insertional mutants of *C. trachomatis* was also recently described for *ct101/mrcA* (Nguyen *et al.*, 2018), while other specific phenotypes of this mutant strain could be complemented (Nguyen *et al.*, 2018). We are currently analyzing whether the intron insertion affects the genes adjacent to *ct105* in the chromosome of *C. trachomatis*. Nevertheless, the lack of an intracellular growth defect is also not uncommon amongst *C. trachomatis* effector gene mutants characterized thus far (Weber *et al.*, 2017; Stanhope *et al.*, 2017; McKuen *et al.*, 2017), which might reflect redundancy in effector function or inexistence of adequate infection models (Galán, 2009). Moreover, in cells infected by the *C. trachomatis ct105::aadA* mutant the Golgi distribution around the inclusion appears to be unaltered, but we cannot exclude that CT105 could be involved in other Golgi-related processes subverted in *C. trachomatis*-infected cells (Pokrovskaya *et al.*, 2012).

We also showed that ectopic expression of CT105 in *Saccharomyces cerevisiae* induces a vacuolar protein sorting (Vps) defect, indicating a potential capacity of the protein to interfere with vesicular trafficking in infected cells. The carboxypeptidase Y - invertase (CPY-Inv) assay has been used to screen for *Legionella pneumophila* type IV secretion effectors interfering with endocytic trafficking (Shohdy *et al.*, 2005; De Felipe *et al.*, 2008). The function of most *Legionella pneumophila* effectors identified in these screens was subsequently described in further detail (Franco *et al.*, 2012; Gaspar and Machner, 2014; Shi *et al.*, 2016; Young *et al.*, 2016). A potential activity of CT105 on vesicular trafficking in infected cells could also affect, e.g., cytokine secretion (Murray and Stow, 2014) or immune signaling (Gleeson, 2014), which would not have an impact on chlamydial intracellular growth in tissue culture cells.

4.5 CT105 IS LIKELY RELEVANT FOR THE TROPISM OF LGV STRAINS

Analysis of the primary structure of CT105 revealed that full-length orthologues were only present in *Chlamydia muridarum* and *Chlamydia suis*, consistent with the fact that these species are the closer relatives of *C. trachomatis* (Sachse *et al.*, 2015). Interestingly, among the truncated and/or duplicated potential orthologues of CT105 found in other *Chlamydia* species, some (CAB376 in *Chlamydia abortus*, CCA_00389 in *Chlamydia caviae*, CF0618 and CF0619 in *Chlamydia felis*, CPSIT_0422 and CPSIT_0421 in *Chlamydia psittaci*) have been proposed to be T3S substrates (Voigt *et al.*, 2012). Furthermore, *ct105* is mostly expressed in *C. trachomatis* LGV strains and a deletion of 74-bp within the predicted promoter region among the non-LGV strains was also observed. There is also a considerable representation of protein-changing substitutions when comparing genital and LGV strains (Borges *et al.*, 2012). Therefore, CT105 displays a striking variability within *C. trachomatis* serovars, revealing LGV-specific genetic and transcriptomic traits. Overall, this suggests that CT105 could have a specific function related with the unique characteristics of infections by these strains, which, unlike ocular and urogenital *C. trachomatis* strains, can infect mononuclear phagocytes and disseminate into regional

lymph nodes (Thomson *et al.*, 2008; Borges and Gomes, 2015). This also indicates that features of the infection by LGV strains could be an evolutionary pressure to maintain an active *ct105* gene.

4.6 OUTLOOK ON OTHER CANDIDATE T3S EFFECTORS OF *C. TRACHOMATIS*

Regarding the *C. trachomatis* proteins CT053, CT082, CT429, CT696 and CT849 (da Cunha *et al.*, 2014), which possess a T3S signal but were not detected in the host cell during chlamydial infection, we cannot conclude that these proteins are not T3S effectors. These proteins could be expressed and/or delivered into host cells in amounts too low, or too much dispersed in the host cytosol, to allow detection by fluorescence microscopy. For these cases, alternative approaches to monitor transport into host cells would be using the split-GFP system (Wang et al., 2018), or reporter proteins such as β-lactamase (Mueller et al., 2015), CyaA (Bauler et al., 2014), or GSK (Bauler et al., 2014). Nevertheless, when ectopically expressed in mammalian cells, EGFP-CT082, EGFP-CT696 and EGFP-CT849 localized at specific sites, further suggesting that these might be chlamydial T3S effectors. Furthermore, CT082 has been shown to interact and be stabilized by CT584, a chlamydial T3S chaperone (Pais *et al.*, 2013). As for CT696, the corresponding gene localizes in a chromosomal region near a known chlamydial T3S substrates genes *tmeA/ct694* and *tmeB/ct695*, which encoding proteins were shown to be delivered into the host cell by *C. trachomatis*. Moreover, T3S effector TmeA is involved in the remodeling of actin during chlamydial entry into host cells (Hower *et al.*, 2009; Bullock *et al.*, 2012; McKuen *et al.*, 2017) and found to be necessary for normal intracellular growth of *C. trachomatis* (McKuen *et al.*, 2017). However, in a previous study using the β-lactamase system as a reporter to monitor protein delivery into host cell, CT696 could also not be detected into the host cell (Mueller et al., 2015). Finally, *ct849* localizes in the chromosome near *ct847*, which encodes for a later cycle T3S effector that interacts with human GCIP, a protein degraded during *C. trachomatis* infection (Chellas-Géry *et al.*, 2007). Also near in the chromosome is *ct848*, which encodes a candidate T3S effector of *C. trachomatis*, as it was shown to be type III secreted by the *Shigella flexneri* T3SS (Subtil *et al.*, 2005). Moreover, CT847, CT848 and CT849, all share a domain of unknown function (DUF720), suggesting that they all could be T3S effectors of *C. trachomatis*.

4.7 HYPOTHETIC MODE OF ACTION FOR CT105 DURING *C. TRACHOMATIS* INFECTION

Taking together all the results, we could speculate a mechanism of action for CT105 during *C. trachomatis* infection. CT105 is expressed in *C. trachomatis* early during infection where it might bind a T3S chaperone and/or be modified by a chlamydial enzyme. Upon delivery into the host cells, CT105 is targeted and associates to the Golgi through its first 100 amino acids where it alters eukaryotic vesicular trafficking. In *Chlamydia*-infected epithelial cells, fragmentation of the Golgi would lead to the re-localization of CT105 to the host plasma membrane where it could be involved in the processes of *Chlamydia* exit from the host cell.

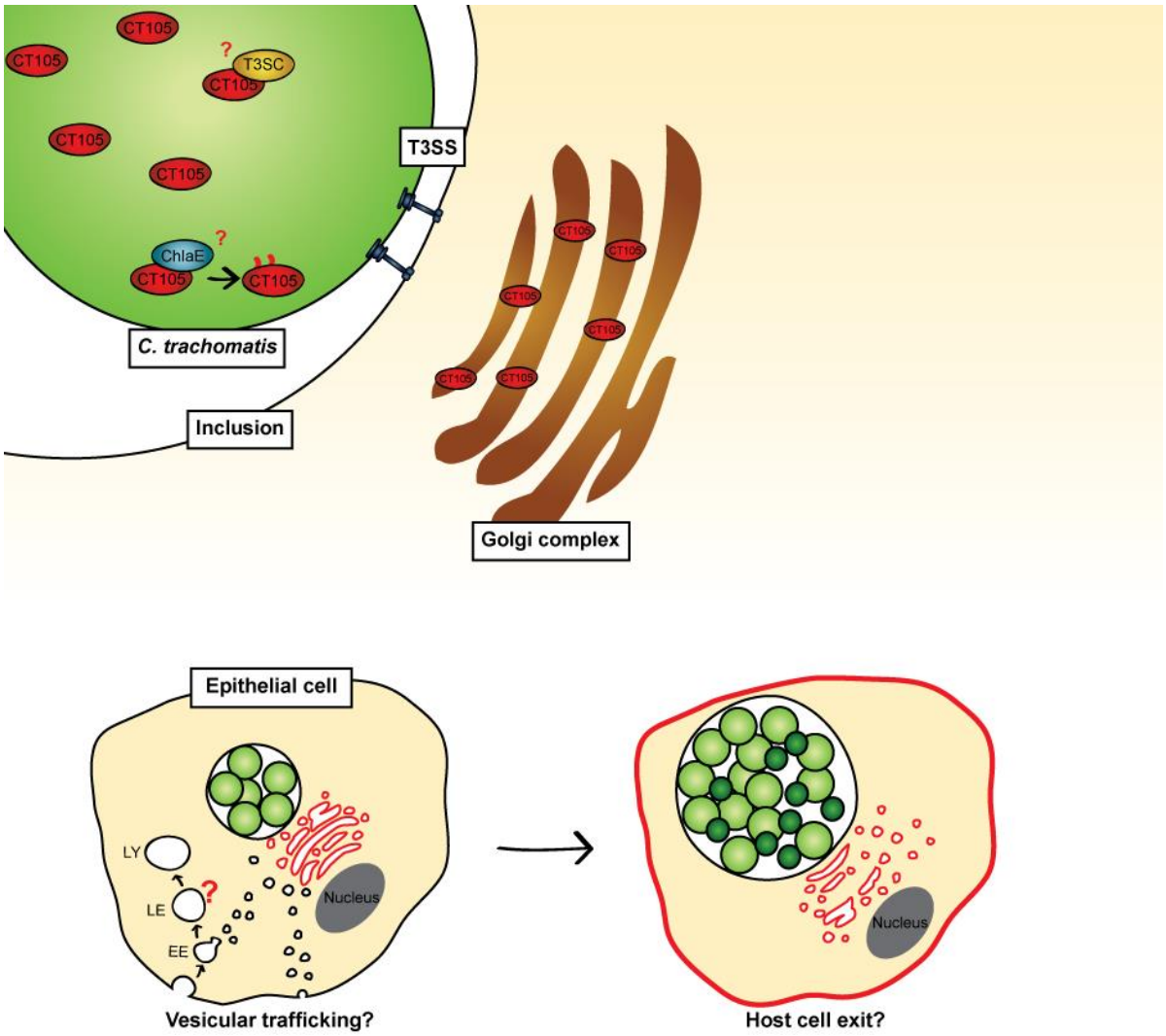

Figure 4.1 Schematic model for CT105 mode of action during *C. trachomatis* infection of epithelial cells. Inside de bacteria CT105 is either modified by a chlamydial enzyme (ChlaE) or/and requires a specific T3S chaperone (T3SC). Upon delivery into the hos cell by a T3SS, CT105 (represented in red) associates with the Golgi, where it could modify (red arrows) the vesicular trafficking pathways (EE, early endosomes; LE, late endosomes; LY; lysosomes) of the host cell. As the developmental cycle progresses and the Golgi becomes more fragmented, CT105 localizes at the plasma membrane where it might contribute to processes of host cell exit.

4.8 FUTURE WORK

Our results suggest a complex mode of action for CT105 during *C. trachomatis* infection both before and after its delivery into the host cell. Here, we summarize the most prominent questions raised from this work.

CT105 was found to potentially require additional bacterial factors to be delivered into the host cell and to be modified within the bacteria. Thus, we could propose the identification of bacterial interacting partners that we hypothesize as T3S chaperones or enzymes capable of catalyzing PTMs. Furthermore, constructing *C. trachomatis* strains expressing additional truncated versions or chimeras of CT105 might give insights in which regions are important for modification and delivery of the protein. Although our data suggests that CT105 is delivered into the host cell by a T3S-dependent mechanism, this causal association could only be confirmed by abolishing T3S using chemical inhibitors or, better, using a *C.*

trachomatis T3S-deficient strain. The latter may not be feasible due to the obligate intracellular lifestyle of *C. trachomatis*.

Regarding the targeting of CT105 to distinct localizations in the host cell, the Golgi targeting region of CT105 is likely comprised within the first 100 amino acids of the protein, but its nature was not identified. We are currently constructing truncated versions of CT105 containing different regions of the first 100 amino acid residues and performing single amino acid mutations in these regions to determine the specific motif that allows the targeting of CT105 to the Golgi. A similar approach should be taken to study the plasma membrane targeting region of CT105, which was also not identified.

Moreover, the whole process that leads to the change of the localization of CT105 must be investigated. For instance, CT105 targeting to the Golgi might be required for its subsequent re-direction to the plasma membrane. Alternatively, CT105 could be directed to the plasma membrane, independently of the previous Golgi localization. In addition, as we have found that the transport of CT105 unlikely occurs through vesicle trafficking, another hypothesis to be examined is whether there could be a modification of the Golgi-targeting region of CT105 during infection or if this could be dependent on the fragmentation of the Golgi or of *Chlamydia*-dependent changes in the lipid and/or protein composition of host cellular membranes.

Thus, analysis of additional truncations of CT105 both in transfected and infected cells would allow a detailed mapping and further identification of protein motifs required to target CT105 to the different regions in the host cell. Moreover, maintenance of a compact Golgi (in infected cells) would be helpful to answer if the change of localization was dependent on the morphology of the Golgi, as the timing of fragmentation and change of localization overlaps in *C. trachomatis*-infected cells. For this, a *C. trachomatis ct813*/*inaC* mutant could be used as in this strain the Golgi fragmentation is abolished (Kokes *et al.*, 2015; Wesolowski *et al.*, 2017).

Furthermore, an analysis of the *C. trachomatis ct105* mutant strain should be performed with emphasis on the effects on the vesicular trafficking of epithelial cells. Additionally, other infection models, such as macrophages and animal models, should be used and infection with *C. trachomatis ct105* mutant strain should be detailed in terms of invasion, intracellular growth, vesicular trafficking and immune signaling responses. Above all, the identification of host cell interacting partners of CT105 would be crucial to a more focused analysis and to the understanding of the function of the protein during *C. trachomatis* infection. We have attempted to use yeast two-hybrid system to identify host interacting partners of CT105 with no success. Moreover, due to the membrane localization of CT105, we tested interaction of this protein with lipids immobilized in a membrane, but again we could not detect any interaction. Currently, we are planning to perform a mass spectrometry analysis of mammalian proteins pulled down by ectopically expressed EGFP-CT105.

4.9 CONCLUSIONS AND FINAL REMARKS

The intracellular lifecycle of *C. trachomatis* requires these bacteria to maintain a fine balance on its interactions with the host cells. While these bacteria exploit the host cell for their replication they also must avoid host cell death to complete its developmental cycle. T3S effectors are thought to play a key role in these interactions.

The work developed in this PhD thesis resulted in the identification of a novel T3S effector of *C. trachomatis*, using the newly discovered methodologies for genetic manipulation of this bacterium. Our main findings were the identification of CT105 as a T3S effector of *C. trachomatis* that localizes to the Golgi and plasma membrane in infected cells at distinct times of the chlamydial developmental cycle, and that can disrupt eukaryotic vesicular trafficking in eukaryotic cells. Furthermore, CT105 appears to reveal LGV-specific features. Considering its striking association with the Golgi complex, we named it CteG (for *C. trachomatis* effector associated with the Golgi).

Overall, this expands the portfolio of known chlamydial effector proteins and uncovers the first *Chlamydia* effector that associates with the Golgi complex. Moreover, it further illustrates that *C. trachomatis* effectors can have distinct subcellular localizations (and possibly different functions) during the chlamydial developmental cycle. Nevertheless, more questions have been raised than those answered and future work should be directed to the identification of CT105/CteG function, subcellular targeting mechanisms, diversity and specificity within *C. trachomatis* and among *Chlamydia* species.

REFERENCES

Abby, S.S., and Rocha, E.P.C. (2012) The non-flagellar type III secretion system evolved from the bacterial flagellum and diversified into host-cell adapted systems. *PLoS Genet* **8**: e1002983 http://www.ncbi.nlm.nih.gov/pubmed/23028376.

Abdelrahman, Y., Ouellette, S.P., Belland, R.J., and Cox, J. V (2016) Polarized Cell Division of Chlamydia trachomatis. *PLOS Pathog* **12**: e1005822 https://doi.org/10.1371/journal.ppat.1005822.

Abdelrahman, Y.M., and Belland, R.J. (2005) The chlamydial developmental cycle. *FEMS Microbiol Rev* **29**: 949–59 http://www.ncbi.nlm.nih.gov/pubmed/16043254.

Abromaitis, S., and Stephens, R.S. (2009) Attachment and Entry of Chlamydia Have Distinct Requirements for Host Protein Disulfide Isomerase. *PLoS Pathog* **5**: e1000357 http://www.ncbi.nlm.nih.gov/pmc/articles/PMC2655716/.

Aeberhard, L., Banhart, S., Fischer, M., Jehmlich, N., Rose, L., Koch, S., *et al.* (2015) The Proteome of the Isolated Chlamydia trachomatis Containing Vacuole Reveals a Complex Trafficking Platform Enriched for Retromer Components. *PLoS Pathog* **11**: e1004883 http://www.ncbi.nlm.nih.gov/pubmed/6042774.

Agaisse, H., and Derré, I. (2013) A C. trachomatis Cloning Vector and the Generation of C. trachomatis Strains Expressing Fluorescent Proteins under the Control of a C. trachomatis Promoter. *PLoS One* **8**.

Agaisse, H., and Derré, I. (2014) Expression of the Effector Protein IncD in Chlamydia trachomatis Mediates Recruitment of the Lipid Transfer Protein CERT and the Endoplasmic Reticulum-Resident Protein VAPB to the Inclusion Membrane. *Infect Immun* **82**: 2037–2047 http://www.ncbi.nlm.nih.gov/pubmed/24595143.

Agrain, C., Sorg, I., Paroz, C., and Cornelis, G.R. (2005) Secretion of YscP from Yersinia enterocolitica is essential to control the length of the injectisome needle but not to change the type III secretion substrate specificity. *Mol Microbiol* **57**: 1415–27 http://www.ncbi.nlm.nih.gov/pubmed/16102009.

Al-Zeer, M.A., Al-Younes, H.M., Kerr, M., Abu-Lubad, M., Gonzalez, E., Brinkmann, V., and Meyer, T.F. (2014) Chlamydia trachomatis remodels stable microtubules to coordinate Golgi stack recruitment to the chlamydial inclusion surface. *Mol Microbiol* **94**: 1285–97 http://www.ncbi.nlm.nih.gov/pubmed/25315131.

Albrecht, M., Sharma, C.M., Reinhardt, R., Vogel, J., and Rudel, T. (2009) Deep sequencing-based discovery of the Chlamydia trachomatis transcriptome. *Nucleic Acids Res* **38**: 868–877.

Allen-Vercoe, E., Toh, M.C.W., Waddell, B., Ho, H., and DeVinney, R. (2005) A carboxy-terminal domain of Tir from enterohemorrhagic Escherichia coli O157:H7 (EHEC O157:H7) required for efficient type III secretion. *FEMS Microbiol Lett* **243**: 355–364 http://dx.doi.org/10.1016/j.femsle.2004.12.027.

Almeida, F., Borges, V., Ferreira, R., Borrego, M.J., Gomes, J.P., and Mota, L.J. (2012) Polymorphisms in Inc Proteins and Differential Expression of inc Genes among Chlamydia trachomatis Strains Correlate with Invasiveness and Tropism of Lymphogranuloma Venereum Isolates. *J Bacteriol* **194**: 6574–6585 http://jb.asm.org/lookup/doi/10.1128/JB.01428-12.

Almeida, F., Luís, M.P., Pereira, I.S., Pais, S. V, and Mota, L.J. (2018) The Human Centrosomal Protein CCDC146 Binds Chlamydia trachomatis Inclusion Membrane Protein CT288 and Is Recruited to the Periphery of the Chlamydia-Containing Vacuole. *Front Cell Infect Microbiol* **8**: 254 https://www.frontiersin.org/article/10.3389/fcimb.2018.00254.

Arnold, R., Brandmaier, S., Kleine, F., Tischler, P., Heinz, E., Behrens, S., *et al.* (2009) Sequence-based prediction of type III secreted proteins. *PLoS Pathog* **5**: e1000376 http://www.ncbi.nlm.nih.gov/pubmed/19390696.

Azuma, Y., Hirakawa, H., Yamashita, A., Cai, Y., Rahman, M.A., Suzuki, H., *et al.* (2006) Genome sequence of the cat pathogen, Chlamydophila felis. *DNA Res* **13**: 15–23 http://www.ncbi.nlm.nih.gov/pubmed/16766509.

Babst, M., Wendland, B., Estepa, E.J., and Emr, S.D. (1998) The Vps4p AAA ATPase regulates membrane association of a Vps protein complex required for normal endosome function. *EMBO J* **17**: 2982–2993.

Bannantine, J.P., Stamm, W.E., Suchland, R.J., and Rockey, D.D. (1998) Chlamydia trachomatis IncA is localized to the inclusion membrane and is recognized by antisera from infected humans and primates. *Infect Immun* **66**: 6017–21 http://www.ncbi.nlm.nih.gov/pubmed/9826388.

Barron, A.L., White, H.J., Rank, R.G., Soloff, B.L., and Moses, E.B. (1981) A new animal model for the study of Chlamydia trachomatis genital infections: infection of mice with the agent of mouse pneumonitis. *J Infect Dis* **143**: 63–6 http://www.ncbi.nlm.nih.gov/pubmed/7217713.

Barry, C.E., Hayes, S.F., and Hackstadt, T. (1992) Nucleoid condensation in Escherichia coli that express a chlamydial histone homolog. *Science* **256**: 377–9 http://www.ncbi.nlm.nih.gov/pubmed/1566085.

Bartra, S.S., and Plano, G. V (2017) Measurement of Effector Protein Translocation Using

Phosphorylatable Epitope Tags and Phospho-Specific Antibodies. *Methods Mol Biol* **1531**: 111–119 http://www.ncbi.nlm.nih.gov/pubmed/27837486.

Bauler, L.D., and Hackstadt, T. (2014) Expression and targeting of secreted proteins from Chlamydia trachomatis. *J Bacteriol* **196**: 1325–34 http://www.ncbi.nlm.nih.gov/pubmed/24443531.

Bayer-Santos, E., Durkin, C.H., Rigano, L.A., Kupz, A., Alix, E., Cerny, O., *et al.* (2016) The Salmonella Effector SteD Mediates MARCH8-Dependent Ubiquitination of MHC II Molecules and Inhibits T Cell Activation. *Cell Host Microbe* **20**: 584–595 http://www.ncbi.nlm.nih.gov/pubmed/27832589.

Beatty, W.L. (2006) Trafficking from CD63-positive late endocytic multivesicular bodies is essential for intracellular development of Chlamydia trachomatis. *J Cell Sci* **119**: 350–9 http://www.ncbi.nlm.nih.gov/pubmed/16410552.

Beatty, W.L. (2008) Late endocytic multivesicular bodies intersect the chlamydial inclusion in the absence of CD63. *Infect Immun* **76**: 2872–81 http://www.ncbi.nlm.nih.gov/pubmed/18426873.

Beatty, W.L., Morrison, R.P., and Byrne, G.I. (1994) Persistent chlamydiae: from cell culture to a paradigm for chlamydial pathogenesis. *Microbiol Rev* **58**: 686–99 http://www.ncbi.nlm.nih.gov/pubmed/7854252.

Belland, R.J., Scidmore, M.A., Crane, D.D., Hogan, D.M., Whitmire, W., McClarty, G., and Caldwell, H.D. (2001) Chlamydia trachomatis cytotoxicity associated with complete and partial cytotoxin genes. *Proc Natl Acad Sci U S A* **98**: 13984–9 http://www.ncbi.nlm.nih.gov/pubmed/11707582.

Bertelli, C., Collyn, F., Croxatto, A., Rückert, C., Polkinghorne, A., Kebbi-Beghdadi, C., *et al.* (2010) The Waddlia genome: a window into chlamydial biology. *PLoS One* **5**: e10890 http://www.ncbi.nlm.nih.gov/pubmed/20531937.

Beyer, A.R., Rodino, K.G., VieBrock, L., Green, R.S., Tegels, B.K., Oliver, L.D., *et al.* (2017) Orientia tsutsugamushi Ank9 is a multifunctional effector that utilizes a novel GRIP-like Golgi localization domain for Golgi-to-endoplasmic reticulum trafficking and interacts with host COPB2. *Cell Microbiol* **19** http://www.ncbi.nlm.nih.gov/pubmed/28103630.

Binet, R., and Maurelli, A.T. (2009) Transformation and isolation of allelic exchange mutants of Chlamydia psittaci using recombinant DNA introduced by electroporation. *Proc Natl Acad Sci U S A* **106**: 292–297 http://www.ncbi.nlm.nih.gov/entrez/query.fcgi?cmd=Retrieve&db=PubMed&dopt=Citation&list_uids=19104068.

Birge, R.B., Kalodimos, C., Inagaki, F., and Tanaka, S. (2009) Crk and CrkL adaptor proteins: networks for physiological and pathological signaling. *Cell Commun Signal* **7**: 13 http://www.ncbi.nlm.nih.gov/pubmed/19426560.

Borges, V., and Gomes, J.P. (2015) Deep comparative genomics among Chlamydia trachomatis lymphogranuloma venereum isolates highlights genes potentially involved in pathoadaptation. *Infect Genet Evol* **32**: 74–88 http://www.ncbi.nlm.nih.gov/pubmed/25745888.

Borges, V., Nunes, A., Ferreira, R., Borrego, M.J., and Gomes, J.P. (2012) Directional evolution of Chlamydia trachomatis towards niche-specific adaptation. *J Bacteriol* **194**: 6143–53 http://jb.asm.org/cgi/doi/10.1128/JB.01291-12.

Boyd, A.P., Lambermont, I., and Cornelis, G.R. (2000) Competition between the Yops of Yersinia enterocolitica for delivery into eukaryotic cells: role of the SycE chaperone binding domain of YopE. *J Bacteriol* **182**: 4811–21 http://www.ncbi.nlm.nih.gov/pubmed/10940022.

Brinkworth, A.J., Malcolm, D.S., Pedrosa, A.T., Roguska, K., Shahbazian, S., Graham, J.E., *et al.* (2011) Chlamydia trachomatis Slc1 is a type III secretion chaperone that enhances the translocation of its invasion effector substrate TARP. *Mol Microbiol* **82**: 131–44 http://www.ncbi.nlm.nih.gov/pubmed/21883523.

Brown, J.S. (2012) Community-acquired pneumonia. *Clin Med* **12**: 538–43 http://www.clinmed.rcpjournal.org/cgi/doi/10.7861/clinmedicine.12-6-538.

Bullock, H.D., Hower, S., and Fields, K.A. (2012) Domain analyses reveal that chlamydia trachomatis CT694 protein belongs to the membrane-localized family of type III effector proteins. *J Biol Chem* **287**: 28078–28086.

Cai, Y., Fukushi, H., Koyasu, S., Kuroda, E., Yamaguchi, T., and Hirai, K. (2002) An etiological investigation of domestic cats with conjunctivitis and upper respiratory tract disease in Japan. *J Vet Med Sci* **64**: 215–9 http://www.ncbi.nlm.nih.gov/pubmed/11999440.

Caldwell, H.D., Wood, H., Crane, D., Bailey, R., Jones, R.B., Mabey, D., *et al.* (2003) Polymorphisms in Chlamydia trachomatis tryptophan synthase genes differentiate between genital and ocular isolates. *J Clin Invest* **111**: 1757–69 http://www.ncbi.nlm.nih.gov/pubmed/12011099.

Campbell, J., Huang, Y., Liu, Y., Schenken, R., Arulanandam, B., and Zhong, G. (2014) Bioluminescence imaging of Chlamydia muridarum ascending infection in mice. *PLoS One* **9**: 1–6.

Carlson, J.H., Hughes, S., Hogan, D., Cieplak, G., Sturdevant, D.E., McClarty, G., *et al.* (2004)

Polymorphisms in the Chlamydia trachomatis cytotoxin locus associated with ocular and genital isolates. *Infect Immun* **72**: 7063–72 http://www.ncbi.nlm.nih.gov/pubmed/15557630.

Carpenter, V., Chen, Y., Dolat, L., and Valdivia, R.H. (2017) The Effector TepP Mediates Recruitment and Activation of Phosphoinositide 3-Kinase on Early Chlamydia trachomatis Vacuoles. *mSphere* **2**: 1–15 http://msphere.asm.org/content/msph/2/4/e00207-17.full.pdf%0Ahttp://www.ncbi.nlm.nih.gov/pubmed/28744480%0Ahttp://www.pubmedcentral.nih.gov/articlerender.fcgi?artid=PMC5518268.

Chellas-Géry, B., Linton, C.N., and Fields, K.A. (2007) Human GCIP interacts with CT847, a novel Chlamydia trachomatis type III secretion substrate, and is degraded in a tissue-culture infection model. *Cell Microbiol* **9**: 2417–30 http://www.ncbi.nlm.nih.gov/pubmed/17532760.

Chen, A.L., Johnson, K.A., Lee, J.K., Sütterlin, C., and Tan, M. (2012) CPAF: A Chlamydial Protease in Search of an Authentic Substrate. *PLoS Pathog* **8**: e1002842 http://www.ncbi.nlm.nih.gov/pubmed/22876181.

Chen, D., Chai, J., Hart, P.J., and Zhong, G. (2009) Identifying catalytic residues in CPAF, a Chlamydia-secreted protease. *Arch Biochem Biophys* **485**: 16–23 http://www.ncbi.nlm.nih.gov/pubmed/19388144.

Chen, D., Lei, L., Flores, R., Huang, Z., Wu, Z., Chai, J., and Zhong, G. (2010) Autoprocessing and self-activation of the secreted protease CPAF in Chlamydia-infected cells. *Microb Pathog* **49**: 164–73 http://www.ncbi.nlm.nih.gov/pubmed/20510344.

Chen, D., Lei, L., Lu, C., Flores, R., DeLisa, M.P., Roberts, T.C., *et al.* (2010) Secretion of the chlamydial virulence factor CPAF requires the Sec-dependent pathway. *Microbiology* **156**: 3031–40 http://www.ncbi.nlm.nih.gov/pubmed/20522495.

Chen, Y.-S., Bastidas, R.J., Saka, H.A., Carpenter, V.K., Richards, K.L., Plano, G. V, and Valdivia, R.H. (2014) The Chlamydia trachomatis type III secretion chaperone Slc1 engages multiple early effectors, including TepP, a tyrosine-phosphorylated protein required for the recruitment of CrkI-II to nascent inclusions and innate immune signaling. *PLoS Pathog* **10**: e1003954 http://www.ncbi.nlm.nih.gov/pubmed/24586162.

Chiu, H.-J., Lin, W.-S., and Syu, W.-J. (2003) Type III secretion of EspB in enterohemorrhagic Escherichia coli O157:H7. *Arch Microbiol* **180**: 218–26 http://www.ncbi.nlm.nih.gov/pubmed/12856107.

Christian, J., Vier, J., Paschen, S.A., and Häcker, G. (2010) Cleavage of the NF-κB Family Protein p65/RelA by the Chlamydial Protease-like Activity Factor (CPAF) Impairs Proinflammatory Signaling in Cells Infected with Chlamydiae. *J Biol Chem* **285**: 41320–41327 http://www.ncbi.nlm.nih.gov/pubmed/21041296.

Clausen, J.D., Christiansen, G., Holst, H.U., and Birkelund, S. (1997) Chlamydia trachomatis utilizes the host cell microtubule network during early events of infection. *Mol Microbiol* **25**: 441–9 http://www.ncbi.nlm.nih.gov/pubmed/9302007.

Clements, A., Smollett, K., Lee, S.F., Hartland, E.L., Lowe, M., and Frankel, G. (2011) EspG of enteropathogenic and enterohemorrhagic E. coli binds the Golgi matrix protein GM130 and disrupts the Golgi structure and function. *Cell Microbiol* **13**: 1429–1439.

Clifton, D.R., Fields, K.A., Grieshaber, S.S., Dooley, C.A., Fischer, E.R., Mead, D.J., *et al.* (2004) A chlamydial type III translocated protein is tyrosine-phosphorylated at the site of entry and associated with recruitment of actin. *Proc Natl Acad Sci U S A* **101**: 10166–71 http://www.ncbi.nlm.nih.gov/pubmed/15199184.

Comanducci, M., Cevenini, R., Moroni, A., Giuliani, M.M., Ricci, S., Scarlato, V., and Ratti, G. (1993) Expression of a plasmid gene of Chlamydia trachomatis encoding a novel 28 kDa antigen. *J Gen Microbiol* **139**: 1083–92 http://www.ncbi.nlm.nih.gov/pubmed/8336105.

Conant, C.G., and Stephens, R.S. (2007) Chlamydia attachment to mammalian cells requires protein disulfide isomerase. *Cell Microbiol* **9**: 222–232 https://doi.org/10.1111/j.1462-5822.2006.00783.x.

Cornelis, G.R. (2006) The type III secretion injectisome. *Nat Rev Microbiol* **4**: 811–25 http://www.ncbi.nlm.nih.gov/pubmed/17041629%5Cnhttp://www.nature.com/doifinder/10.1038/nrmicro1526.

Cossé, M.M., Barta, M.L., Fisher, D.J., Oesterlin, L.K., Niragire, B., Perrinet, S., *et al.* (2018) The Loss of Expression of a Single Type 3 Effector (CT622) Strongly Reduces Chlamydia trachomatis Infectivity and Growth. *Front Cell Infect Microbiol* **8**: 145 http://www.ncbi.nlm.nih.gov/pubmed/29868501.

Costa, T.R.D., Felisberto-Rodrigues, C., Meir, A., Prevost, M.S., Redzej, A., Trokter, M., and Waksman, G. (2015) Secretion systems in Gram-negative bacteria: structural and mechanistic insights. *Nat Rev Microbiol* **13**: 343–359 http://dx.doi.org/10.1038/nrmicro3456.

Cunha, M. da, Milho, C., Almeida, F., Pais, S. V, Borges, V., Maurício, R., *et al.* (2014) Identification of

type III secretion substrates of Chlamydia trachomatis using Yersinia enterocolitica as a heterologous system. *BMC Microbiol* **14**: 40 http://bmcmicrobiol.biomedcentral.com/articles/10.1186/1471-2180-14-40.

Cunha, M. da, Pais, S. V, Bugalhão, J.N., and Mota, L.J. (2017) The Chlamydia trachomatis type III secretion substrates CT142, CT143, and CT144 are secreted into the lumen of the inclusion. *PLoS One* **12**: e0178856 https://doi.org/10.1371/journal.pone.0178856.

Curak, J., Rohde, J., and Stagljar, I. (2009) Yeast as a tool to study bacterial effectors. *Curr Opin Microbiol* **12**: 18–23 http://www.ncbi.nlm.nih.gov/pubmed/19150254.

Darsow, T., Odorizzi, G., and Emr, S.D. (2000) Invertase fusion proteins for analysis of protein trafficking in yeast. *Methods Enzymol* **327**: 95–106 http://www.ncbi.nlm.nih.gov/pubmed/11044977.

Darville, T., and Hiltke, T.J. (2010) Pathogenesis of genital tract disease due to Chlamydia trachomatis. *J Infect Dis* **201 Suppl**: S114-25 http://www.ncbi.nlm.nih.gov/pubmed/20524234.

Delevoye, C., Nilges, M., Dehoux, P., Paumet, F., Perrinet, S., Dautry-Varsat, A., and Subtil, A. (2008) SNARE protein mimicry by an intracellular bacterium. *PLoS Pathog* **4**.

Derré, I., Swiss, R., and Agaisse, H. (2011) The lipid transfer protein CERT interacts with the Chlamydia inclusion protein IncD and participates to ER-Chlamydia inclusion membrane contact sites. *PLoS Pathog* **7**.

Drozdetskiy, A., Cole, C., Procter, J., and Barton, G.J. (2015) JPred4: a protein secondary structure prediction server. *Nucleic Acids Res* **43**: W389-94 http://www.ncbi.nlm.nih.gov/pubmed/25883141.

Dugan, J., Andersen, A.A., and Rockey, D.D. (2007) Functional characterization of IScs605, an insertion element carried by tetracycline-resistant Chlamydia suis. *Microbiology* **153**: 71–79.

Dugan, J., Rockey, D.D., Jones, L., Arthur, A., and Andersen, A.A. (2004) Tetracycline Resistance in *Chlamydia suis* Mediated by Genomic Islands Inserted into the Chlamydial inv -Like Gene Tetracycline Resistance in Chlamydia suis Mediated by Genomic Islands Inserted into the Chlamydial inv -Like Gene. *Antimicrob Agents Chemother* **48**: 3989–3995.

Dumoux, M., Menny, A., Delacour, D., and Hayward, R.D. (2015) A Chlamydia effector recruits CEP170 to reprogram host microtubule organization. *J Cell Sci* **128**: 3420–34 http://www.ncbi.nlm.nih.gov/pubmed/26220855.

Durand, N.J., Nicolas, J., and Favre, M. (1913) Lymphogranulomatose inguinale subaiguë d'origine génitale probable, peut-être vénérienne. *Bull la Société des Médecins des Hôpitaux Paris* **35**: 274–288.

Elwell, C.A., Ceesay, A., Kim, J.H., Kalman, D., and Engel, J.N. (2008) RNA interference screen identifies Abl kinase and PDGFR signaling in Chlamydia trachomatis entry. *PLoS Pathog* **4**: e1000021 http://www.ncbi.nlm.nih.gov/pubmed/18369471.

Elwell, C.A., Czudnochowski, N., Dollen, J. von, Johnson, J.R., Nakagawa, R., Mirrashidi, K., *et al.* (2017) Chlamydia interfere with an interaction between the mannose-6-phosphate receptor and sorting nexins to counteract host restriction. *Elife* **6** http://www.ncbi.nlm.nih.gov/pubmed/28252385.

Everett, K.D. (2000) Chlamydia and Chlamydiales: more than meets the eye. *Vet Microbiol* **75**: 109–26 http://linkinghub.elsevier.com/retrieve/pii/S0378113500002133.

Everett, K.D., Bush, R.M., and Andersen, A.A. (1999) Emended description of the order Chlamydiales, proposal of Parachlamydiaceae fam. nov. and Simkaniaceae fam. nov., each containing one monotypic genus, revised taxonomy of the family Chlamydiaceae, including a new genus and five new s. *Int J Syst Bacteriol* **49 Pt 2**: 415–440.

Falcón-Pérez, J.M., Nazarian, R., Sabatti, C., and Dell'Angelica, E.C. (2005) Distribution and dynamics of Lamp1-containing endocytic organelles in fibroblasts deficient in BLOC-3. *J Cell Sci* **118**: 5243–55 http://www.ncbi.nlm.nih.gov/pubmed/16249233.

Fehlner-Gardiner, C., Roshick, C., Carlson, J.H., Hughes, S., Belland, R.J., Caldwell, H.D., and McClarty, G. (2002) Molecular basis defining human Chlamydia trachomatis tissue tropism. A possible role for tryptophan synthase. *J Biol Chem* **277**: 26893–903 http://www.ncbi.nlm.nih.gov/pubmed/12011099.

Feldman, M.F., and Cornelis, G.R. (2003) The multitalented type III chaperones: All you can do with 15 kDa. *FEMS Microbiol Lett* **219**: 151–158.

Felipe, K.S. De, Glover, R.T., Charpentier, X., Anderson, O.R., Reyes, M., Pericone, C.D., and Shuman, H.A. (2008) Legionella eukaryotic-like type IV substrates interfere with organelle trafficking. *PLoS Pathog* **4**.

Ferreira, R., Borges, V., Nunes, A., Borrego, M.J., and Gomes, J.P. (2013) Assessment of the load and transcriptional dynamics of Chlamydia trachomatis plasmid according to strains' tissue tropism. *Microbiol Res* **168**: 333–339.

Fields, K.A., and Hackstadt, T. (2000) Evidence for the secretion of Chlamydia trachomatis CopN by a type III secretion mechanism. *Mol Microbiol* **38**: 1048–60

http://www.ncbi.nlm.nih.gov/pubmed/11123678.
Fischer, A., Harrison, K.S., Ramirez, Y., Auer, D., Chowdhury, S.R., Prusty, B.K., *et al.* (2017) Chlamydia trachomatis-containing vacuole serves as deubiquitination platform to stabilize Mcl-1 and to interfere with host defense. *Elife* **6**: 1–27.
Franco, I.S., Shohdy, N., and Shuman, H.A. (2012) The Legionella pneumophila effector VipA is an actin nucleator that alters host cell organelle trafficking. *PLoS Pathog* **8**.
Furtado, A.R., Essid, M., Perrinet, S., Balañá, M.E., Yoder, N., Dehoux, P., and Subtil, A. (2013) The chlamydial OTU domain-containing protein ChlaOTU is an early type III secretion effector targeting ubiquitin and NDP52. *Cell Microbiol* **15**: 2064–79 http://www.ncbi.nlm.nih.gov/pubmed/23869922.
Galán, J.E. (2009) Common themes in the design and function of bacterial effectors. *Cell Host Microbe* **5**: 571–9 http://www.ncbi.nlm.nih.gov/pubmed/19527884.
Galán, J.E., Lara-Tejero, M., Marlovits, T.C., and Wagner, S. (2014) Bacterial Type III Secretion Systems: Specialized Nanomachines for Protein Delivery into Target Cells. *Annu Rev Microbiol* **68**: 415–438 http://www.ncbi.nlm.nih.gov/pmc/articles/PMC4388319/.
Galán, J.E., and Wolf-Watz, H. (2006) Protein delivery into eukaryotic cells by type III secretion machines. *Nature* **444**: 567–573 http://www.ncbi.nlm.nih.gov/pubmed/17136086.
Gaspar, A.H., and Machner, M.P. (2014) VipD is a Rab5-activated phospholipase A1 that protects Legionella pneumophila from endosomal fusion. *Proc Natl Acad Sci* **111**: 4560–4565 http://www.pnas.org/cgi/doi/10.1073/pnas.1316376111.
Ge, J., Gong, Y.-N., Xu, Y., and Shao, F. (2012) Preventing bacterial DNA release and absent in melanoma 2 inflammasome activation by a Legionella effector functioning in membrane trafficking. *Proc Natl Acad Sci U S A* **109**: 6193–8 http://www.ncbi.nlm.nih.gov/pubmed/22474394.
Gehre, L., Gorgette, O., Perrinet, S., Prevost, M.-C., Ducatez, M., Giebel, A.M., *et al.* (2016) Sequestration of host metabolism by an intracellular pathogen. *Elife* **5**: e12552 http://www.ncbi.nlm.nih.gov/pubmed/26981769.
Gleeson, P.A. (2014) The role of endosomes in innate and adaptive immunity. *Semin Cell Dev Biol* **31**: 64–72 http://www.ncbi.nlm.nih.gov/pubmed/24631355.
Gomes, J.P., Nunes, A., Bruno, W.J., Borrego, M.J., Florindo, C., and Dean, D. (2006) Polymorphisms in the nine polymorphic membrane proteins of Chlamydia trachomatis across all serovars: evidence for serovar Da recombination and correlation with tissue tropism. *J Bacteriol* **188**: 275–86 http://www.ncbi.nlm.nih.gov/pubmed/16352844.
Gong, S., Lei, L., Chang, X., Belland, R., and Zhong, G. (2011) Chlamydia trachomatis secretion of hypothetical protein CT622 into host cell cytoplasm via a secretion pathway that can be inhibited by the type III secretion system inhibitor compound 1. *Microbiology* **157**: 1134–44 http://www.ncbi.nlm.nih.gov/pubmed/21233161.
Gong, S., Yang, Z., Lei, L., Shen, L., and Zhong, G. (2013) Characterization of chlamydia trachomatis plasmid-encoded open reading frames. *J Bacteriol* **195**: 3819–3826.
Gophna, U., Ron, E.Z., and Graur, D. (2003) Bacterial type III secretion systems are ancient and evolved by multiple horizontal-transfer events. *Gene* **312**: 151–63 http://www.ncbi.nlm.nih.gov/pubmed/12909351.
Gottlieb, S.L., Deal, C.D., Giersing, B., Rees, H., Bolan, G., Johnston, C., *et al.* (2016) The global roadmap for advancing development of vaccines against sexually transmitted infections: Update and next steps. *Vaccine* **34**: 2939–2947 http://www.ncbi.nlm.nih.gov/pubmed/27105564.
Grangeasse, C., Stülke, J., and Mijakovic, I. (2015) Regulatory potential of post-translational modifications in bacteria. *Front Microbiol* **6**: 500 http://www.ncbi.nlm.nih.gov/pubmed/26074895.
Grieshaber, S.S., Grieshaber, N.A., and Hackstadt, T. (2003) Chlamydia trachomatis uses host cell dynein to traffic to the microtubule-organizing center in a p50 dynamitin-independent process. *J Cell Sci* **116**: 3793–802 http://www.ncbi.nlm.nih.gov/pubmed/12902405.
Gruenheid, S., Sekirov, I., Thomas, N.A., Deng, W., O'Donnell, P., Goode, D., *et al.* (2004) Identification and characterization of NleA, a non-LEE-encoded type III translocated virulence factor of enterohaemorrhagic Escherichia coli O157:H7. *Mol Microbiol* **51**: 1233–49 http://www.ncbi.nlm.nih.gov/pubmed/14982621.
Gurumurthy, R.K., Chumduri, C., Karlas, A., Kimmig, S., Gonzalez, E., Machuy, N., *et al.* (2014) Dynamin-mediated lipid acquisition is essential for Chlamydia trachomatis development. *Mol Microbiol* **94**: 186–201 http://www.ncbi.nlm.nih.gov/pubmed/25116793.
Hackstadt, T., Todd, W.J., and Caldwell, H.D. (1985) Disulfide-mediated interactions of the chlamydial major outer membrane protein: role in the differentiation of chlamydiae? *J Bacteriol* **161**: 25–31 http://www.ncbi.nlm.nih.gov/pubmed/2857160.
Halberstaedter, L., and Prowazek, S. von (1907) Zur Aetiologie des Trachoms. *Dtsch Medizinische Wochenschrift* **33**: 1285–7.

Hammond, G.R. V, Fischer, M.J., Anderson, K.E., Holdich, J., Koteci, A., Balla, T., and Irvine, R.F. (2012) PI4P and PI(4,5)P2 are essential but independent lipid determinants of membrane identity. *Science* **337**: 727–30 http://www.ncbi.nlm.nih.gov/pubmed/22722250.

Hansen-Wester, I., and Hensel, M. (2001) Salmonella pathogenicity islands encoding type III secretion systems. *Microbes Infect* **3**: 549–59 http://www.ncbi.nlm.nih.gov/pubmed/11418329.

Harris, S.R., Clarke, I.N., Seth-Smith, H.M.B., Solomon, A.W., Cutcliffe, L.T., Marsh, P., *et al.* (2012) Whole-genome analysis of diverse Chlamydia trachomatis strains identifies phylogenetic relationships masked by current clinical typing. *Nat Genet* **44**: 413–9, S1 http://www.ncbi.nlm.nih.gov/pubmed/22406642.

Harryman, L., Blee, K., and Horner, P. (2014) Chlamydia trachomatis and non-gonococcal urethritis. *Medicine (Baltimore)* **42**: 327–332 http://linkinghub.elsevier.com/retrieve/pii/S135730391400067X.

Hartley, J.C., Stevenson, S., Robinson, A.J., Littlewood, J.D., Carder, C., Cartledge, J., *et al.* (2001) Conjunctivitis due to Chlamydophila felis (Chlamydia psittaci feline pneumonitis agent) acquired from a cat: case report with molecular characterization of isolates from the patient and cat. *J Infect* **43**: 7–11 http://www.ncbi.nlm.nih.gov/pubmed/11597148.

Hefty, P.S., and Stephens, R.S. (2007) Chlamydial type III secretion system is encoded on ten operons preceded by sigma 70-like promoter elements. *J Bacteriol* **189**: 198–206 http://www.ncbi.nlm.nih.gov/pubmed/17056752.

Heinzen, R.A., Scidmore, M.A., Rockey, D.D., and Hackstadt, T. (1996) Differential interaction with endocytic and exocytic pathways distinguish parasitophorous vacuoles of Coxiella burnetii and Chlamydia trachomatis. *Infect Immun* **64**: 796–809 http://www.ncbi.nlm.nih.gov/pmc/articles/PMC173840/.

Heuer, D., Rejman Lipinski, A., Machuy, N., Karlas, A., Wehrens, A., Siedler, F., *et al.* (2009) Chlamydia causes fragmentation of the Golgi compartment to ensure reproduction. *Nature* **457**: 731–5 http://www.ncbi.nlm.nih.gov/pubmed/19060882.

Hicks, S.W., Charron, G., Hang, H.C., and Galán, J.E. (2011) Subcellular targeting of Salmonella virulence proteins by host-mediated S-palmitoylation. *Cell Host Microbe* **10**: 9–20 http://www.ncbi.nlm.nih.gov/pubmed/21767808.

Ho, T.D., and Starnbach, M.N. (2005) The Salmonella enterica serovar typhimurium-encoded type III secretion systems can translocate Chlamydia trachomatis proteins into the cytosol of host cells. *Infect Immun* **73**: 905–11 http://www.ncbi.nlm.nih.gov/pubmed/15664932.

Hobolt-Pedersen, A.S., Christiansen, G., Timmerman, E., Gevaert, K., and Birkelund, S. (2009) Identification of Chlamydia trachomatis CT621, a protein delivered through the type III secretion system to the host cell cytoplasm and nucleus. *FEMS Immunol Med Microbiol* **57**: 46–58.

Hogan, R.J., Mathews, S.A., Mukhopadhyay, S., Summersgill, J.T., and Timms, P. (2004) Chlamydial persistence: beyond the biphasic paradigm. *Infect Immun* **72**: 1843–55 http://www.ncbi.nlm.nih.gov/pubmed/15039303.

Horn, M. (2008) Chlamydiae as Symbionts in Eukaryotes. *Annu Rev Microbiol* **62**: 113–131 http://www.annualreviews.org/doi/10.1146/annurev.micro.62.081307.162818.

Hou, S., Dong, X., Yang, Z., Li, Z., Liu, Q., and Zhong, G. (2015) Chlamydial plasmid-encoded virulence factor Pgp3 neutralizes the antichlamydial activity of human cathelicidin LL-37. *Infect Immun* **83**: 4701–4709.

Hou, S., Sun, X., Dong, X., Lin, H., Tang, L., Xue, M., and Zhong, G. (2018) Chlamydial plasmid-encoded virulence factor Pgp3 interacts with human cathelicidin peptide LL-37 to modulate immune response. *Microbes Infect* 6–11 https://doi.org/10.1016/j.micinf.2018.06.003.

Hovis, K.M., Mojica, S., McDermott, J.E., Pedersen, L., Simhi, C., Rank, R.G., *et al.* (2013) Genus-optimized strategy for the identification of chlamydial type III secretion substrates. *Pathog Dis* **69**: 213–22 http://www.ncbi.nlm.nih.gov/pubmed/23873765.

Hower, S., Wolf, K., and Fields, K.A. (2009) Evidence that CT694 is a novel Chlamydia trachomatis T3S substrate capable of functioning during invasion or early cycle development. *Mol Microbiol* **72**: 1423–37 http://www.ncbi.nlm.nih.gov/pubmed/19460098.

Huang, Z., Feng, Y., Chen, D., Wu, X., Huang, S., Wang, X., *et al.* (2008) Structural Basis for Activation and Inhibition of the Secreted Chlamydia Protease CPAF. *Cell Host Microbe* **4**: 529–542 http://www.ncbi.nlm.nih.gov/pubmed/19064254.

Hueck, C.J. (1998) Type III protein secretion systems in bacterial pathogens of animals and plants. *Microbiol Mol Biol Rev* **62**: 379–433 http://www.ncbi.nlm.nih.gov/pubmed/9618447.

Hybiske, K., and Stephens, R.S. (2007) Mechanisms of host cell exit by the intracellular bacterium Chlamydia. *Proc Natl Acad Sci U S A* **104**: 11430–5 http://www.ncbi.nlm.nih.gov/pubmed/17592133.

Illingworth, M., Hooppaw, A.J., Ruan, L., Fisher, D.J., and Chen, L. (2017) Biochemical and Genetic Analysis of the Chlamydia GroEL Chaperonins. *J Bacteriol* **199**: e00844-16

http://jb.asm.org/lookup/doi/10.1128/JB.00844-16.
Inoue, T., Heo, W. Do, Grimley, J.S., Wandless, T.J., and Meyer, T. (2005) An inducible translocation strategy to rapidly activate and inhibit small GTPase signaling pathways. *Nat Methods* **2**: 415–8 http://www.ncbi.nlm.nih.gov/pubmed/15908919.
INSA Inquiry 2015-2016 (2016) .
Iriarte, M., and Cornelis, G.R. (1998) YopT, a new Yersinia Yop effector protein, affects the cytoskeleton of host cells. *Mol Microbiol* **29**: 915–29 http://www.ncbi.nlm.nih.gov/pubmed/9723929.
Jewett, T.J., Dooley, C.A., Mead, D.J., and Hackstadt, T. (2008) Chlamydia trachomatis tarp is phosphorylated by src family tyrosine kinases. *Biochem Biophys Res Commun* **371**: 339–44 http://www.ncbi.nlm.nih.gov/pubmed/18442471.
Jewett, T.J., Fischer, E.R., Mead, D.J., and Hackstadt, T. (2006) Chlamydial TARP is a bacterial nucleator of actin. *Proc Natl Acad Sci U S A* **103(42)**: 15599–15604 http://www.pubmedcentral.nih.gov/articlerender.fcgi?artid=1622868&tool=pmcentrez&rendertype=abstract.
Jewett, T.J., Miller, N.J., Dooley, C.A., and Hackstadt, T. (2010) The conserved tarp actin binding domain is important for chlamydial invasion. *PLoS Pathog* **6**: 1–11.
Jiwani, S., Ohr, R.J., Fischer, E.R., Hackstadt, T., Alvarado, S., Romero, A., and Jewett, T.J. (2012) Chlamydia trachomatis Tarp cooperates with the Arp2/3 complex to increase the rate of actin polymerization. *Biochem Biophys Res Commun* **420**: 816–821.
Johnson, C.M., and Fisher, D.J. (2013) Site-specific, insertional inactivation of inca in chlamydia trachomatis using a group II intron. *PLoS One* **8**.
Jorgensen, I., Bednar, M.M., Amin, V., Davis, B.K., Ting, J.P.Y., McCafferty, D.G., and Valdivia, R.H. (2011) The Chlamydia Protease CPAF Regulates Host and Bacterial Proteins to Maintain Pathogen Vacuole Integrity and Promote Virulence. *Cell Host Microbe* **10**: 21–32 http://www.ncbi.nlm.nih.gov/pubmed/21767809.
Kalman, S., Mitchell, W., Marathe, R., Lammel, C., Fan, J., Hyman, R.W., *et al.* (1999) Comparative genomes of Chlamydia pneumoniae and C. trachomatis. *Nat Genet* **21**: 385–9 http://www.ncbi.nlm.nih.gov/pubmed/10192388.
Kari, L., Goheen, M.M., Randall, L.B., Taylor, L.D., Carlson, J.H., Whitmire, W.M., *et al.* (2011) Generation of targeted Chlamydia trachomatis null mutants. *Proc Natl Acad Sci U S A* **108**: 7189–7193.
Key, C.E., and Fisher, D.J. (2017) Use of Group II Intron Technology for Targeted Mutagenesis in Chlamydia trachomatis. *Methods Mol Biol* **1498**: 163–177 http://www.ncbi.nlm.nih.gov/pubmed/27709575.
Kim, B.H., Kim, H.G., Kim, J.S., Jang, J.I., and Park, Y.K. (2007) Analysis of functional domains present in the N-terminus of the SipB protein. *Microbiology* **153**: 2998–3008 http://mic.microbiologyresearch.org/content/journal/micro/10.1099/mic.0.2007/007872-0.
Kim, B.S., and Satchell, K.J.F. (2016) MARTX effector cross kingdom activation by Golgi-associated ADP-ribosylation factors. *Cell Microbiol* **18**: 1078–93 http://www.ncbi.nlm.nih.gov/pubmed/26780191.
Kim, J., Thanabalasuriar, A., Chaworth-Musters, T., Fromme, J.C., Frey, E.A., Lario, P.I., *et al.* (2007) The bacterial virulence factor NleA inhibits cellular protein secretion by disrupting mammalian COPII function. *Cell Host Microbe* **2**: 160–71 http://www.ncbi.nlm.nih.gov/pubmed/18005731.
Kokes, M., Dunn, J.D., Granek, J.A., Nguyen, B.D., Barker, J.R., Valdivia, R.H., and Bastidas, R.J. (2015) Integrating chemical mutagenesis and whole-genome sequencing as a platform for forward and reverse genetic analysis of Chlamydia. *Cell Host Microbe* **17**: 716–725 http://dx.doi.org/10.1016/j.chom.2015.03.014.
Kovach, M.E., Phillips, R.W., Elzer, P.H., Roop, R.M., and Peterson, K.M. (1994) pBBR1MCS: a broad-host-range cloning vector. *Biotechniques* **16**: 800–2 http://www.ncbi.nlm.nih.gov/pubmed/8068328.
Kumar, Y., Cocchiaro, J., and Valdivia, R.H. (2006) The obligate intracellular pathogen Chlamydia trachomatis targets host lipid droplets. *Curr Biol* **16**: 1646–51 http://www.ncbi.nlm.nih.gov/pubmed/16920627.
Kumar, Y., and Valdivia, R.H. (2008) Actin and Intermediate Filaments Stabilize the Chlamydia trachomatis Vacuole by Forming Dynamic Structural Scaffolds. *Cell Host Microbe* **4**: 159–169 http://www.ncbi.nlm.nih.gov/pubmed/18692775.
Laar, M.J.W. van de, and Morré, S.A. (2007) Chlamydia: a major challenge for public health. *Euro Surveill* **12**: E1-2 http://www.ncbi.nlm.nih.gov/pubmed/17997923.
Lad, S.P., Li, J., Silva Correia, J. da, Pan, Q., Gadwal, S., Ulevitch, R.J., and Li, E. (2007) Cleavage of p65/RelA of the NF- B pathway by Chlamydia. *Proc Natl Acad Sci* **104**: 2933–2938 http://www.ncbi.nlm.nih.gov/pubmed/17301240.

Lad, S.P., Yang, G., Scott, D.A., Wang, G., Nair, P., Mathison, J., *et al.* (2007) Chlamydial CT441 is a PDZ domain-containing tail-specific protease that interferes with the NF-kappaB pathway of immune response. *J Bacteriol* **189**: 6619–25 http://www.ncbi.nlm.nih.gov/pubmed/17631635.

Lane, B.J., Mutchler, C., Khodor, S. Al, Grieshaber, S.S., and Carabeo, R.A. (2008) Chlamydial entry involves TARP binding of guanine nucleotide exchange factors. *PLoS Pathog* **4**.

Lee, J.K., Enciso, G.A., Boassa, D., Chander, C.N., Lou, T.H., Pairawan, S.S., *et al.* (2018) Replication-dependent size reduction precedes differentiation in Chlamydia trachomatis. *Nat Commun* **9**: 45 http:https://doi.org/10.1038/s41467-017-02432-0.

Lee, S.F., Kelly, M., McAlister, A., Luck, S.N., Garcia, E.L., Hall, R.A., *et al.* (2008) A C-terminal class I PDZ binding motif of EspI/NleA modulates the virulence of attaching and effacing Escherichia coli and Citrobacter rodentium. *Cell Microbiol* **10**: 499–513 http://www.ncbi.nlm.nih.gov/pubmed/17979986.

Letzelter, M., Sorg, I., Mota, L.J., Meyer, S., Stalder, J., Feldman, M., *et al.* (2006) The discovery of SycO highlights a new function for type III secretion effector chaperones. *EMBO J* **25**: 3223–33 http://www.ncbi.nlm.nih.gov/pubmed/16794578.

Li, Z., Chen, C., Chen, D., Wu, Y., Zhong, Y., and Zhong, G. (2008) Characterization of fifty putative inclusion membrane proteins encoded in the Chlamydia trachomatis genome. *Infect Immun* **76**: 2746–57 http://www.ncbi.nlm.nih.gov/pubmed/18391011.

Li, Z., Chen, D., Zhong, Y., Wang, S., and Zhong, G. (2008) The chlamydial plasmid-encoded protein pgp3 is secreted into the cytosol of Chlamydia-infected cells. *Infect Immun* **76**: 3415–3428.

Lin, Y.-H., Doms, A.G., Cheng, E., Kim, B., Evans, T.R., and Machner, M.P. (2015) Host Cell-catalyzed S -Palmitoylation Mediates Golgi Targeting of the Legionella Ubiquitin Ligase GobX. *J Biol Chem* **290**: 25766–25781 http://www.ncbi.nlm.nih.gov/pubmed/26316537.

Lindner, K. (1910) Zur atiologie der gonokokken-freien urethritis. *Wien Klin Wochenschr* **8**: 283–284.

Lippincott-Schwartz, J., Yuan, L.C., Bonifacino, J.S., and Klausner, R.D. (1989) Rapid redistribution of Golgi proteins into the ER in cells treated with brefeldin A: evidence for membrane cycling from Golgi to ER. *Cell* **56**: 801–13 http://www.ncbi.nlm.nih.gov/pubmed/2647301.

Liu, Y., Chen, C., Gong, S., Hou, S., Qi, M., Liu, Q., *et al.* (2014) Transformation of Chlamydia muridarum reveals a role for Pgp5 in suppression of plasmid-dependent gene expression. *J Bacteriol* **196**: 989–998.

Liu, Y., Huang, Y., Yang, Z., Sun, Y., Gong, S., Hou, S., *et al.* (2014) Plasmid-encoded Pgp3 is a major virulence factor for Chlamydia muridarum to induce hydrosalpinx in mice. *Infect Immun* **82**: 5327–5335.

Lloyd, S.A., Norman, M., Rosqvist, R., and Wolf-Watz, H. (2001) Yersinia YopE is targeted for type III secretion by N-terminal, not mRNA, signals. *Mol Microbiol* **39**: 520–31 http://www.ncbi.nlm.nih.gov/pubmed/11136471.

Login, F.H., and Wolf-Watz, H. (2015) YscU/FlhB of Yersinia pseudotuberculosis Harbors a C-terminal Type III Secretion Signal. *J Biol Chem* **290**: 26282–91 http://www.ncbi.nlm.nih.gov/pubmed/26338709.

Longbottom, D., and Coulter, L.J. (2003) Animal chlamydioses and zoonotic implications. *J Comp Pathol* **128**: 217–244.

Lovett, M., Kuo, C.C., Holmes, K., and Falkow, S. (1980) Plasmids of the genus Chlamydia. *Curr Chemother Infect Dis* **2**: 1250–1252.

Lowden, N.M., Yeruva, L., Johnson, C.M., Bowlin, A.K., and Fisher, D.J. (2015) Use of aminoglycoside 3' adenyltransferase as a selection marker for Chlamydia trachomatis intron-mutagenesis and in vivo intron stability. *BMC Res Notes* **8**: 570 http://bmcresnotes.biomedcentral.com/articles/10.1186/s13104-015-1542-9.

Löwer, M., and Schneider, G. (2009) Prediction of type III secretion signals in genomes of gram-negative bacteria. *PLoS One* **4**: e5917 http://www.ncbi.nlm.nih.gov/pubmed/19526054.

Lutter, E.I., Barger, A.C., Nair, V., and Hackstadt, T. (2013) Chlamydia trachomatis inclusion membrane protein CT228 recruits elements of the myosin phosphatase pathway to regulate release mechanisms. *Cell Rep* **3**: 1921–31 http://www.ncbi.nlm.nih.gov/pubmed/23727243.

Lutter, E.I., Bonner, C., Holland, M.J., Suchland, R.J., Stamm, W.E., Jewett, T.J., *et al.* (2010) Phylogenetic analysis of Chlamydia trachomatis Tarp and correlation with clinical phenotype. *Infect Immun* **78**: 3678–88 http://www.ncbi.nlm.nih.gov/pubmed/20605986.

Lutter, E.I., Martens, C., and Hackstadt, T. (2012) Evolution and conservation of predicted inclusion membrane proteins in chlamydiae. *Comp Funct Genomics* **2012**: 362104 http://www.ncbi.nlm.nih.gov/pubmed/22454599.

Mabey, D., and Peeling, R.W. (2002) Lymphogranuloma venereum. *Sex Transm Infect* **78**: 90–2 http://www.ncbi.nlm.nih.gov/pubmed/12081191.

Marenne, M.-N., Journet, L., Mota, L.J., and Cornelis, G.R. (2003) Genetic analysis of the formation of the Ysc-Yop translocation pore in macrophages by Yersinia enterocolitica: role of LcrV, YscF and YopN. *Microb Pathog* **35**: 243–58 http://www.ncbi.nlm.nih.gov/pubmed/14580388.

Markham, A.P., Jaafar, Z.A., Kemege, K.E., Middaugh, C.R., and Hefty, P.S. (2009) Biophysical characterization of Chlamydia trachomatis CT584 supports its potential role as a type III secretion needle tip protein. *Biochemistry* **48**: 10353–61 http://www.ncbi.nlm.nih.gov/pubmed/19769366.

Martin-Iguacel, R., Llibre, J.M., Nielsen, H., Heras, E., Matas, L., Lugo, R., *et al.* (2010) Lymphogranuloma venereum proctocolitis: a silent endemic disease in men who have sex with men in industrialised countries. *Eur J Clin Microbiol Infect Dis* **29**: 917–925 http://www.ncbi.nlm.nih.gov/pubmed/20509036.

Matsumoto, A. (1973) Fine structures of cell envelopes of Chlamydia organisms as revealed by freeze-etching and negative staining techniques. *J Bacteriol* **116**: 1355–63 http://www.ncbi.nlm.nih.gov/pubmed/4127629.

Matsumoto, A., Izutsu, H., Miyashita, N., and Ohuchi, M. (1998) Plaque Formation by and Plaque Cloning of Chlamydia trachomatis Biovar Trachoma These include : Plaque Formation by and Plaque Cloning of Chlamydia trachomatis Biovar Trachoma. *J ClinMicrobiol* **36**: 3013–3019.

McKuen, M.J., Mueller, K.E., Bae, Y.S., and Fields, K.A. (2017) Fluorescence-Reported Allelic Exchange Mutagenesis Reveals a Role for Chlamydia trachomatis TmeA in Invasion That Is Independent of Host AHNAK. *Infect Immun* **85**: e00640-17 http://iai.asm.org/lookup/doi/10.1128/IAI.00640-17.

Mehlitz, A., Banhart, S., Hess, S., Selbach, M., and Meyer, T.F. (2008) Complex kinase requirements for Chlamydia trachomatis Tarp phosphorylation. *FEMS Microbiol Lett* **289**: 233–240.

Mehlitz, A., Banhart, S., Mäurer, A.P., Kaushansky, A., Gordus, A.G., Zielecki, J., *et al.* (2010) Tarp regulates early Chlamydia-induced host cell survival through interactions with the human adaptor protein SHC1. *J Cell Biol* **190**: 143–157.

Mendonça, A.G., Alves, R.J., and Pereira-Leal, J.B. (2011) Loss of genetic redundancy in reductive genome evolution. *PLoS Comput Biol* **7**: e1001082 http://www.ncbi.nlm.nih.gov/pubmed/21379323.

Meyer, T. (2016) Diagnostic Procedures to Detect Chlamydia trachomatis Infections. *Microorganisms* **4**: 25 http://www.mdpi.com/2076-2607/4/3/25.

Michiels, T., and Cornelis, G.R. (1991) Secretion of hybrid proteins by the Yersinia Yop export system. *J Bacteriol* **173**: 1677–85 http://www.ncbi.nlm.nih.gov/pubmed/1999387.

Miller, C.N., Smith, E.P., Cundiff, J.A., Knodler, L.A., Bailey Blackburn, J., Lupashin, V., and Celli, J. (2017) A Brucella Type IV Effector Targets the COG Tethering Complex to Remodel Host Secretory Traffic and Promote Intracellular Replication. *Cell Host Microbe* **22**: 317–329.e7 http://www.ncbi.nlm.nih.gov/pubmed/28844886.

Mirrashidi, K.M., Elwell, C.A., Verschueren, E., Johnson, J.R., Frando, A., Dollen, J. Von, *et al.* (2015) Global Mapping of the Inc-Human Interactome Reveals that Retromer Restricts Chlamydia Infection. *Cell Host Microbe* **18**: 109–21 http://www.ncbi.nlm.nih.gov/pubmed/24655651.

Misaghi, S., Balsara, Z.R., Catic, A., Spooner, E., Ploegh, H.L., and Starnbach, M.N. (2006) Chlamydia trachomatis-derived deubiquitinating enzymes in mammalian cells during infection. *Mol Microbiol* **61**: 142–50 http://www.ncbi.nlm.nih.gov/pubmed/16824101.

Mital, J., and Hackstadt, T. (2011) Role for the SRC family kinase Fyn in sphingolipid acquisition by chlamydiae. *Infect Immun* **79**: 4559–68 http://www.ncbi.nlm.nih.gov/pubmed/21896774.

Mital, J., Lutter, E.I., Barger, A.C., Dooley, C.A., and Hackstadt, T. (2015) Chlamydia trachomatis inclusion membrane protein CT850 interacts with the dynein light chain DYNLT1 (Tctex1). *Biochem Biophys Res Commun* **462**: 165–70 http://dx.doi.org/10.1016/j.bbrc.2015.04.116.

Miyagawa, Y., Mitamura, T., Yaoi, H., Ishii, N., and Okanishi, J. (1935) Studies on the virus of lymphogranuloma inguinale Nicolas, Favre and Durand. *Jpn J Exp Med* **13**: 733–738.

Miyairi, I., Mahdi, O.S., Ouellette, S.P., Belland, R.J., and Byrne, G.I. (2006) Different growth rates of Chlamydia trachomatis biovars reflect pathotype. *J Infect Dis* **194**: 350–7 http://www.ncbi.nlm.nih.gov/pubmed/16826483.

Moore, E.R., Mead, D.J., Dooley, C.A., Sager, J., and Hackstadt, T. (2011a) The trans-Golgi SNARE syntaxin 6 is recruited to the chlamydial inclusion membrane. *Microbiology* **157**: 830–8 http://www.ncbi.nlm.nih.gov/pubmed/21109560.

Moore, E.R., Mead, D.J., Dooley, C.A., Sager, J., and Hackstadt, T. (2011b) The trans-Golgi SNARE syntaxin 6 is recruited to the chlamydial inclusion membrane. *Microbiology* **157**: 830–8 http://www.ncbi.nlm.nih.gov/pubmed/21124879.

Moulder, J.W. (1966) The Relation of the Psittacosis Group (Chlamydiae) to Bacteria and Viruses. *Annu Rev Microbiol* **20**: 107–130 http://www.annualreviews.org/doi/10.1146/annurev.mi.20.100166.000543.

Mu, Y., Cai, P., Hu, S., Ma, S., and Gao, Y. (2014) Characterization of diverse internal binding specificities of PDZ domains by yeast two-hybrid screening of a special peptide library. *PLoS One* **9**: e88286 http://www.ncbi.nlm.nih.gov/pubmed/24505465.

Mueller, K.E., and Fields, K.A. (2015) Application of β-lactamase reporter fusions as an indicator of effector protein secretion during infections with the obligate intracellular pathogen Chlamydia trachomatis. *PLoS One* **10**: 1–18.

Mueller, K.E., Wolf, K., and Fields, K.A. (2016) Gene deletion by fluorescence-reported allelic exchange mutagenesis in Chlamydia trachomatis. *MBio* **7**: 1–9.

Murray, R.Z., and Stow, J.L. (2014) Cytokine Secretion in Macrophages: SNAREs, Rabs, and Membrane Trafficking. *Front Immunol* **5**: 538 http://www.ncbi.nlm.nih.gov/pubmed/25386181.

Muschiol, S., Boncompain, G., Vromman, F., Dehoux, P., Normark, S., Henriques-Normark, B., and Subtil, A. (2011) Identification of a family of effectors secreted by the type III secretion system that are conserved in pathogenic Chlamydiae. *Infect Immun* **79**: 571–80 http://www.ncbi.nlm.nih.gov/pubmed/21078856.

Negrate, G. Le, Krieg, A., Faustin, B., Loeffler, M., Godzik, A., Krajewski, S., and Reed, J.C. (2008) Chla Dub1 of Chlamydia trachomatis suppresses NF-κB activation and inhibits IκBα ubiquitination and degradation. *Cell Microbiol* **10**: 1879–1892 http://www.ncbi.nlm.nih.gov/pubmed/18503636.

Nguyen, B.D., and Valdivia, R.H. (2012) Virulence determinants in the obligate intracellular pathogen Chlamydia trachomatis revealed by forward genetic approaches. *Proc Natl Acad Sci U S A* **109**: 1263–8 http://www.ncbi.nlm.nih.gov/pubmed/22232666%5Cnhttp://www.pubmedcentral.nih.gov/articlerender.fcgi?artid=PMC3268281.

Nguyen, B.D., and Valdivia, R.H. (2013) Forward genetic approaches in Chlamydia trachomatis. *J Vis Exp* e50636 http://www.ncbi.nlm.nih.gov/pubmed/24192560.

Nguyen, P.H., Lutter, E.I., and Hackstadt, T. (2018) Chlamydia trachomatis inclusion membrane protein MrcA interacts with the inositol 1,4,5-trisphosphate receptor type 3 (ITPR3) to regulate extrusion formation. *PLoS Pathog* **14**: e1006911 http://www.ncbi.nlm.nih.gov/pubmed/29543918.

O'Connell, C.M., and Ferone, M.E. (2016) Chlamydia trachomatis Genital Infections. *Microb cell (Graz, Austria)* **3**: 390–403 http://microbialcell.com/researcharticles/chlamydia-trichomatis-genital-infections.

O'Connell, C.M., and Nicks, K.M. (2006) A plasmic-cured Chlamydia muridarum strain displays altered plaque morphology and reduced infectivity in cell culture. *Microbiology* **152**: 1601–1607.

Omsland, A., Sixt, B.S., Horn, M., and Hackstadt, T. (2014) Chlamydial metabolism revisited: interspecies metabolic variability and developmental stage-specific physiologic activities. *FEMS Microbiol Rev* **38**: 779–801 http://www.ncbi.nlm.nih.gov/pubmed/24484402.

Ouellette, S.P. (2018) Feasibility of a Conditional Knockout System forChlamydiaBased on CRISPR Interference. *Front Cell Infect Microbiol* **8**: 59 http://www.ncbi.nlm.nih.gov/pubmed/29535977%0Ahttp://www.pubmedcentral.nih.gov/articlerender.fcgi?artid=PMC5835046.

Ouellette, S.P., and Carabeo, R.A. (2010a) A Functional Slow Recycling Pathway of Transferrin is Required for Growth of Chlamydia. *Front Microbiol* **1**: 112 http://www.ncbi.nlm.nih.gov/pubmed/21607082.

Ouellette, S.P., and Carabeo, R.A. (2010b) A Functional Slow Recycling Pathway of Transferrin is Required for Growth of Chlamydia. *Front Microbiol* **1**: 112 http://www.ncbi.nlm.nih.gov/pubmed/25293760.

Ouellette, S.P., Dorsey, F.C., Moshiach, S., Cleveland, J.L., and Carabeo, R.A. (2011) Chlamydia Species-Dependent Differences in the Growth Requirement for Lysosomes. *PLoS One* **6**: e16783 https://doi.org/10.1371/journal.pone.0016783.

Pais, S. V, Milho, C., Almeida, F., and Mota, L.J. (2013) Identification of Novel Type III Secretion Chaperone-Substrate Complexes of Chlamydia trachomatis. *PLoS One* **8**: e56292 http://dx.plos.org/10.1371/journal.pone.0056292.

Palmer, L., and Falkow, S. (1986) A common plasmid of Chlamydia trachomatis. *Plasmid* **16**: 52–62 http://linkinghub.elsevier.com/retrieve/pii/0147619X8690079X.

Parsot, C., Hamiaux, C., and Page, A.L. (2003) The various and varying roles of specific chaperones in type III secretion systems. *Curr Opin Microbiol* **6**: 7–14.

Patel, J.C., Hueffer, K., Lam, T.T., and Galán, J.E. (2009) Diversification of a Salmonella virulence protein function by ubiquitin-dependent differential localization. *Cell* **137**: 283–94 http://www.ncbi.nlm.nih.gov/pubmed/19379694.

Patton, M.J., Chen, C.-Y., Yang, C., McCorrister, S., Grant, C., Westmacott, G., *et al.* (2018) Plasmid Negative Regulation of CPAF Expression Is Pgp4 Independent and Restricted to Invasive Chlamydia

trachomatis Biovars. *MBio* **9** http://www.ncbi.nlm.nih.gov/pubmed/29382731.
Patton, M.J., McCorrister, S., Grant, C., Westmacott, G., Fariss, R., Hu, P., *et al.* (2016) Chlamydial Protease-Like Activity Factor and Type III Secreted Effectors Cooperate in Inhibition of p65 Nuclear Translocation. *MBio* **7** http://www.ncbi.nlm.nih.gov/pubmed/27677792.
Paumet, F., Wesolowski, J., Garcia-Diaz, A., Delevoye, C., Aulner, N., Shuman, H.A., *et al.* (2009) Intracellular bacteria encode inhibitory SNARE-like proteins. *PLoS One* **4**: e7375 http://www.ncbi.nlm.nih.gov/pubmed/19823575.
Pennini, M.E., Perrinet, S., Dautry-Varsat, A., and Subtil, A. (2010) Histone methylation by NUE, a novel nuclear effector of the intracellular pathogen Chlamydia trachomatis. *PLoS Pathog* **6**: e1000995 http://www.ncbi.nlm.nih.gov/pubmed/20657819.
Pickett, M.A., Everson, J.S., Pead, P.J., and Clarke, I.N. (2005) The plasmids of Chlamydia trachomatis and Chlamydophila pneumoniae (N16): Accurate determination of copy number and the paradoxical effect of plasmid-curing agents. *Microbiology* **151**: 893–903.
Pirbhai, M., Dong, F., Zhong, Y., Pan, K.Z., and Zhong, G. (2006) The Secreted Protease Factor CPAF Is Responsible for Degrading Pro-apoptotic BH3-only Proteins in Chlamydia trachomatis -infected Cells. *J Biol Chem* **281**: 31495–31501 http://www.ncbi.nlm.nih.gov/pubmed/16940052.
Pokrovskaya, I.D., Szwedo, J.W., Goodwin, A., Lupashina, T. V, Nagarajan, U.M., and Lupashin, V. V (2012) Chlamydia trachomatis hijacks intra-Golgi COG complex-dependent vesicle trafficking pathway. *Cell Microbiol* **14**: 656–68 http://www.ncbi.nlm.nih.gov/pubmed/22233276.
Polkinghorne, A., Hanger, J., and Timms, P. (2013) Recent advances in understanding the biology, epidemiology and control of chlamydial infections in koalas. *Vet Microbiol* **165**: 214–223 http://dx.doi.org/10.1016/j.vetmic.2013.02.026.
Poston, T.B., Gottlieb, S.L., and Darville, T. (2017) Status of vaccine research and development of vaccines for Chlamydia trachomatis infection. *Vaccine* http://dx.doi.org/10.1016/j.vaccine.2017.01.023.
Prusty, B.K., Chowdhury, S.R., Gulve, N., and Rudel, T. (2018) Peptidase Inhibitor 15 (PI15) Regulates Chlamydial CPAF Activity. *Front Cell Infect Microbiol* **8**: 183 http://www.ncbi.nlm.nih.gov/pubmed/29900129.
Rajeeve, K., Das, S., Prusty, B.K., and Rudel, T. (2018) Chlamydia trachomatis paralyses neutrophils to evade the host innate immune response. *Nat Microbiol* **3**: 824–835 http://www.ncbi.nlm.nih.gov/pubmed/29946164.
Rank, R.G., Bowlin, A.K., Reed, R.L., and Darville, T. (2003) Characterization of chlamydial genital infection resulting from sexual transmission from male to female guinea pigs and determination of infectious dose. *Infect Immun* **71**: 6148–54 http://www.ncbi.nlm.nih.gov/pubmed/14573630.
Rank, R.G., and Sanders, M.M. (1992) Pathogenesis of endometritis and salpingitis in a guinea pig model of chlamydial genital infection. *Am J Pathol* **140**: 927–936 http://www.ncbi.nlm.nih.gov/pubmed/1562052%5Cnhttp://www.ncbi.nlm.nih.gov/pmc/articles/PMC1886353/pdf/amjpathol00088-0169.pdf.
Read, T.D., Brunham, R.C., Shen, C., Gill, S.R., Heidelberg, J.F., White, O., *et al.* (2000) Genome sequences of Chlamydia trachomatis MoPn and Chlamydia pneumoniae AR39. *Nucleic Acids Res* **28**: 1397–406 http://www.ncbi.nlm.nih.gov/pubmed/10684935.
Read, T.D., Myers, G.S.A., Brunham, R.C., Nelson, W.C., Paulsen, I.T., Heidelberg, J., *et al.* (2003) Genome sequence of Chlamydophila caviae (Chlamydia psittaci GPIC): examining the role of niche-specific genes in the evolution of the Chlamydiaceae. *Nucleic Acids Res* **31**: 2134–47 http://www.ncbi.nlm.nih.gov/pubmed/12682364.
Rejman Lipinski, A., Heymann, J., Meissner, C., Karlas, A., Brinkmann, V., Meyer, T.F., and Heuer, D. (2009) Rab6 and Rab11 regulate Chlamydia trachomatis development and golgin-84-dependent Golgi fragmentation. *PLoS Pathog* **5**: e1000615 http://www.ncbi.nlm.nih.gov/pubmed/19816566.
Reyburn, H. (2010) New WHO guidelines for the treatment of malaria. *BMJ* **340**: c2637–c2637 http://www.ncbi.nlm.nih.gov/pubmed/25103303.
Ricci, S., Cevenini, R., Cosco, E., Comanducci, M., Ratti, G., and Scarlato, V. (1993) Transcriptional analysis of the Chlamydia trachomatis plasmid pCT identifies temporally regulated transcripts, anti-sense RNA and sigma 70-selected promoters. *Mol Gen Genet* **237**: 318–26 http://www.ncbi.nlm.nih.gov/pubmed/7683369.
Ricci, S., Ratti, G., and Scarlato, V. (1995) Transcriptional regulation in the Chlamydia trachomatis pCT plasmid. *Gene* **154**: 93–98.
Rockey, D.D., Scidmore, M.A., Bannantine, J.P., and Brown, W.J. (2002) Proteins in the chlamydial inclusion membrane. *Microbes Infect* **4**: 333–340.
Rodríguez-Escudero, I., Roelants, F.M., Thorner, J., Nombela, C., Molina, M., and Cid, V.J. (2005) Reconstitution of the mammalian PI3K/PTEN/Akt pathway in yeast. *Biochem J* **390**: 613–23

http://www.ncbi.nlm.nih.gov/pubmed/15913452.
Ronzone, E., and Paumet, F. (2013) Two coiled-coil domains of Chlamydia trachomatis IncA affect membrane fusion events during infection. *PLoS One* **8**: e69769 http://www.ncbi.nlm.nih.gov/pubmed/23936096.
Ronzone, E., Wesolowski, J., Bauler, L.D., Bhardwaj, A., Hackstadt, T., and Paumet, F. (2014) An α-helical core encodes the dual functions of the chlamydial protein IncA. *J Biol Chem* **289**: 33469–80 http://www.ncbi.nlm.nih.gov/pubmed/25324548.
Roulis, E., Polkinghorne, A., and Timms, P. (2013) Chlamydia pneumoniae: Modern insights into an ancient pathogen. *Trends Microbiol* .
Rzomp, K.A., Moorhead, A.R., and Scidmore, M.A. (2006) The GTPase Rab4 interacts with Chlamydia trachomatis inclusion membrane protein CT229. *Infect Immun* **74**: 5362–5373.
Rzomp, K.A., Scholtes, L.D., Briggs, B.J., Whittaker, G.R., and Scidmore, M.A. (2003) Rab GTPases are recruited to chlamydial inclusions in both a species-dependent and species-independent manner. *Infect Immun* **71**: 5855–70 http://www.ncbi.nlm.nih.gov/pubmed/14500507.
Sachse, K., Bavoil, P.M., Kaltenboeck, B., Stephens, R.S., Kuo, C.-C., Rosselló-Móra, R., and Horn, M. (2015) Emendation of the family Chlamydiaceae: proposal of a single genus, Chlamydia, to include all currently recognized species. *Syst Appl Microbiol* **38**: 99–103 http://dx.doi.org/10.1016/j.syapm.2014.12.004.
Sachse, K., Laroucau, K., Riege, K., Wehner, S., Dilcher, M., Creasy, H.H., *et al.* (2014) Evidence for the existence of two new members of the family Chlamydiaceae and proposal of Chlamydia avium sp. nov. and Chlamydia gallinacea sp. nov. *Syst Appl Microbiol* **37**: 79–88 http://dx.doi.org/10.1016/j.syapm.2013.12.004.
Saka, H.A., Thompson, J.W., Chen, Y.-S., Dubois, L.G., Haas, J.T., Moseley, A., and Valdivia, R.H. (2015) Chlamydia trachomatis Infection Leads to Defined Alterations to the Lipid Droplet Proteome in Epithelial Cells. *PLoS One* **10**: e0124630 http://www.ncbi.nlm.nih.gov/pubmed/25909443.
Salcedo, S.P., and Holden, D.W. (2003) SseG, a virulence protein that targets Salmonella to the Golgi network. *EMBO J* **22**: 5003–14 http://www.ncbi.nlm.nih.gov/pubmed/14517239.
Samudrala, R., Heffron, F., and McDermott, J.E. (2009) Accurate prediction of secreted substrates and identification of a conserved putative secretion signal for type III secretion systems. *PLoS Pathog* **5**: e1000375 http://www.ncbi.nlm.nih.gov/pubmed/19390620.
Sang, Y., Ren, J., Ni, J., Tao, J., Lu, J., and Yao, Y.-F. (2016) Protein Acetylation Is Involved in Salmonella enterica Serovar Typhimurium Virulence. *J Infect Dis* **213**: 1836–45 http://www.ncbi.nlm.nih.gov/pubmed/26810370.
Sang, Y., Ren, J., Qin, R., Liu, S., Cui, Z., Cheng, S., *et al.* (2017) Acetylation Regulating Protein Stability and DNA-Binding Ability of HilD, thus Modulating Salmonella Typhimurium Virulence. *J Infect Dis* **216**: 1018–1026 http://www.ncbi.nlm.nih.gov/pubmed/28329249.
Schachter, J. (1999) Infection and Disease Epidemiology. In *Chlamydia: Intracellular Biology, Pathogenesis and Immunity*. Stephens, R.S. (ed.). ASM Press, Washington DC. pp. 139–169.
Schesser, K., Frithz-Lindsten, E., and Wolf-Watz, H. (1996) Delineation and mutational analysis of the Yersinia pseudotuberculosis YopE domains which mediate translocation across bacterial and eukaryotic cellular membranes. *J Bacteriol* **178**: 7227–33 http://www.ncbi.nlm.nih.gov/pubmed/8955406.
Schindelin, J., Arganda-Carreras, I., Frise, E., Kaynig, V., Longair, M., Pietzsch, T., *et al.* (2012) Fiji: an open-source platform for biological-image analysis. *Nat Methods* **9**: 676–82 http://www.ncbi.nlm.nih.gov/pubmed/22743772.
Scidmore, M.A. (2005) Cultivation and Laboratory Maintenance of Chlamydia trachomatis. *Curr Protoc Microbiol* **Chapter 11**: Unit 11A.1 http://www.ncbi.nlm.nih.gov/pubmed/18770550.
Seaman, M.N.J. (2012) The retromer complex - endosomal protein recycling and beyond. *J Cell Sci* **125**: 4693–4702 http://jcs.biologists.org/cgi/doi/10.1242/jcs.103440.
Selyunin, A.S., Sutton, S.E., Weigele, B.A., Reddick, L.E., Orchard, R.C., Bresson, S.M., *et al.* (2011) The assembly of a GTPase-kinase signalling complex by a bacterial catalytic scaffold. *Nature* **469**: 107–11 http://www.ncbi.nlm.nih.gov/pubmed/21170023.
Seth-Smith, H.M.B., Harris, S.R., Skilton, R.J., Radebe, F.M., Golparian, D., Shipitsyna, E., *et al.* (2013) Whole-genome sequences of Chlamydia trachomatis directly from clinical samples without culture. *Genome Res* **23**: 855–866.
Sexually transmitted infections (STIs) Fact Sheet, World Health Organization (WHO) (2016) .
Shaw, A., Christiansen, G., Roepstorff, P., and Birkelund, S. (2000) Genetic differences in the Chlamydia trachomatis tryptophan synthase alpha-subunit can explain variations in serovar pathogenesis. *Microbes Infect* **2**: 581–92 http://www.ncbi.nlm.nih.gov/pubmed/10884608.
Shaw, E.I., Dooley, C.A., Fischer, E.R., Scidmore, M.A., Fields, K.A., and Hackstadt, T. (2000) Three

temporal classes of gene expression during the Chlamydia trachomatis developmental cycle. *Mol Microbiol* **37**: 913–25 http://www.ncbi.nlm.nih.gov/pubmed/10972811.

Shaw, R.K., Smollett, K., Cleary, J., Garmendia, J., Straatman-Iwanowska, A., Frankel, G., and Knutton, S. (2005) Enteropathogenic Escherichia coli type III effectors EspG and EspG2 disrupt the microtubule network of intestinal epithelial cells. *Infect Immun* **73**: 4385–90 http://www.ncbi.nlm.nih.gov/pubmed/15972534.

Shi, X., Halder, P., Yavuz, H., Jahn, R., and Shuman, H.A. (2016) Direct targeting of membrane fusion by SNARE mimicry: Convergent evolution of *Legionella* effectors. *Proc Natl Acad Sci* **113**: 8807–8812 http://www.pnas.org/lookup/doi/10.1073/pnas.1608755113.

Shohdy, N., Efe, J.A., Emr, S.D., and Shuman, H. a (2005) Pathogen effector protein screening in yeast identifies *Legionella* factors that interfere with membrane trafficking. *Proc Natl Acad Sci U S A* **102**: 4866–71 http://www.pubmedcentral.nih.gov/articlerender.fcgi?artid=555709&tool=pmcentrez&rendertype=abstract.

Sigar, I.M., Schripsema, J.H., Wang, Y., Clarke, I.N., Cutcliffe, L.T., Seth-Smith, H.M.B., *et al.* (2014) Plasmid deficiency in urogenital isolates of Chlamydia trachomatis reduces infectivity and virulence in a mouse model. *Pathog Dis* **70**: 61–69.

Sisko, J.L., Spaeth, K., Kumar, Y., and Valdivia, R.H. (2006) Multifunctional analysis of Chlamydia-specific genes in a yeast expression system. *Mol Microbiol* **60**: 51–66.

Sixt, B.S., Bastidas, R.J., Finethy, R., Baxter, R.M., Carpenter, V.K., Kroemer, G., *et al.* (2017) The Chlamydia trachomatis Inclusion Membrane Protein CpoS Counteracts STING-Mediated Cellular Surveillance and Suicide Programs. *Cell Host Microbe* **21**: 113–121.

Snavely, E.A., Kokes, M., Dunn, J.D., Saka, H.A., Nguyen, B.D., Bastidas, R.J., *et al.* (2014) Reassessing the role of the secreted protease CPAF in Chlamydia trachomatis infection through genetic approaches. *Pathog Dis* **71**: 336–51 http://www.ncbi.nlm.nih.gov/pubmed/24838663.

Song, L., Carlson, J.H., Whitmire, W.M., Kari, L., Virtaneva, K., Sturdevant, D.E., *et al.* (2013) Chlamydia trachomatis plasmid-encoded pgp4 is a transcriptional regulator of virulence-associated genes. *Infect Immun* **81**: 636–644.

Sorg, I., Wagner, S., Amstutz, M., Müller, S.A., Broz, P., Lussi, Y., *et al.* (2007) YscU recognizes translocators as export substrates of the Yersinia injectisome. *EMBO J* **26**: 3015–24 http://www.ncbi.nlm.nih.gov/pubmed/17510628.

Sory, M.P., Boland, A., Lambermont, I., and Cornelis, G.R. (1995) Identification of the YopE and YopH domains required for secretion and internalization into the cytosol of macrophages, usig the cyaA gene fusion approach. *Proc Natl Acad Sci U S A* **92**: 11998–2002 http://www.ncbi.nlm.nih.gov/pubmed/8618831.

Sory, M.P., and Cornelis, G.R. (1994) Translocation of a hybrid YopE-adenylate cyclase from Yersinia enterocolitica into HeLa cells. *Mol Microbiol* **14**: 583–94 http://www.ncbi.nlm.nih.gov/pubmed/7885236.

Spaeth, K.E., Chen, Y.-S., and Valdivia, R.H. (2009) The Chlamydia type III secretion system C-ring engages a chaperone-effector protein complex. *PLoS Pathog* **5**: e1000579 http://www.ncbi.nlm.nih.gov/pubmed/19750218.

Stanhope, R., Flora, E., Bayne, C., and Derré, I. (2017) IncV, a FFAT motif-containing Chlamydia protein, tethers the endoplasmic reticulum to the pathogen-containing vacuole. *Proc Natl Acad Sci U S A* **114**: 12039–12044 http://www.ncbi.nlm.nih.gov/pubmed/29078338.

Stephens, R.S. (1998) Genome Sequence of an Obligate Intracellular Pathogen of Humans: Chlamydia trachomatis. *Science (80-)* **282**: 754–759 http://www.ncbi.nlm.nih.gov/pubmed/9784136%5Cnhttp://www.sciencemag.org/content/282/5389/754.full.pdf.

Stephens, R.S., Myers, G., Eppinger, M., and Bavoil, P.M. (2009) Divergence without difference: phylogenetics and taxonomy of Chlamydia resolved. *FEMS Immunol Med Microbiol* **55**: 115–119 http://www.ncbi.nlm.nih.gov/pubmed/25246403.

Stone, C.B., Sugiman-Marangos, S., Bulir, D.C., Clayden, R.C., Leighton, T.L., Slootstra, J.W., *et al.* (2012) Structural characterization of a novel Chlamydia pneumoniae type III secretion-associated protein, Cpn0803. *PLoS One* **7**: e30220 http://www.ncbi.nlm.nih.gov/pubmed/22272312.

Su, H., Raymond, L., Rockey, D.D., Fischer, E., Hackstadt, T., and Caldwell, H.D. (1996) A recombinant Chlamydia trachomatis major outer membrane protein binds to heparan sulfate receptors on epithelial cells. *Proc Natl Acad Sci U S A* **93**: 11143–8 http://www.ncbi.nlm.nih.gov/pubmed/8855323.

Subbarayal, P., Karunakaran, K., Winkler, A.-C., Rother, M., Gonzalez, E., Meyer, T.F., and Rudel, T. (2015) EphrinA2 receptor (EphA2) is an invasion and intracellular signaling receptor for Chlamydia trachomatis. *PLoS Pathog* **11**: e1004846 http://www.ncbi.nlm.nih.gov/pubmed/25906164.

Subtil, A., Delevoye, C., Balañá, M.-E., Tastevin, L., Perrinet, S., and Dautry-Varsat, A. (2005) A directed screen for chlamydial proteins secreted by a type III mechanism identifies a translocated protein and numerous other new candidates. *Mol Microbiol* **56**: 1636–47 http://www.ncbi.nlm.nih.gov/pubmed/15916612.

Tam, J.E., Davis, C.H., and Wyrick, P.B. (1994) Expression of recombinant DNA introduced into Chlamydia trachomatis by electroporation. *Can J Microbiol* **40**: 583–591.

Tang, L., Chen, J., Zhou, Z., Yu, P., Yang, Z., and Zhong, G. (2015) Chlamydia-secreted protease CPAF degrades host antimicrobial peptides. *Microbes Infect* **17**: 402–8 http://www.ncbi.nlm.nih.gov/pubmed/25752416.

Taylor, H.R., Burton, M.J., Haddad, D., West, S., and Wright, H. (2014) Trachoma. *Lancet (London, England)* **384**: 2142–52 http://www.ncbi.nlm.nih.gov/pubmed/25043452.

Thalmann, J., Janik, K., May, M., Sommer, K., Ebeling, J., Hofmann, F., *et al.* (2010) Actin Re-Organization Induced by Chlamydia trachomatis Serovar D - Evidence for a Critical Role of the Effector Protein CT166 Targeting Rac. *PLoS One* **5**: e9887 http://www.ncbi.nlm.nih.gov/pubmed/20360858.

Thanabalasuriar, A., Koutsouris, A., Weflen, A., Mimee, M., Hecht, G., and Gruenheid, S. (2010) The bacterial virulence factor NleA is required for the disruption of intestinal tight junctions by enteropathogenic Escherichia coli. *Cell Microbiol* **12**: 31–41 http://www.ncbi.nlm.nih.gov/pubmed/19712078.

Thomas, N.S., Lusher, M., Storey, C.C., and Clarke, I.N. (1997) Plasmid diversity in Chlamydia. *Microbiology* **143**: 1847–1854 http://mic.microbiologyresearch.org/content/journal/micro/10.1099/00221287-143-6-1847.

Thompson, C.C., Griffiths, C., Nicod, S.S., Lowden, N.M., Wigneshweraraj, S., Fisher, D.J., and McClure, M.O. (2015) The Rsb Phosphoregulatory Network Controls Availability of the Primary Sigma Factor in Chlamydia trachomatis and Influences the Kinetics of Growth and Development. *PLoS Pathog* **11**: 1–22.

Thomson, N.R., Holden, M.T.G., Carder, C., Lennard, N., Lockey, S.J., Marsh, P., *et al.* (2008) Chlamydia trachomatis: genome sequence analysis of lymphogranuloma venereum isolates. *Genome Res* **18**: 161–71 http://www.ncbi.nlm.nih.gov/pubmed/18032721.

Thomson, N.R., Yeats, C., Bell, K., Holden, M.T.G., Bentley, S.D., Livingstone, M., *et al.* (2005) The Chlamydophila abortus genome sequence reveals an array of variable proteins that contribute to interspecies variation. *Genome Res* **15**: 629–40 http://www.ncbi.nlm.nih.gov/pubmed/15837807.

Tomalka, A.G., Stopford, C.M., Lee, P.-C., and Rietsch, A. (2012) A translocator-specific export signal establishes the translocator-effector secretion hierarchy that is important for type III secretion system function. *Mol Microbiol* **86**: 1464–81 http://www.ncbi.nlm.nih.gov/pubmed/23121689.

Tomson, F.L., Viswanathan, V.K., Kanack, K.J., Kanteti, R.P., Straub, K. V, Menet, M., *et al.* (2005) Enteropathogenic Escherichia coli EspG disrupts microtubules and in conjunction with Orf3 enhances perturbation of the tight junction barrier. *Mol Microbiol* **56**: 447–64 http://www.ncbi.nlm.nih.gov/pubmed/15813736.

Trachoma Fact Sheet, World Health Organization (WHO) (2018) .

Uphoff, C.C., and Drexler, H.G. (2011) Detecting mycoplasma contamination in cell cultures by polymerase chain reaction. *Methods Mol Biol* **731**: 93–103 http://www.ncbi.nlm.nih.gov/pubmed/21516400.

Voigt, A., Schöfl, G., and Saluz, H.P. (2012) The chlamydia psittaci genome: A comparative analysis of intracellular pathogens. *PLoS One* .

Vromman, F., Perrinet, S., Gehre, L., and Subtil, A. (2016) The DUF582 Proteins of Chlamydia trachomatis Bind to Components of the ESCRT Machinery, Which Is Dispensable for Bacterial Growth In vitro. *Front Cell Infect Microbiol* **6**: 1–14 http://journal.frontiersin.org/article/10.3389/fcimb.2016.00123/full.

Walker, E., Lee, E.J., Timms, P., and Polkinghorne, A. (2015) Chlamydia pecorum infections in sheep and cattle: A common and under-recognised infectious disease with significant impact on animal health. *Vet J* **206**: 252–260 http://dx.doi.org/10.1016/j.tvjl.2015.09.022.

Wang, J., Zhang, Y., Lu, C., Lei, L., Yu, P., and Zhong, G. (2010) A genome-wide profiling of the humoral immune response to Chlamydia trachomatis infection reveals vaccine candidate antigens expressed in humans. *J Immunol* **185**: 1670–1680.

Wang, X., Hybiske, K., and Stephens, R.S. (2017) Orchestration of the mammalian host cell glucose transporter proteins-1 and 3 by Chlamydia contributes to intracellular growth and infectivity. *Pathog Dis* **75** http://academic.oup.com/femspd/article/doi/10.1093/femspd/ftx108/4411801.

Wang, X., Hybiske, K., and Stephens, R.S. (2018) Direct visualization of the expression and localization of chlamydial effector proteins within infected host cells. *Pathog Dis* **76**

https://academic.oup.com/femspd/article/doi/10.1093/femspd/fty011/4830102.
Wang, Y., Kahane, S., Cutcliffe, L.T., Skilton, R.J., Lambden, P.R., and Clarke, I.N. (2011) Development of a transformation system for chlamydia trachomatis: Restoration of glycogen biosynthesis by acquisition of a plasmid shuttle vector. *PLoS Pathog* **7**.
Wang, Y., Sun, M., Bao, H., Zhang, Q., and Guo, D. (2013) Effective identification of bacterial type III secretion signals using joint element features. *PLoS One* **8**: e59754 http://www.ncbi.nlm.nih.gov/pubmed/23593149.
Weber, M.M., Lam, J.L., Dooley, C.A., Noriea, N.F., Hansen, B.T., Hoyt, F.H., *et al.* (2017) Absence of Specific Chlamydia trachomatis Inclusion Membrane Proteins Triggers Premature Inclusion Membrane Lysis and Host Cell Death. *Cell Rep* **19**: 1406–1417 http://dx.doi.org/10.1016/j.celrep.2017.04.058.
Weber, M.M., Noriea, N.F., Bauler, L.D., Lam, J.L., Sager, J., Wesolowski, J., *et al.* (2016) A Functional Core of IncA Is Required for Chlamydia trachomatis Inclusion Fusion. *J Bacteriol* **198**: 1347–55 http://www.ncbi.nlm.nih.gov/pubmed/26883826.
Weber, M.M., Noriea, N.F., Bauler, L.D., Lam, J.L., Sager, J., Wesolowski, J., *et al.* (2016) A Functional Core of IncA Is Required for Chlamydia trachomatis Inclusion Fusion. *J Bacteriol* **198**: 1347–55 http://www.ncbi.nlm.nih.gov/pubmed/26883826.
Wesolowski, J., Weber, M.M., Nawrotek, A., Dooley, C.A., Calderon, M., St Croix, C.M., *et al.* (2017) Chlamydia Hijacks ARF GTPases To Coordinate Microtubule Posttranslational Modifications and Golgi Complex Positioning. *MBio* **8**: 1–14 http://www.ncbi.nlm.nih.gov/pubmed/28465429.
Wickstrum, J., Sammons, L.R., Restivo, K.N., and Hefty, P.S. (2013) Conditional Gene Expression in Chlamydia trachomatis Using the Tet System. *PLoS One* **8**: 1–11.
Woestyn, S., Sory, M.P., Boland, A., Lequenne, O., and Cornelis, G.R. (1996) The cytosolic SycE and SycH chaperones of Yersinia protect the region of YopE and YopH involved in translocation across eukaryotic cell membranes. *Mol Microbiol* **20**: 1261–71 http://www.ncbi.nlm.nih.gov/pubmed/8809777.
Yang, C., Starr, T., Song, L., Carlson, J.H., Sturdevant, G.L., Beare, P.A., *et al.* (2015) Chlamydial lytic exit from host cells is plasmid regulated. *MBio* **6**: 1–9.
Yang, Z., Soderholm, A., Lung, T.W.F., Giogha, C., Hill, M.M., Brown, N.F., *et al.* (2015) SseK3 Is a Salmonella Effector That Binds TRIM32 and Modulates the Host's NF-κB Signalling Activity. *PLoS One* **10**: e0138529 http://www.ncbi.nlm.nih.gov/pubmed/26394407.
Yang, Z., Tang, L., Shao, L., Zhang, Y., Zhang, T., Schenken, R., *et al.* (2016) The Chlamydia-Secreted Protease CPAF Promotes Chlamydial Survival in the Mouse Lower Genital Tract. *Infect Immun* **84**: 2697–702 http://www.ncbi.nlm.nih.gov/pubmed/27382018.
Yao, J., Abdelrahman, Y.M., Robertson, R.M., Cox, J. V, Belland, R.J., White, S.W., and Rock, C.O. (2014) Type II Fatty Acid Synthesis Is Essential for the Replication of Chlamydia trachomatis. *J Biol Chem* **289**: 22365–22376 http://www.ncbi.nlm.nih.gov/pubmed/24958721.
Yao, J., Cherian, P.T., Frank, M.W., and Rock, C.O. (2015) Chlamydia trachomatis Relies on Autonomous Phospholipid Synthesis for Membrane Biogenesis. *J Biol Chem* **290**: 18874–88 http://www.ncbi.nlm.nih.gov/pubmed/25995447.
Yao, J., Dodson, V.J., Frank, M.W., and Rock, C.O. (2015) Chlamydia trachomatis Scavenges Host Fatty Acids for Phospholipid Synthesis via an Acyl-Acyl Carrier Protein Synthetase. *J Biol Chem* **290**: 22163–22173 http://www.ncbi.nlm.nih.gov/pubmed/26195634.
Yen, H., Sugimoto, N., and Tobe, T. (2015) Enteropathogenic Escherichia coli Uses NleA to Inhibit NLRP3 Inflammasome Activation. *PLoS Pathog* **11**: e1005121 http://www.ncbi.nlm.nih.gov/pubmed/26332984.
Young, B.H., Caldwell, T.A., McKenzie, A.M., Kokhan, O., and Berndsen, C.E. (2016) Characterization of the structure and catalytic activity of Legionella pneumophila VipF. *Proteins* **84**: 1422–30 http://www.ncbi.nlm.nih.gov/pubmed/27315603.
Yu, X.-J., Liu, M., and Holden, D.W. (2016) Salmonella Effectors SseF and SseG Interact with Mammalian Protein ACBD3 (GCP60) To Anchor Salmonella -Containing Vacuoles at the Golgi Network. *MBio* **7**: e00474-16 http://mbio.asm.org/lookup/doi/10.1128/mBio.00474-16.

ANNEXES

Table A.1 Plasmids used in this work.

Plasmid	Description	Source/Reference	Chapter
pBOMB4-Tet-mCherry	*C. trachomatis* vector for expression of proteins, under the control of a tetracycline-inducible promotor (Amp^R).	(Bauler and Hackstadt, 2014)	3.2
p2TK2--SW2	*C. trachomatis* vector for expression of proteins (Amp^R).	(Agaisse and Derré, 2013)	3.1
pSVP247	Derivative of p2TK2--SW2 (Agaisse *et al.*, 2013) for expression of proteins with a C-terminal double HA (2HA) tag. Contains the terminator of the *incDEFG* operon (T*incD*) of *C. trachomatis* L2/434 (Amp^R).	(da Cunha *et al.*, 2017)	3.1
pSVP277	Derivative of p2TK2--SW2 (Agaisse *et al.*, 2013) for expression of proteins with a C-terminal GSK peptide. Contains the terminator of the *incDEFG* operon (T*incD*) of *C. trachomatis* L2/434. A DNA fragment containing the DNA sequence of the GSK peptide was amplified by PCR using primers 1749 and 1751. The DNA sequence of T*incD* was amplified by PCR from DNA of *C. trachomatis* L2/434 using primers 1750 and 1483. The two products were fused by overlapping PCR using primers 1749 and 1483; the resulting DNA product was digested with NotI and SalI and ligated into those sites of p2TK2-SW2 (Amp^R).	This work	3.1
pSVP268	Derivative of p2TK2--SW2 (Agaisse *et al.*, 2013) for expression of proteins with a C-terminal adenylate cyclase (CyaA). Contains the terminator of the *incDEFG* operon (T*incD*) of *C. trachomatis* L2/434. A DNA fragment containing *cyaA* was amplified by PCR from pJB2581 using primers 1693 and 1695. The DNA sequence of T*incD* was amplified by PCR from DNA of *C. trachomatis* L2/434 using primers 1694 and 1696. The DNA fragments of *cyaA* and T*incD* were fused by overlapping PCR using primers 1693 and 1696. The resulting DNA product was digested with NdeI and NotI and ligated into those sites of p2TK2-SW2 (Amp^R).	This work	3.1
pLJM3	Derivative of the low copy vector pBBR1MCS-2 (Kovach *et al.*, 1994). Expresses YopE under the control of its own promoter (P*yopE*) (Km^R).	(Marenne *et al.*, 2003)	3.1
pEGFP-N1	Transfection vector. Fusions at the N-terminus of EGFP under the control of the CMV promoter (Km^R).	Clontech	3.1
pEGFP-C1	Transfection vector. Fusions at the N-terminus of EGFP under the control of the CMV promoter (Km^R).	Clontech	3.1
pLAMP1-mGFP	Transfection vector encoding human LAMP1 fused to monomeric GFP (mGFP) (Km^R)	Addgene plasmid # 34831 (Falcon-Perez *et al.*, 2005)	3.2
Lyn11-FRB-mcherry	Mammalian expression vector encoding a Lyn Src kinase N-terminal sequence (Lyn11) fused to FRB (fragment of mTOR that binds rapamycin) and to mCherry.	Addgene plasmid # 38004 (Hammond *et al.*, 2012)	3.2
pmEGFP-N1/pALT1	Mammalian transfection vector for expression of proteins fused to the N-terminus of mEGFP under the control of the *CMV* promoter (Km^R). The DNA fragment encoding mEGFP was amplified by PCR from pLAMP1-mEGFP using primers 1851 and 1852. The resulting DNA product was digested with AgeI and NotI and ligated into those sites of pGFP-N1.	This work	3.2
pmEGFP-C1/pALT2	Mammalian transfection vector for expression of proteins fused to the C-terminus of mEGFP under the control of the *CMV* promoter (Km^R). The DNA fragment encoding mEGFP was amplified by PCR from pLAMP1-mEGFP using primers 1852 and 1853. The resulting DNA product was digested with XhoI and NotI and ligated into those sites of pGFP-C1.	This work	3.2

pEF6/*Myc*-His A	Mammalian transfection vector for expression of proteins, under the control of the *EF-1α* promoter (Km^R).	Thermo Fisher Scientific	3.2
pDFTT3*aadA*	Group II intron donor plasmid.	(Key *et al.*, 2017)	3.3
pYES2-GFP	Yeast vector for expression of proteins fused to the C-terminus of GFP, under the control of a galactose-inducible promoter (Amp^R).	(Rodriguez-Escudero *et al.*, 2005)	3.3
pKS84	Yeast vector for expression of proteins fused to the N-terminus of GFP, under the control of a galactose-inducible promoter (Amp^R).	(de Felipe *et al.*, 2008)	3.3
pCM46	Transfection vector encoding EGFP-CT053. A DNA fragment containing *ct053* was amplified from *C. trachomatis* L2/434 chromosomal DNA using primers 997 and 998. The resulting DNA product was digested with HindIII and SalI and inserted into those sites of pEGFP-C1 (Km^R).	This work	3.1
pSG13	Transfection vector encoding EGFP-CT082. A DNA fragment containing *ct082* was amplified from *C. trachomatis* L2/434 chromosomal DNA using primers 650 and 651. The resulting DNA product was digested with XhoI and BamHI and inserted into those sites of pEGFP-C1 (Km^R).	This work	3.1
pSG19	Transfection vector encoding EGFP-CT105. A DNA fragment containing *ct105* was amplified from *C. trachomatis* L2/434 chromosomal DNA using primers 652 and 653. The resulting DNA product was digested with SalI and KpnI and inserted into those sites of pEGFP-C1 (Km^R).	This work	3.1
pSG10	Transfection vector encoding EGFP-CT429. A DNA fragment containing *ct429* was amplified from *C. trachomatis* L2/434 chromosomal DNA using primers 670 and 671. The resulting DNA product was digested with XhoI and BamHI and inserted into those sites of pEGFP-C1 (Km^R).	This work	3.1
pLJM1070	Transfection vector encoding EGFP-CT696. A DNA fragment containing *ct696* was amplified from *C. trachomatis* L2/434 chromosomal DNA using primers 938 and 939. The resulting DNA product was digested with XhoI and SalI and inserted into those sites of pEGFP-C1 (Km^R).	This work	3.1
pSG9	Transfection vector encoding EGFP-CT849. A DNA fragment containing *ct849* was amplified from *C. trachomatis* L2/434 chromosomal DNA using primers 684 and 685. The resulting DNA product was digested with XhoI and BamHI and inserted into those sites of pEGFP-C1 (Km^R).	This work	3.1
pSVP261/pCT053-2HA	Expresses CT053-2HA under the control of the predicted *ct053* promoter. A DNA fragment containing *ct053* and its endogenous promoter was amplified from *C. trachomatis* L2/434 chromosomal DNA using primers 1677 and 1678. The resulting DNA product was digested with KpnI and NotI and inserted into those sites of pSVP247 (Amp^R).	This work	3.1
pSVP263/pCT082-2HA	Expresses CT082-2HA under the control of the predicted *ct082* promoter. A DNA fragment containing c*t082* and its endogenous promoter was amplified from *C. trachomatis* L2/434 chromosomal DNA using primers 1679 and 1549. The resulting DNA product was digested with KpnI and NotI and inserted into those sites of pSVP247 (Amp^R).	This work	3.1
pSVP264/pCT105-2HA	Expresses CT105-2HA under the control of the predicted *ct105* promoter. A DNA fragment containing c*t105* and its endogenous promoter was amplified from *C. trachomatis* L2/434 chromosomal DNA using primers 1680 and 1552. The resulting DNA product was digested with KpnI and NotI and inserted into those sites of pSVP247 (Amp^R).	This work	3.1, 3.2, 3.3
pSVP265/pCT429-2HA	Expresses CT429-2HA under the control of the predicted *ct429* promoter. A DNA fragment containing c*t429* and its endogenous promoter was amplified from *C. trachomatis*	This work	3.1

	L2/434 chromosomal DNA using primers 1681 and 1682. The resulting DNA product was digested with KpnI and NotI and inserted into those sites of pSVP247 (Amp^R).		
pSVP266/pCT696-2HA	Expresses CT696-2HA under the control of the predicted *ct696* promoter. A DNA fragment containing c*t696* and its endogenous promoter was amplified from *C. trachomatis* L2/434 chromosomal DNA using primers 1685 and 1564. The resulting DNA product was digested with KpnI and NotI and inserted into those sites of pSVP247 (Amp^R).	This work	3.1
pSVP267/pCT849-2HA	Expresses CT849-2HA under the control of the predicted *ct849* promoter. A DNA fragment containing c*t849* and its endogenous promoter was amplified from *C. trachomatis* L2/434 chromosomal DNA using primers 1686 and 1687. The resulting DNA product was digested with KpnI and NotI and inserted into those sites of pSVP247 (Amp^R).	This work	3.1
pFA3	Expresses the mature form of TEM-1 β-lactamase (TEM-1) under the *yopE* promoter (Km^R).	(Almeida *et al.*, 2012)	3.1
pRM11	Expresses $CT105_{20}$-TEM-1 under the control of the *yopE* promoter (Km^R).	(da Cunha *et al.*, 2014)	3.1
pMBC1	Expresses $CT105_{40}$-TEM-1 under the control of the *yopE* promoter. A DNA fragment encoding the first 40 amino acids of CT105 was amplified from pRM7 using primers 28 and 1801. TEM-1 was amplified from pFA3 using primers 1802 and 60. The two DNA fragments were then fused by overlapping PCR using primers 28 and 60. The resulting DNA product was digested with NdeI and HindIII and inserted into those sites of pLJM3 (Km^R).	This work	3.1
pRM7	Expresses $CT105_{FL}$-2HA under the control of the *yopE* promoter (Km^R).	(da Cunha *et al.*, 2014)	3.1
pMBC2	Expresses $CT105_{\Delta 20}$-2HA under the control of the *yopE* promoter. A DNA fragment encoding CT105 without its first 20 amino acids was amplified from *C. trachomatis* L2/434 chromosomal DNA using primers 1799 and 174. The resulting DNA product was digested with NdeI and KpnI and inserted into those sites of pLJM3 (Km^R).	This work	3.1
pMBC3	Expresses $CT105_{\Delta 40}$-2HA under the control of the *yopE* promoter. A DNA fragment encoding CT105 without its first 40 amino acids was amplified from *C. trachomatis* L2/434 chromosomal DNA using primers 1800 and 174. The resulting DNA product was digested with NdeI and KpnI and inserted into those sites of pLJM3 (Km^R).	This work	3.1
pMBC5/$pCT105_{\Delta 20}$-2HA	Expresses $CT105_{\Delta 20}$-2HA under the control of the predicted *ct105* promoter. A DNA fragment encoding the predicted *ct105* promoter was amplified from pSVP264 using primers 1680 and 1812. A DNA fragment encoding CT105 without its first 20 amino acids was amplified from *C. trachomatis* L2/434 chromosomal DNA using primers 1813 and 1552. The two DNA fragments were then fused by overlapping PCR using primers 1680 and 1552. The resulting DNA product was digested with KpnI and NotI and inserted into those sites of pSVP247 (Amp^R).	This work	3.1
pSVP302/pTet-CT105-2HA	Expresses CT105-2HA under the control of the tetracycline-inducible promoter (P_{tet}). A DNA fragment containing P_{tet} was amplified from pBOMB4-Tet-mCherry using primers 1803 and 1804. A DNA fragment containing *ct105* was amplified from *C. trachomatis* L2/434 chromosomal DNA using primers 1805 and 1552. The two DNA fragments were then fused by overlapping PCR using primers 1803 and 1552. The resulting DNA product was digested with KpnI and NotI and inserted into those sites of pSVP247 (Amp^R).	This work	3.2
pSVP294	Transfection vector encoding LYN11-mEGFP. A DNA fragment encoding Lyn11 was amplified from pLYN11-FRB-mCherry using primers 1824 and 1848. A DNA fragment encoding mEGFP was amplified from pLAMP-1-mEGFP using primers 1847 and 1851. The two coding	This work	3.2

	regions were fused by overlapping PCR using primers 1858 and 1859. The resulting DNA product was digested with HindIII and NotI and inserted into those sites of pEGFP-N1 (Km^R).		
pALT4	Transfection vector encoding mEGFP-CT105. A DNA fragment containing *ct105* was amplified from *C. trachomatis* L2/434 chromosomal DNA using primers 652 and 653. The resulting DNA product was digested with KpnI and SalI and inserted into those sites of pmEGFP-C1 (Km^R).	This work	3.2
pSVP292	Transfection vector encoding CT105-2HA. A DNA fragment encoding CT105-2HA was amplified from pSVP264 using primers 1780 and 1783. The resulting DNA product was digested with KpnI and NotI and inserted into those sites of pEF6/*Myc*-His A (Amp^R).	This work	3.2
pSVP310	Transfection vector encoding mEGFP-$CT105_{1\text{-}100}$. A DNA fragment encoding the first 100 amino acid residues of CT105 was amplified from *C. trachomatis* L2/434 chromosomal DNA using primers 652 and 2128. The resulting DNA product was digested with KpnI and SalI and inserted into those sites of pmEGFP-C1 (Km^R).	This work	3.2
pSVP314	Transfection vector encoding mEGFP-$CT105_{\Delta 100}$. A DNA fragment encoding CT105 without its first 100 amino acid residues (but maintaining the ATG start codon) was amplified from *C. trachomatis* L2/434 chromosomal DNA using primers 2155 and 653. The resulting DNA product was digested with KpnI and SalI and inserted into those sites of pmEGFP-C1 (Km^R).	This work	3.2
pSVP303	Transfection vector encoding mEGFP-$CT105_{1\text{-}320}$. A DNA fragment encoding the first 320 amino acid residues of CT105 was amplified from *C. trachomatis* L2/434 chromosomal DNA using primers using primers 652 and 2129. The resulting DNA product was digested with KpnI and SalI and inserted into those sites of pmEGFP-C1 (Km^R).	This work	3.2
pSVP316	Transfection vector encoding mEGFP-$CT105_{\Delta 320}$. A DNA fragment encoding CT105 without its first 320 amino acid residues (but maintaining the ATG start codon) was amplified from *C. trachomatis* L2/434 chromosomal DNA using primers 2161 and 653. The resulting DNA product was digested with KpnI and SalI and inserted into those sites of pmEGFP-C1 (Km^R).	This work	3.2
pSVP311	Transfection vector encoding mEGFP-$CT105_{\Delta 100\text{-}320}$. A DNA fragment encoding the first 100 amino acid residues of CT105 was amplified from *C. trachomatis* L2/434 chromosomal DNA using primers 652 and 2125. A DNA fragment encoding the region from the amino acid residue 320 to the C-terminus of CT105 was amplified from *C. trachomatis* L2/434 chromosomal DNA using primers 2124 and 653. The two DNA products were fused by overlapping PCR using primers 652 and 653. The resulting DNA product was digested with KpnI and SalI and inserted into those sites of pmEGFP-C1 (Km^R).	This work	3.2
pSVP315	Encodes mEGFP-$CT105_{PDZ}$. A DNA fragment encoding CT105 with the last 3 amino acids (PDZ domain) mutated to alanine was amplified from *C. trachomatis* L2/434 chromosomal DNA using primers 652 and 2157. The resulting DNA product was digested with SalI and KpnI and inserted into those sites of pmEGFP-C1 (Km^R).	This work	3.2
pALT3	Transfection vector encoding CT105-mEGFP. A DNA fragment containing *ct105* was amplified from *C. trachomatis* L2/434 chromosomal DNA using primers 1778 and 1779. The resulting DNA product was digested with SalI and AgeI and inserted into those sites of pmEGFP-N1 (Km^R).	This work	3.2
pSVP307	Transfection vector encoding $CT105_{1\text{-}100}$-mEGFP. A DNA fragment encoding the first 100 amino acid residues of	This work	3.2

	CT105 was amplified from *C. trachomatis* L2/434 chromosomal DNA using primers 1778 and 2126. The resulting DNA product was digested with SalI and AgeI and inserted into those sites of pmEGFP-N1 (Km^R).		
pSVP308	Transfection vector encoding $CT105_{1-320}$-mEGFP. A DNA fragment encoding the first 320 amino acid residues of CT105 was amplified from *C. trachomatis* L2/434 chromosomal DNA using primers 1778 and 2127. The resulting DNA product was digested with SalI and AgeI and inserted into those sites of pmEGFP-N1 (Km^R).	This work	3.2
pSVP309	Transfection vector encoding $CT105_{\Delta 100-320}$-mEGFP. A DNA fragment encoding the first 100 amino acid residues of CT105 was amplified from *C. trachomatis* L2/434 chromosomal DNA using primers 1778 and 2125. A DNA fragment encoding the region from the amino acid residue 320 to the C-terminus of CT105 was amplified from *C. trachomatis* L2/434 chromosomal DNA using primers 2124 and 1779. The two DNA products were fused by overlapping PCR using primers 1778 and 1779. The resulting DNA product was digested with SalI and AgeI and inserted into those sites of pmEGFP-N1 (Km^R).	This work	3.2
pSVP304/pTet-$CT105_{1-100}$-2HA	Expresses $CT105_{1-100}$-2HA under the control of the tetracycline-inducible promoter (P_{tet}). A DNA fragment containing P_{tet} was amplified from pBOMB4-Tet-mCherry using primers 1803 and 1804. A DNA fragment encoding the first 100 amino acid residues of CT105 was amplified from *C. trachomatis* L2/434 chromosomal DNA using primers 1805 and 2122. The two DNA fragments were then fused by overlapping PCR using primers 1803 and 2122. The resulting DNA product was digested with KpnI and NotI and inserted into those sites of pSVP247 (Amp^R).	This work	3.2
pSVP305/ pTet-$CT105_{1-320}$-2HA	Expresses $CT105_{1-320}$-2HA under the control of the tetracycline-inducible promoter (P_{tet}). A DNA fragment containing P_{tet} was amplified from pBOMB4-Tet-mCherry using primers 1803 and 1804. A DNA fragment encoding the first 320 amino acid residues of CT105 was amplified from *C. trachomatis* L2/434 chromosomal DNA using primers 1805 and 2123. The two DNA fragments were then fused by overlapping PCR using primers 1803 and 2123. The resulting DNA product was digested with KpnI and NotI and inserted into those sites of pSVP247 (Amp^R).	This work	3.2
pSVP306/ pTet-$CT105_{\Delta 100-320}$-2HA	Expresses $CT105_{\Delta 100-320}$-2HA under the control of the tetracycline-inducible promoter (P_{tet}). A DNA fragment containing P_{tet} was amplified from pBOMB4-Tet-mCherry using primers 1803 and 1804. A DNA fragment encoding the first 100 amino acid residues of CT105 was amplified from *C. trachomatis* L2/434 chromosomal DNA using primers 1778 and 2125. A DNA fragment encoding the region from the amino acid residue 320 to the C-terminus of CT105 was amplified from *C. trachomatis* L2/434 chromosomal DNA using primers 2124 and 1779. The two DNA fragments encoding CT105 were fused using primers 1778 and 1779. The resulting DNA fragment was fused with the fragment encoding P_{tet} using primers 1805 and 1552. The resulting DNA product was digested with KpnI and NotI and inserted into those sites of pSVP247 (Amp^R).	This work	3.2
pDFTT296	Derivative of pDFTT3*aadA* carrying a group II intron targeting sequence of *ctl0360* from *C. trachomatis* strain L2/434 (orthologue of *ct105* in strain D/UW3). The 5' intron sequence was amplified by PCR using primers 1860, 1861, 1862, and 1922. The resulting ~350 bp DNA product was digested with HindIII and BsrG1 and ligated into those sites of pDFTT3*aadA* (Spc^R).	This work	3.3

pSVP319	Expresses CT105::aadA-2HA under the control of the predicted *ct105* promoter. A DNA fragment containing c*t105::aadA* and its endogenous promoter was amplified from *C. trachomatis* L2/434 *ct105::aadA* chromosomal DNA using primers 2254 and 1552. The resulting DNA product was digested with AgeI and NotI and inserted into those sites of pSVP247 (Amp^R).	This work	3.3
pCM35	Yeast expression vector expressing GFP-CT105 under the control of a galactose-inducible promoter. A DNA fragment containing *ct105* was amplified from *C. trachomatis* L2/434 chromosomal DNA using primers 799 and 812. The resulting DNA product was digested with BglII and PstI, and with PstI and NotI. The two DNA fragments obtained were inserted into BamHI and NotI sites of pGFP-YES2 (Amp^R).	This work	3.3
pSVP293	Yeast expression vector encoding CT105-EGFP under the control of a galactose-inducible promoter. A DNA fragment containing *ct105* was amplified from *C. trachomatis* L2/434 chromosomal DNA using primers 1784 and 1785. The resulting DNA product was inserted into pKS84 by homologous recombination in yeast (Amp^R).	This work	3.3

Table A.2 Oligonucleotides used in this work.

Number	Description	Sequence (5' → 3')	Restriction site
28	Forward primer to construct pMBC1	GAT TAAGTTGGGTAACGCC	-
60	Reverse primer to construct pMBC1	CCCAAGCTTTTACCAATGCTTAATCAGTGA GG	HindIII
174	Reverse primer to construct pMBC2, pMBC3	GATCGGTACCCTAAGCATAATCAGGAACAT CATACGGATAGATAGAGGAGCTTTGCACACC	KpnI
650	Forward primer to construct pSG13	GATCCTCGAGCTTCAATTTCTGGAAGTGG	XhoI
651	Reverse primer to construct pSG13	GATCGGATCCTCATGAATCGCCGCCTG CATCC	BamHI
652	Forward primer to construct pSG19, pALT4, pSVP310, pSVP303, pSVP311, pSVP315	GATCGATCGTCGACTCATTTGGTATTGGTAGT GC	SalI
653	Reverse primer to construct pSG19, pALT4, pSVP314, pSVP316, pSVP311	GATCGGTACCCTAGATAGAGGAGCTTTGCACA CC	KpnI
670	Forward primer to construct pSG10	GATCCTCGAGCTACGACATATCCTGTACCTC	XhoI
671	Reverse primer to construct pSG10	GATCGGATCCTTATGAACGGCTCTTCTTACG	BamHI
684	Forward primer to construct pSG9	GATCCTCGAGCTTCAGCACCAACCTCACAGG	XhoI
685	Reverse primer to construct pSG9	GATCGGATCCTTAAGACAGGGGTTTATTTAAT TGG	BamHI
799	Reverse primer to construct pCM35	ATAAGAATGCGGCCGCCTAGATAGAGGAGCT TTGCACACC	NotI
812	Forward primer to construct pCM35	GATCAGATCTTCATTTGGTATTGGTAGTGC	BglII
938	Forward primer to construct pLJM1070	GATCCTCGAGCTCTATTAGATTCTCGTTTCCC	XhoI
939	Reverse primer to construct pLJM1070	GATCGTCGACCTAACGAGCTTCCTTACGGAAA G	SalI
997	Forward primer to construct pCM46	GATCAAGCTTCTAAAAGTGAGCGTTTAAAAAA ATTAG	HindIII
998	Reverse primer to construct pCM46	GATCGTCGACTTACCATTCATTCGCGTCAGG	SalI
1483	Reverse primer to construct pSVP277	GATCGTCGACGTCTTAGGAGCTTTTTGCAATG C	SalI
1549	Reverse primer to construct pSVP263	GATCGCGGCCGCGTGAATCGCCGCCTGCATC CTC	NotI
1552	Reverse primer to construct pSVP264, pMBC5, pSVP302 and pSVP319, pSVP306	GATCGCGGCCGCGGATAGAGGAGCTTTGCAC ACC	NotI
1564	Reverse primer to construct pSVP266	GATCGCGGCCGCGACGAGCTTCCTTACGGAA AGTTCC	NotI
1677	Forward primer to construct pSVP261	GATCGGTACCTTTCCATGAAGAATCCATCG	KpnI
1678	Reverse primer to construct pSVP261	GATCGCGGCCGCGCCATTCATTCGCGTCAGG ATC	NotI
1679	Forward primer to construct pSVP263	GATCGGTACCGGTTAGGCATGAGTGCCTGC	KpnI
1680	Forward primer to construct pSVP264, pMBC5	GATCGGTACCTTCTTTATTATTGAGAAACG	KpnI
1681	Forward primer to construct pSVP265	GATCGGTACCTTATGAGCGAGGTTGTGAGC	KpnI
1682	Reverse primer to construct pSVP265	GATCGCGGCCGCGTGAACGGCTCTTCTTACG TCCACG	NotI
1685	Forward primer to construct pSVP266	GATCGGTACCGCAAATTGTTAATGCAAACG	KpnI

1686	Forward primer to construct pSVP267	GATCGGTACCTTCCAAAATCCTTTTTAGGG	KpnI
1687	Reverse primer to construct pSVP267	GATCGCGGCCGCGAGACAGGGGTTTATTTAA TTGG	NotI
1693	Forward primer to construct pSVP268	GGGAATTCCATATGATGCAGCAATCGCATCAG GC	NdeI
1694	Forward overlap primer to construct pSVP268	G GAA CGC CAG GAT TCC GGC TAT TAA GGA TGA CAT GTG ATT CGC GTA GG	-
1695	Reverse overlap primer to construct pSVP268	CC TAC GCG AAT CAC ATG TCA TCC TTA ATA GCC GGA ATC CTG GCG TTC C	-
1696	Reverse primer to construct pSVP268	GATCGCGGCCGCGTCTTAGGAGCTTTTTGCAA TGC	NotI
1749	Forward primer to construct pSVP277	GATCGCGGCCGCATGAGTGGTCGCCCTCGCA CTACTAGTTTCGCTGAAAGTTGA	NotI
1750	Forward overlap primer to construct pSVP277	CTAGTTTCGCTGAAAGTTGAGGATGACATGTG ATTCGCGTAGG	
1751	Reverse overlap primer to construct pSVP277	CCTACGCGAATCACATGTCATCCTCAACTTTC AGCGAAACTAG	
1778	Forward primer to construct pALT3, pSVP307, pSVP308, pSVP309, pSVP306	GATCGTCGACACCATGAGCTTTGGTATTGGTA GTGCTTG	SalI
1779	Reverse primer to construct pALT3, pSVP309, pSVP306	GATCACCGGTGGGATAGAGGAGCTTTGCACA CCTGC	AgeI
1780	Forward primer to construct pSVP292	GATCGGTACCACCATGAGCTTTGGTATTGGTA GTGCTTG	KpnI
1783	Reverse primer to construct pSVP292	GATCGCGGCCGCTTAAGCATAATCAGGAACAT CATACG	NotI
1784	Forward primer to construct pSVP293	GTTAATATACCTCTATACTTTAACGTCAAGGAG AAAAAAC ATGTCATTTGGTATTGGTAGTGC	-
1785	Reverse primer to construct pSVP293	GGATGGGCACCACTCCAGTGAAAAGTTCTTCT CCTTTACTGATAGAGGAGCTTTGCACACC	-
1799	Forward primer to construct pMBC2	GGAATTCCATATGGGCAGTGAGGGTAACAGC GAA GAAGG	NdeI
1800	Forward primer to construct pMBC3	GGAATTCCATATGTCTGGTGCTGCTTCTGCTG TAT GCC	NdeI
1801	Reverse overlap primer to construct pMBC1	CACCAGCGTTTCTGGGTGACCTGAGGCGGCG TCT GAACCCG	-
1802	Forward overlap primer to construct pMBC1	CGGGTTCAGACGCCGCCTCAGGTCACCCAGA AAC GCTGGTG	-
1803	Forward primer to construct pSVP302, pSVP304, pSVP305, pSVP306	GATCGGTACCTTAAGACCCACTTTCACATTTAA	KpnI
1804	Reverse overlap primer to construct pSVP302, pSVP304, pSVP305, pSVP306	CTACCAATACCAAATGACATTTCACTTTTCTCT ATCACTGATAGGGAGTGG	-
1805	Forward overlap primer to construct pSVP302, pSVP304, pSVP305, pSVP306	CCACTCCCTATCAGTGATAGAGAAAAGTGAAA TGTCATTTGGTATTGGTAG	-
1812	Reverse overlap primer to construct pMBC5	CCTTCTTCGCTGTTACCCTCACTGCCCATACC TTT AACTCCCGG	-
1813	Forward overlap primer to construct pMBC5	CCGGGAGTTAAAGGTATGGGCAGTGAGGGTA ACA GCGAAGAAGG	-
1824	Forward primer to construct pSVP294	GATCAAGCTTACCATGGGATGTATAAAATCAA AAGGGAAAGACAGCAGA	HindIII
1847	Forward overlap primer to construct pSVP294	TCAAAAGGGAAAGACAGCAGAGTGAGCAAGG GCGAGGAGCTG	-
1848	Reverse overlap primer to construct pSVP294	CAGCTCCTCGCCCTTGCTCACTCTGCTGTCTT TCCCTTTTGA	-
1851	Reverse primer to construct pmEGFP-N1 and pSVP294	GATCGCGGCCGCTTACTTGTACAGCTCGTCCA TGCC	NotI
1852	Forward primer to construct pmEGFP-N1 and pmEGFP-C1	GATCACCGGTCGCCACCATGGTGAGCAAGGG CGAGCTG	AgeI

1853	Reverse primer to construct pmEGFP-C1	GATCCTCGAGACTTGTCAGCTCGTCCATGCC	XhoI
1858	Forward primer to construct pSVP294	GATCAAGCTTACCATGGGATG	HindIII
1859	Reverse primer to construct pSVP294	GATCGCGGCCGCTTACTTGTAC	NotI
1860	Group II intron retargeting (CT105_261|262s_IBS1/2)	AAAAAAGCTTATAATTATCCTTACATGGCGGACGCGTGCGCCCAGATAGGGTG	-
1861	Group II intron retargeting (CT105_261|262s EBS1/delta)	CAGATTGTACAAATGTGGTGATAACAGATAAGTCGGACGCGGTAACTTACCTTTCTTTGT	-
1862	Group II intron retargeting (CT105_261|262s EBS2)	TGAACGCAAGTTTCTAATTTCGGTTCCATGTCGATAGAGGAAAGTGTCT	-
1922	Group II intron retargeting (EBS universal)	CGAAATTAGAAACTTGCGTTCAGTAAAC	-
1932	Forward primer for *16S* RT-qPCR	GCGAAGGCGCTTTTCTAATTTAT	-
1933	Reverse primer for *16S* RT-qPCR	CCAGGGTATCTAATCCTGTTTGCT	.
1934	Forward primer for *ct105* RT-qPCR	ATGGAGCCGTTTGTGTGGTT	-
1935	Reverse primer for *ct105* RT-qPCR	CCTTCTTCGCTGTTACCCTCACT	-
2122	Reverse primer for pSVP304	GATCGCGGCCGCGACTAGCAGAATATTTTTGGTAGC	NotI
2123	Reverse primer for pSVP305	GATCGCGGCCGCGACACGCACTTGCGCAGCAAGGC	NotI
2124	Forward overlap primer to construct pSVP311, pSVP309, pSVP306	ACCAAAAATATTCTGCTAGTGGATATCCTTCTTGCGGATG	-
2125	Reverse overlap primer to construct pSVP311, pSVP309, pSVP306	CATCCGCAAGAAGGATATCCACTAGCAGAATATTTTTGGT	-
2126	Reverse primer to construct pSVP307	GATCACCGGTGGACTAGCAGAATATTTTTGGTAGC	AgeI
2127	Reverse primer to construct pSVP308	GATCACCGGTGGACACGCACTTGCGCAGCAAGGC	AgeI
2128	Reverse primer to construct pSVP310	GATCGGTACCCTAACTAGCAGAATATTTTTGGTAGC	KpnI
2129	Reverse primer to construct pSVP303	GATCGGTACCCTAACACGCACTTGCGCAGCAAGGC	KpnI
2155	Forward primer to construct pSVP314	GATCGATCGTCGACGGAGTAAGTCTTACATCTATATCC	SalI
2161	Forward primer to construct pSVP316	GATCGATCGTCGACGGATATCCTTCTTGCGGATGTGC	SalI
2254	Forward primer to construct pSVP319	GATCACCGGTCCTTCTTTATTATTGAGAAACG	AgeI
2157	Reverse primer to construct pSVP315	GATCGGTACCCTAGGCAGCGGCGCTTTGCACACCTGCTTTCTGTGC	KpnI

Table A.3 *Saccharomyces cerevisiae* strains used in this work

Strains	Genotype	Source/Reference
NSY01	BHY10 diploid a/α, CPY-Inv, *inv*$^-$, *ura*$^-$	(Shohdy *et al.*, 2005)
SCIF00	NSY01 *Pgal-gfp* (pKS84)	(Franco *et al.*, 2012)
SCIF01	NSY01 *Pgal-vipA-gfp* (pIF206)	(Franco *et al.*, 2012)
SCNS00	NSY01 *Pgal-vps4*^{E233Q}	(Shohdy *et al.*, 2005)
SCSVP01	NSY01 *Pgal-gfp-ct105* (pCM35)	This work
SCSVP02	NSY01 *Pgal-ct105-gfp* (pSVP293)	This work